Uses of Recycled Concrete in Michigan

Final Report
to the
Michigan Concrete Paving Association
and the
Michigan Promotion Fund

Department of Civil and Environmental Engineering
The University of Michigan
College of Engineering

Ann Arbor, MI 48109-2125

TESTING AND RESEARCH SECTION
CONSTRUCTION AND TECHNOLOGY DIVISION
RESEARCH REPORT NO. RC-1457

Uses of Recycled Concrete in Michigan

Final Report
to the
Michigan Concrete Paving Association
and the
Michigan Promotion Fund

By: Will Hansen
Associate Professor
Department of Civil and Environmental Engineering
University of Michigan, Ann Arbor

Participating Research Fellows:
Phil Mohr, Kathryn Messner, Moideen Mathari, and
Carlos Fernandez-Baca

November 9, 1995

Table of Contents

Acknowledgments

The research described in this report was proposed and sponsored by the Michigan Concrete Paving Association (MCPA) and the Michigan Promotion Fund (MPF). Dr. Hansen wishes to extend his sincere appreciation and thanks to Mr. Gerald McCarthy, Managing Director of MCPA for the whole hearted cooperation and support he granted throughout the execution of this project. The author also thanks Dr. Mark B. Snyder, University of Minnesota for helping to design the field study program, and for conducting the crack texture measurements. Mr. Elo Yde of Laboratoriet A/S was gracious in performing petrographic analysis, and providing useful insights into the condition and performance of the concrete.

Several graduate students from the Materials and Geotechnical divisions of the Department of Civil Engineering participated in this research and in the preparation of this report. The author extends his special thanks to Messrs. Phil Mohr, Moideen Mathari, and Carlos Fernandez-Baca and Miss Kathryn Messner for their support in field and laboratory operations and in the preparation of this report.

Work in this project could not have been carried out without the cooperation of many officials of the Michigan Department of Transportation (MDOT). Our sincere thanks are to Messrs. Dave Smiley, Vern Barnhart, Dennis Dodson, Bob Kelly, Kurt Bancroft and Chris Byrum of MDOT. Mr. Dave Smiley was instrumental in coordinating all activities which required MDOT support. Messrs. Vern Barnhart and Dennis Dodson were with us for all of the field operations of this project and provided a valuable database of construction information. The expertise and efficiency of the coring crew under the direction of Bob Kelly, the FWD crew led by Kurt Bancroft, and the many others who participated in the field operation allowed for the effective collection of data. Mr. Chris Byrum extended a supporting hand giving timely suggestions and comments on this project.

The author also wishes to thank Dr. Starr Kohn of the Soil & Materials Engineers, Inc. (SME) for his valuable suggestions and for generously loaning out the DCP equipment used in this project. Mr. Jack Kzeski of Interstate Highway Construction, Inc. provided useful construction data and observations. For this the author is grateful.

Executive Summary

Two recycled Portland cement concrete (PCC) pavement projects constructed between 1984 and 1986 along I-94 were selected by the University of Michigan (U of M) research team to study the effects of truck traffic, concrete mix composition, pavement design, and foundation design on field performance. This study leads to recommendations to the sponsors, Michigan Concrete Paving Association and Michigan Promotion Fund, for improved field performance of recycled jointed reinforced concrete pavement (JRCP) in Michigan. The approach used, has consisted of an extensive field and laboratory investigation including field crack mapping, coring, Falling Weight Deflectometer (FWD) measurements of joints and cracks, petrographic testing of the concretes, fracture texture determination of concrete cracks, dynamic cone penetrometer tests of the base and subbase, and interviews with the contractor and Michigan Department of Transportation (MDOT) pavement personnel. The U of M laboratory study consisted of analysis of cores and soil samples from the field, and freeze-thaw (F-T) evaluation of recycled concrete coarse aggregates using Michigan Test Methods (MTM) testing procedures.

The two projects investigated were: Lawrence (CSN-80023-20993) West bound (WB), and Galesburg (CSN 39022-20736) in both WB and East bound (EB) directions for same station locations.

The Lawrence pavement project, constructed in 1984, consists of an 8.9 mile long, two lane, standard width, 10 inch thick, and recycled JRCP slab with 41 ft. joint spacing. This section has tied PCC shoulders with 14 ft. joint spacing. Four test sections, each approximately 400 ft. long, having 4 inch thick drainage courses of different materials ranging from open-graded drainage course (OGDC), to 5% cement-stabilized peastone base, to a dense-graded base course (DGBC). Three sections were recycled, and one section was an experimental peastone concrete of only 8 mm maximum aggregate size, as compared to 30 mm maximum aggregate size for the recycled mixes. PMS (Pavement Management System) distress data obtained by MDOT for the first time in 1993 by means of video tapes indicated that the performance of this project was, on the whole, marginal. Third point transverse cracks were pronounced, propagating into the design lane from the shoulder joints. This cracking pattern is referred to as sympathy cracking. A 10 inch dense-graded subbase was used throughout the Lawrence project.

The Galesburg project, located just east of Kalamazoo, is an 8.7 mile long recycled JRCP in both directions. The EB section was constructed in 1985, WB one year later. WB and EB are separated by a concrete barrier wall with WB built on fill, and EB built on a cut slope. The shoulder joints lined up with the 41 ft. slab joints. PMS distress data showed widely different performance in the two directions. WB had little visible distress, whereas EB was in very poor condition with a distress point of 50 or more over approximately a two mile section, which was chosen for further investigation. EB showed extensive transverse working cracks, shattered slabs, corner breaks, 1 inch to 1.25 inch joint faulting and

asphalt patches. For this project the pipe underdrain lies under the right wheel path of the driving lane in both directions confirmed by field coring. EB contained a 4 inch OGDC, 8G modified, whereas WB contained a modified 5G recycled OGDC. A 10 inch dense-graded subbase was used for the Galesburg project. The major question here was why EB and WB show such vastly different field performances for practically the same mix designs, drainage course designs, pavement designs, and contractor.

Pavement performance evaluation using the American Association of State Highway and Transportation Officials (AASHTO) serviceability criteria, assuming a terminal serviceability index of 2.5, indicates that several of the 6 pavement sections should have failed due to the estimated number of 18 kip. equivalent single axle loads (ESAL's). According to AASHTO, WB Galesburg should not have failed yet whereas EB is predicted to fail. The reasons are: (1) slightly higher truck traffic EB; (2) smaller average slab thickness EB (10.1 inch versus 10.4 in. WB); (3) substantially better concrete quality WB versus EB. The 9 year old pavement WB had an average compressive strength of 6,775 psi. versus 5,901 psi. EB (10 years of age) obtained from mid-panel cores. This resulted in a lower estimated 28 day flexural strength used in the AASHTO pavement design method; (4) a lower foundation support value was estimated for EB than WB based on FWD and DCP results. When combined, these four factors caused the predicted failure of the EB pavement section. The remaining service life of the WB lane is predicted to be only a few more years. It appears that the failure of these sections is due to factors other than the use of recycled concrete.

Falling Weight Deflectometer data were used to evaluate the load transfer efficiency (LTE) across joints, between slab and shoulder and across cracks. The LTE across joints (50% to 60%) and between pavement and shoulder (35% to 40%) were found to be similar for both Galesburg sections. However, the load transfer across cracks varied considerably. The LTE of one of two cracks detected in the 1000 ft section in WB was above 90%. The second crack was so small that it was difficult to locate, and was not tested for LTE. The average load transfer value of the EB was only about 30%, indicating the severity of the cracks. The low LTE across cracks EB is mainly due to the loss of support and lack of aggregate interlock associated with crack opening.

FWD data was used to backcalculate the effective soil modulus, and the DCP results were used to calculate the base and subbase combined layer moduli. This analysis indicated weaker soil moduli EB than WB. Based on FWD backcalculation, the average predicted subgrade modulus was about 32,000 psi., while EB had a value predicted at 19,000 psi. Similarly, based on the estimates made using the DCP results, the average base and subbase combined modulus was as high as 178,000 psi. WB, while that of EB was only about 149,000 psi. Thus EB has a higher propensity toward loss of support and larger slab deflections.

Microscopic analysis of the concrete in the Galesburg project indicates that the EB section has extremely inhomogeneous cement paste in the new concrete, with a water/cement ratio (WC) ranging from 0.35 to 0.60. In addition, large numbers of microcracks were found in the new and recycled cement paste of the EB section. WB has considerably more homogeneous cement paste (WC of 0.35 to 0.40) and fewer microcracks. These clues indicate a lower quality concrete EB than WB. Indications of the low quality of the recycled aggregate EB were given in interviews with the contractor, who explained that it was much easier to break up the old EB concrete than the WB concrete.

In the Lawrence project sections, the recycled sections over open graded and dense graded bases respectively, passed the serviceability criteria test, while a peastone concrete over OGDC and a recycled concrete over 5% cement-stabilized peastone base course failed the AASHTO serviceability test. It should be noted that the 5% cement-stabilized peastone did not form a rigid layer as would a typical stabilized base course. Instead, the peastone broke apart easily, and during sampling it was difficult to obtain any specimens where the peastone remained cemented together. While lower concrete strength and stiffness were the major factors for the predicted failure of the peastone concrete section, lower thickness and lower foundation layer moduli caused the predicted failure of the recycled concrete section over 5% cement stabilized peastone base. Even though the recycled section over open-graded base showed severe cracking in the field, the AASHTO serviceability criteria test shows some remaining service life. This was mainly because of the higher concrete strength and stiffness, and higher thickness of the slab. The discrepancy between the AASHTO design prediction and the field performance for this section may be due to a number of factors not taken into account by AASHTO (such as sympathy cracking, shrinkage cracking, etc.).

The LTE across joints, between slab and shoulder, and across cracks were determined for the Lawrence sections. The LTE across joints was low (50% to 60%) for two of the Lawrence sections, the peastone concrete over OGDC and the recycled section over 5% cement stabilized peastone base. The other two sections, the recycled sections over dense graded base and open graded base, had LTE across joints as high as 80%. The LTE between pavement and shoulder was found to be similar for all Lawrence sections (30% to 50%). The LTE across cracks varied between 35% and 60%, with the section over the dense graded base having the highest value.

These LTE values show that the dowel bars aid significantly in the transfer of loads across the joints. The aggregate interlock alone in many of the sections is not sufficient to provide enough load transfer due to truck traffic. This is evidenced by the poor LTE's across cracks. The visual condition of the joints is excellent for all sections, with virtually no visual damage to any of the joints.

Load transfer efficiency values across the transverse cracks, calculated from falling weight deflectometer data, gives an indication of the quality of aggregate interlock in the various pavements. Aggregate interlock is one of the major factors that helps long term performance by providing effective transfer of loading from one crack or joint surface to the other. In the Lawrence project, a peastone concrete shows poor load transfer. This can be traced back to the small (8mm max. size), rounded, and poorly graded peastone aggregate, which provides poor aggregate interlock. Several recycled concrete sections studied also show poor load transfer, though they contain aggregate of 30 mm. top size. The initial texture of the fractured face is a function of the coarse aggregate characteristics (gradation, number of crushed faces, particle density, etc.), the bond that develops between the aggregate and the paste prior to fracture, and the relative strengths of the paste and aggregate at time of fracture. The erosion of the fractured face depends mainly upon the degree of grain interlock or fracture texture that is initially between the crack faces (crack or joint opening), the magnitude of the loads that cross the crack or joint, and the level of foundation support. To improve aggregate interlock in recycled concretes, an experiment adding premium virgin aggregate of large size should be conducted. The optimal blend and virgin aggregate size should be investigated.

In the Lawrence project, a recycled concrete over dense graded base course has performed comparatively better than the recycled concretes over other base types. This conclusion was obtained from visual inspection showing fewer working cracks and FWD results indicating high load transfer across joints and cracks. The cause of this improved performance is not known. One factor that stands out is the uniformity of the foundation support in the dense graded section. The overall stiffness of the foundation in this section, though, is comparatively low (106,000 psi. for the combined base and subbase modulus, and 22,500 for the subgrade modulus). As per the FWD backcalculation, the average subgrade moduli for the Lawrence sections varied between 21,000 psi. and 33,000 psi. Similarly, based on the estimates made using the DCP results, the average base and subbase combined modulus varied between 100,000 psi. and 176,000 psi. It does not appear that the national study on recycled concrete being conducted by Dr. Snyder from the University of Minnesota is investigating this issue of the effects of dense graded bases. Thus, further study is recommended.

The quality of recycled aggregate to be used in recycled concrete is very important to the overall performance of the new concrete. Freeze-thaw testing shows that recycled aggregates may not meet current MTM requirements for freeze-thaw durability. Recycled aggregates have high water absorption capacities and are highly sensitive to degree of saturation in the vacuum saturation procedure. Recycled aggregates should be considered for use in pavements on a case by case basis.

1. Introduction

1.1 Objectives

The goal of this study is to determine the factors that lead to distress in recycled concrete pavements. The project is divided into two areas: field study and laboratory analysis. The field investigation focuses on two areas of concern: the quality of the pavement slab and the quality of the underlying foundation materials. Because many factors play a role in the performance of a pavement, numerous tests have been conducted to identify the critical contributing causes of deterioration in these pavement sections.

Studies of Concrete Slab Quality

-Crack Mapping and Photographic Record for visual analysis of pavement performance.

-Falling Weight Deflectometer (FWD) testing for evaluation of concrete stiffness and load transfer.

-Concrete Strength and Stiffness testing of cored specimens for concrete quality.

-Petrographic Analysis of cored concrete samples for composition and microcracking patterns.

-Surface texture measurement of fractured surfaces to determine crack deterioration and aggregate interlock load transfer potential.

Studies of Foundation Quality

-FWD testing for estimation of effective soil stiffness, and measurement of relative influence area and slab deflection.

-Dynamic Cone Penetrometer (DCP) testing to estimate the relative stiffnesses and compaction of base and subbase layers.

-Soil Gradation Analysis to estimate layer permeabilities, filter criterion, and for checking adherence to gradation specifications.

In addition to field investigations and analysis of construction records, traffic data has been analyzed in order to seek out clues to the varied performances of the different test sections.

Construction and Traffic Data Analysis

-Review of design life and serviceability calculations based on measured field and laboratory data.

-Analysis of mix designs.

-Investigations of construction and air temperature data.

Laboratory study has been performed on recycled concrete coarse aggregates to aid in understanding performance in the field.

<u>Laboratory Study of Recycled Aggregate</u>
-Aggregate properties determination including absorption, unit weight, and bulk specific gravity.
-Freeze-thaw durability testing under different degrees of saturation.

1.2 Scope of Work

Two recycled pavement projects in Michigan were chosen for investigation on the basis of their potential merit in identifying factors critical to recycled concrete pavement performance. Field and laboratory tests were conducted on pavement samples from both of these projects. Additionally, recycled aggregate was acquired for durability testing from a recent paving project.

The first project chosen is one where recycled concrete was placed on a series of different base course types. An experimental virgin aggregate peastone concrete was also placed in this project, allowing for comparison between virgin and recycled aggregate concretes under similar field conditions. A cracking pattern that has developed in all of these test sections allows for comparison of load transfer efficiency after cracking has occurred. This project will be referred to as the Lawrence project, and is described in section 2 of this report.

The second project chosen for study contains two test sections of recycled pavement on open-graded drainage courses (OGDC). While similar materials, mix designs and procedures were used in constructing these two pavement sections, their performances are radically different. Identifying likenesses and differences in these pavements leads to an understanding of their varied levels of deterioration. This project is identified as the Galesburg project, and is discussed in section 3 of this report.

Test Section Identifications

Section No.	Project Location	Type of PCC Aggregate	Type of Base Course
MI 1-1	Lawrence	Peastone	Open-graded
MI 1-2	Lawrence	Recycled	Open-graded
MI 1-3	Lawrence	Recycled	5% Cement-stabilized peastone
MI 1-4	Lawrence	Recycled	Dense-graded
MI 2-1	Galesburg (West Bound)	Recycled	Recycled, Open-graded
MI 2-2	Galesburg (East Bound)	Recycled	Open-graded

Table #1: Explanation of section references by project location, aggregate type, and base course type.

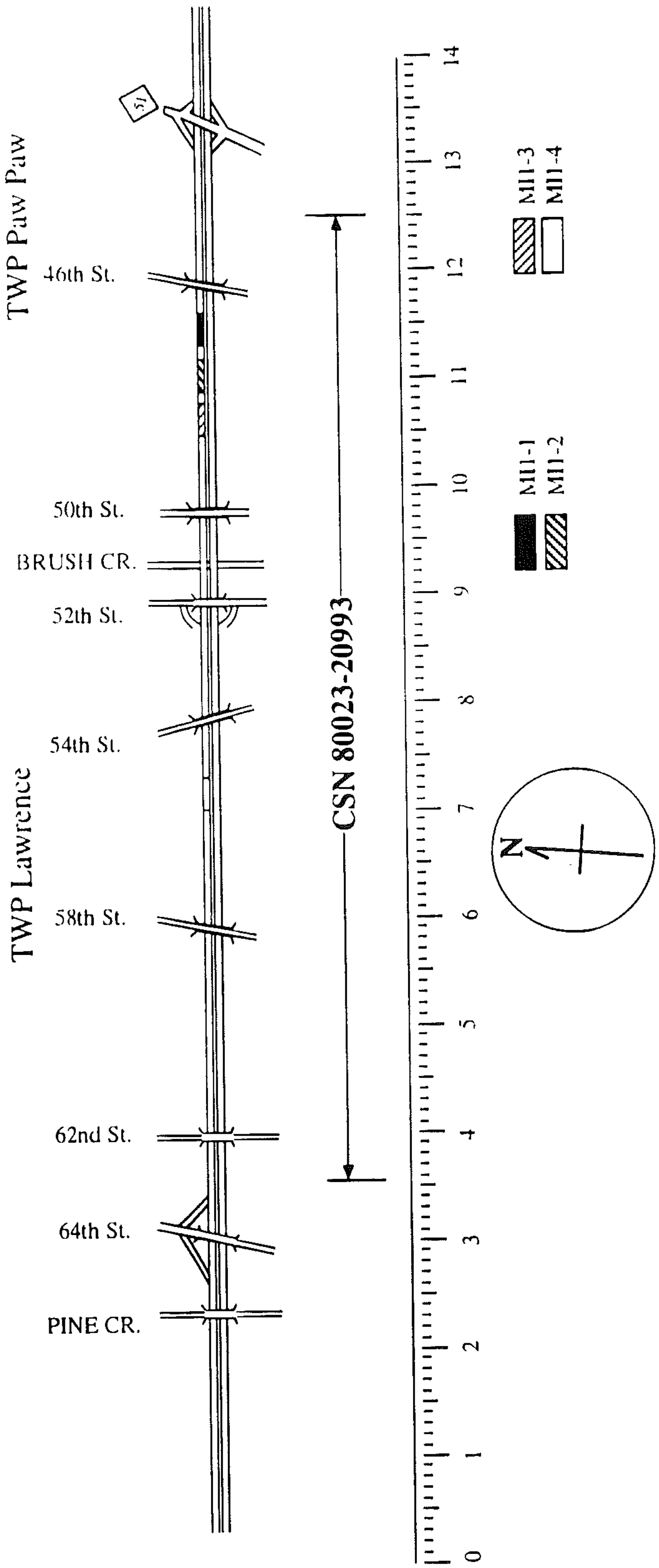

Figure 1: Control section log for Lawrence project showing test section locations.

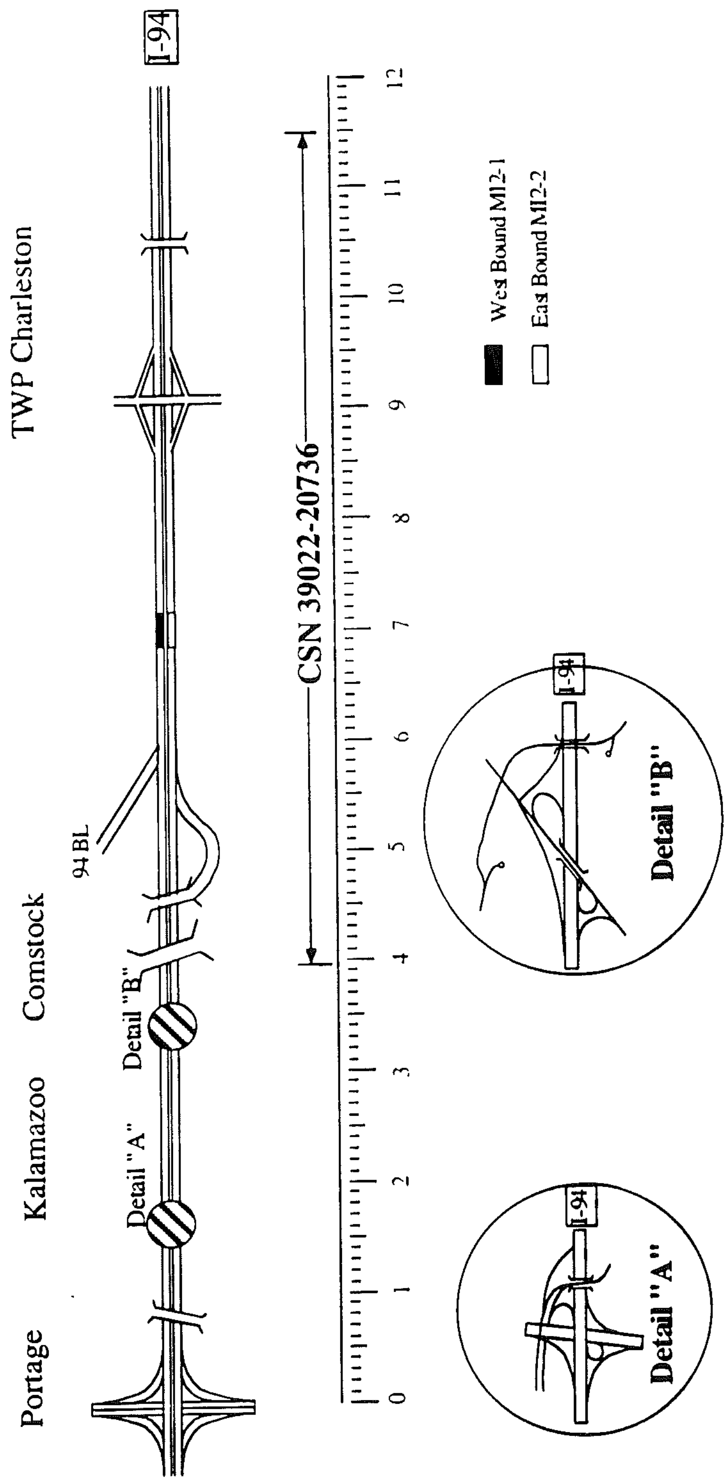

Figure 2: Control section log for Galesburg project showing test section locations.

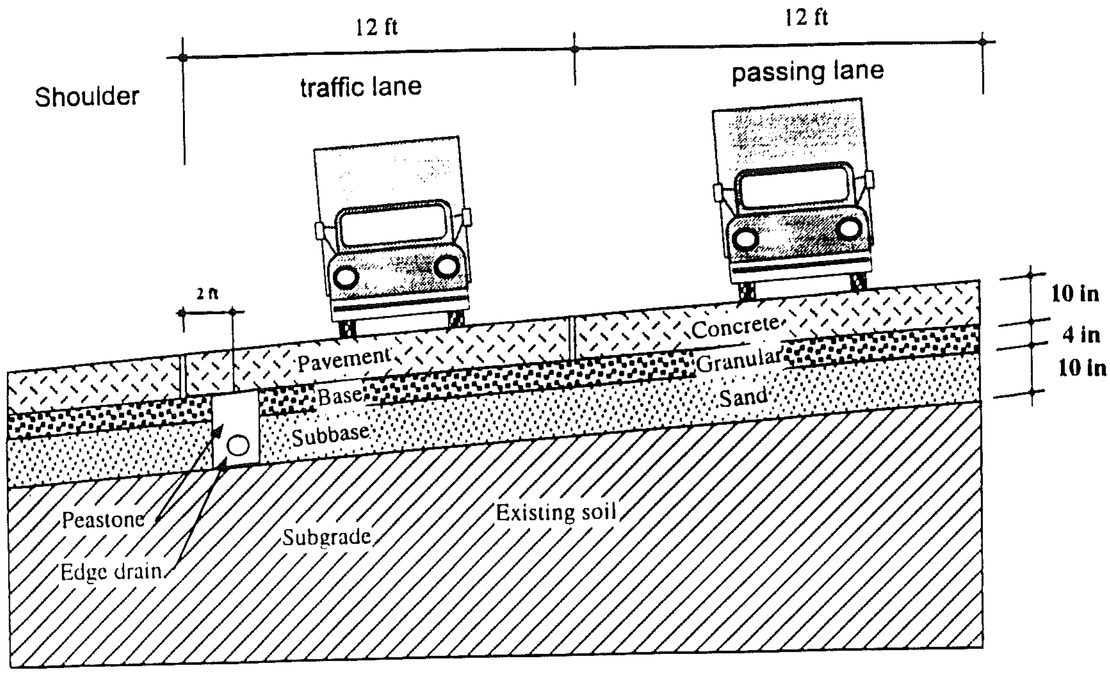

Figure 3: Typical view of pavement system cross-section for both the Lawrence and Galesburg projects.

The recycled aggregate tested for durability was acquired from a paving project on I-96 near Brighton, Michigan. This material was being used as a base course for new pavement construction on that site. Durability testing of aggregates is discussed in section 4 of this report.

2. The Lawrence Project

2.1 Project Description

The Lawrence project is located on West bound I-94 near Lawrence, Michigan and is referred to with the label MI1. This project, with Control Section Number (CSN) 80023-20993, was constructed by Eisenhouer Construction Company at a cost $7,993,808 in 1984. Within this 8.9-mile project, four separate pavement sections were examined. The first section (labeled MI1-1) is an experimental concrete with virgin peastone aggregate used over an open-graded drainage course (OGDC). The contractor used this peastone concrete to test whether it would be acceptable for large-scale use in a later project. This peastone concrete section is considered the control section in the context of this project because it is a non-recycled concrete. The tested section is approximately 400-ft. long, with a 41-ft. joint spacing, two 12-ft. wide lanes and a nominal 10-in. pavement thickness. The paved shoulder has a 14-ft. joint spacing. Only the design traffic lane has been examined in this study.

The other three pavement sections in the Lawrence project have the same joint spacings and dimensions as the control section. The second section (labeled MI1-2) is a recycled pavement over OGDC. The third section (labeled MI1-3) is a recycled pavement over a 5% cement-stabilized peastone base course. The final section (labeled MI1-4) is a recycled pavement over a dense-graded base course (DGBC). Detailed location information is found in Appendix 1 of this report.

Photo #1: Typical crack pattern in section MI1-1, peastone concrete on open-graded drainage course.

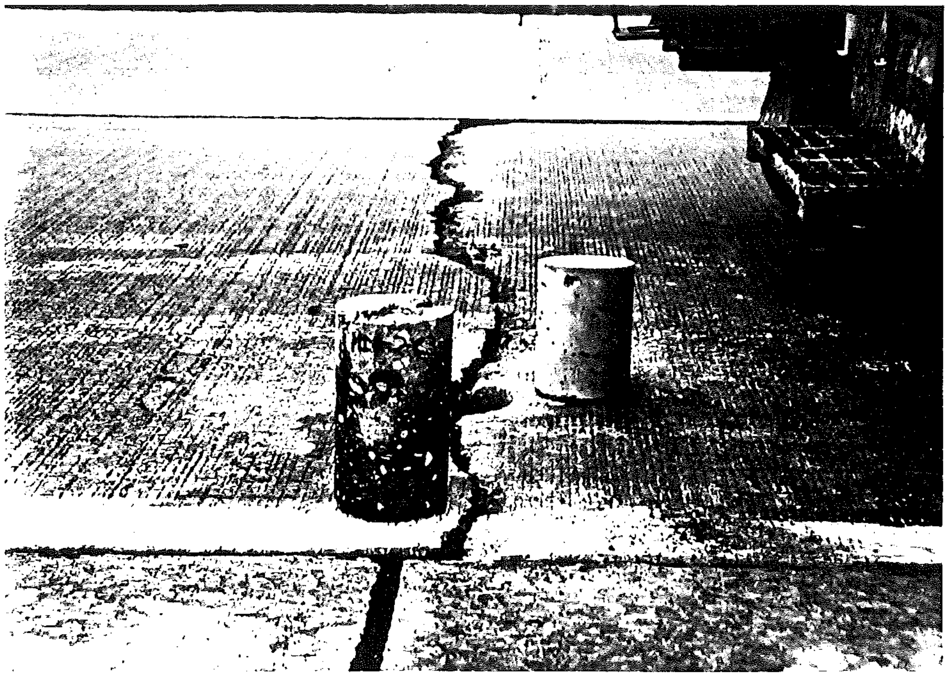

Photo #2: Typical crack in section MI1-2, recycled concrete on open-graded drainage course.

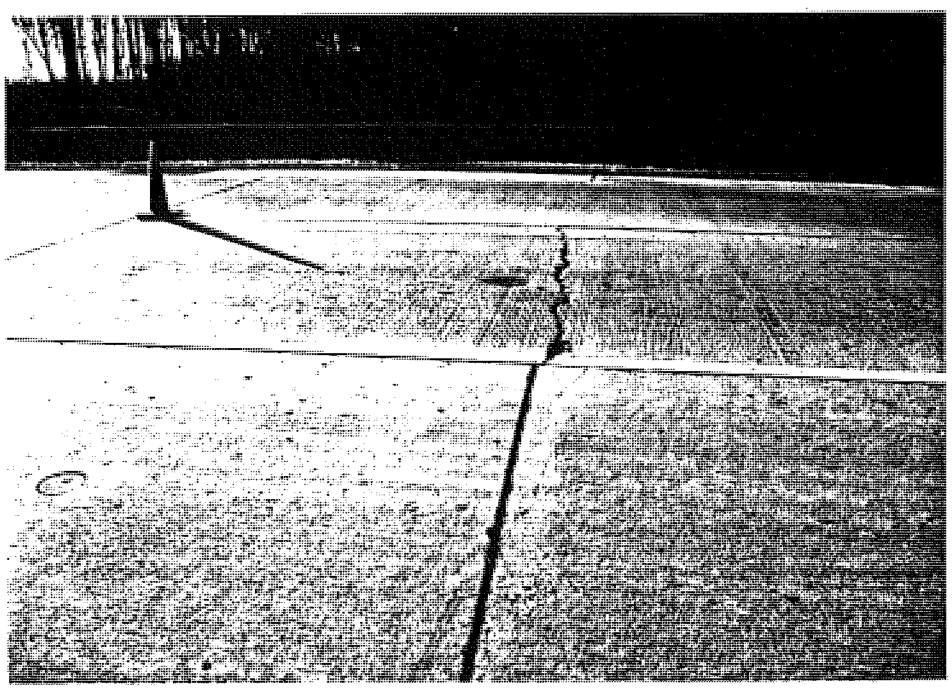

Photo #3: Typical crack pattern in section MI 1-3, recycled concrete on 5% cement-stabilized peastone base course.

Photo #4: Typical crack in section MI1-4, recycled concrete on dense-graded base course.

2.2 Project Findings

2.2.1 Overview of Findings

The Lawrence project provides an opportunity to compare recycled and virgin concretes that have been placed over various types of base course materials. Because the four test sections of the Lawrence project all exhibit similar cracking patterns, the process of crack deterioration is of interest. While it is known that the transverse cracks propagate from shoulder joints, the crack severities differ for the four test sections. This behavior lends itself to a study of load transfer efficiency across cracks and transverse joints. Investigations into the concrete materials, foundation materials, traffic and environmental factors during and after placement lead to additional clues to the varied performances of these pavements.

Control Peastone Concrete

The peastone concrete exhibits significant cracking and crack deterioration, including some faulting and spalling. It has both lower strength and stiffness than the recycled concretes and was placed on a warm sunny day with problems occurring during placement. It is possible that early cracking occurred, which deteriorated at a rapid rate. The cracking was likely initiated and/or propagated by the 1/3-point shoulder joint design. The free movement of the jointed shoulder tied to the slab likely caused the opening of the cracks and the rupture of the temperature steel. It is possible that the deterioration is related to poor aggregate interlock. The straightness of cracking through the thickness of the pavement in joints and cracked sections also contributes to early deterioration. This is evidenced by poor load transfer across the cracks and transverse joints.

A performance evaluation for serviceability based on the AASHTO[1] design procedure showed that the estimated actual ESAL's for the 11 years of service life exceed the allowable ESAL's in this section.

Alkali Silica Reactivity (ASR) is detected in microanalysis of the pavement, though it is likely not a major factor in the general deterioration of the slab. Foundation stiffness appears adequate for this pavement section.

Recycled Pavements

The three recycled concrete pavement sections delineate the sensitivity of recycled pavements to field conditions. While each of these pavement sections suffers from sympathy cracks which propagate from third point shoulder joints, the rate of deterioration for each section is of interest. The load transfer efficiency across the cracks for these sections indicates that aggregate interlock is not sufficient in these recycled pavements to adequately prevent crack movement and deterioration. It should be noted that testing under warmer temperature conditions would be expected to improve load transfer somewhat. In addition, uniformity of foundation support appears critical to good performance in recycled concretes. See Figure #4 for a summary of load transfer values, and Appendix #4 for a detailed discussion of the load transfer data.

The recycled pavement placed over 5% cement-stabilized peastone base (MI1-3) has experienced severe crack deterioration. This is likely related to the high slab deflection in the test section. The high deflection in the slab may be attributable to the low stiffness of the subgrade material. Low load transfer across transverse joints and cracks and high load transfer to the shoulder are more characteristic of this pavement section relative to the other sections studied. Large deflections in the slab combined with a high degree of influence from shoulder joints may lead to the severe cracking evident in this test section. ASR has been detected in petrographic analysis of this pavement section, though it is not considered a leading cause of distress.

The two remaining test sections: recycled concrete over OGDC and DGBC, sections MI1-2 and MI1-4 respectively, show performance that is likely influenced by different factors than the other test sections. Both of these pavement sections have high load transfer across joints and low load transfer to the shoulder. Both sections show similar slab deflections, and similar deflection basins. Both exhibit relatively high concrete strengths and stiffnesses and low foundation stiffnesses.

In the foundation layers, it appears that the uniformity of the support is of greater importance than the stiffness of the support. In section MI1-4 (over DGBC), the foundation support is very uniform throughout. This pavement performs better, even though the overall foundation stiffness is not as high. Better performance for this section is characterized by lower severity cracking than is seen in the other sections. Faulting and spalling, though present, are not normal for this test section.

A performance evaluation for serviceability based on the AASHTO pavement design procedure showed that the estimated actual ESAL's for the 11 years of service life exceed the allowable ESAL's in sections MI1-1 and MI1-3.

Another significant difference in performance between these two pavements can be traced back to the original placement of the slabs. Because MI1-2 was placed on a clear warm day, and difficulties with quick setting of the concrete were noted by the inspector, it is very possible that early cracking (cracking before the joints were sawed) occurred in this concrete. Inhomogeneity in the cement paste in the upper portion of the concrete, as well as shrinkage cracks found in the field, support this hypothesis. The other section, MI1-4, was placed on a cloud-covered, rainy day, and no difficulties were reported during placement. This pavement, in turn, has performed considerably better.

2.2.2 Performance Evaluation

A performance evaluation based on the AASHTO pavement design procedure indicates that allowable equivalent single axle loads (ESAL's) are lower than the estimated actual ESAL's in sections MI1-1 and MI1-3. This shows that these sections have already reached their threshold serviceability values after 11 years of pavement service. In the case of sections MI1-2 and MI1-4, some service life remains.

AASHTO Serviceability Check

(Lawrence Project)

Section	Age in years (Until 1995)	Load repetitions (ESAL's)		Remarks
		Total allowable	Estimated Actual* to date	
MI1-1	11	11,176,010	13,658,149	Fail
MI1-2	11	20,168,810	13,658,149	Pass
MI1-3	11	11,279,980	13,658,149	Fail
MI1-4	11	15,698,400	13,658,149	Pass

* Based on data obtained from MDOT

Table #2: Summary of traffic analysis for the Lawrence project.

Section MI1-1 fails the AASHTO procedure because of comparatively low concrete quality and low load transfer across joints. Section MI1-2 did not fail in the analysis even though field performance is poor. One of the reasons for this may be that the loss of support assumed in the analysis may not be representative of the actual field value. The concrete properties such as the strength and modulus of the section are comparatively better than those seen in section MI1-1. A detailed description of the input parameters used for this analysis is located in Appendix #11.

2.2.3 Concrete Slab Quality

Crack Mapping and Photographic Record

A crack mapping study indicates a pattern of cracks in the slabs of all four sections at the slab 1/3-points. These cracks correspond to 1/3-point transverse joints in the adjoining shoulder. The test section that stands out in the Lawrence Project for its notably better performance than the other sections is MI1-4, recycled pavement on dense-graded base. In the first three sections (MI1-1, MI1-2, MI1-3), this sympathy cracking is severe and considerable crack spalling has occurred. The cracks can be identified as working cracks, and some evidence of pumping is found. MI1-4 exhibits the same cracking patterns, but the severity of the cracks is considerably lower. Few working cracks are present in this section.

Many sympathy cracks in all four sections run through both traffic lanes, but spalling and significant crack deterioration are mostly observed in the design lane. The sympathy cracks generally run very straight across the pavement, often following the tining grooves. In all four sections, the joints are intact and appear in good condition. No longitudinal cracking has occurred in the pavements, and few cracks other than the sympathy cracks are found. Appendix 2 contains the crack mapping reports for these pavement sections.

Photographs of cracks found in each of the Lawrence project test sections verify the results of the crack mapping study. Photos #1-4 depict cracks that are typical to each pavement section. Additional photos are found in Appendix 2.

Load Transfer and Crack Texture

Falling Weight Deflectometer analysis of the four Lawrence test sections gives indications of load transfer across transverse joints and to the shoulder.

Load transfer efficiency across the transverse sympathy cracks gives an indication of aggregate interlock. While many factors may affect formation and movement of cracks, aggregate interlock is the primary mechanism for transfer of load across the crack faces. Once cracks have formed, in this case through sympathy cracking, the aggregate interlock provides protection from movement that leads to rapid deterioration due to spalling, pumping and the like. Slab length is also critical in determining the effectiveness of aggregate interlock. A long slab will experience greater movement, allowing cracks to open more, and aggregate interlock to be less effective.

Load transfer efficiencies are highly variable among the various cracks of all of the pavement sections. This is due to great differences in performance from crack to crack. When taken as an average for each section, though, the general trend in crack performance is seen. While no section has high load transfer, section MI1-4 performs slightly better than the other sections. This is indicative of better concrete quality and/or better foundation quality.

The severity of many of the sympathy cracks in the recycled and peastone concretes alike and the low load transfer efficiencies for these cracks indicate the lack of adequate aggregate interlock. It is likely that the small nominal aggregate size plays a role for the peastone, and lack of premium grade aggregate is a factor for the recycled aggregate. Premium aggregate is important to preserve the texture of the shearing faces of cracks. Weaker aggregates are more likely to break down, causing the cracks to become smooth.

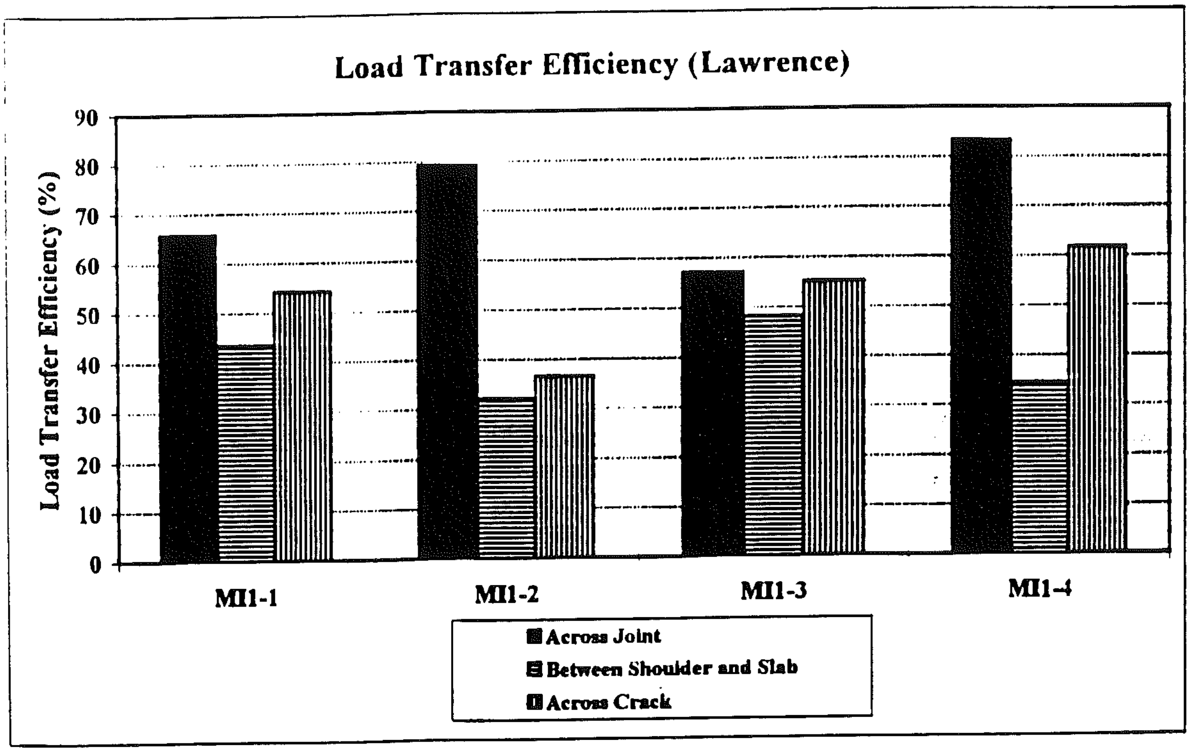

Figure #4: FWD analysis: load transfer for Lawrence project

Load transfer at the transverse joints is greatest in the recycled pavement over dense graded base (MI1-4). High load transfer across transverse joints is important to avoid load concentrations and excessive deflection of the slab edges. The good load transfer may be brought about by a uniform and stable foundation support. It also indicates proper functioning of the doweled joints in providing efficient transfer of vehicle loads.

Load transfer to the shoulder is low in all sections relative to load transfer across transverse joints. This is particularly the case for MI1-2 and MI1-4, recycled concrete on OGDC and DGBC respectively. Due to the detrimental 1/3-point transverse shoulder joint design, poor load transfer to the shoulder may actually be beneficial to the slab. Poor load transfer reduces the influence of the 1/3-point shoulder joints on the pavement slab, reducing the severity of sympathy cracking. FWD analysis results are presented in Appendix 4.

Load transfer efficiency across the joints is also evidenced by analysis of cores from joints of the four pavement sections. Micro-structure analysis was performed on a core from each section. The cored joint from Section MI1-4 fares the best, with a visual macro-texture rating of "very good". MI1-2 is rated "good", while MI1-3 and MI1-1 are rated "fair" and "poor" respectively. The macro-texture rating refers to the texture provided by the coarse aggregate. The peastone concrete has a poor rating because the small rounded aggregate provides little texture or aggregate interlock in the crack beneath the joint. "Good" and "very good" ratings indicate good aggregate interlock and tight joints where little damage has occurred from joint movement.

A gross texture rating has also been assigned to each of the joint cores, indicating the straightness of the crack through the core. The greater the incline of the crack, the higher the rating. All three recycled sections receive "fair" ratings while the peastone concrete rates "poor".

Surface texture analysis has also been performed on cored specimens from the third point sympathy cracks of the pavement sections. In general, the cracks tend to have a lower macro-texture rating than the joints of their respective pavement sections. This is indicative of greater movement in the cracks than in the joints. Cracks are dependent on aggregate interlock to prevent movement, while joints are protected from shearing by dowel bars.

Core Identification	**Visual Rating**	
	Macro	**Gross**
Joints:		
MI 1-1-J2	poor	poor
MI 1-2-J2	good	fair
MI 1-3-J2	fair	fair
MI 1-4-J2	very good	fair
Cracks:		
MI 1-1-C2	poor	fair
MI 1-2-C2	poor	good-fair
MI 1-3-C2	poor-fair	poor
MI 1-4-C2	poor	poor

Table 3: Crack texture for Lawrence project

The macro-texture ratings for all four crack specimens are "poor" or "poor to fair". Gross texture ratings indicate that the specimen from section MI1-2 (recycled over OGDC) performs the best. The low rating of the MI1-4 specimen (recycled over DGBC) is due to the fact that the specimen tested comes from one of the few severe cracks within the test section. This result is likely not representative for the test section where only few such cracks are found. Complete crack analysis data is located in Appendix 9.

The cracks and joints for all sections show evidence of fines within the cracks. These fines represent leacheates (white deposits), corrosion products (gray/brown deposits), and soil migration (brown deposits). Exposed dowel bars and temperature steel have corroded severely. Abrasions indicative of wear are not pronounced in the joints

Concrete Material Properties

Concrete strengths in all of the recycled sections are well above the 3500 psi. design strength, with strengths consistently above 6000 psi., when tested in accordance with ASTM C42[2]. Elastic moduli of these concretes range from $3.5x10^6$ psi. to $4.2x10^6$ psi. as determined in accordance with ASTM C469[3]. A high modulus value indicates a stiff concrete, where low deflection can be expected. The peastone concrete exhibits both lower strength and lower stiffness than the recycled concretes. This result can likely be attributed to the poor gradation and small grain size of the peastone aggregate. In addition, the rounded particle shape contributes to the low strength and stiffness. The weakness in this concrete is likely in the adhesion zones between the aggregate and paste. The large number of microcracks in this region indicate that the aggregate paste bond is deficient. See Appendix 3 for strength and stiffness data.

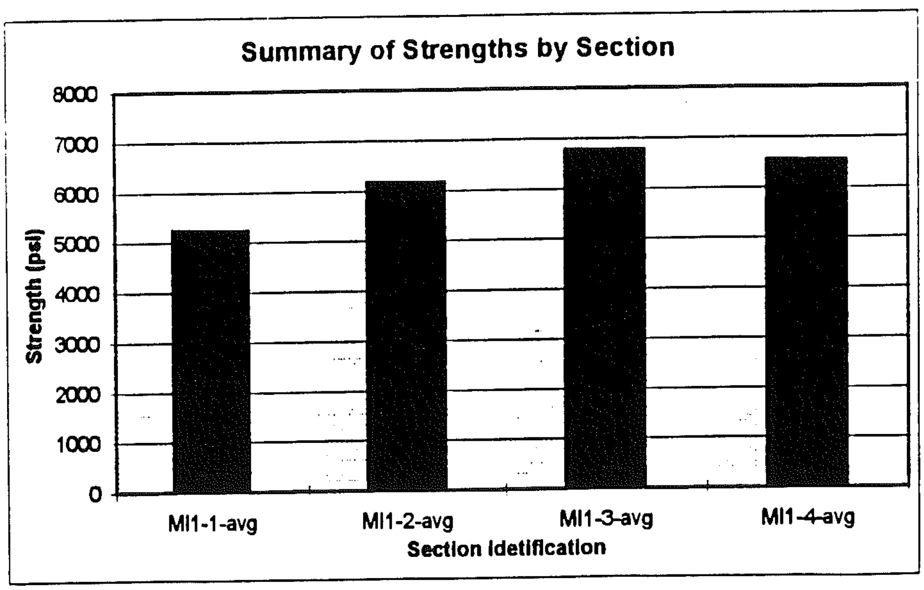

Figure 5: Concrete compressive strength for Lawrence project.

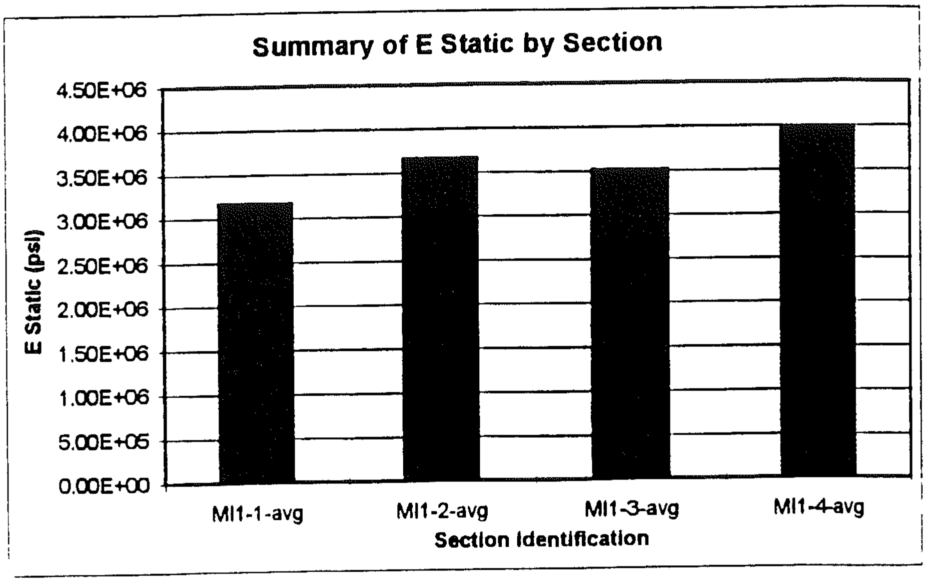

Figure 6: Concrete stiffness for Lawrence project

Petrographic Analysis

Petrographic analysis performed on mid-slab cores from all four pavement sections identifies microcracking patterns, concrete composition, and aggregate reactivity.

In the recycled concretes, considerably more microcracking is found in the new concrete than in the recycled aggregate. Though no aggregate durability information is available from the time of recycling of the original pavement, this crack pattern is one indicator that the recycled aggregate is probably of good durability.

Microcracking in Lawrence Project Concrete Samples

Core	Thin Section	Microcracks/mm²			
		New Concrete		Recycled Conc. Agg.	
		Cement Paste	Adhesion Zone	Cement Paste	Adhesion Zone
MI1-1-M2	Surface Middle Bottom	0.14	0.57*	--	--
MI1-1-M4	Surface	0.09	0.12	--	--
MI1-2-M2	Surface Middle Bottom	0.52*	0.34	0.38	0.21
MI1-2-M4	Surface	0.95*	0.22	0.14	0.07
MI1-3-M2	Surface Middle Bottom	0.60*	0.26	0.46	0.21
MI1-3-M4	Surface	0.71*	0.31	0.33	0.14
MI1-4-M2	Surface Middle Bottom	0.53*	0.22	0.16	0.02
MI1-4-M4	Surface	0.41	0.21	0.31	0.14

Cracks less than 0.01 mm are considered in this quantitative determination in 10 fields of sight (5.8 mm^2) on each thin section.

(*) High amount of microcracks.

Table 4: Microcracks for Lawrence project

Microcracking is more prevalent in the cement paste than at aggregate-paste adhesion zones in the recycled concretes studied. Good adhesion between the recycled aggregates and new cement paste is common to all three recycled pavement sections. In many cases it is difficult to distinguish between the old and new concrete. This is likely due to the similarity in the constituencies of the old and new concretes. Recycled coarse aggregate typically contains 20-30% by volume of attached cement paste[4], which adheres well to new cement paste.

Of the three recycled pavements, there was noticeable adhesion zone cracking in the upper portions of two of the pavement sections (MI1-2 and MI1-3). This is an indication of early cracking possibly caused by drying shrinkage. In section MI1-4, good adhesion is noted in the top portion of the concrete.

The large number of microcracks in the new cement paste of the recycled concretes indicates problems in the early stages of curing. The upper portions of the specimens have inhomogeneous cement paste, with highly variable water/cement ratios. Bleeding and drying shrinkage could both be of concern.

In the peastone concrete, the adhesion zones show more significant cracking than the cement paste. This is indicative of a poorer bond between the smooth rounded aggregate and the cement paste than is seen in the recycled concretes. The small size, poor gradation, and rounded shape of the peastone aggregate gives a higher adhesion zone volume per volume of concrete than is found in a typical paving concrete. This mismatch is also likely to be the cause of the reduced overall strength and stiffness of the peastone concrete.

Photo #5: Microphoto of a sample from section MI1-3, taken in transparent light. Scale: 1 cm = 0.26 mm. ASR gel is present in the recycled concrete. No cracking is observed that can be attributed to ASR.

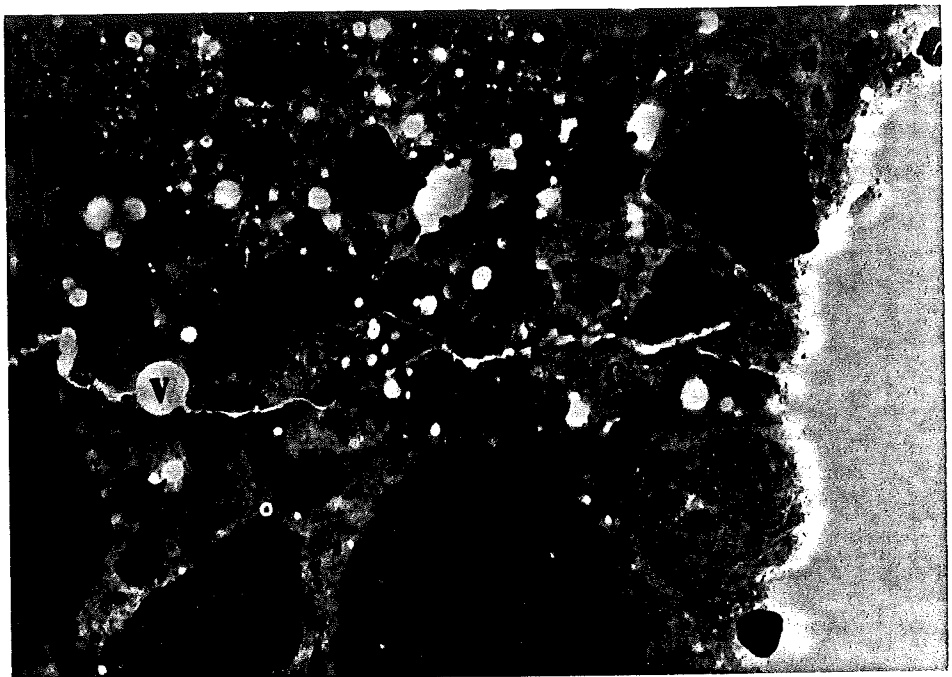

Photo #6: Microphoto of sample from section MI1-3, taken in fluorescent light. Scale: 1 cm = .26 mm. Fine crack penetrating the cement paste perpendicular to the surface, see arrows. No aggregates are penetrated, indicating early cracking. Aggregates are marked "A", cement paste "C" and air "V".

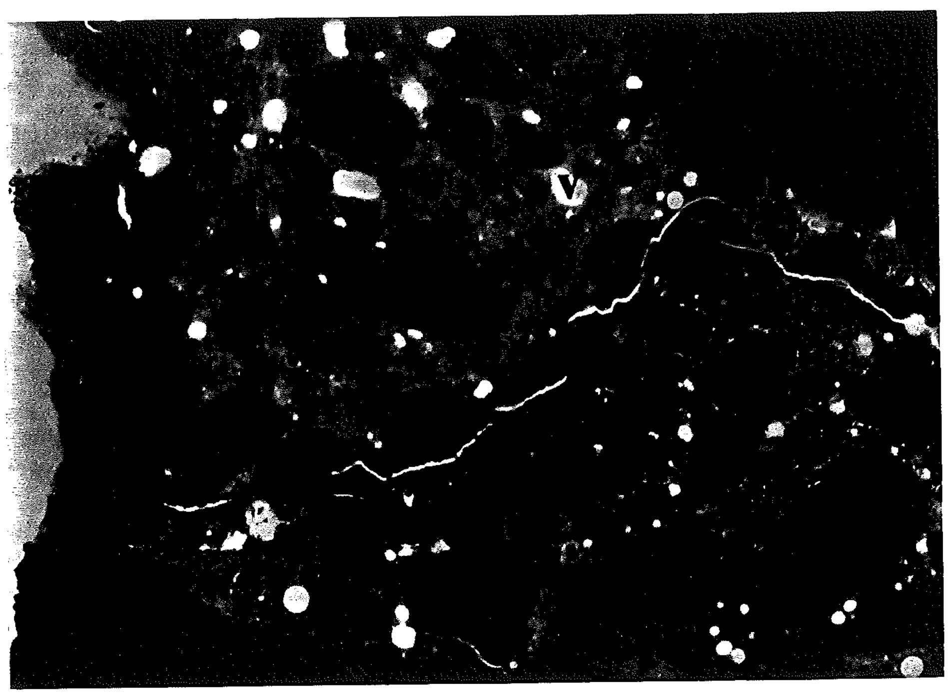

Photo #7: Microphoto of sample from section MI1-4, taken in fluorescent light. Scale: 1 cm = 0.26 mm. Fine crack is penetrating surface area and running perpendicular into the concrete. The crack penetrates aggregates, see arrows, which indicates formation in later state. aggregates are marked "A", cement paste 'C" and air voids "V".

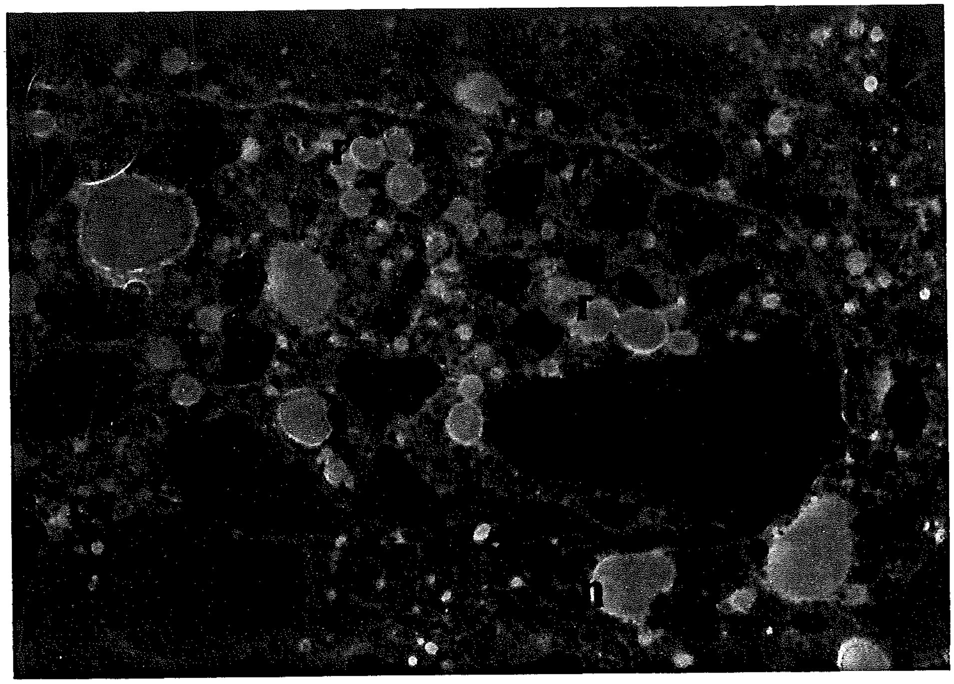

Photo #8: Microphoto of sample from section MI1-2 taken in fluorescent light. Scale: 1 cm = 0.26 mm. The cement paste contains microcracks along adhesion zone to recycled concrete, see arrows. Recycled concrete is marked "R" and new concrete "N".

Alkali-silica reactivity (ASR) can be identified in several cores, and some expansive gel is found interspersed throughout the cores. Some ettringite crystals have formed in air voids and ASR is evident around some aggregates. While only low amounts of ASR have been detected, the presence of porous chert, sandstone and opal indicate a propensity toward ASR, especially in the presence of de-icing salts and a humid environment. Although ASR is present, the cracking patterns for the slabs do not appear to be typical of ASR type distress, and ASR is not considered a major factor in the deterioration of the slabs.

Photos #5-8 give evidence of the micro-cracking and ASR in specimens from the Lawrence project. Additional micro-images are depicted in Appendix 6.

2.2.4 Construction Records and Mix Design

Construction records indicate many problems, including difficulty with the mix setting up very fast in section MI1-2 (recycled over OGDC). The peastone concrete (MI1-1) also developed problems during placement. The inspector's report indicates a weak looking mix with bleeding encountered during normal vibration. The first two loads had to be discarded and an overrun was experienced due to deep wet cores. In addition, weather conditions were noted to be warm and sunny for the placement of MI1-1, MI1-2, and MI1-3, while MI1-4 was placed in cloudy and rainy weather. The likelihood of problems during the early stages of curing is amplified by hot summer weather. Construction data is located in Appendix 7.

AIR TEMPERATURE ON THE DAY OF CONCRETE PLACEMENT
(Data collected from weather stations located close to the project section)

Section	Date	Temperature (Degrees F)		Location
		Low	High	
MI1-1	8/15/84	58	85	Kalamazoo
		51	86	Benton Harbor
MI1-2	8/14/84	60	86	Kalamazoo
		51	78	Benton Harbor
MI1-3	8/9/84	68	90	Kalamazoo
		63	92	Benton Harbor
MI1-4	9/4/84	49	68	Kalamazoo
		43	71	Benton Harbor

Temperature data is compiled from "Climatological Data: Michigan"
U.S. Department of Commerce[5]

Table 5: Temperatures on the day of placement. Data obtained from nearby weather stations.

The mix design records show that the fine aggregate was composed of 50% of recycled fines for sections MI1-2 and MI1-3 while only 30% was used for MI1-4. It has been reported that a higher percentage of recycled fines may cause higher abrasion and formation of leacheates in concrete. MI1-4, where lower amounts of recycled fines were used, showed comparatively less crack deterioration and improved performance.

2.2.5 Quality of Foundation Materials

Investigations into the foundation layers are vital to gain information about stability of the foundation and drainage under the pavement slab. Base and subbase courses are used to protect the pavement system from environmental factors effecting the existing roadbed. Among these factors are frost heave, pumping, shrinkage and swelling[6].

Falling weight deflectometer testing gives an indication of effective soil stiffness of the foundation, relative load influence area, and slab deflection. Predicted effective soil stiffness is a combined stiffness of the base, subbase and subgrade layers. The subgrade has the most influence on the value because of it's semi-infinite thickness, compared to very limited base and subbase thicknesses. Dynamic Cone Penetration testing gives a qualitative value of base and subbase stiffnesses. Load influence area is a measure of the width of the deflection bowl. A high influence area represents a well-distributed load.

The three recycled pavement sections all show relatively high deflections and concrete moduli when compared to the peastone concrete, yielding low back-calculated effective soil stiffnesses for these sections. The peastone concrete, which has low deflection and low concrete stiffness shows high back-calculated soil stiffness.

DCP blowcounts indicate little difference between open graded and dense-graded base stiffnesses. The subbase layers do show lower blow counts under the dense-graded base, though uniformity of support is very good beneath this section.

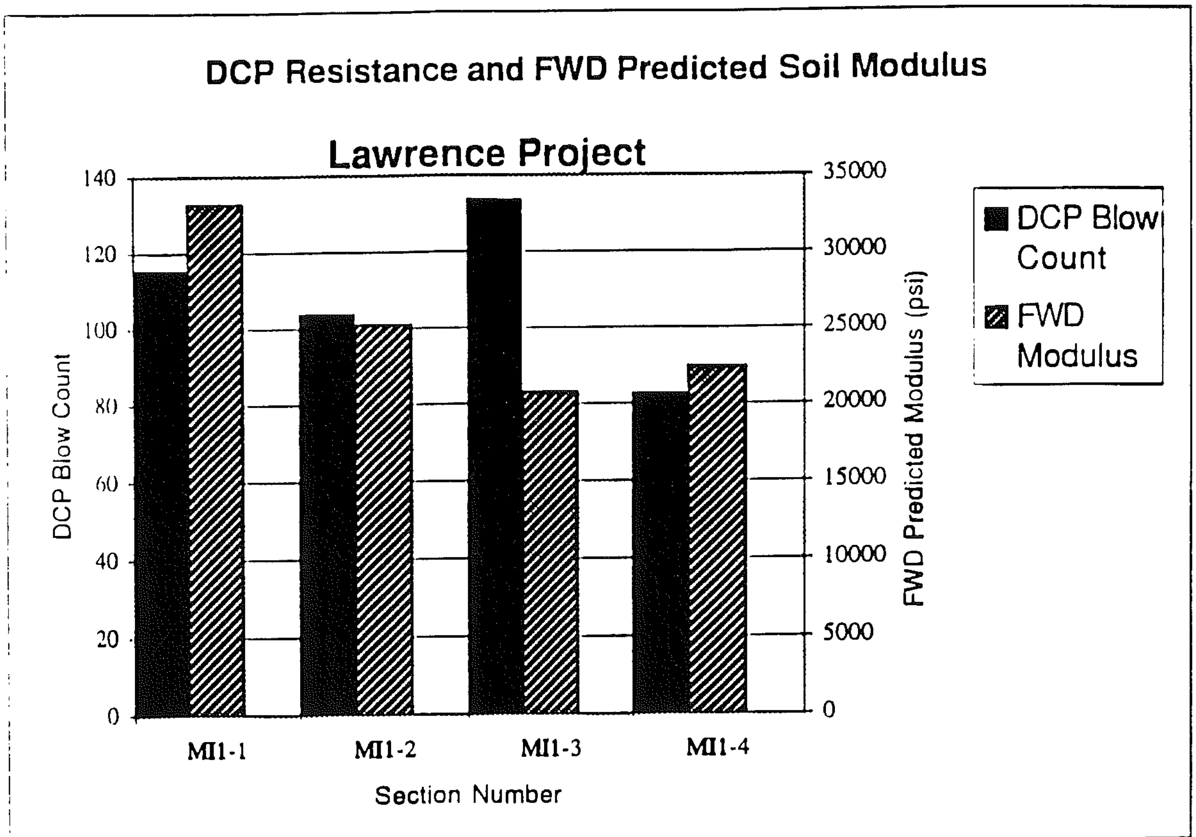

Figure 7: Foundation support stiffness; FWD-DCP study for the Lawrence project

When DCP and FWD results are plotted together, general conclusions about the foundation layers can be drawn. The peastone concrete section (MI1-1) shows relatively high stiffnesses for all foundation layers. The recycled over stabilized peastone section (MI1-3) shows relatively stiff base and subbase layers, and a very weak subgrade. FWD results show large deflection and large influence area in this section, indicating a low subgrade stiffness. This weak subgrade layer may be a leading cause of pavement distress. The remaining sections, MI1-2 and MI1-4 both show relatively low stiffnesses in all layers. Section MI1-4, though, has a very uniform foundation support, reducing stress concentrations in the slab. This uniformity in the support appears to make up for the low stiffness. See appendices 4 and 8 for complete FWD and DCP data.

It should be noted that the 5% cement-stabilized peastone base did not have the consistency of a typical stabilized base course. The 5% cement that was added to the peastone did not hold the peastone rigidly in place, but rather crumbled easily. It was difficult to get cohesive sample of the stabilized peastone out of the ground without it breaking up completely. Thus, this base course performed less like a lean concrete and more like an open-graded base course.

The lack of evidence of pumping in any of the pavement sections indicates that there is adequate filtration provided by the various foundation layers. Analysis of filter criteria indicates some migration of materials, particularly fines between the subbase and subgrade layers.

Gradation analysis indicates that frost heave and/or shrinkage and swelling effects are not likely to be a problem in the Lawrence project sections. This is due to a relatively low percentage of fines in the subgrade materials.

Drainage of water from pavements is very critical to their performance. A poorly drained base course combined with increased traffic may lead to premature failure. In the test sections, rapid drainage of water is provided by OGDC layers, while the DGBC acts as a waterproofing layer for the underlying materials. Clogged drains have been observed in some locations. Poor drainage may be one of the contributing factors for the early distress in these test sections. If indeed drainage is a problem, then as the slab cracks, the adverse effect due to poor drainage also gets more severe.

Gradation data is located in Appendix 5 of this report.

3. Galesburg Project

3.1 Project Description

The second project is located on I-94 East and West bound near Galesburg, Michigan and will be referred to as the Galesburg Project (labeled MI2). This project, with CSN 39022-20736, was constructed by Eisenhouer Construction Company at a cost of $12,896,579. Two 1000-ft. test sections were chosen from this 8.7-mile paving project. One section is West bound (MI2-1) and one is East bound (MI2-2) at the same station locations. The East bound section was constructed in 1985, while West bound was built in 1986. The chosen sections are representative of the pavement in each direction. Both sections contain recycled pavement over an open-graded drainage course. Each of the tested sections has 41-ft. joint spacing, two 12-ft. wide lanes and a 10-inch thick slab. The paved shoulder has joints spaced at 41 ft., coincident with pavement joints. Only the design traffic lane was examined for each test section.

The highway in the area where these sections are located is in a cut-fill region. The West bound lane is built on fill, while the East bound lane is cut into a slope. The directions are split by a concrete barrier median. The cut-fill slope is not severe, and there is little slope longitudinally. Information regarding the precise location of this project is found in Appendix 1.

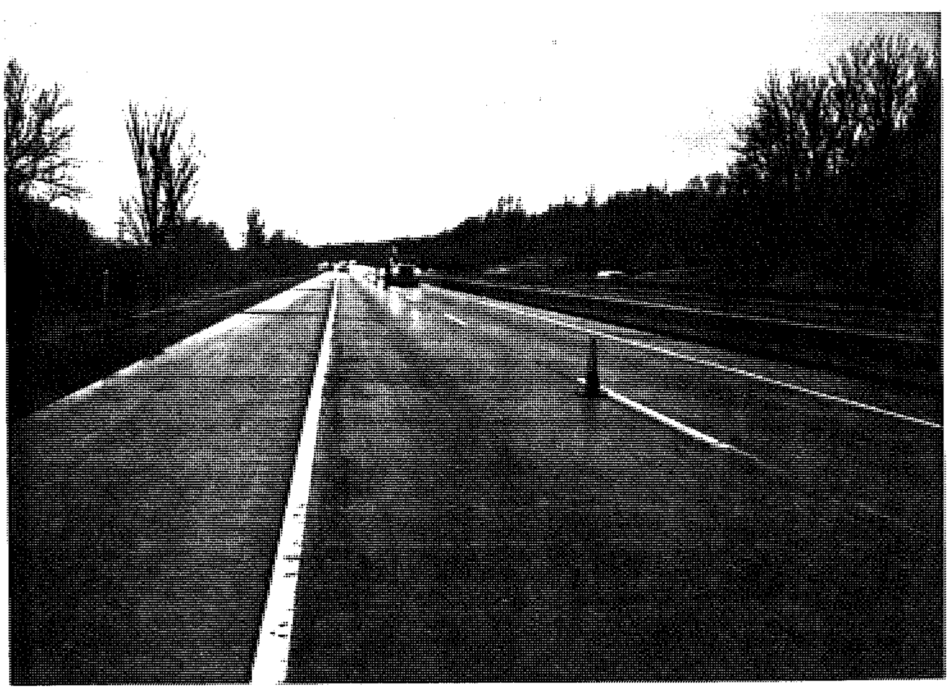

Photo #9: Overview of section MI2-1 (West bound Galesburg).

Photo #10: View of section MI2-2 (East bound Galesburg) showing transverse and longitudinal cracking. Note that asphalt patching has been placed to fill in a lane shoulder dropoff of roughly one inch.

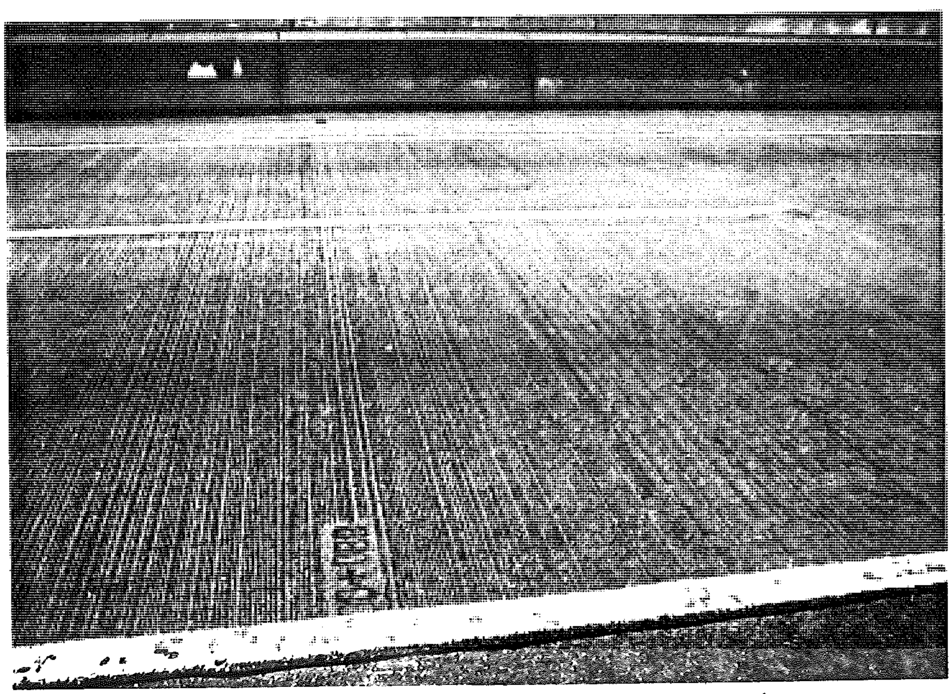

Photo #11: Typical view of the pavement in the West bound test section.

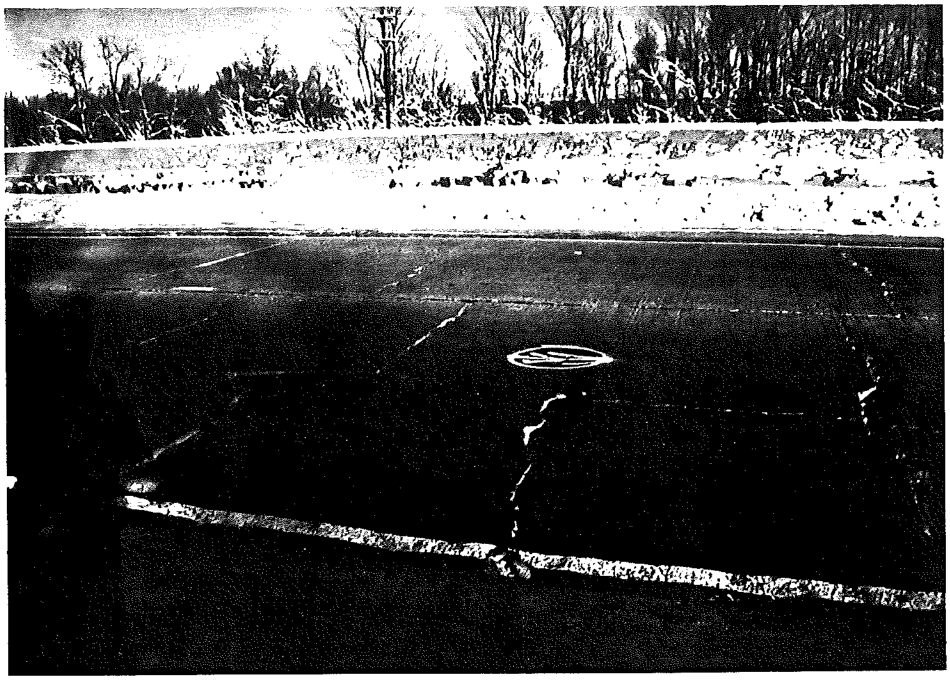

Photo #12: Pavement in the East bound test section (MI2-2). Notice the shattered slab and the spalling at the cracks.

3.2 Project Findings

3.2.1 Overview of Findings

The Galesburg project exhibits very peculiar performance: West bound (MI2-1) is in excellent condition, and East bound (MI2-2) is nearing the need for total replacement after roughly the same life span; East bound is 1 year older.

There are several factors that may contribute to these dichotomous behaviors. The quality of the recycled material appears to affect both the concrete material properties and the slab performance. Material of poorer quality was recycled East bound than that recycled West bound. This is evidenced by low concrete strength and stiffness on a macro level. Under microscopic investigation, numerous microcracks are seen in the cement paste of the new concrete as well as in the paste regions of the recycled aggregate. This cracking in the recycled aggregate is indicative of a weak material. The aggregate quality may have led to lower concrete strength and rapid crack formation and deterioration.

A large number of microcracks in the new cement paste East bound, as well as a highly variable water/cement ratio in the new cement paste indicate possible difficulty with the mix at the time of placement. Many of the microcracks run around aggregates, while others run through the aggregates in the East bound lanes. Cracking around aggregate is typical of early cracking, when the soft paste is the path of least resistance. After extensive curing, cracks tend to run through aggregates and follow a straighter path. East bound has both types of microcracks.

Lack of adequate drainage beneath the slab may have been a factor in the deterioration East bound. Pumping and loss of support have been observed in this section. These types of distress can sometimes be explained by excess water being trapped beneath the pavement, weakening the foundation support.

Traffic analysis indicates a higher number of equivalent single axle loads (ESAL's) East bound than West bound. The AASHTO Design Method (a serviceability-based design method) has been used to determine allowable ESAL's for the two pavement sections based on measured values from field testing. It can be seen that East bound has exceeded its service life while West bound has not, based on current and back-calculated field conditions.

3.2.2 Performance Evaluation

A performance evaluation based on the AASHTO pavement design procedure shows that the East bound section of the Galesburg project has reached the threshold value of its serviceability while West bound still has some remaining service life. The current rate of traffic is about 7.3% higher in the East bound direction than in the West bound direction. The thickness of the pavement slab is higher West bound at an average of 10.4 in. versus an average thickness of 10.1 in East bound. Higher concrete strength and stiffness West bound, as well as higher foundation layer stiffnesses also lead to improved performance of the West bound section. While none of these factors alone are enough to make East bound fail and West bound pass the AASHTO serviceability check, the combined effects of these factors can be enough to drive East bound to a failing state.

An estimation of actual total ESAL's experienced by West bound to date are roughly 15% lower than the estimated total ESAL's to date East bound. ESAL's have been estimated from figures provided by MDOT for current traffic and yearly growth rates. Allowable ESAL's are about 70% higher West bound.

AASHTO Serviceability Check

(Galesburg Project)

Section	Age in years (Until 1995)	Load repetitions (ESAL's)		Remarks
		Total allowable	Estimated Actual* to date	
MI2-1 (West bound)	9	18,481,760	16,356,698	Pass
MI2-2 (East bound)	10	10,845,930	13,861,600	Fail

* Based on data obtained from MDOT

Table #6: Performance evaluation of the Galesburg test sections.

3.2.3 Concrete Slab Quality

Crack Mapping and Photographic Record

A visual examination of the two test sections has been conducted, including crack mapping and making a photographic record. West bound (MI2-1) contains very few cracks, with only two minor transverse cracks detected, one being so small that it was overlooked during the first walk-through of the site. The joints are visually in excellent condition throughout the site, as are lane-shoulder connections. In the East bound section (MI2-2), severe cracking is found in many slabs, as well as several shattered areas, faulted cracks, and faulted lane-shoulder connections. Several asphalt patches have been placed and one concrete slab replacement has been conducted. Loss of support is evident in several of the shattered sections, and slab sections can be observed rocking and bouncing under truck traffic. Pumping is evidenced by contamination of crack and joint surfaces East bound. Both longitudinal and transverse cracks are common to this test section. The photographic record and crack mapping may be found in Appendix 2 of this report.

Load Transfer and Crack Analysis

FWD testing has been performed on the two test sections, giving an indication of load transfer across transverse joints, cracks, and to the shoulder. There is some variability in the individual test results for each section. West bound, the first roughly 150 feet of the test section show poor load transfer and foundation stiffness. The remaining 850 feet exhibit good load transfer and stiffness. East bound, the values are more uniform, but comparatively lower in load transfer. Average load transfer across transverse joints is higher West bound than East bound. This is to be expected with West bound's better performance (though it is surprising that the first 150 feet of West bound have performed as well as they have).

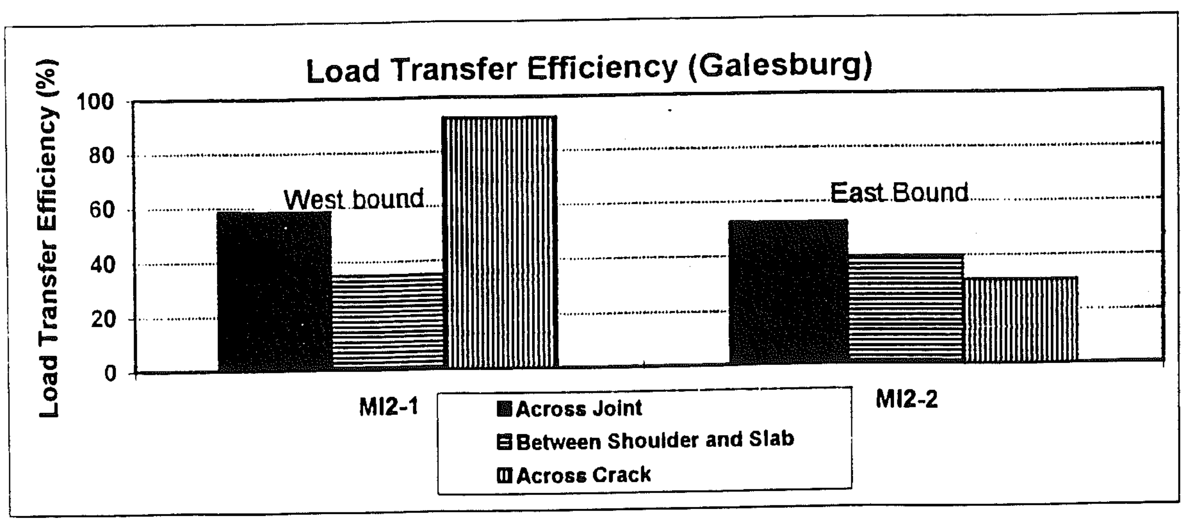

Figure #8: FWD analysis: load transfer for Galesburg project.

Good load transfer across transverse joints protects the pavement against load concentrations and excessive deflections. Load transfer to the shoulder has less influence on pavement performance. This is especially the case for the Galesburg project, where shoulder joints coincide with slab joints, and sympathy cracking is not a factor. Load transfer to the shoulders is low in both test sections, with East bound showing a slightly higher average value, and West bound showing considerable variability. Appendix 4 contains the FWD test data.

Load transfer across transverse cracks indicates that the West bound cracks are very tight with very little crack movement encountered. East bound load transfer is poor indicating little interlock of aggregates, large slab movements, and wide crack openings.

Crack analysis has been performed on cored specimens from cracks and joints in the two test sections. Visual surface texture analysis shows that the joints rate better than the cracks based on macro analysis of both sections. This can be expected because dowel bars provide shear load transfer in joints, while cracks rely on aggregate interlock alone. In addition, joint sealants protect against infiltration of debris in joints, while cracks remain open. The macro-texture rating refers to the texture provided by the coarse aggregate. The macro-texture ratings for the cracks of MI2-1 and MI2-2 are both "poor." The joints, however, show that MI2-1 is rated better than MI2-2 with ratings of "good" and "fair to poor" respectively. The good rating for MI2-1 indicates good aggregate interlock, working dowel bars and tight joints in this section.

Surface Texture Data Summary

Core Identification	Visual Rating	
	Macro	Gross
Joints:		
MI 2-1-J2 (WB)	good	good
MI 2-2-J2 (EB)	fair-poor	fair-poor
Cracks:		
MI 2-1-C2 (WB)	poor	good
MI 2-2-C2 (EB)	poor	good

Table 7: Crack texture of the Galesburg test sections.

Each section is also assigned a gross texture rating which indicates the straightness of the crack through the core. The gross-texture rating for the cracks of both West bound (MI2-1) and East bound (MI2-2) is "good." The joints West bound rate better than those East bound, with gross-texture ratings of "good" West bound and "fair to poor" East bound.

The cracks and joints for West bound appear to have experienced less movement and wear than those from East bound. The crack cores taken from West bound show a fine crack from top to bottom which remained very tight even after coring. The aggregate and cement paste along the crack surface in the West bound joints appear free from abrasions indicative of wear. One West bound joint does show corrosion of the dowel bar with evidence of wear on the concrete near the bottom of the dowel bar. The cores for East bound, however, tend to show more signs of wear. Abrasions and wear in both the cracks and joints East bound indicate vertical deflections of the slabs. More fine materials have infiltrated the cracks and joints of East bound than in West bound. This is indicative of pumping which leads to further loss of support and increased deflection.

Concrete Material Properties

Concrete strengths and stiffnesses for the Galesburg project were determined by laboratory testing of cored samples. Figures #9 and #10 summarize average test results for all tested specimens of each section. Individual test results for strength and stiffness testing are presented in Appendix #3.

Strength and static elastic modulus testing have been performed on mid-slab cores from both East and West bound test sections. Significantly higher strength, roughly 900 psi, is found in the West bound concrete. Static Young's modulus testing indicated similar concrete stiffness East and West bound, West bound being slightly higher. While both East and West bound are well above the 3500 psi required, the higher strength West bound could be indicative of higher quality materials and a better quality mix used. Discussions with the pavement contractor support this hypothesis.

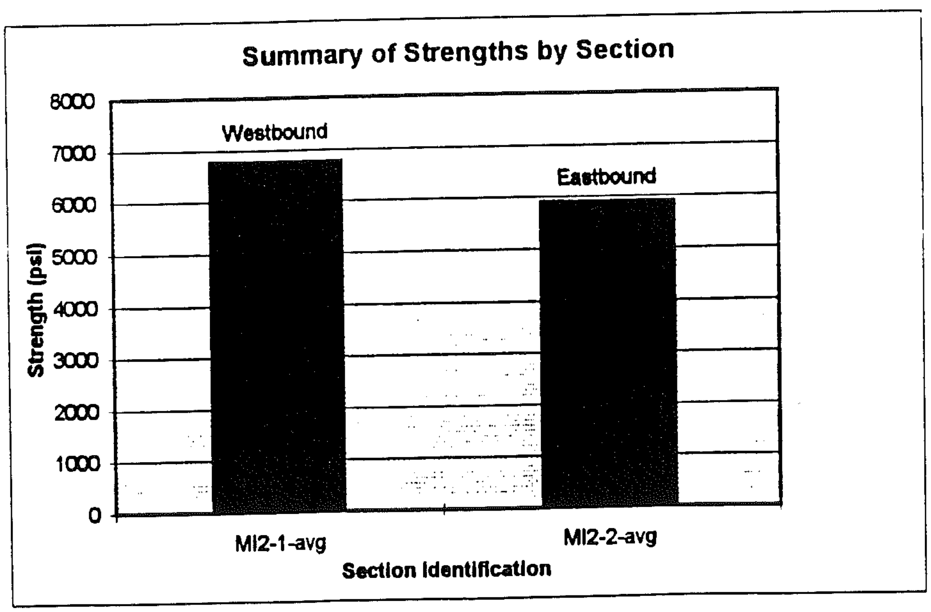

Figure #9: Strength of pavement slab for Galesburg project.

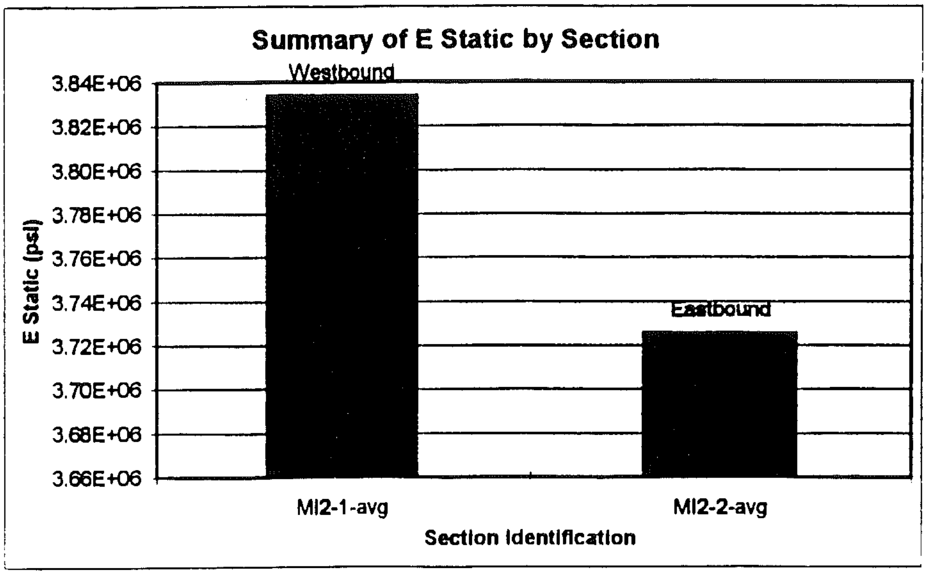

Figure #10: Stiffness of pavement slab for Galesburg project.

Construction Records and Mix Design

Discussions with the contractor and review of construction records indicate that the pre-existing road West bound (MI2-1) was much stronger than the pre-existing road East bound (MI2-1). The contractor indicates that it was much more difficult to remove and break up the West bound roadway. Additionally, the East bound roadway was formed of two layers of visibly different materials. When recycled, these two layers were mixed together.

No recycled fine aggregate was used in either pavement section. This is an important difference from the Lawrence project, where up to 50% of the fines were recycled. Recycled fine aggregate can be detrimental to the wear resistance of the concrete.

Petrographic Analysis

Petrographic analysis performed on mid-slab cores gives indications of the composition of the concrete as well as aggregate reactivity and microcracking patterns.

Microcracking analysis indicates significantly more microcracking in the East bound test section (MI2-2) than in the West bound section (MI2-1). There is a large number of microcracks in the recycled concrete aggregate as well as the new concrete in the East bound direction. West bound exhibits few microcracks throughout. As with the Lawrence project, more microcracking is present in the cement paste than in the adhesion zones. East bound, the concrete suffers from a highly non-uniform water/cement ratio in the new cement paste, ranging from 0.35 to 0.60. The West bound paste is much more homogeneous, with w/c ranging from 0.35 to 0.40.

Core	Thin Section	Microcracks/mm²			
		New Concrete		Old Concrete (recycled)	
		Cement Paste	Adhesion Zone	Cement Paste	Adhesion Zone
MI2-1-M2	Surface Middle Bottom	0.23	0.10	0.14	0.05
MI2-1-M4	Surface	0.22	0.14	0.17	0.16
MI2-2-M2	Surface Middle Bottom	0.41	0.14	0.84*	0.18
MI2-2-M4	Surface	0.78*	0.36	0.33	0.12

Cracks less than 0.01 mm are considered in this quantitative determination in 10 fields of sight on each thin section.
(*) High amount of microcracks.

Table 8: Microcracks for Galesburg project

The highly inhomogeneous paste East bound and the large number of microcracks gives an indication of poor quality concrete in this section. This is confirmed by strength data.

Reactive alkali-silica gel is found in some specimens of the East bound pavement, though not in large quantities. The ASR does not lead to significant cracking in the examined sections, and the extent to which it may be a factor in the deterioration of these concretes is unknown. No ASR has been detected West bound.

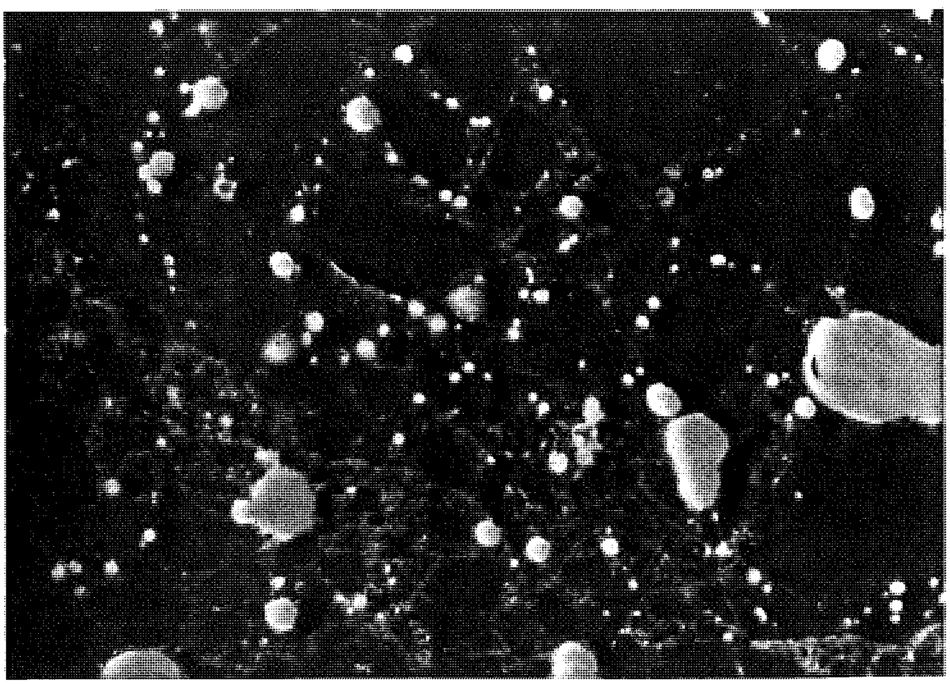

Photo #13 Microphoto of a sample from section MI2-1 (West bound Galesburg) taken in fluorescent light. Scale:1 cm = 0.26 mm. Some minor cracking is evident in the cement paste.

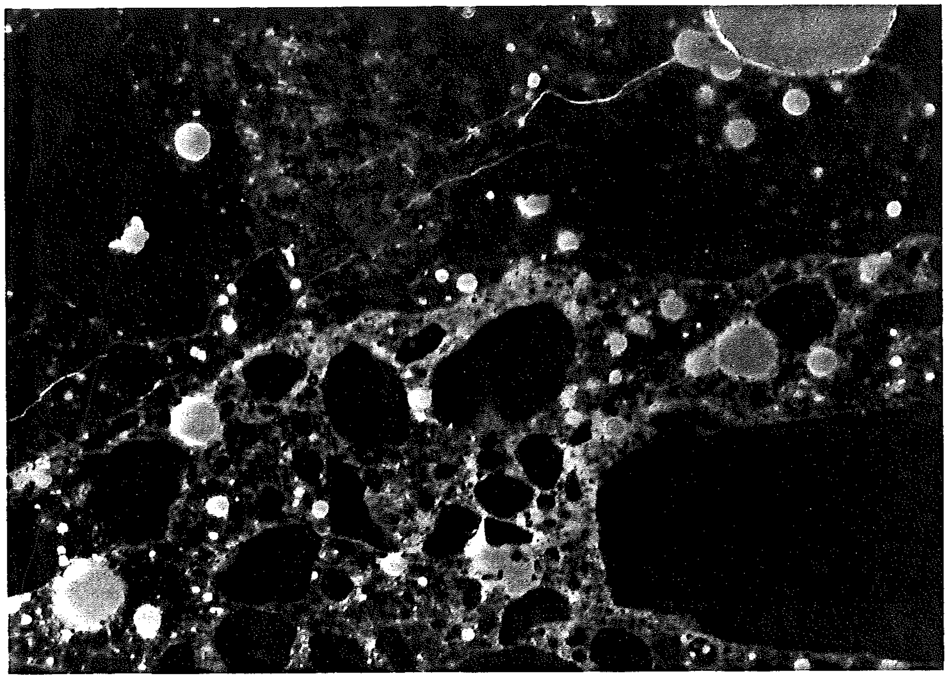

Photo #14 Microphoto of a sample from section MI2-2 (East bound Galesburg) taken in fluorescent light. Scale: 1 cm = 0.26 mm. Cracking is seen through the cement paste as well as through the aggregate.

3.2.4 Quality of Foundation Materials

To qualify materials under the concrete slab, an extensive field testing program was developed using the DCP and FWD tests. A predicted value of modulus of the combined base, subbase and subgrade layers has been obtained from FWD testing. This effective modulus is heavily affected by the subgrade, due it's semi-infinite thickness, as compared to very limited base and subbase thicknesses. This test has been compared with a summation of the representative number of DCP blows of the base and subbase. The following chart shows DCP and FWD results plotted together to give an overall picture of foundation stiffnesses.

The DCP tests on the West bound section show higher values than East bound. This is the case for both base and subbase materials. The required number of blows for penetration gives a qualitative representation of soil compaction. Lower DCP blowcount may be attributable to poorer soil compaction in the East bound test section.

FWD testing also provides considerable information on the overall quality of foundation materials. Mid-slab deflections are considerably lower for West bound than for East bound. It should be noted that only one reliable test result is available East bound for this comparison. This is because the East bound pavement is so shattered that the validity of the remaining tests is questionable. Low deflection and a wide shallow deflection bowl West bound are indicative of the high area of influence from loading and high effective stiffness of the soil compared to low influence area and effective soil stiffness East bound. Influence area is a measure of load distribution, with a high relative influence area indicating a large compression bowl and good load distribution through the system. Effective soil stiffness is calculated using the Bousdef program and the measured concrete stiffness from lab testing. Lower effective stiffness East bound could possibly be attributed to a weaker subgrade.

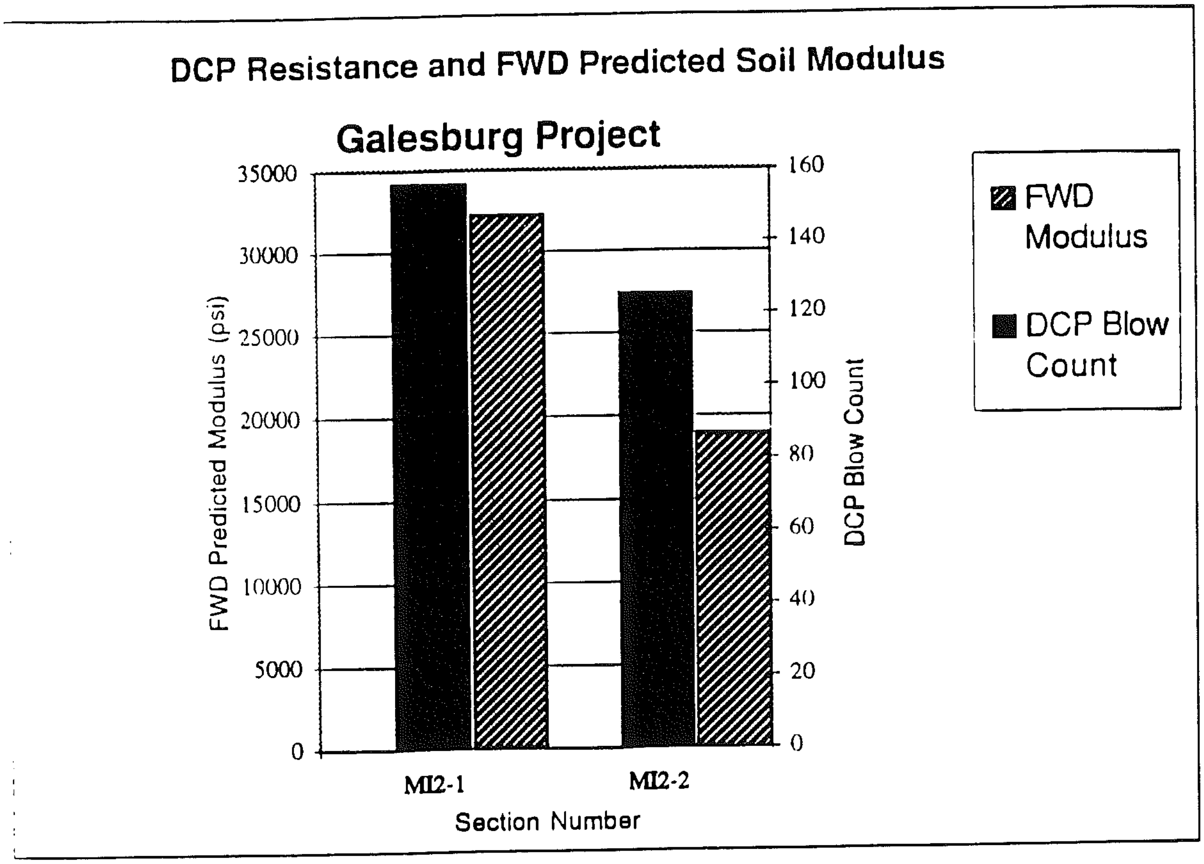

Figure #11 DCP and FWD analysis of foundation stiffness for the Galesburg project.

Gradation analysis of the foundation materials has been conducted. The base course West bound (MI2-1) is recycled aggregate with a 6A Modified 5G gradation. See Appendix 5. East bound (MI2-2), the base gradation is 8G Modified. Subbases for East and West are well graded materials. There is some variability in the gradation of these materials, especially West bound (MI2-1). The subbases likely have a low susceptibility to frost heave due to a low percentage of fines. The subgrades East and West bound are somewhat different, with East bound being densely graded and West bound being uniformly graded. Frost heave susceptibility appears not to be an issue in either section's subgrade.[7] Filter criteria for the base courses indicate that both the West and East bound materials are adequate filters for the subbase layers, though some contamination of cracks and joints with fines is found East bound. The subbases of both sections fail as filters for the subgrades because of migration of fines upward.

In both East and West bound, drainage beneath the slab is provided by the open graded base course. This drains into a geotextile wrapped corrugated pipe edge drain beneath the outer wheel path, approximately 2-3 ft. inside the outer lane from the shoulder. West bound (MI2-1), a drain pipe in the edge drain carries water to outlets at the edge of the pavement. East bound (MI2-2) water is drained from the edge drain into catch basins in the median connected to the storm drain system. West bound, one of four drains was clogged on inspection, with two others working only at partial capacity. East bound, the condition of the drains is not known. A core was drilled in the East bound test section to verify that the edge drain was properly placed; it was. Due to the cut/fill slopes in this project, the West bound section would tend to drain naturally to some extent even if the drains were clogged. East bound however, it is possible that water would become trapped beneath the pavement if drains were not working properly.

4. Laboratory Study of Recycled Aggregate Durability

As performance of a recycled pavement seems to be linked to the quality of the recycled aggregate, it may be important to examine the durability of such aggregates prior to use. The accepted method in Michigan for determining aggregate durability is freeze-thaw testing. The procedure used is a standard ASTM procedure, modified by Michigan Test Methods 113-115 (MTM) [8-10]. The MTM specifications call for a 24-hour vacuum saturation of coarse aggregates prior to batching freeze-thaw specimens.

Recycled aggregates were obtained from I-96 near Brighton, Michigan, where they were being used as base course material in a new paving project. Material properties testing indicated a unit weight of 84.39 pcf, a specific gravity of 2.35 (oven dry basis), and an absorption capacity of 5.26% for this aggregate. Previous research performed by the Michigan Department of Transportation (MDOT) indicated a range of 2.31-2.40 for specific gravity and 3.43 to 5.00% absorption for various recycled aggregates from Interstates 96 and 94.[11,12] These values confirm that the Brighton aggregate has properties typical of recycled aggregates.

AGGREGATE PROPERTIES

Bulk Specific Gravity (Oven dry basis)	2.35
Bulk Specific Gravity (Saturated, surface dry basis)	2.48
Absorption Percent	5.26
Dry Unit Weight (pcf)	84.39

Properties calculated using MTM 24 hour vacuum saturation procedures.

Table #9 Aggregate properties of Recycled I-96 concrete from Brighton, Michigan.

Three separate batches of freeze-thaw specimens were made and tested using the Brighton aggregate. A significant dependence on degree of saturation was noted, possibly due to the high absorption capacity of the aggregate. When saturated to current MTM specifications, the aggregate exhibited an expansion of 0.083% per 100 freeze-thaw cycles. This puts the aggregate in the marginal durability range. For the other batches, some vacuum pressure was released during backfilling of the vacuum chamber, causing the final pressure to be below MTM required levels. These batches performed far better, showing less than 1/2 of the expansion seen in the MTM qualifying batch. This indicates a high degree of sensitivity to degree of vacuum saturation. This sensitivity is likely due to the high absorption capacity of the Brighton aggregate. As absorption properties of different recycled aggregates can vary significantly, durability testing should be performed on each recycled aggregate of interest prior to use. Furthermore, research by Stephen W. Foster of the Federal Highway Administration[12] indicated that freeze-thaw durability of recycled aggregates is greatly dependent on the quality of the original aggregate used, and performance should be judged on a case-by-case basis.

FREEZE-THAW BATCHING DATA

		BATCH NUMBER			
CONCRETE MIX DATA		**1**	**2**	**3**	**Average**
Date Made		11/10/94	11/15/94	11/22/94	
Slump (inches)		2	2.5	2.75	2.42
Unit weight of Concrete (pcf)		141.82	141.02	140.60	141.15
Actual Cement Content (pcy)		530	524	524	526
Water-cement ratio by weight		0.43	0.46	0.44	0.45
Air Content (%)		6.2	6.6	8.2	7.0
Compressive Strength (psi)	7 days	4220	3435	3175	3610
	28 days	4644	4416	4726	4595
Vacuum Pressure (in-hg)*		28.0	28.6	27.4	
Freeze-Thaw Durability (% Expansion per 100 cycles)	Beam 1	0.025	0.107	0.032	
	Beam 2	0.023	0.063	0.038	
	Beam 3	0.021	0.083	0.039	
	Average	0.023	0.084	0.036	0.048

REMARKS:
*MTM specifies 28.5+0.2 in-hg of vacuum pressure.

Table #10 Freeze-thaw durability data for recycled I-96 aggregate.

5. Recommendations and Conclusions

Many factors that affect the performance of recycled pavement are also common to virgin aggregate concretes. A performance evaluation of the test sections indicates that traffic loading and pavement thickness play a major role in the deterioration of several of the pavement sections. Using a thicker pavement slab can help to reduce pavement damage.

Based on the four 410-ft. test sections of the Lawrence project, the recycled concrete on dense-graded base (MI1-4) out-performs recycled concretes on other base types (MI1-2, MI1-3) as well as a control peastone concrete on open-graded base (MI1-1). It appears that it is not so much the stiffness, but the uniformity of foundation support that improves the performance of MI1-4.

The effect of the foundation layers on recycled concrete performance is not conclusive, though it is seen that excessive deflection can cause significant damage to the pavement. Good compaction of base and subbbase layers is advantageous as is a stiff subgrade. Uniform foundation stiffness can reduce stress concentrations in the slab.

Load transfer efficiency across cracks and transverse joints has a significant effect on slab performance. High load transfer across cracks is indicative of good aggregate interlock and adequate foundation support. Load transfer across joints is indicative of properly working joints with the doweled connections moving as they are designed to do. Poor load transfer across joints indicates ineffective joints.

Because of the aggregate/paste mix in recycled aggregates, the long-term shearing resistance of the aggregate may be lower than for many virgin aggregates. This could in turn lead to a decrease in aggregate interlock, causing more rapid deterioration of existing cracks. In the case of peastone concrete, small aggregate size and rounded aggregate shape lead to poor aggregate interlock.

This project also shows the sensitivity of recycled concretes to both field conditions and environmental factors. Data shows that hot weather during placement was associated with recycled sections that deteriorated rapidly, while a better product was produced during cooler placement weather. Early shrinkage cracking and inhomogeneous concrete were noted for the sections placed at high temperatures.

In the Lawrence project, where sympathy cracking and shrinkage cracking were active in some sections, rapid deterioration has been noted. In the section where early shrinkage cracking is not noted, sympathy cracking has been much slower to develop.

Based on the evidence seen in the Galesburg project (MI2), it is probable that the quality of the recycled aggregate plays a major role in the performance of the new concrete. If this conclusion can be made, perhaps through further study, then determination of an aggregate's durability is vital prior to its use in a recycled concrete.

The use of freeze-thaw testing is an accepted method for aggregate durability testing and can be applied to recycled aggregates. Because of the high absorption capacity of many recycled aggregates, freeze-thaw dilation may be excessive under MTM guidelines. The use of large size premium virgin aggregate in conjunction with recycled aggregate can increase aggregate durability as well as improve aggregate interlock and abrasion resistance.

Appendix 1: Project Locations

Both projects discussed in this report, the Lawrence project (MI1) and the Galesburg project (MI2) are located on I-94 near Kalamazoo, Michigan. The projects are highlighted on an area map to indicate their general locations. Next a brief description of each test section is given, followed by the precise locations of all core samples taken.

The Lawrence project, located near Lawrence and Paw Paw, Michigan is an 8.9 mile project containing virgin and recycled concretes on various base types. Within the project, four test sections, each of approximately 400 feet in length, have been investigated. These test sections include virgin and recycled concretes over open graded, dense graded, and 5% cement stabilized peastone base courses.

The Galesburg project, located between Galesburg and Kalamazoo, Michigan, is an 8.7 mile long project containing recycled concrete over open graded base courses. Two 1000 foot long test sections have been investigated - one east bound and one west bound at the same station locations.

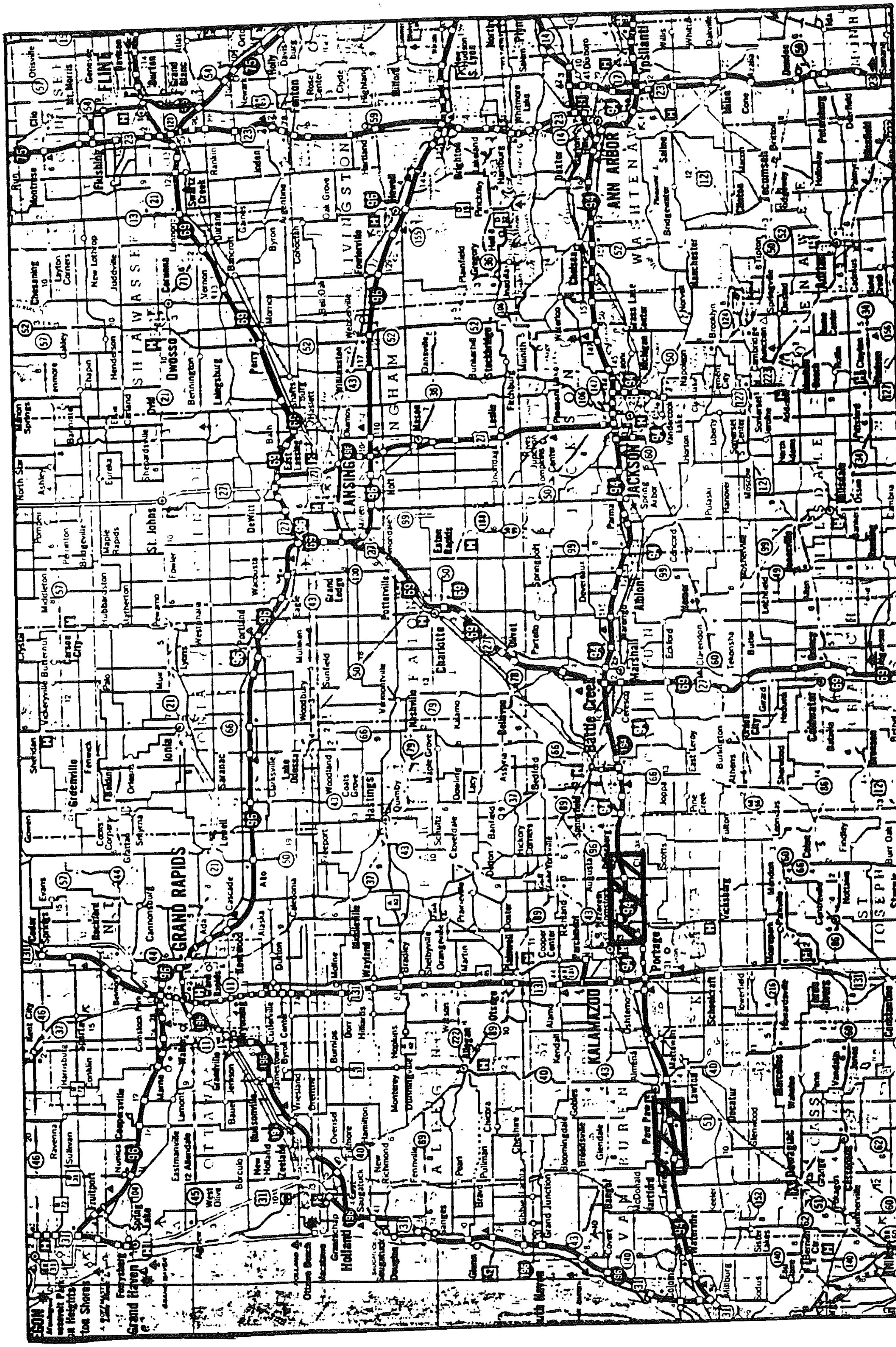
GRAND RAPIDS
LANSING
KALAMAZOO
JACKSON
ANN ARBOR
FLINT
OWOSSO
Battle Creek
Holland
Grand Haven
Ypsilanti
Hastings
Charlotte
Marshall
Albion
Portage
St. Johns
Ionia
Greenville
Coldwater
Hillsdale
Adrian
Tecumseh
Howell
Brighton
Fenton
Mason
Eaton Rapids
Grand Ledge
Allegan
Otsego
Paw Paw
Sturgis
Three Rivers
Dowagiac
Cassopolis
Niles

INDEX OF TEST SECTIONS

Section MI1-1 Lawrence - I 94 West Bound

Control Section - Peastone Pavement on Open-Graded Drainage Course
Beginning Station 652+25'
Ending Station 648+00'
Coring Date 11-17-94

Section MI1-2 Lawrence - I 94 West Bound

Recycled Pavement on Open-Graded Drainage Course
Beginning Station 645+00'
Ending Station 640+00'
Coring Date 11-17-94

Section MI1-3 Lawrence - I 94 West Bound

Recycled Pavement on 5% Cement-Stabilized Peastone Base Course
Beginning Station 515+00'
Ending Station 510+00'
Coring Date 11-18-94

Section MI1-4 Lawrence - I 94 West Bound

Recycled Pavement on Dense-Graded Base Course
Beginning Station 414+00'
Ending Station 410+00'
Coring Date 11-29-94

Section MI2-1 Galesburg - I 94 West Bound

Recycled pavement on Recycled Open-Graded Drainage Course
Beginning Station 880+00'
Ending Station 870+00'
Coring Date 12-6-94

Section MI2-2 Galesburg - I 94 East Bound

Recycled Concrete on Open-Graded Drainage Course
Beginning Station 870+00'
Ending Station 880+00'
Coring Date 12-8-94

Stationing of Pavement Cores

Job	Section	Pavement Core Type	Core #	Station	Length	Job	Section	Pavement Core Type	Core #	Station	Length
MI1	1	Mid-Panel	1	651+90'	9.75" *	MI2	1	Mid-Panel	1	879+48.5'	10.25"
MI1	1	Mid-Panel	2	650+55'	10" *	MI2	1	Mid-Panel	2	877+40'	10.25"
MI1	1	Mid-Panel	3	649+75'	10.5"	MI2	1	Mid-Panel	3	875+32'	10"
MI1	1	Mid-Panel	4	649+35'	10.25"	MI2	1	Mid-Panel	4	873+36'	10.75"
MI1	1	Mid-Panel	5	648+54'	10.25"	MI2	1	Mid-Panel	5	870+55'	10"
MI1	1	Joint	1	651+49'	10"	MI2	1	Joint	1	879+28'	10"
MI1	1	Joint	2	650+63'	10"	MI2	1	Joint	2	874+78.5'	10.75"
MI1	1	Joint	3	648+57'	10"	MI2	1	Joint	3	871+48.7'	10.25"
MI1	1	Crack	1	651+60'	10.25"	MI2	1	Crack	1	874+91'	11"
MI1	1	Crack	2	650+40'	10.25"	MI2	1	Crack	2	872+92'	11"
MI1	1	Crack	3	648+49'	10.25'	MI2	1	Mid-Crack		872+92'	10.25"
MI1	2	Mid-Panel	1	644+81.5'	8.75" *	MI2	2	Mid-Panel	1	872+75'	10"
MI1	2	Mid-Panel	2	643+94.5'	10.5"	MI2	2	Mid-Panel	2	874+50.5'	10"
MI1	2	Mid-Panel	3	642+77.5'	10.5"	MI2	2	Mid-Panel	3	875+70'	9.75"
MI1	2	Mid-Panel	4	641+51'	10.5"	MI2	2	Mid-Panel	4	877+8'	9.75"
MI1	2	Mid-Panel	5	640+31.5'	10" *	MI2	2	Mid-Panel	5	879+38'	10"
MI1	2	Joint	1	644+88'	10.25"	MI2	2	Joint	1	875+15.7'	10.5"
MI1	2	Joint	2	642+82.75'	10.25"	MI2	2	Joint	2	876+30.5'	10.25"
MI1	2	Joint	3	640+34.5'	10"	MI2	2	Joint	3	878+77'	10"
MI1	2	Crack	1	644+60.5'	10.25"	MI2	2	Crack	1	871+63'	10"
MI1	2	Crack	2	642+60.75'	10.25"	MI2	2	Crack	2	874+86.4'	10.75"
MI1	2	Crack	3	640+42.5'	10"	MI2	2	Crack	3	876+35.8'	10.25"
MI1		Shrink-crack			10"						
MI1	3	Mid-Panel	1	514+85.5'	10.25" *						
MI1	3	Mid-Panel	2	513+59'	10.5"						
MI1	3	Mid-Panel	3	512+35'	10.25"						
MI1	3	Mid-Panel	4	511+36.5'	9. 5"						
MI1	3	Mid-Panel	5	510+55.5'	9.25" *						
MI1	3	Joint	1	514+92'	10.25"						
MI1	3	Joint	2	512+45.67'	10"						
MI1	3	Joint	3	511+24'	9"						
MI1	3	Crack	1	514+24.67'	10"						
MI1	3	Crack	2	510+76'	9.25"						
MI1	3	Crack	3	510+12.75'	9"						
MI1	3	Crack		511+42.5'	9.5"						
MI1	4	Mid-Panel	1	413+65'	9.5" *						
MI1	4	Mid-Panel	2	412+57.25'	9.75"						
MI1	4	Mid-Panel	3	411+73'	9.5"						
MI1	4	Mid-Panel	4	410+91'	9.5"						
MI1	4	Mid-Panel	5	410+22'	9" *						
MI1	4	Joint	1	412+88.5'	9.25"						
MI1	4	Joint	2	412+7.25'	9.25"						
MI1	4	Joint	3	410+43'	9.25"						
MI1	4	Crack	1	413+85.5'	9.5"						
MI1	4	Crack	2	411+93.67'	9.5"						
MI1	4	Crack	3	411+11'	9.5"						
MI1	4	Shoulder	1	413+85'	9.25"						
MI1	4	Shoulder	2	413+45'	9.25"						
MI1	4	Shoulder	3	412+34'	9.5"						

* Core has been cut

Appendix 2: Crack Mapping and Photographic Record

This appendix includes crack mapping and photographic records of the six test sections. These visual records of the pavement sections are useful both to give an overall picture of the performance of each section and to provide clues to the specific causes of distress.

Crack mapping studies have been performed on the pavement sections to show locations of transverse joints (▬▬) and cracks (∿∿). Coring locations have been added (●). In general, only the design lane has been mapped for cracking patterns. No crack mapping has been performed on section MI1-2.

The sympathy crack pattern found in the Lawrence Project is clearly visible in the crack maps (crack severity is not shown). It can be seen that the same type of cracking is present for all Lawrence sections.

The differences between East and West bound Galesburg can be seen from the crack maps of these two test sections. Only two small cracks are found West bound, while numerous cracks and pavement shatters are recorded throughout the East bound section.

A photographic record has been made to visually depict the cracking in each pavement section. Several photos from each test section have been chosen to show typical pavement behavior for that section. In addition, information regarding cut/fill slopes and base course materials is provided by the photographs. Crack severity for cracks from the different test sections can be seen from the photographic record.

In the Lawrence project, sections MI1-1, MI1-2, and MI1-3 all exhibit numerous severe working cracks such as those seen in the photos. Some faulting and spalling is typical of these sympathy cracks. Section MI1-4 tends to exhibit less severe cracks, though some working cracks are present in this section as well. All four Lawrence test sections are on relatively level terrain. The differences in the base course materials are visible in the core hole photos.

The Galesburg project photos show stark differences between the East and West bound pavement sections. East bound is nearing the need for total replacement, while West bound is in excellent condition. East bound is in a cut region, while West bound is on a fill slope.

MI1-1

PROJECT NO. 80023-20993A SURVEY DATE 11-17-95 SURVEYED BY ______ PAVEMENT WIDTH 24 ft *

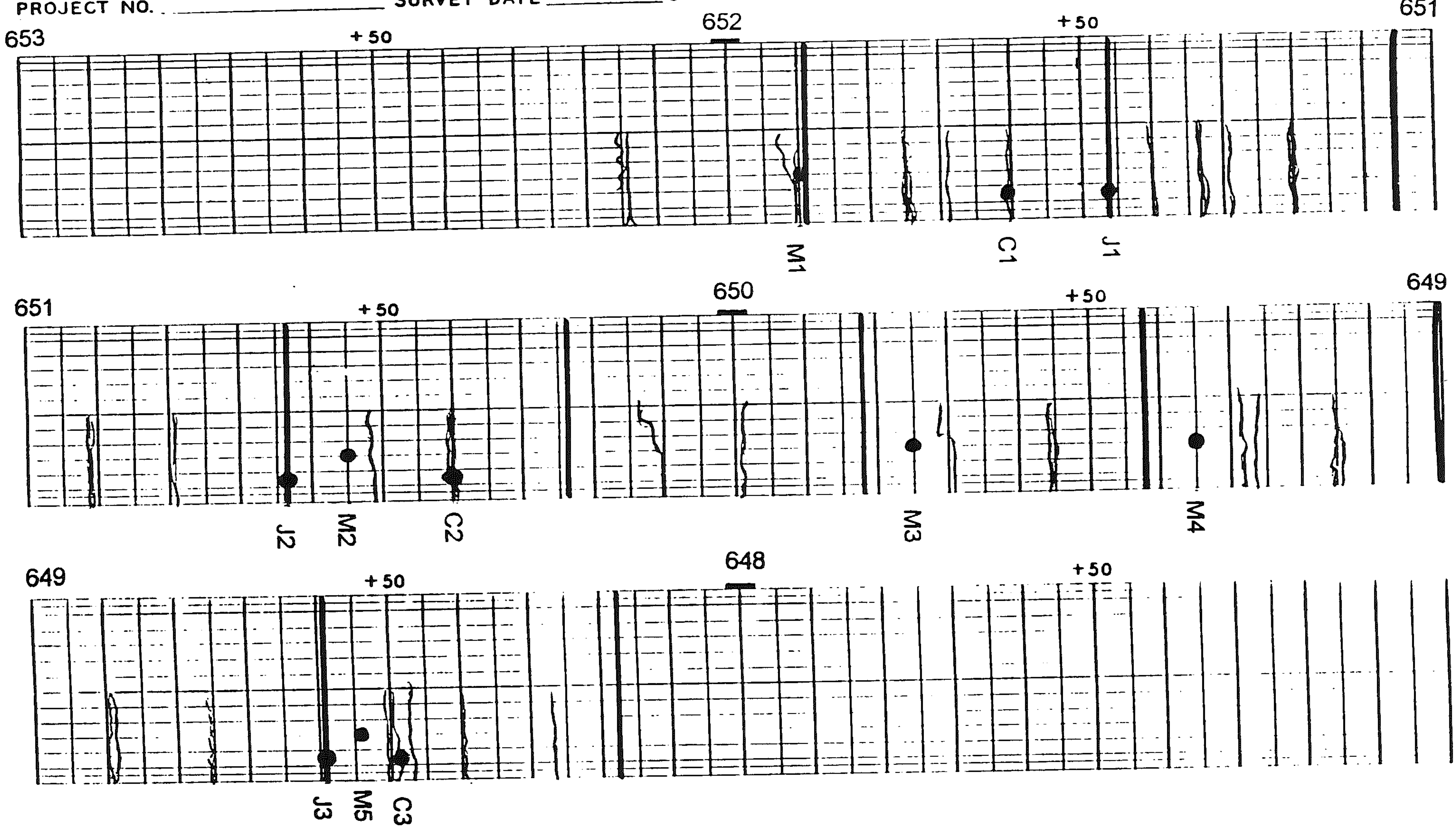

* Crack mapping was only performed in the traffic lane.

MI1-3

PROJECT NO. 80023-20993A SURVEY DATE 11-18-94 SURVEYED BY ________ PAVEMENT WIDTH 24 ft *

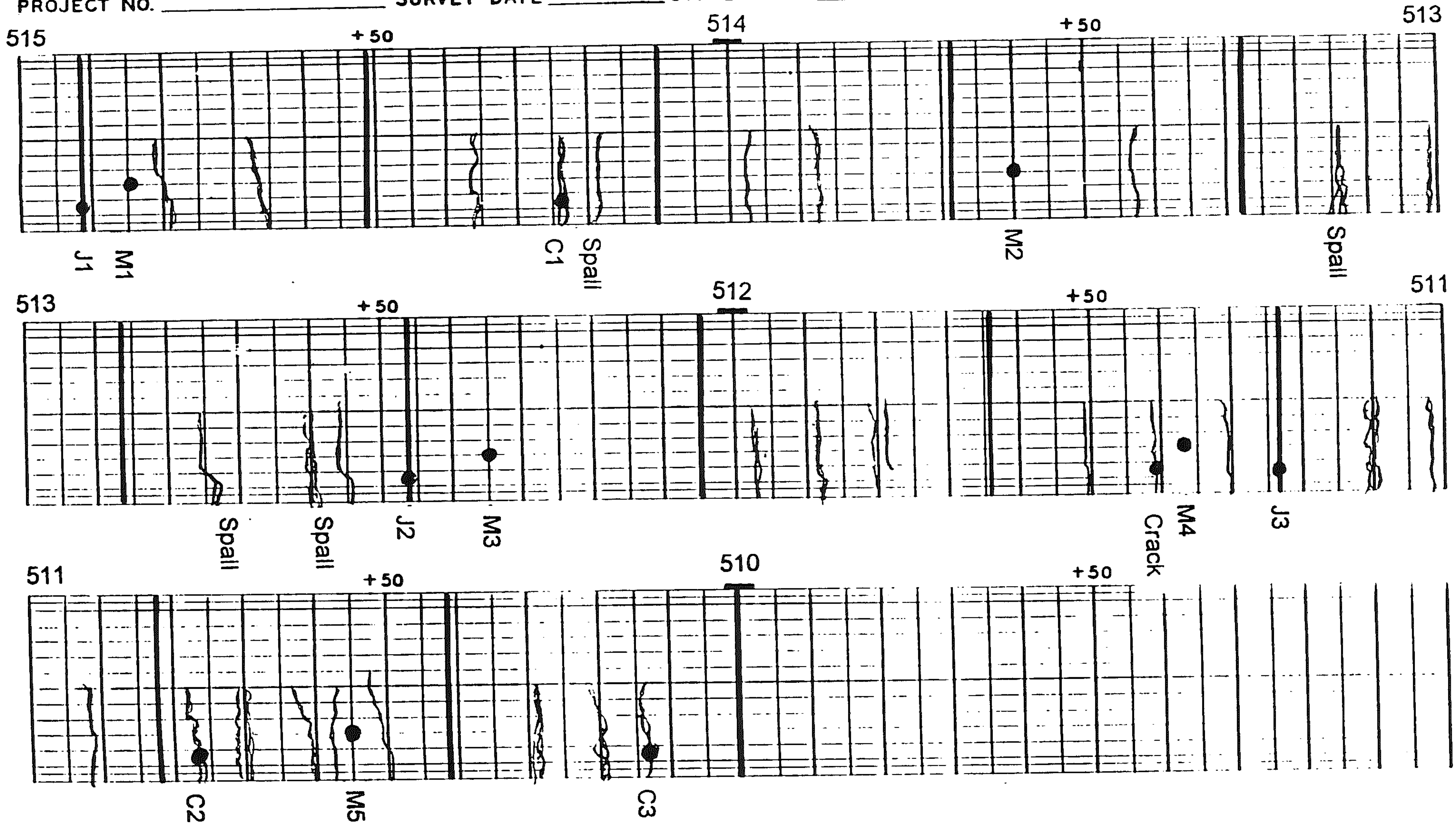

* Crack mapping was only performed in the traffic lane.

MI1-4

PROJECT NO. 80023-20993A SURVEY DATE 11-29-94 SURVEYED BY ________ PAVEMENT WIDTH 24 ft *

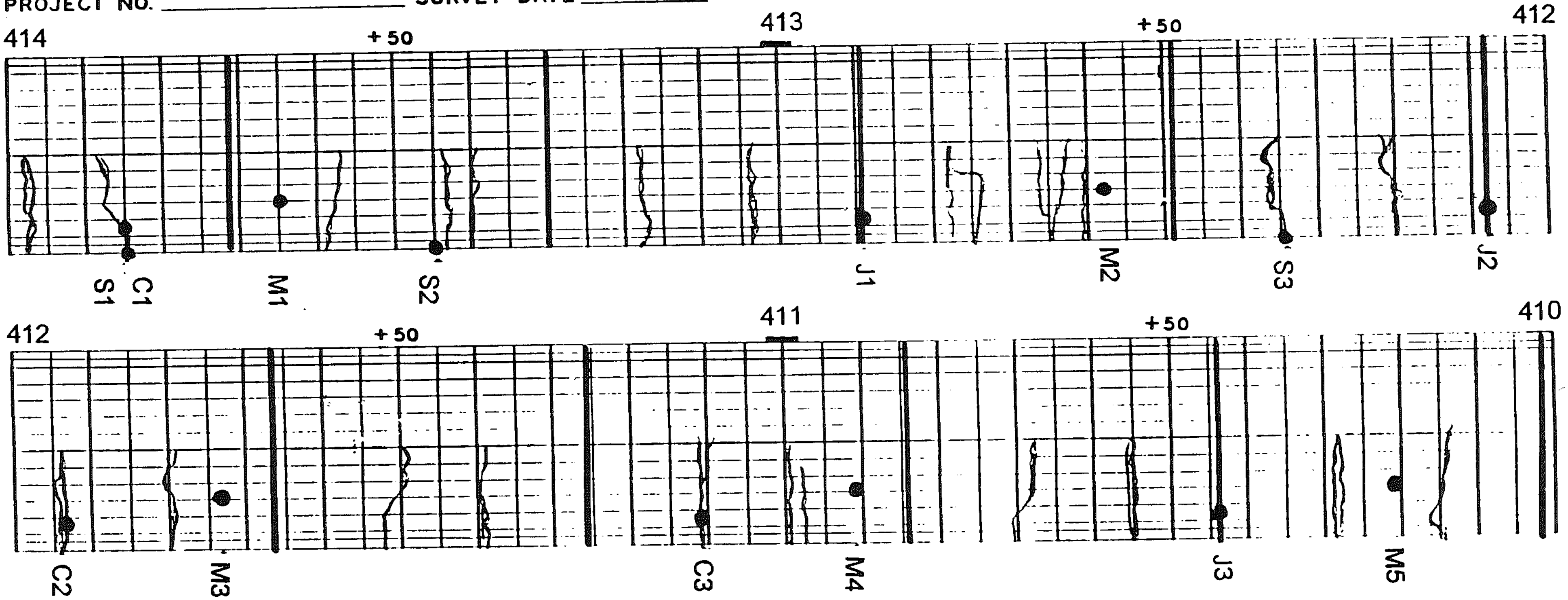

* Crack mapping was only performed in the traffic lane.

M2-1

PROJECT NO. 39022-20736A SURVEY DATE 12-6-94 SURVEYED BY ______ PAVEMENT WIDTH 24 f.

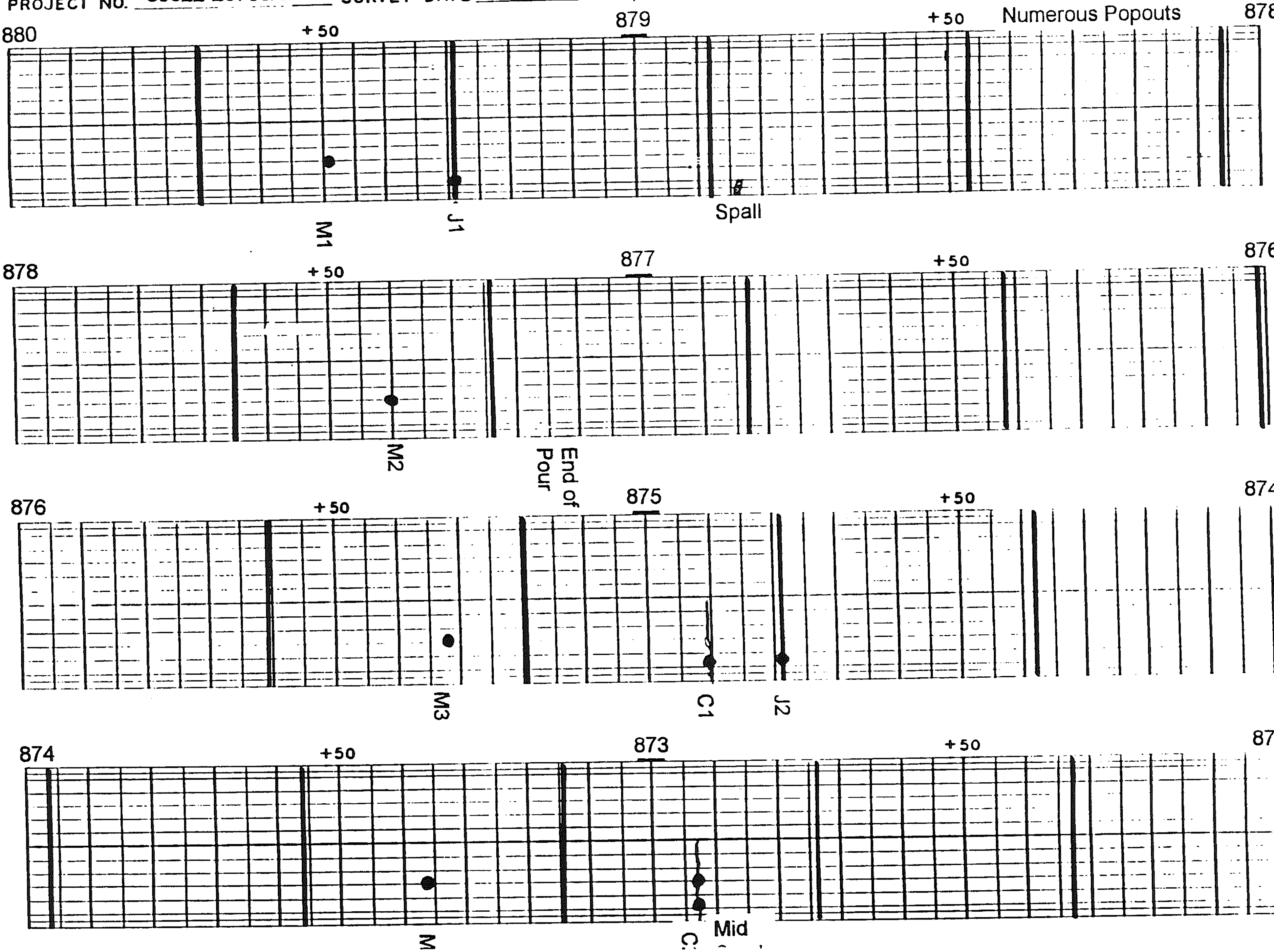

MDOT 1015 (11/81)

MI2-1

PROJECT NO. 39022-20736A SURVEY DATE 12-6-94 SURVEYED BY ______ PAVEMENT WIDTH 24 ft

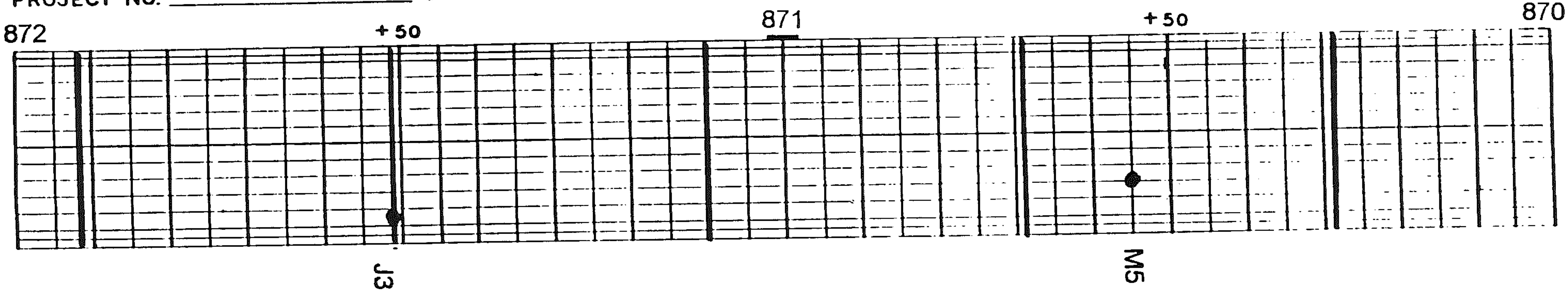

MI2-2

PROJECT NO. 39022-20736A SURVEY DATE 12-8-94 SURVEYED BY ________ PAVEMENT WIDTH 24 ft

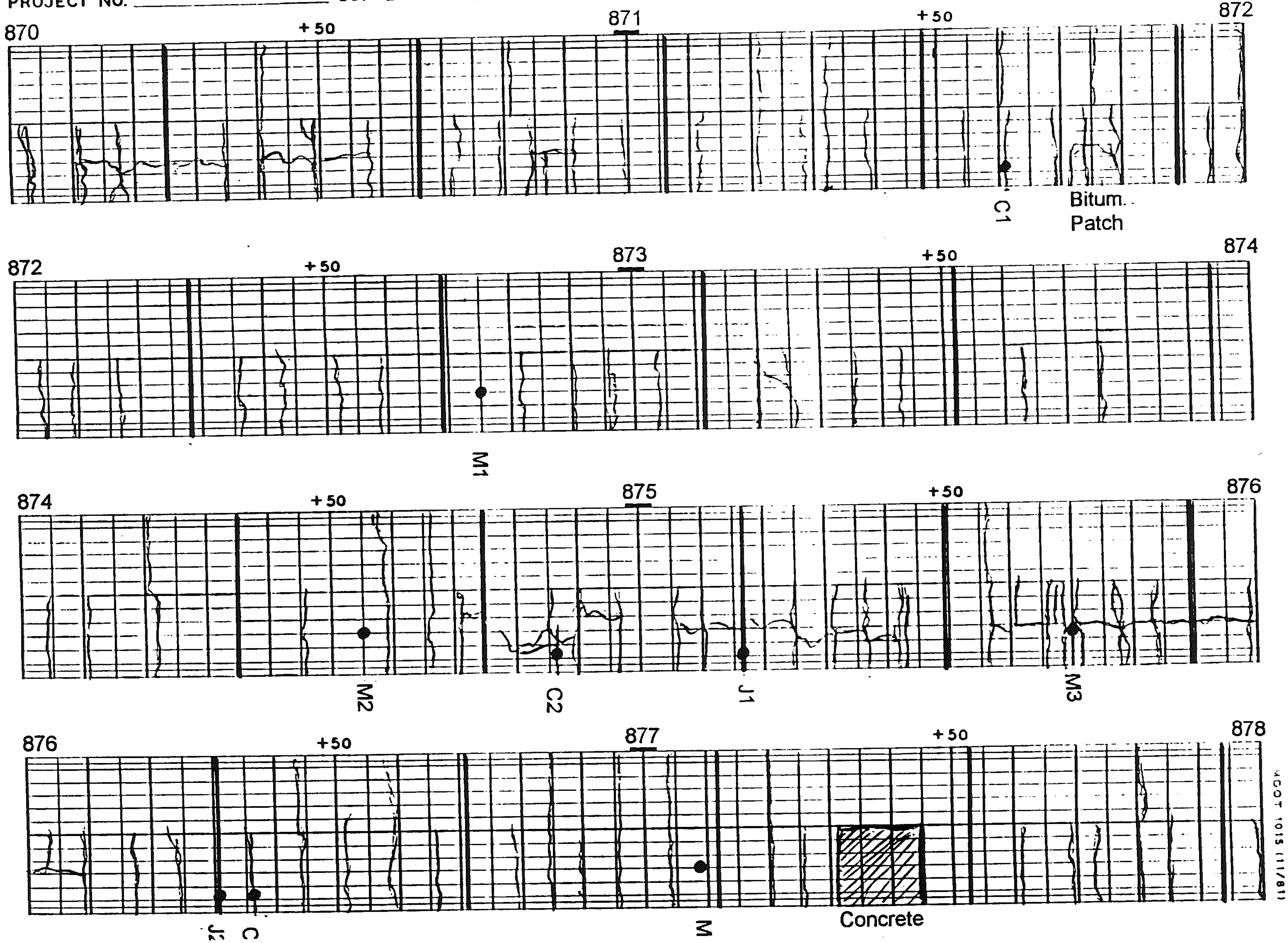

MI2-2

PROJECT NO. 39022-20736A SURVEY DATE 12-8-95 SURVEYED BY ______ PAVEMENT WIDTH 24 ft

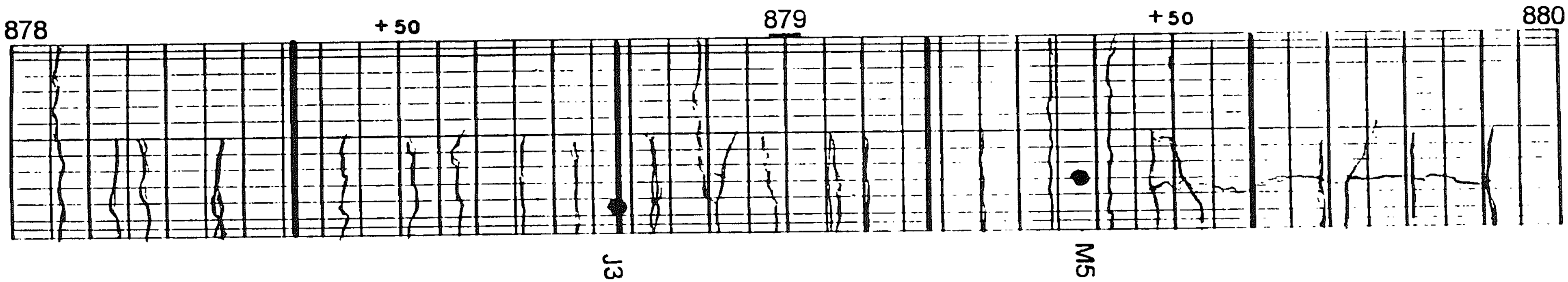

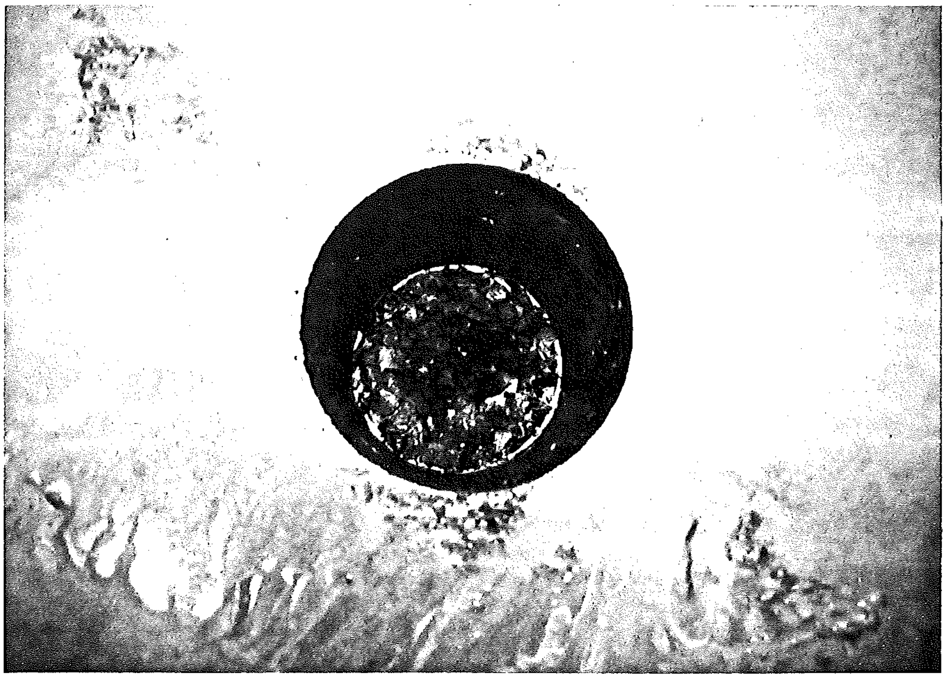

View of mid-panel core hole in section MI1-1. Note the OGDC exposed at the bottom of the hole. Water used in coring the concrete drained quickly.

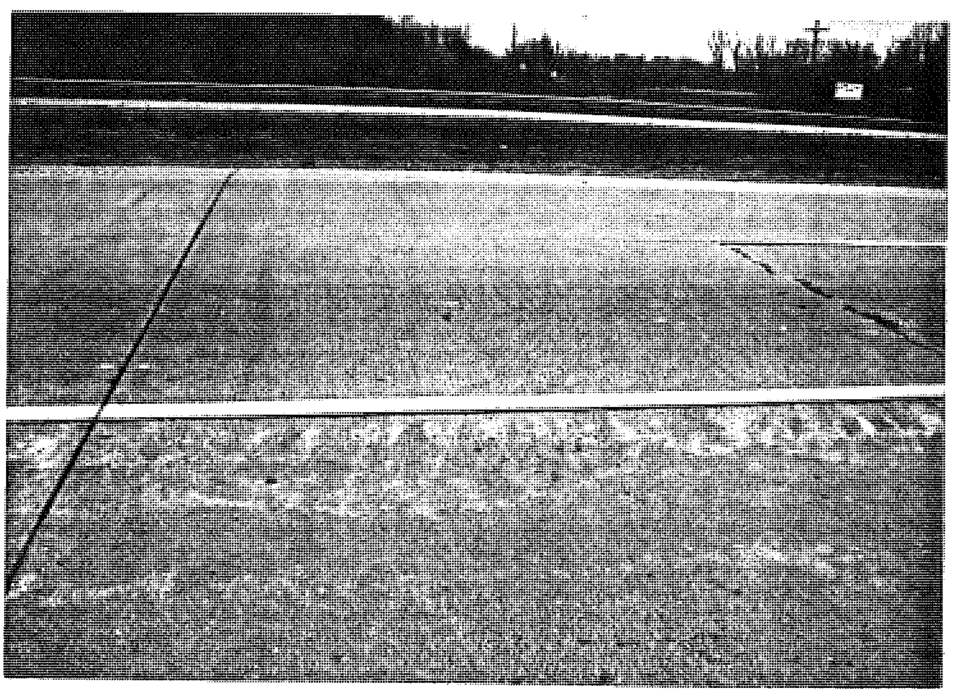

View of typical transverse joint and sympathy crack in section MI1-1. Note the good appearance of the joint and spalling in the crack. An FWD Test location is marked by white spots on the transverse joint.

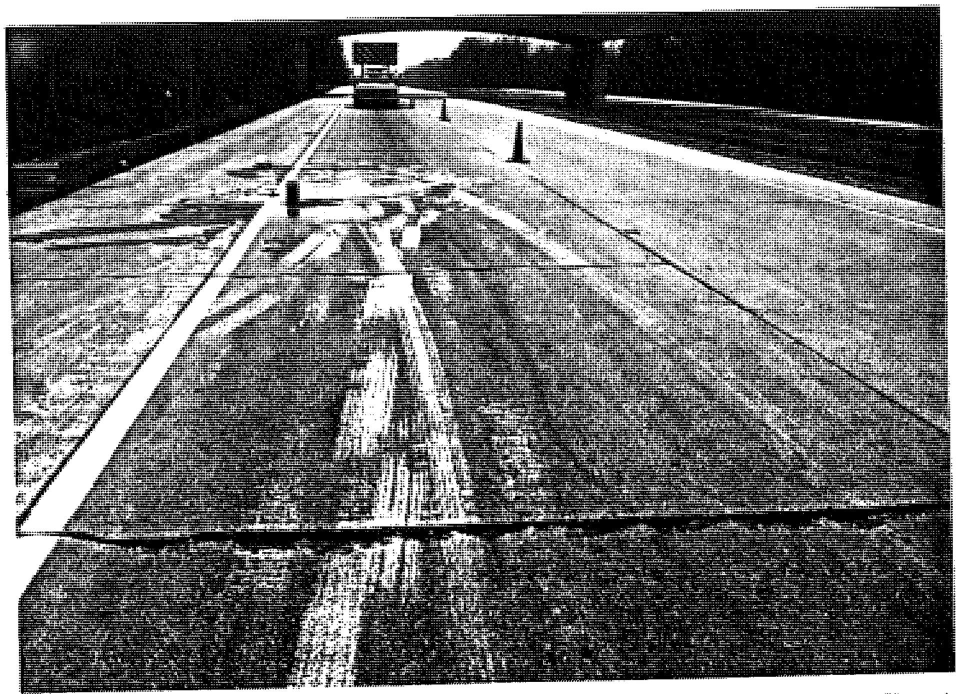

View of several spalled sympathy cracks near the beginning of section MI1-1. The slope on the left shoulder is the bridge embankment. In general, the test section is on level ground.

Close-up view of a sympathy crack in section MI1-1. The crack propogates from the 1/3 point shoulder joint and is severely spalled in the design lane.

Close-up view of a core hole through a transverse joint in section MI1-2. The joint is in good condition. The OGDC is visible in the core hole. Coring water drained rapidly from the hole.

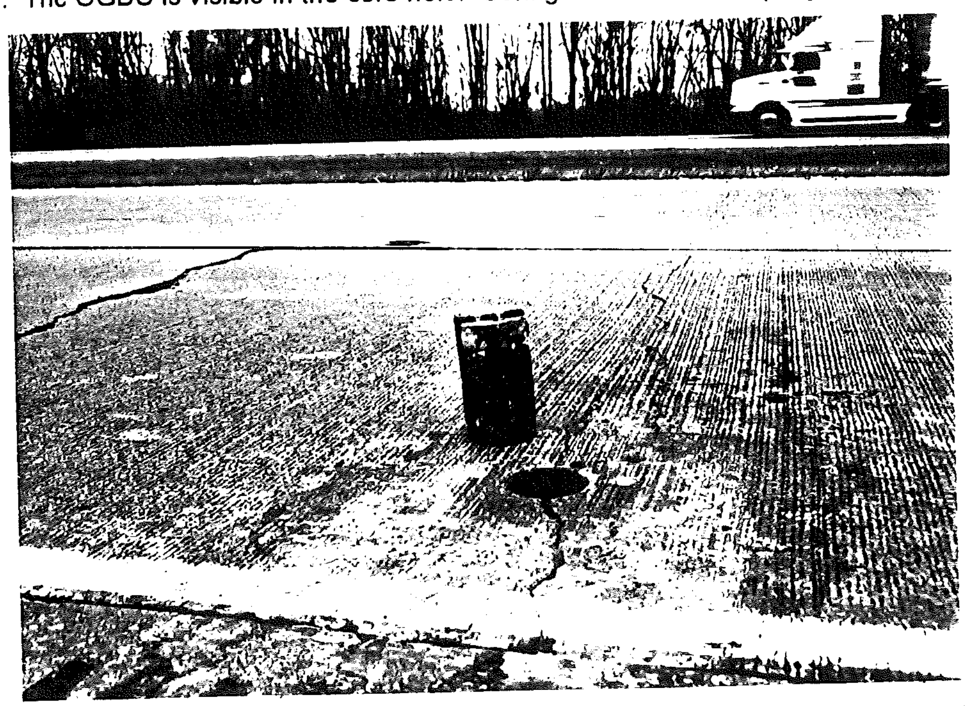

This photo shows two cracks of different severities in section MI1-2. Spalled and faulted cracks are common to this pavement section, though as seen here, some less severe cracks are also present. The more severe crack in this photo is a sympathy crack, while the other is not.

Close-up view of a cored sample in section MI-2 showing a shrinkage crack. The crack follows the tining pattern in the pavement, and extends approximately one inch deep into the concrete. This section contains recycled concrete.

Overview of part of section MI1-2. Note the level terrain. Seen here are core holes from midpanel, crack, and joint section cores. The sympathy cracking pattern is evident.

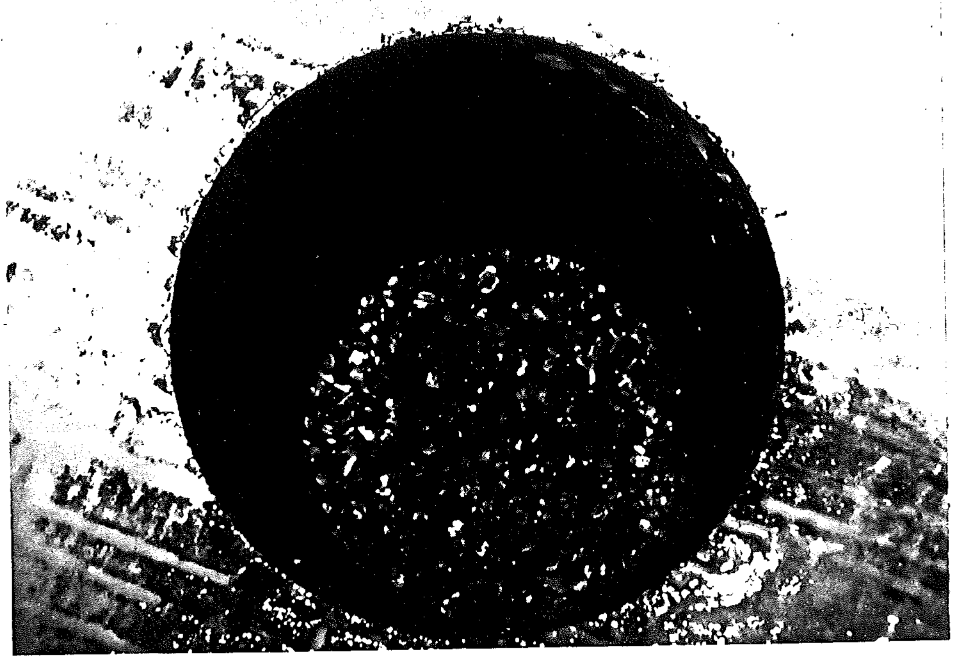

View of midpanel core hole in section MI1-3. The 5% cement stabilized peastone base course is visible in the bottom of the hole. Water from coring drained rapidly through the base course.

Overview of section MI1-3, showing a spalled sympathy crack in the foreground. The terrain is relatively level in this test section.

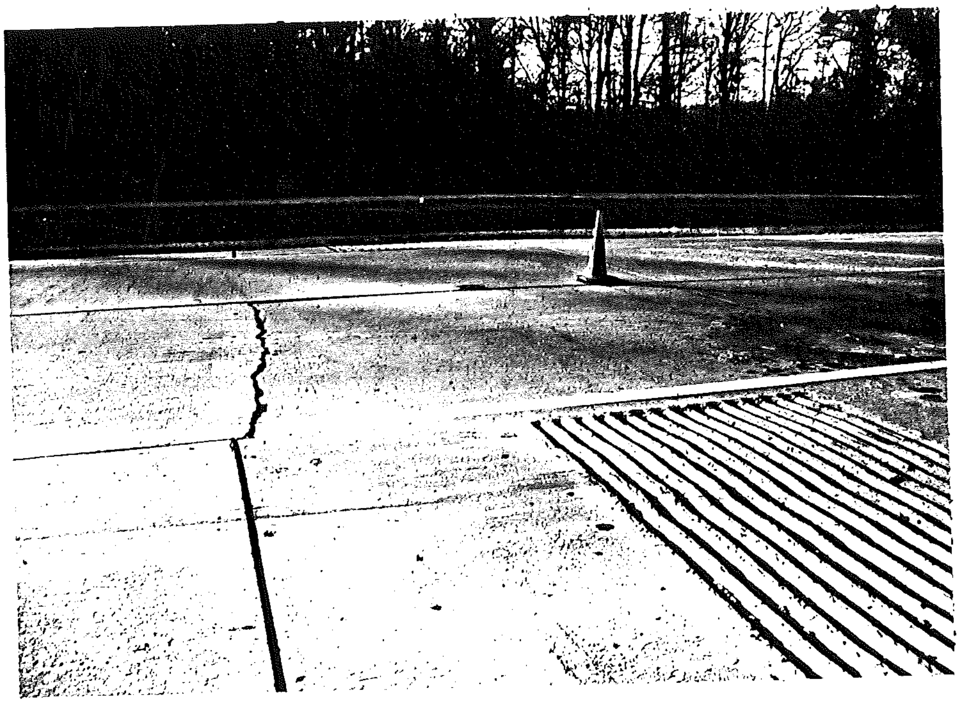

View of a typical spalled sympathy crack in section MI1-3. Propagating from the 1/3 point shoulder joint, this severe crack is found only in the design lane.

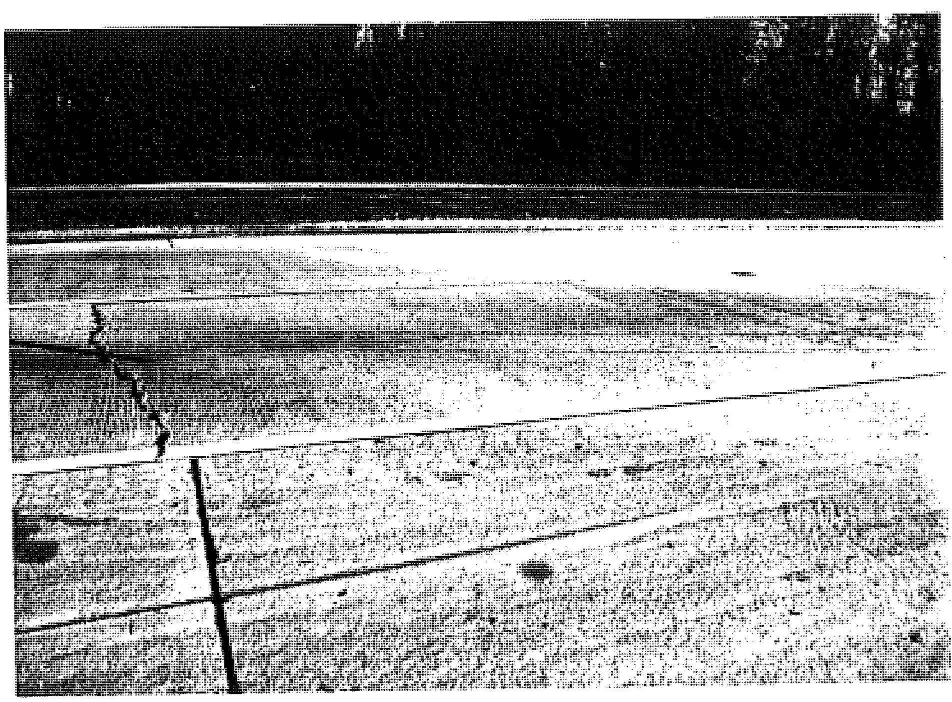

View of an offset sympathy crack which is deteriorated in the design lane. There is no damage in the passing lane. An intact transverse joint is visible in the right hand corner of the photo.

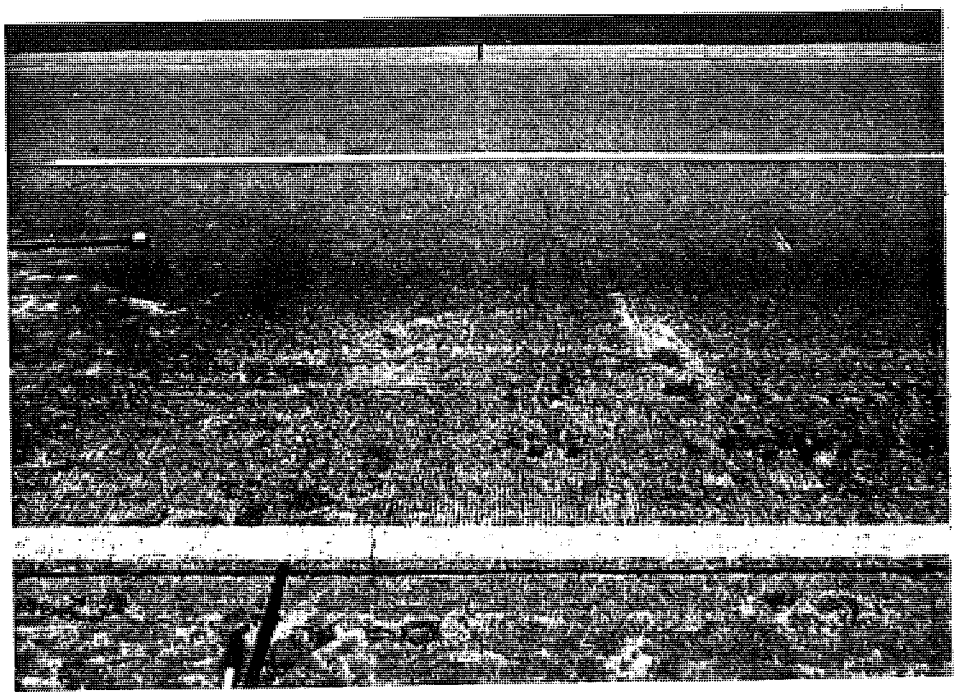

View of sympathy crack from section MI1-4. This photo is typical of many sympathy cracks in the section, showing little or no spalling or faulting.

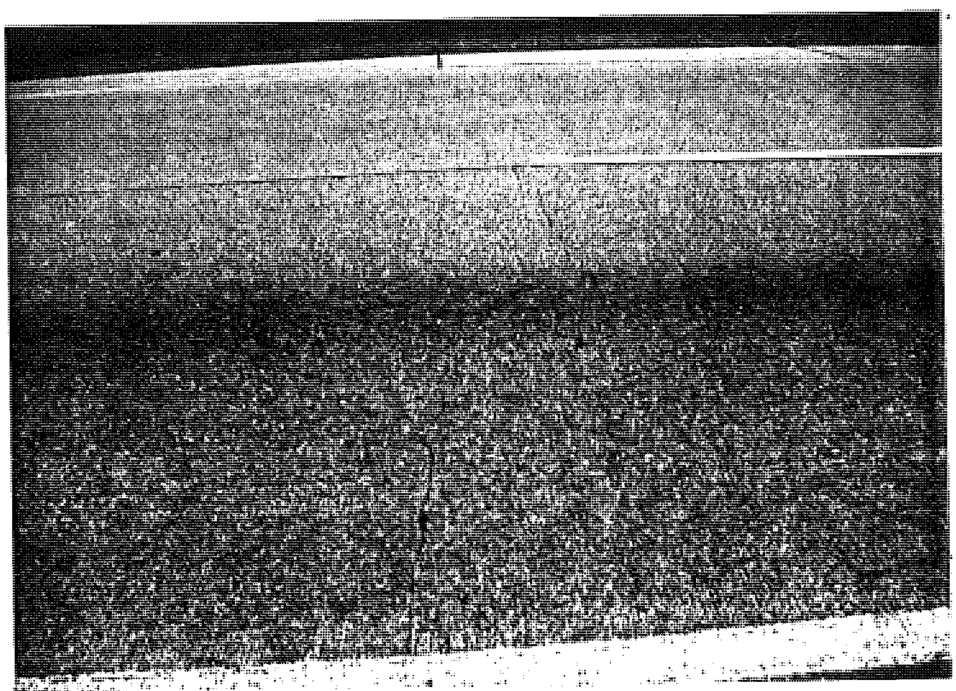

View of a low severity sympathy crack in section MI1-4. While some severe cracks are present in this test section, minor cracks such as this one are common.

Looking down a core hole from one of the few severe cracks in section MI1-4. Water used in coring remained in the core hole long after coring was completed. The DGBC thus shows a visibly lower water permeability.

Overview of section MI1-4. This, as all sections of the Lawrence project, is on relatively level ground, with little cut or fill necessary. An intact transverse joint is visible in the foreground.

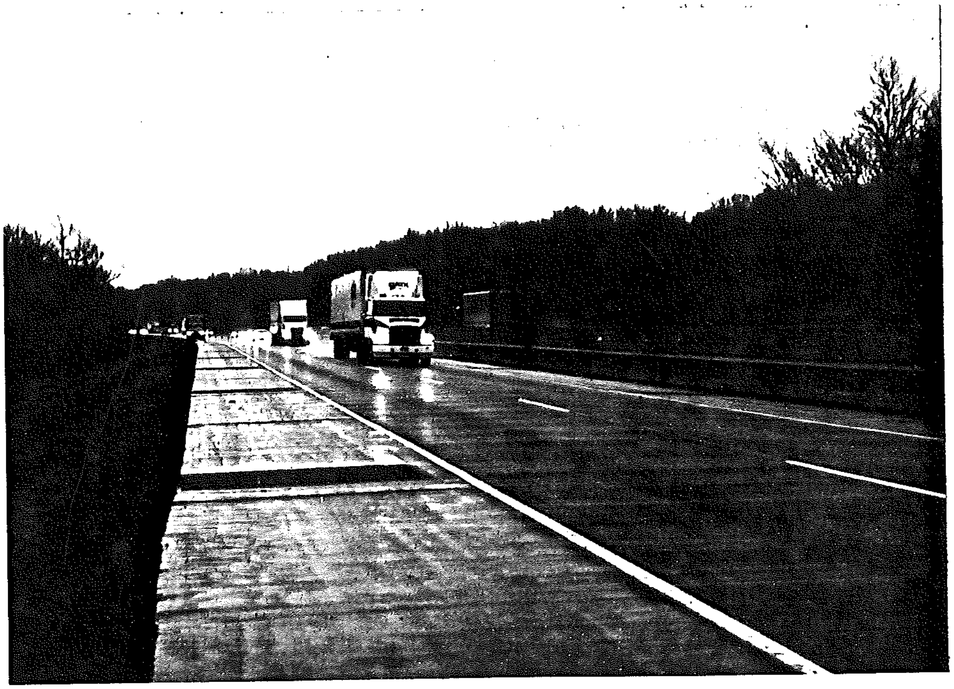

Overview of section MI2-1. This section (west bound) is on a gentle fill slope. The pavement is in excellent condition, with only two minor cracks found in the test section.

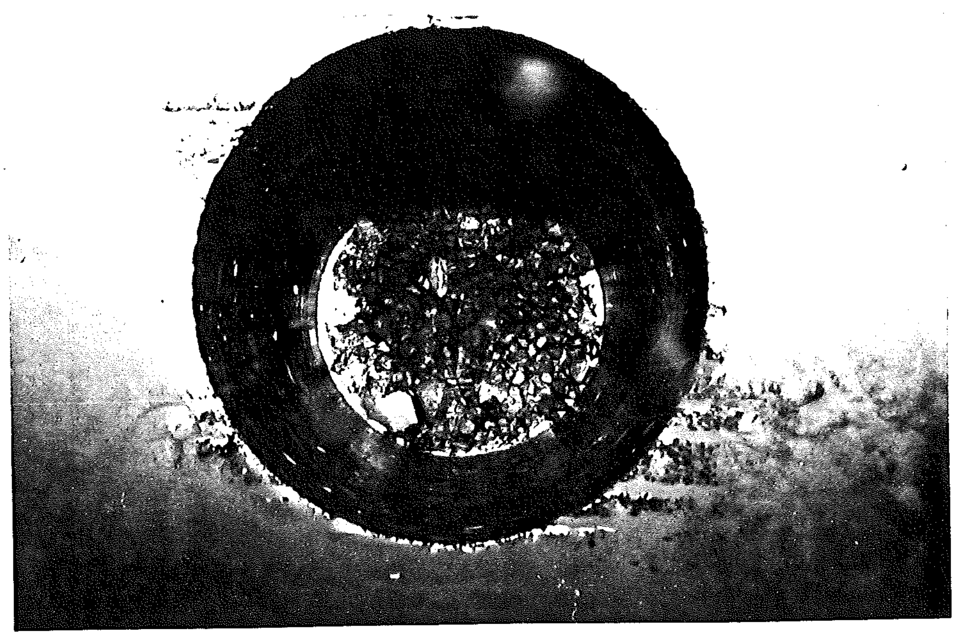

View of midpanel core hole in section MI2-1. Note the OGDC at the bottom of the hole. Water used in coring the concrete drained quickly.

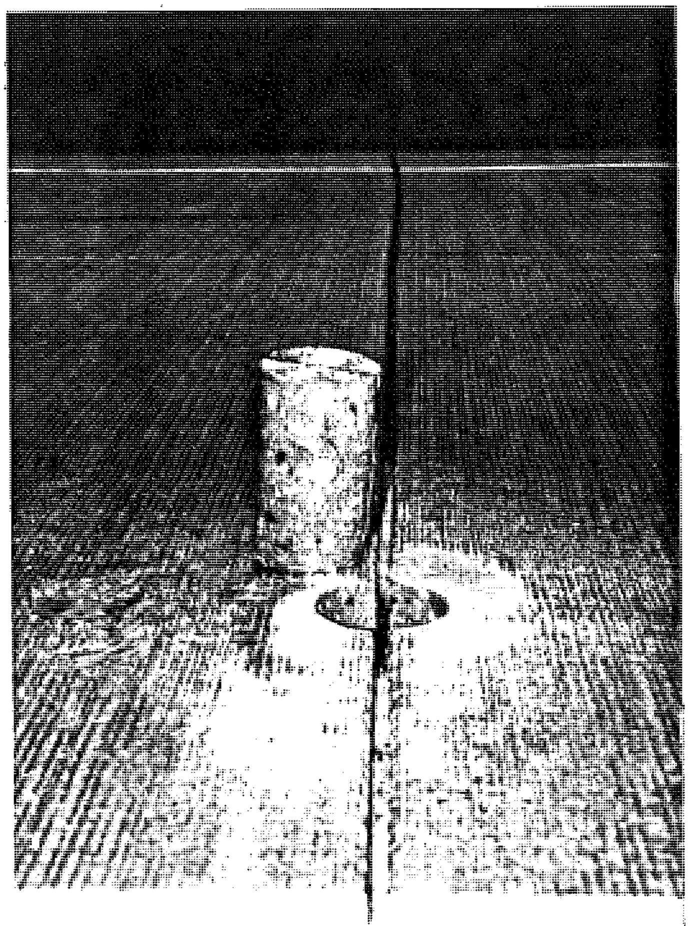

View of a typical transverse joint in section MI2-1 and the core of that joint. Note the good appearance of the joint and the dowel bar in the core.

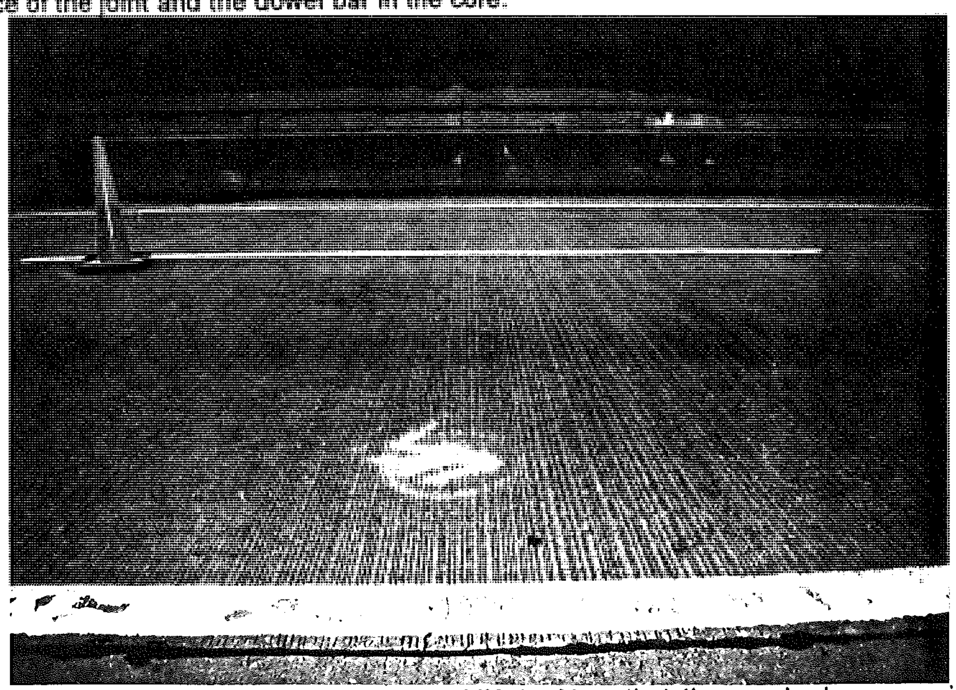

View of one of the two cracks found in section MI2-1. Note that the crack shows no signs of spalling or faulting.

View of transverse and longitudinal cracking in section MI2-2 (east bound). Note the severity of the cracks including faulting. Asphalt patching is already in place to fill in the lane-shoulder dropoff.

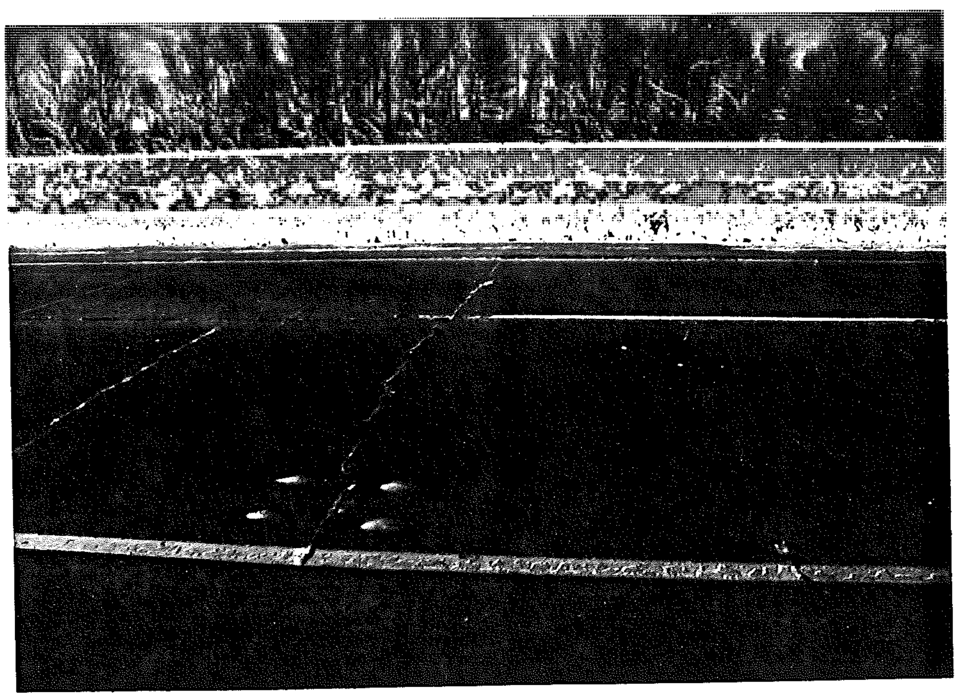

Transverse cracking in section MI2-2. Note the cracking across both lanes. Spalling of the cracks is evident.

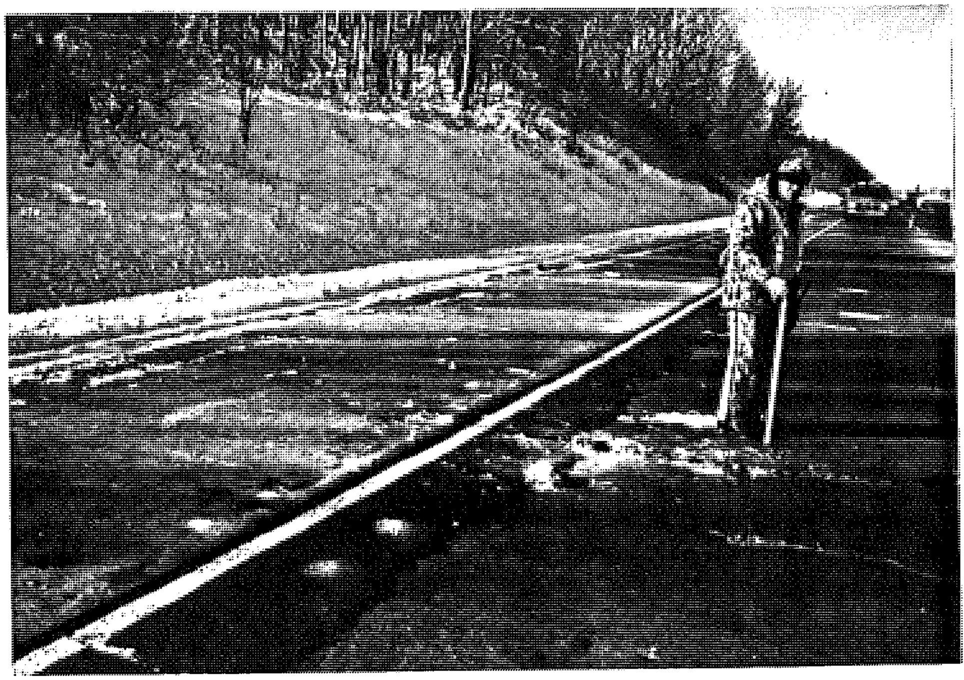

View of the cut slope in section MI2-2. Note the faulted cracks and lane shoulder dropoff that has been filled in with an asphalt patch.

View of crack core hole in section MI2-2. Note the severe settlement of the panel with faulting of approximately one inch.

Appendix 3: Strength and Stiffness

The modulus of elasticity of the concrete was determined in two specimens from each pavement section following the specifications of ASTM C469-65 (reapproved 1975). The recovered concrete cores were cut on one end and trimmed on the other to provide level end surfaces and to remove any skew that existed in the specimen. The cores were measured, weighed, sulfur capped, and saturated in water prior to testing. During testing, each specimen was loaded cyclically 3 times to a load of 80 kips to reach a strain of about 45% of the predicted ultimate strain. The first trial was used to seat the gages and the following two trials were recorded for the modulus computations. The stress-strain data was plotted and the best fit linear correlation was determined for each specimen.

After the cyclic loading for modulus determination, the strain measuring apparatus was removed and the specimen was loaded to failure in order to determine ultimate compressive strength. The ultimate strength was adjusted by a length to diameter ratio correction factor to get the final strength of each specimen. Compressive strength testing was performed in accordance with ASTM C42-90.

The first page of this appendix shows the summary table and corresponding graphs for modulus of elasticity and strength of the tested concrete cores. The following pages show the stress-strain curves with the supporting data for all of the specimens tested. The last page of the appendix shows the curve that provides the strength correction factor for length to diameter ratio. This curve is based on the corresponding values for correction given in the 1975 version of the C42-90 ASTM standards.

Summary of Results

Specimen	Strength (psi)	E Static (psi)
MI1-1-M1	5566	3.46E+06
MI1-1-M5 *	4921	2.89E+06
MI1-1-avg	**5244**	**3.18E+06**
MI1-2-M1 *	5883	3.79E+06
MI1-2-M5	6449	3.54E+06
MI1-2-avg	**6166**	**3.67E+06**
MI1-3-M5	6785	3.51E+06
MI1-3-avg	**6785**	**3.51E+06**
MI1-4-M1	6882	4.18E+06
MI1-4-M5	6224	3.75E+06
MI1-4-avg	**6553**	**3.97E+06**
MI2-1-M1	7012	3.93E+06
MI2-1-M5	6538	3.74E+06
MI2-1-avg	**6775**	**3.83E+06**
MI2-2-M1	5971	3.74E+06
MI2-2-M5	5831	3.71E+06
MI2-2-avg	**5901**	**3.73E+06**

* Testing done at a slower rate. All the other specimens were tested as per ASTM C469, rate 35±5 psi/sec.

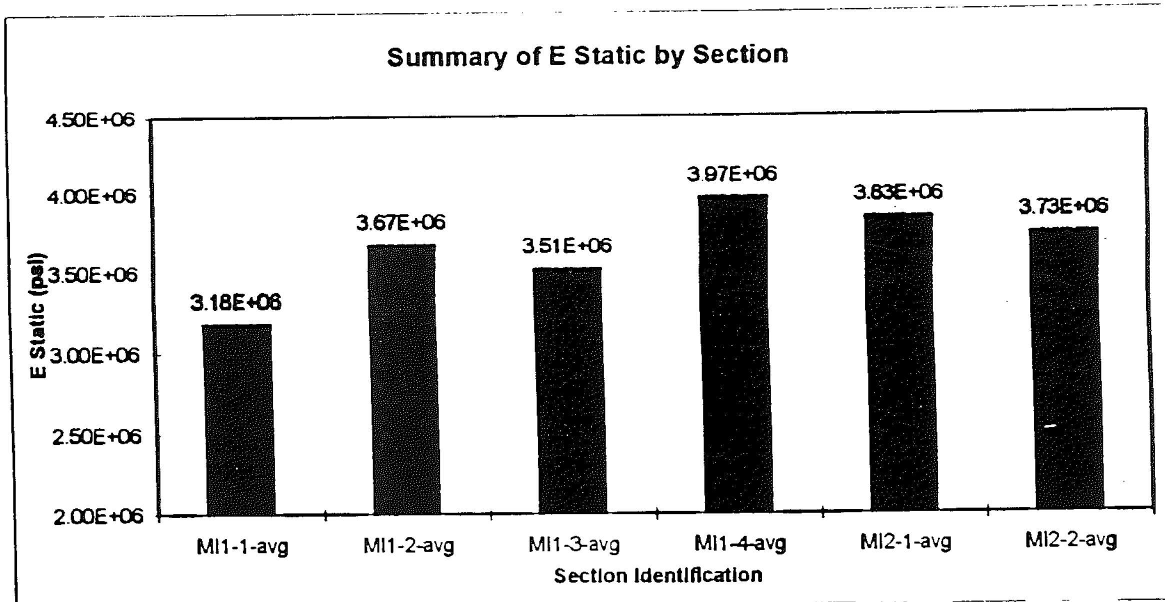

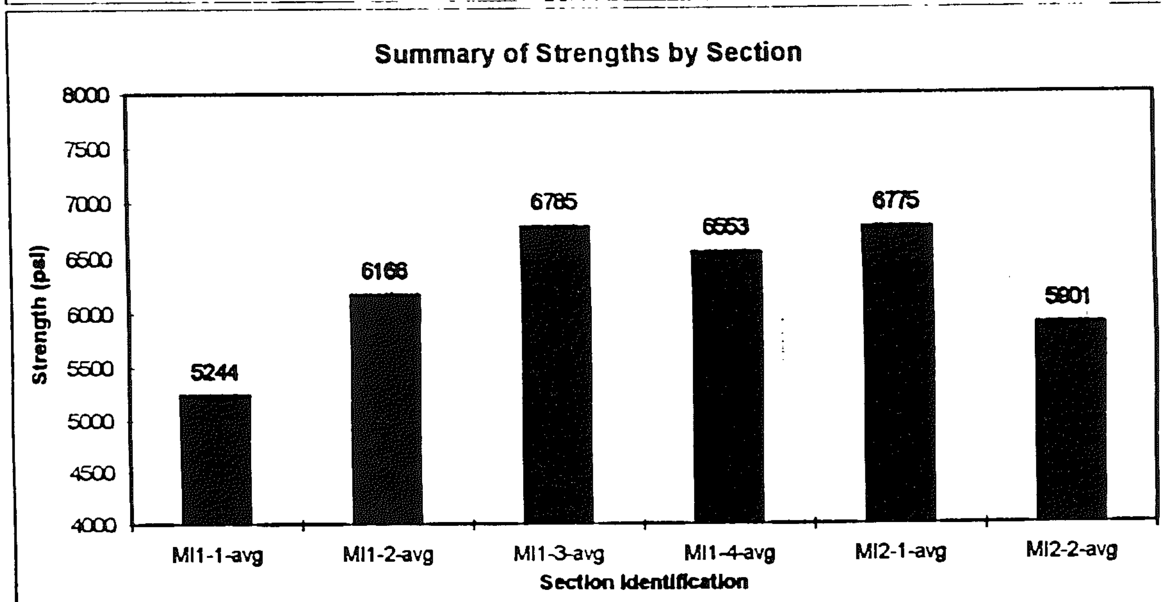

Static Modulus of Elasticity of Recycled Concrete.

(Drilled Cores)
Specimen: MI1-1-M1
Diameter: 5.93 in
Capped Length: 9.80 in
l/d Ratio: 1.65
Corr.Factor: 0.973
X-Section Area: 27.62 in2
Dist. between points of control: 6.1 in

Load lb	Vert.Gage(in) Trial 1	Trial 2	Average	Vert.Deff. dv (in)	Vert.Strn. (--)	Vert.Stress psi	E Static psi
0.00	0.0000	0.0000	0.0000	0.00000	0.00000	0.00	
5000.00	0.0005	0.0004	0.0005	0.00023	0.00004	181.04	4.91E+06
10000.00	0.0013	0.0013	0.0013	0.00065	0.00011	362.08	3.40E+06
20000.00	0.0026	0.0027	0.0027	0.00133	0.00022	724.15	3.33E+06
30000.00	0.0041	0.0042	0.0042	0.00208	0.00034	1086.23	3.19E+06
40000.00	0.0054	0.0055	0.0055	0.00273	0.00045	1448.31	3.24E+06
50000.00	0.0063	0.0071	0.0067	0.00335	0.00055	1810.38	3.30E+06
60000.00	0.0081	0.0082	0.0082	0.00408	0.00067	2172.46	3.25E+06
70000.00	0.0094	0.0096	0.0095	0.00475	0.00078	2534.54	3.25E+06
80000.00	0.0107	0.0110	0.0109	0.00543	0.00089	2896.61	3.26E+06
						Average Elastic Mod:	3.46E+06

Ult. Load (kip): 158.0
Ult. Strength (psi): 5721
Corr Strength (psi) 5566

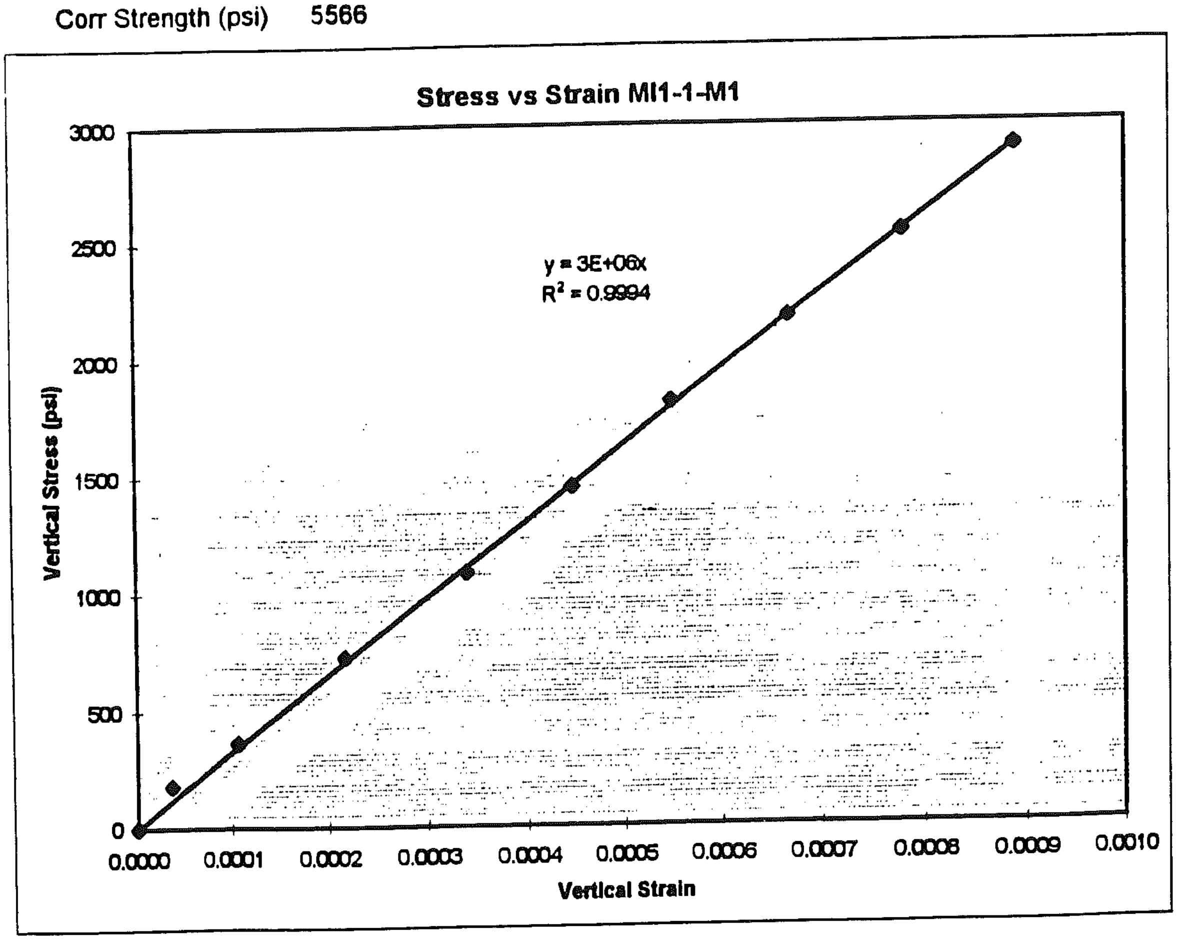

Static Modulus of Elasticity of Recycled Concrete.

(Drilled Cores)
Specimen: **MI1-1-M5**

Diameter:	5.94 in		Corr.Factor:	0.972
Capped Length:	9.725 in		X-Section Area:	27.71 in2
l/d Ratio:	1.64			

Dist. between points of control: 6.1 in

Load lb	Vert.Gage(in) Trial 1	Trial 2	Average	Vert.Deff. dv (in)	Vert.Strn. (--)	Vert.Stress psi	E Static psi
0.00	0.0000	0.0000	0.0000	0.00000	0.00000	0.00	
5000.00	0.0007	0.0007	0.0007	0.00035	0.00006	180.43	3.14E+06
10000.00	0.0016	0.0016	0.0016	0.00080	0.00013	360.86	2.75E+06
20000.00	0.0033	0.0033	0.0033	0.00165	0.00027	721.72	2.67E+06
30000.00	0.0048	0.0049	0.0049	0.00243	0.00040	1082.58	2.72E+06
40000.00	0.0062	0.0063	0.0063	0.00313	0.00051	1443.43	2.82E+06
50000.00	0.0075	0.0077	0.0076	0.00380	0.00062	1804.29	2.90E+06
60000.00	0.0089	0.0090	0.0090	0.00448	0.00073	2165.15	2.95E+06
70000.00	0.0101	0.0103	0.0102	0.00510	0.00084	2526.01	3.02E+06
80000.00	0.0115	0.0115	0.0115	0.00575	0.00094	2886.87	3.06E+06
					Average Elastic Mod:		2.89E+06

Ult. Load (kip): 140.3
Ult. Strength (psi): 5063
Corr Strength (psi) 4921

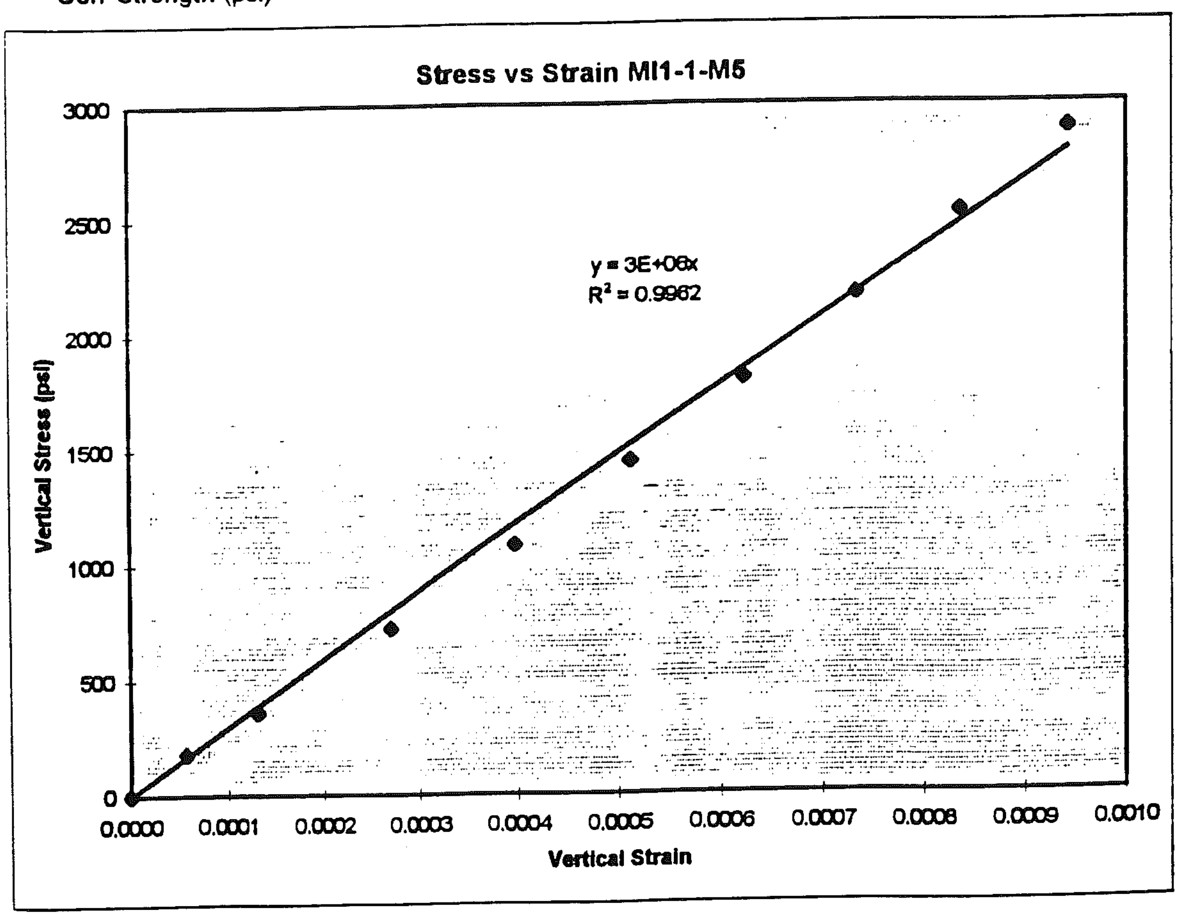

Static Modulus of Elasticity of Recycled Concrete.

(Drilled Cores)
Specimen: **MI1-2-M1**

Diameter:	5.925 in	Corr.Factor:	0.961
Capped Length:	8.95 in	X-Section Area:	27.57 in2
l/d Ratio:	1.51		
Dist. between points of control:		6.1 in	

Load	Vert.Gage(in)			Vert.Deff.	Vert.Strn.	Vert.Stress	E Static
lb	Trial 1	Trial 2	Average	dv (in)	(--)	psi	psi
0.00	0.0000	0.0000	0.0000	0.00000	0.00000	0.00	
5000.00	0.0005	0.0004	0.0005	0.00023	0.00004	181.34	4.92E+06
10000.00	0.0011	0.0011	0.0011	0.00055	0.00009	362.69	4.02E+06
20000.00	0.0024	0.0024	0.0024	0.00120	0.00020	725.38	3.69E+06
30000.00	0.0038	0.0038	0.0038	0.00190	0.00031	1088.06	3.49E+06
40000.00	0.0050	0.0050	0.0050	0.00250	0.00041	1450.75	3.54E+06
50000.00	0.0063	0.0063	0.0063	0.00315	0.00052	1813.44	3.51E+06
60000.00	0.0075	0.0074	0.0075	0.00373	0.00061	2176.13	3.56E+06
70000.00	0.0086	0.0086	0.0086	0.00430	0.00070	2538.82	3.60E+06
					Average Elastic Mod:		3.79E+06

Ult. Load (kip): 168.8
Ult. Strength (psi): 6122
Corr Strength (psi) 5883

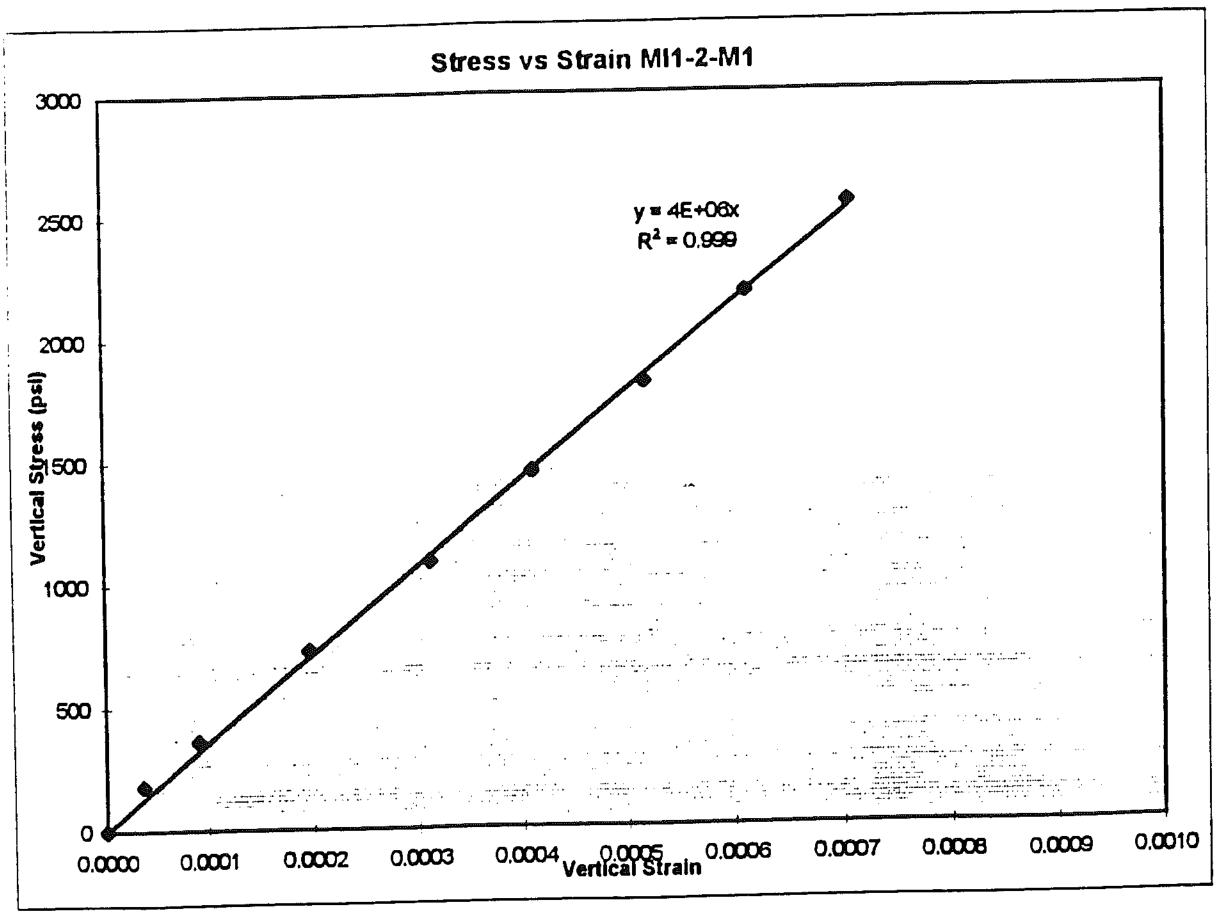

Static Modulus of Elasticity of Recycled Concrete.

(Drilled Cores)

Specimen: **MI1-2-M5**

Diameter: 5.94 in | Corr.Factor: 0.976

Capped Length: 10.05 in | X-Section Area: 27.71 in2

l/d Ratio: 1.69

Dist. between points of control: 6.1 in

Load lb	Vert.Gage(in) Trial 1	Trial 2	Average	Vert.Deff. dv (in)	Vert.Strn. (--)	Vert.Stress psi	E Static psi
0.00	0.0000	0.0000	0.0000	0.00000	0.00000	0.00	
5000.00	0.0006	0.0007	0.0007	0.00033	0.00005	180.43	3.39E+06
10000.00	0.0012	0.0014	0.0013	0.00065	0.00011	360.86	3.39E+06
20000.00	0.0027	0.0027	0.0027	0.00135	0.00022	721.72	3.26E+06
30000.00	0.0037	0.0038	0.0038	0.00188	0.00031	1082.58	3.52E+06
40000.00	0.0049	0.0050	0.0050	0.00248	0.00041	1443.43	3.56E+06
50000.00	0.0060	0.0063	0.0062	0.00308	0.00050	1804.29	3.58E+06
60000.00	0.0071	0.0072	0.0072	0.00358	0.00059	2165.15	3.69E+06
70000.00	0.0083	0.0082	0.0083	0.00413	0.00068	2526.01	3.74E+06
80000.00	0.0093	0.0094	0.0094	0.00468	0.00077	2886.87	3.77E+06
					Average Elastic Mod:		3.54E+06

Ult. Load (kip): 183.1

Ult. Strength (psi): 6607

Corr Strength (psi) 6449

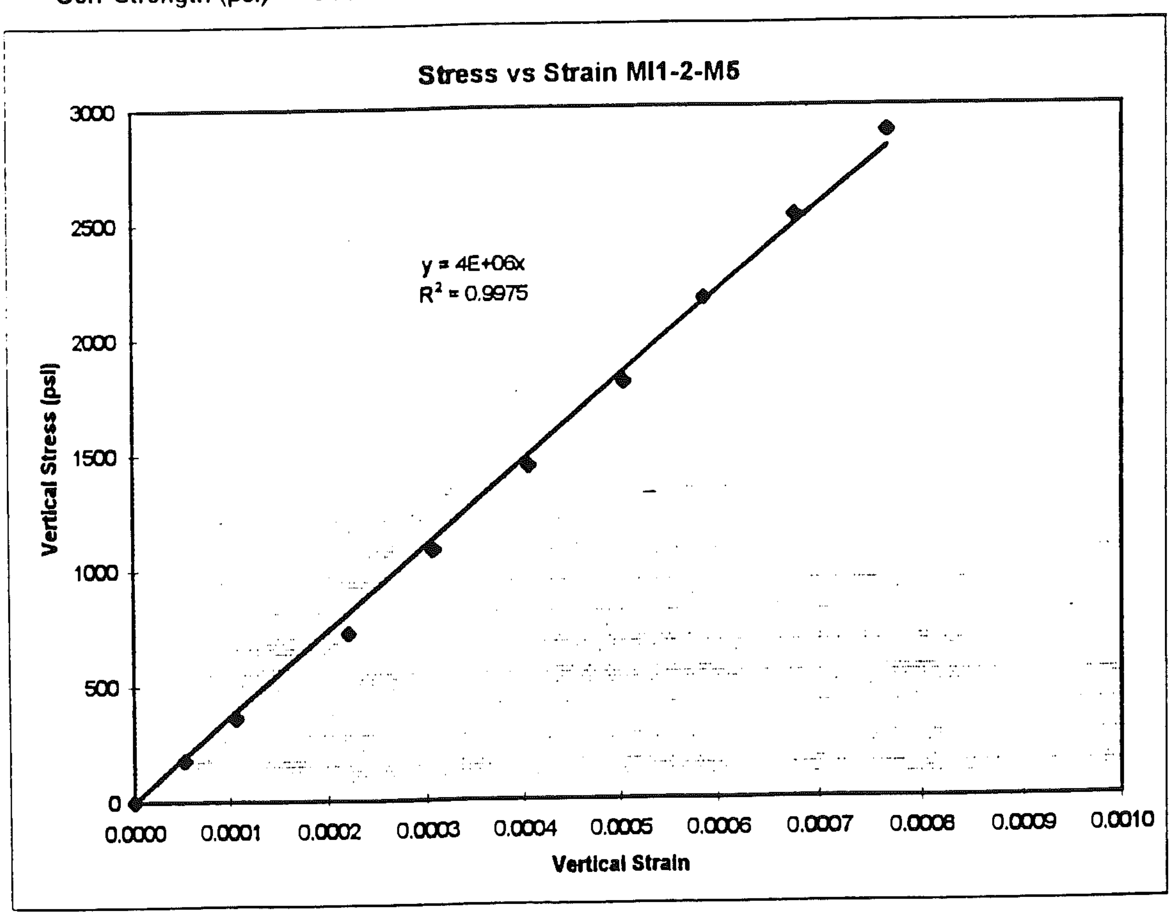

Static Modulus of Elasticity of Recycled Concrete.

(Drilled Cores)
Specimen: **MI1-3-M5**
Diameter: 5.93 in
Capped Length: 9.4 in
l/d Ratio: 1.59
Dist. between points of control: 6.1 in

Corr.Factor: 0.969
X-Section Area: 27.62 in2

Load lb	Vert.Gage(in) Trial 1	Trial 2	Average	Vert.Deff. dv (in)	Vert.Strn. (--)	Vert.Stress psi	E Static psi
0.00	0.0000	0.0000	0.0000	0.00000	0.00000	0.00	
5000.00	0.0005	0.0007	0.0006	0.00030	0.00005	181.04	3.68E+06
10000.00	0.0012	0.0013	0.0013	0.00063	0.00010	362.08	3.53E+06
20000.00	0.0025	0.0027	0.0026	0.00130	0.00021	724.15	3.40E+06
30000.00	0.0038	0.0040	0.0039	0.00195	0.00032	1086.23	3.40E+06
40000.00	0.0053	0.0053	0.0053	0.00265	0.00043	1448.31	3.33E+06
50000.00	0.0065	0.0065	0.0065	0.00325	0.00053	1810.38	3.40E+06
60000.00	0.0074	0.0074	0.0074	0.00370	0.00061	2172.46	3.58E+06
70000.00	0.0087	0.0085	0.0086	0.00430	0.00070	2534.54	3.60E+06
80000.00	0.0097	0.0095	0.0096	0.00480	0.00079	2896.61	3.68E+06
					Average Elastic Mod:		3.51E+06

Ult. Load (kip): 193.4
Ult. Strength (psi): 7003
Corr Strength (psi) 6785

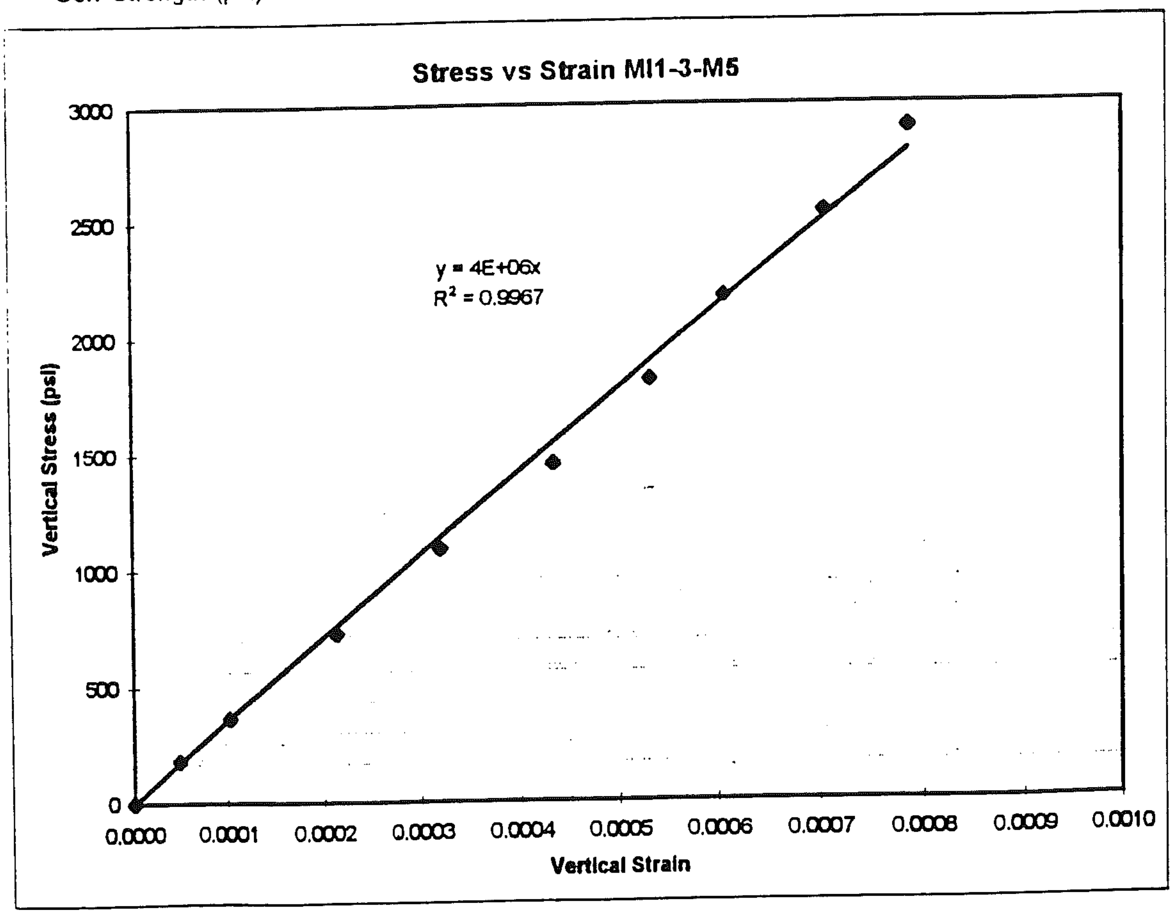

Static Modulus of Elasticity of Recycled Concrete.

(Drilled Cores)
Specimen: **MI1-4-M1**

Diameter:	5.94 in	Corr.Factor:	0.970
Capped Length:	9.55 in	X-Section Area:	27.71 in2
l/d Ratio:	1.61		

Dist. between points of control: 6.1 in

Load lb	Vert.Gage(in) Trial 1	Trial 2	Average	Vert.Deff. dv (in)	Vert.Strn. (--)	Vert.Stress psi	E Static psi
0.00	0.0000	0.0000	0.0000	0.00000	0.00000	0.00	
5000.00	0.0004	0.0007	0.0006	0.00028	0.00005	180.43	4.00E+06
10000.00	0.0011	0.0012	0.0012	0.00058	0.00009	360.86	3.83E+06
20000.00	0.0023	0.0022	0.0023	0.00113	0.00018	721.72	3.91E+06
30000.00	0.0032	0.0032	0.0032	0.00160	0.00026	1082.58	4.13E+06
40000.00	0.0041	0.0042	0.0042	0.00208	0.00034	1443.43	4.24E+06
50000.00	0.0051	0.0051	0.0051	0.00255	0.00042	1804.29	4.32E+06
60000.00	0.0058	0.0061	0.0060	0.00298	0.00049	2165.15	4.44E+06
70000.00	0.0070	0.0071	0.0071	0.00353	0.00058	2526.01	4.37E+06
80000.00	0.0080	0.0080	0.0080	0.00400	0.00066	2886.87	4.40E+06
					Average Elastic Mod:		4.18E+06

Ult. Load (kip): 196.6
Ult. Strength (psi): 7094
Corr Strength (psi) 6882

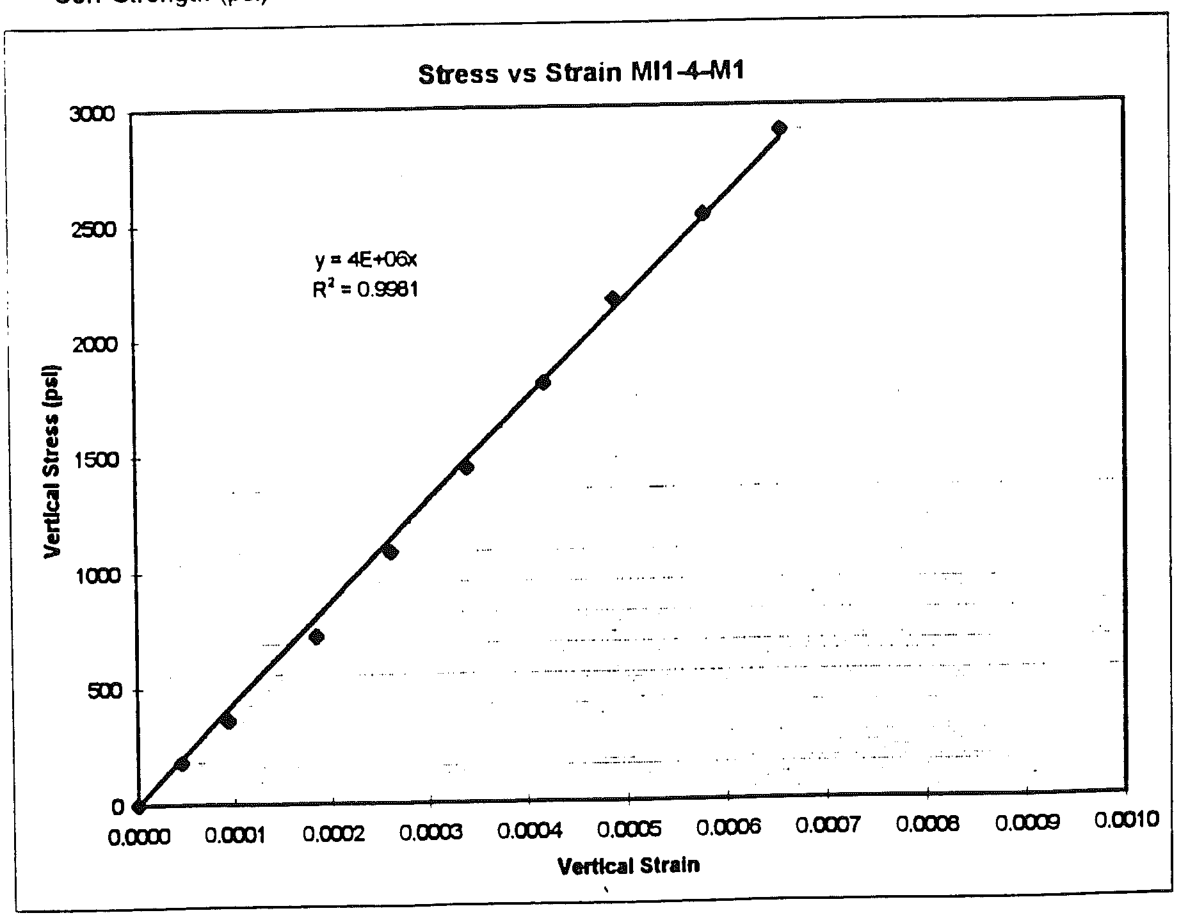

Static Modulus of Elasticity of Recycled Concrete.

(Drilled Cores)
Specimen: **MI1-4-M5**
Diameter: 5.96 in
Capped Length: 9.0 in
l/d Ratio: 1.51
Dist. between points of control: 6.1 in

Corr.Factor: 0.961
X-Section Area: 27.90 in2

Load lb	Vert.Gage(in) Trial 1	Trial 2	Average	Vert.Deff. dv (in)	Vert.Strn. (--)	Vert.Stress psi	E Static psi
0.00	0.0000	0.0000	0.0000	0.00000	0.00000	0.00	
5000.00	0.0007	0.0006	0.0007	0.00033	0.00005	179.22	3.36E+06
10000.00	0.0014	0.0013	0.0014	0.00068	0.00011	358.44	3.24E+06
20000.00	0.0025	0.0024	0.0025	0.00123	0.00020	716.88	3.57E+06
30000.00	0.0036	0.0035	0.0036	0.00178	0.00029	1075.32	3.70E+06
40000.00	0.0047	0.0047	0.0047	0.00235	0.00039	1433.76	3.72E+06
50000.00	0.0055	0.0057	0.0056	0.00280	0.00046	1792.20	3.90E+06
60000.00	0.0065	0.0066	0.0066	0.00328	0.00054	2150.65	4.01E+06
70000.00	0.0074	0.0075	0.0075	0.00373	0.00061	2509.09	4.11E+06
80000.00	0.0084	0.0084	0.0084	0.00420	0.00069	2867.53	4.16E+06
					Average Elastic Mod:		3.75E+06

Ult. Load (kip): 180.7
Ult. Strength (psi): 6477
Corr Strength (psi): 6224

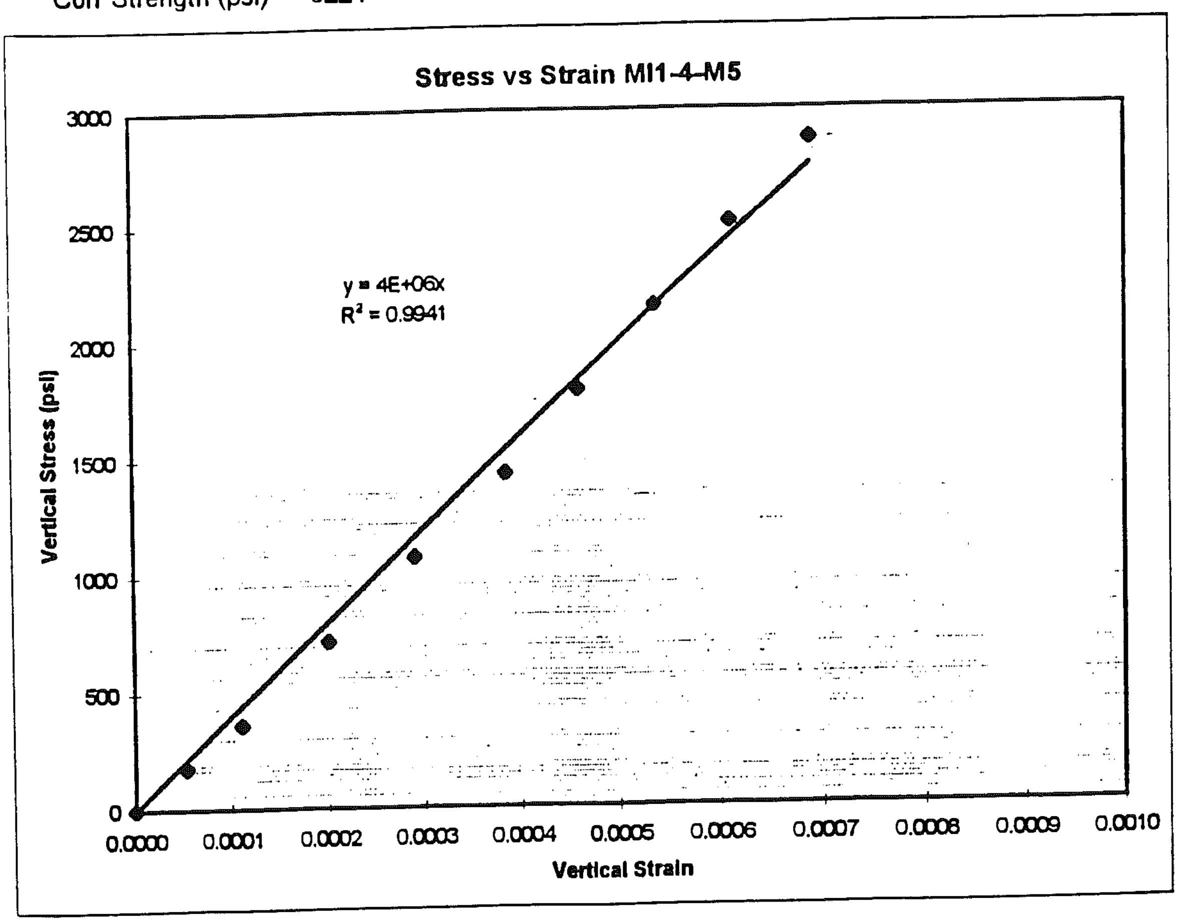

Static Modulus of Elasticity of Recycled Concrete.

(Drilled Cores)
Specimen: **MI2-1-M1**

Diameter: 5.94 in
Capped Length: 9.9 in
l/d Ratio: 1.66
Dist. between points of control: 6.1 in

Corr.Factor: 0.973
X-Section Area: 27.71 in2

Load lb	Vert.Gage(in) Trial 1	Trial 2	Average	Vert.Deff. dv (in)	Vert.Strn. (--)	Vert.Stress psi	E Static psi
0.00	0.0000	0.0000	0.0000	0.00000	0.00000	0.00	
5000.00	0.0005	0.0006	0.0006	0.00028	0.00005	180.43	4.00E+06
10000.00	0.0013	0.0013	0.0013	0.00065	0.00011	360.86	3.39E+06
20000.00	0.0023	0.0025	0.0024	0.00120	0.00020	721.72	3.67E+06
30000.00	0.0036	0.0035	0.0036	0.00178	0.00029	1082.58	3.72E+06
40000.00	0.0045	0.0044	0.0045	0.00223	0.00036	1443.43	3.96E+06
50000.00	0.0055	0.0054	0.0055	0.00273	0.00045	1804.29	4.04E+06
60000.00	0.0064	0.0064	0.0064	0.00320	0.00052	2165.15	4.13E+06
70000.00	0.0074	0.0073	0.0074	0.00368	0.00060	2526.01	4.19E+06
80000.00	0.0083	0.0082	0.0083	0.00413	0.00068	2886.87	4.27E+06
					Average Elastic Mod:		3.93E+06

Ult. Load (kip): 199.7
Ult. Strength (psi): 7206
Corr Strength (psi) 7012

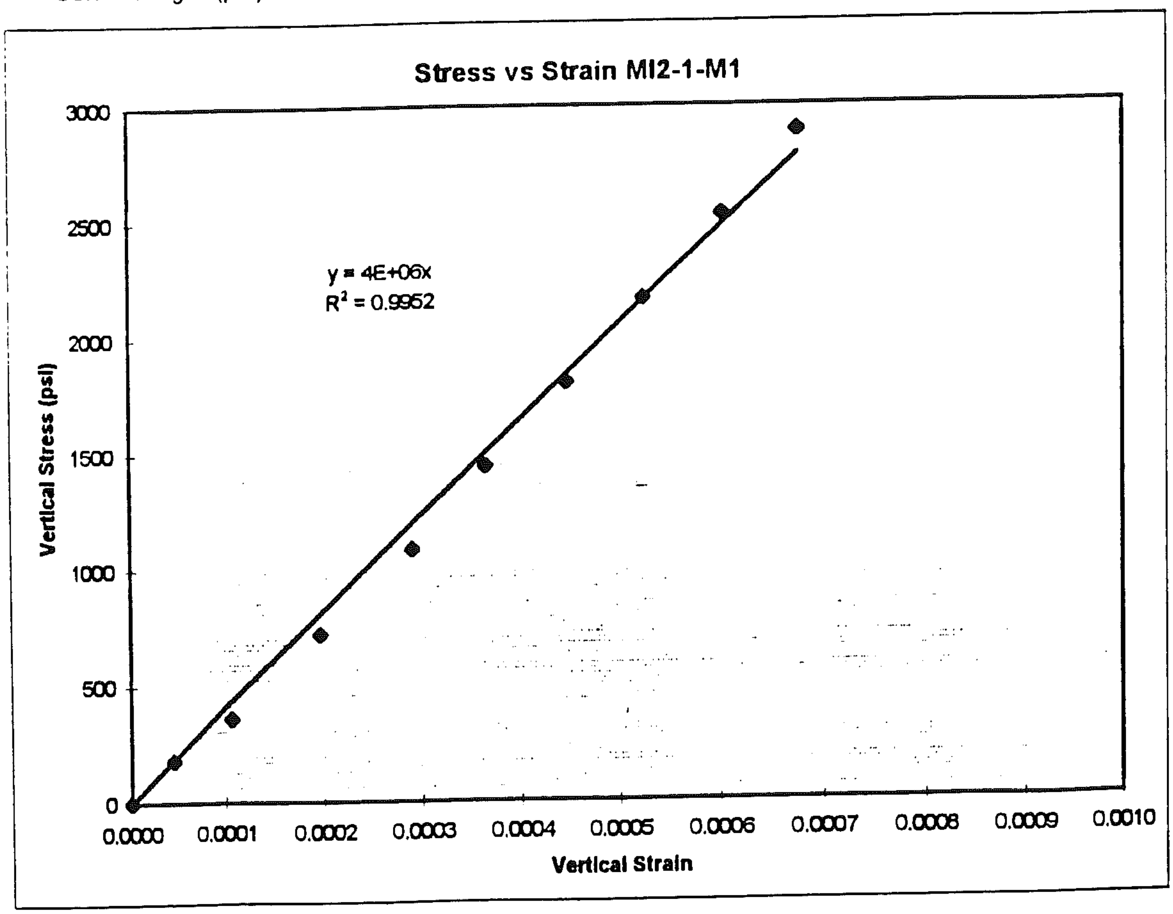

Static Modulus of Elasticity of Recycled Concrete.

(Drilled Cores)
Specimen: **MI2-1-M5**
Diameter: 5.91 in
Capped Length: 9.5 in
l/d Ratio: 1.61
Corr.Factor: 0.970
X-Section Area: 27.43 in2
Dist. between points of control: 6.1 in

Load lb	Vert.Gage(in) Trial 1	Vert.Gage(in) Trial 2	Vert.Gage(in) Average	Vert.Deff. dv (in)	Vert.Strn. (--)	Vert.Stress psi	E Static psi
0.00	0.0000	0.0000	0.0000	0.00000	0.00000	0.00	
5000.00	0.0006	0.0007	0.0007	0.00033	0.00005	182.27	3.42E+06
10000.00	0.0012	0.0013	0.0013	0.00063	0.00010	364.53	3.56E+06
20000.00	0.0024	0.0026	0.0025	0.00125	0.00020	729.06	3.56E+06
30000.00	0.0037	0.0037	0.0037	0.00185	0.00030	1093.59	3.61E+06
40000.00	0.0047	0.0047	0.0047	0.00235	0.00039	1458.13	3.78E+06
50000.00	0.0056	0.0058	0.0057	0.00285	0.00047	1822.66	3.90E+06
60000.00	0.0068	0.0069	0.0069	0.00343	0.00056	2187.19	3.90E+06
70000.00	0.0078	0.0079	0.0079	0.00393	0.00064	2551.72	3.97E+06
80000.00	0.0090	0.0090	0.0090	0.00450	0.00074	2916.25	3.95E+06
					Average Elastic Mod:		3.74E+06

Ult. Load (kip): 184.9
Ult. Strength (psi): 6740
Corr Strength (psi) 6538

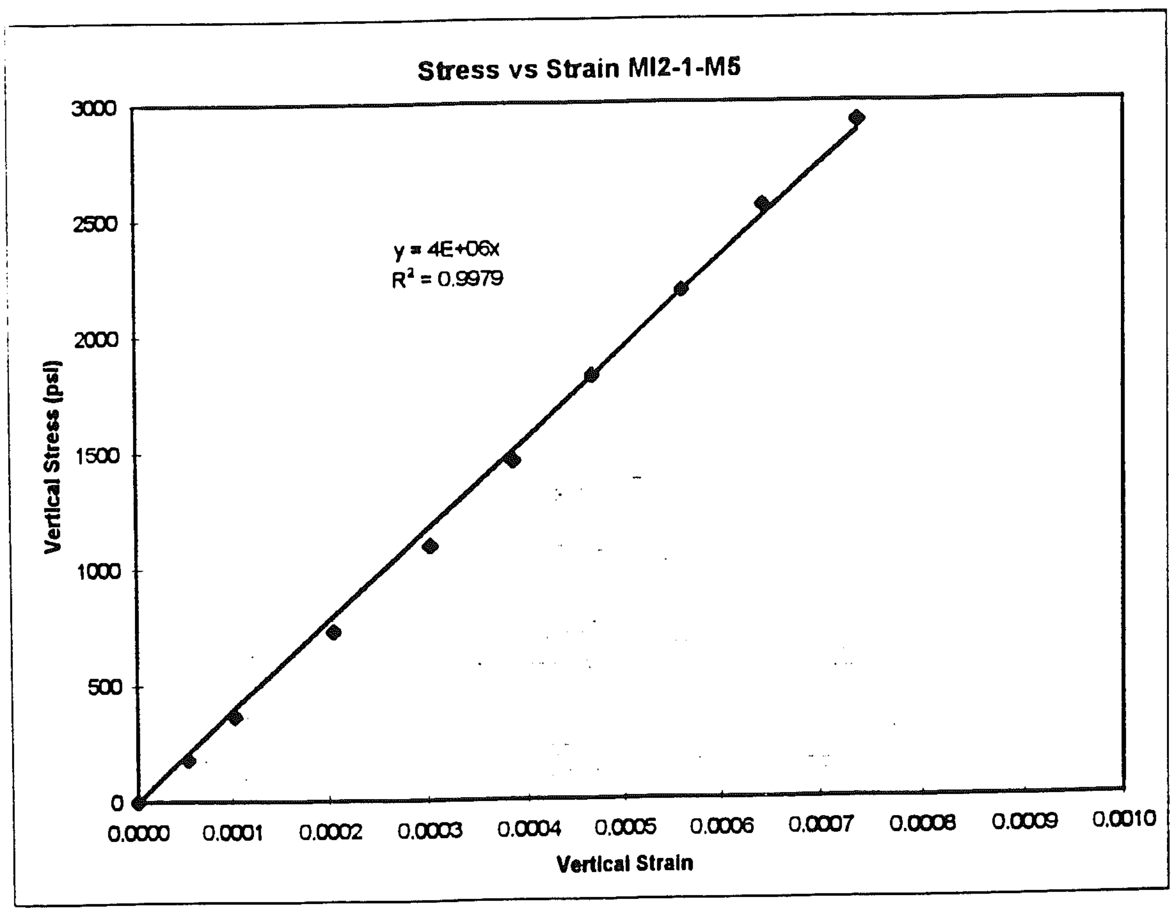

Static Modulus of Elasticity of Recycled Concrete.

(Drilled Cores)
Specimen: **MI2-2-M1**

Diameter: 5.94 in
Capped Length: 9.4 in
l/d Ratio: 1.57
Dist. between points of control: 6.1 in

Corr.Factor: 0.966
X-Section Area: 27.71 in2

Load lb	Vert.Gage(in) Trial 1	Trial 2	Average	Vert.Deff. dv (in)	Vert.Strn. (--)	Vert.Stress psi	E Static psi
0.00	0.0000	0.0000	0.0000	0.00000	0.00000	0.00	
5000.00	0.0007	0.0007	0.0007	0.00035	0.00006	180.43	3.14E+06
10000.00	0.0014	0.0014	0.0014	0.00070	0.00011	360.86	3.14E+06
20000.00	0.0024	0.0025	0.0025	0.00123	0.00020	721.72	3.59E+06
30000.00	0.0036	0.0035	0.0036	0.00178	0.00029	1082.58	3.72E+06
40000.00	0.0045	0.0047	0.0046	0.00230	0.00038	1443.43	3.83E+06
50000.00	0.0056	0.0056	0.0056	0.00280	0.00046	1804.29	3.93E+06
60000.00	0.0065	0.0065	0.0065	0.00325	0.00053	2165.15	4.06E+06
70000.00	0.0078	0.0074	0.0076	0.00380	0.00062	2526.01	4.05E+06
80000.00	0.0084	0.0085	0.0085	0.00423	0.00069	2886.87	4.17E+06
						Average Elastic Mod:	3.74E+06

Ult. Load (kip): 171.3
Ult. Strength (psi): 6182
Corr Strength (psi) 5971

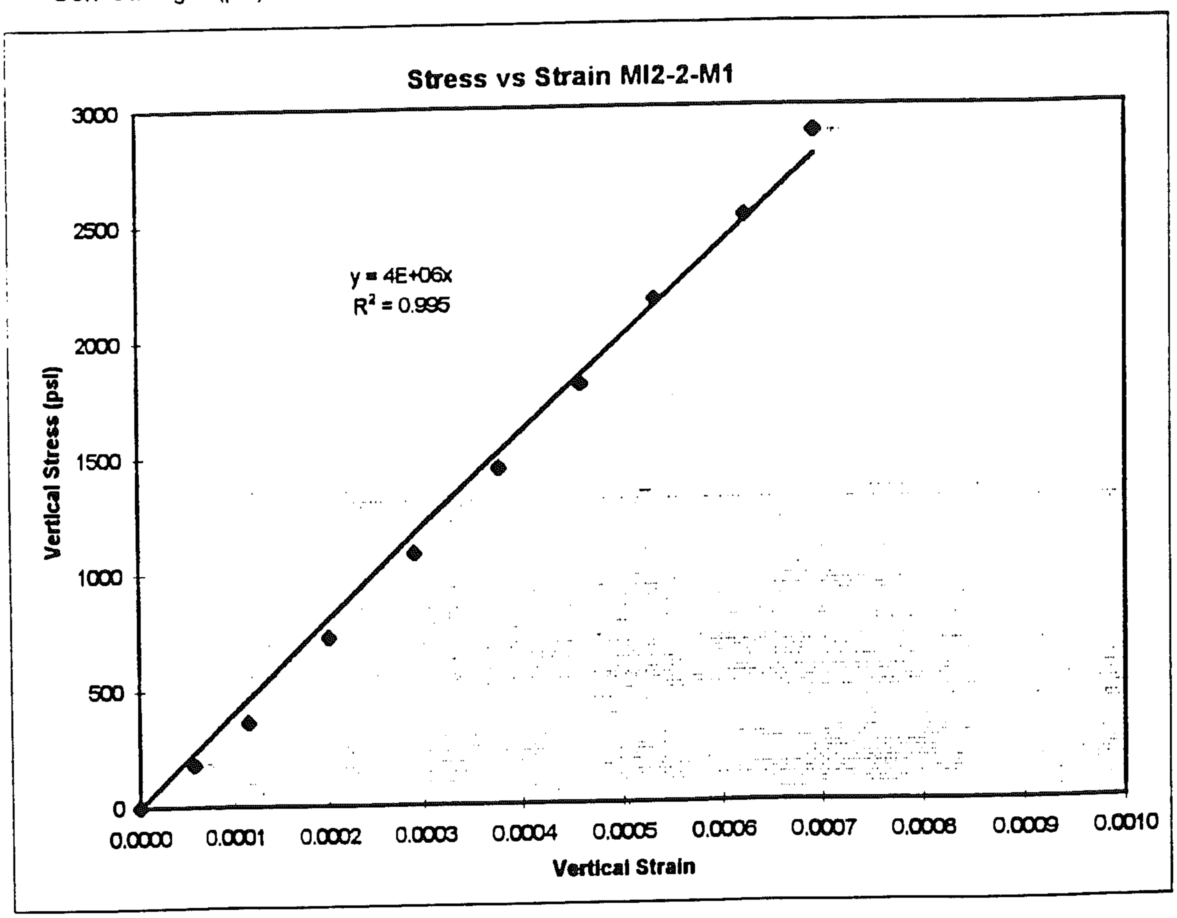

Static Modulus of Elasticity of Recycled Concrete.

(Drilled Cores)

Specimen: **MI2-2-M5**

Diameter: 5.94 in

Capped Length: 9.7 in

l/d Ratio: 1.63

Corr.Factor: 0.971

X-Section Area: 27.71 in2

Dist. between points of control: 6.1 in

Load lb	Vert.Gage(in) Trial 1	Trial 2	Average	Vert.Deff. dv (in)	Vert.Strn. (--)	Vert.Stress psi	E Static psi
0.00	0.0000	0.0000	0.0000	0.00000	0.00000	0.00	
5000.00	0.0007	0.0008	0.0008	0.00038	0.00006	180.43	2.93E+06
10000.00	0.0014	0.0014	0.0014	0.00070	0.00011	360.86	3.14E+06
20000.00	0.0025	0.0024	0.0025	0.00123	0.00020	721.72	3.59E+06
30000.00	0.0036	0.0035	0.0036	0.00178	0.00029	1082.58	3.72E+06
40000.00	0.0047	0.0046	0.0047	0.00233	0.00038	1443.43	3.79E+06
50000.00	0.0056	0.0055	0.0056	0.00278	0.00045	1804.29	3.97E+06
60000.00	0.0066	0.0065	0.0066	0.00328	0.00054	2165.15	4.03E+06
70000.00	0.0075	0.0074	0.0075	0.00373	0.00061	2526.01	4.14E+06
80000.00	0.0087	0.0085	0.0086	0.00430	0.00070	2886.87	4.10E+06
						Average Elastic Mod:	3.71E+06

Ult. Load (kip): 166.4

Ult. Strength (psi): 6005

Corr Strength (psi) 5831

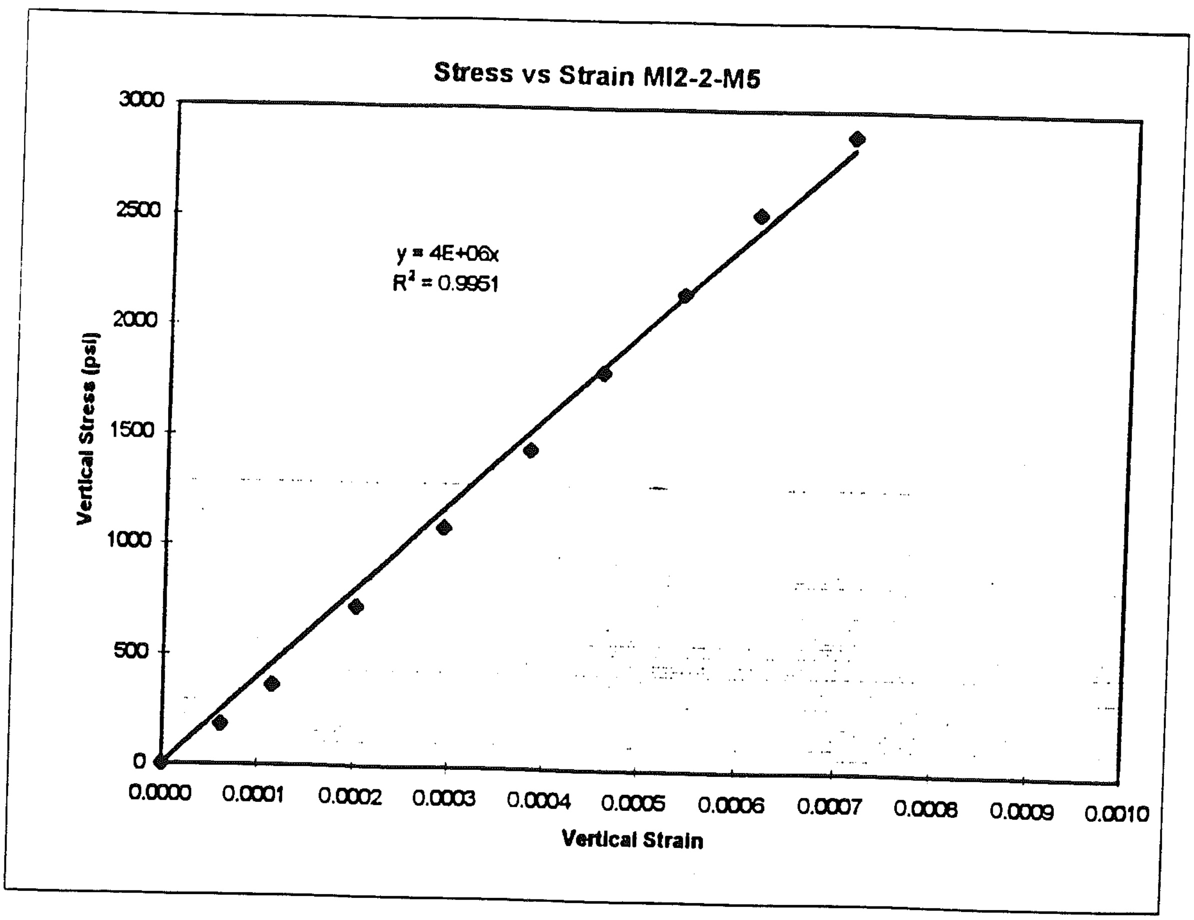

Cylinder Strength Correction Factor for Length to Diameter Ratio

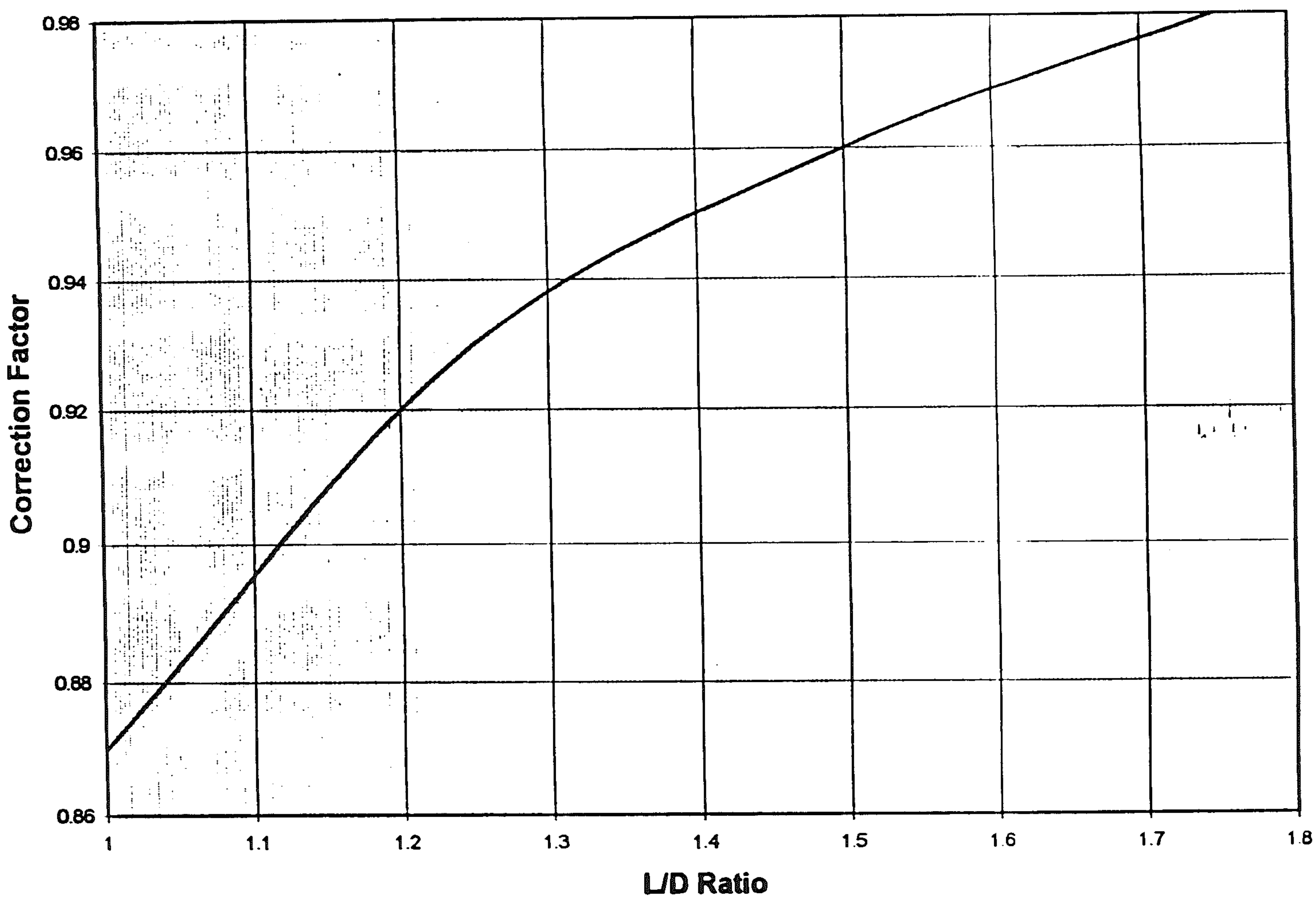

Appendix 4: Falling Weight Deflectometer Testing

This appendix presents the results of an analysis performed on a set of Falling Weight Deflectometer (FWD) tests conducted at various sections of the two projects. The rigid pavement sections made with recycled concrete aggregates were compared to a control section made of peastone aggregates. The deflection bowls, elastic modulus of the PCC and modulus of subgrade reaction, k of the supporting medium were compared. A manual computation method suggested by Ioannides[13] and the BOUSDEF computer program were used in the backcalculation of the modulus.

When loads are placed on the surface of the pavement, it will deflect downward to form a bowl shaped depression known as a deflection basin. The size, depth, and shape of the deflection basin are a function of several variables, including the thickness and stiffness of the pavement, the underlying materials, and the magnitude of the load. A PCC pavement with a high elastic modulus will spread the load over a large area resulting in a shallow deflection basin. The pavement deflection will increase as the load increases. However, this increase in deflection is not linear in most cases as the aggregates and foundation materials are stress dependent. In a Falling Weight Deflectometer test, the deflections are measured at various radial offsets with respect to the center of the load plate. These deflection measurements define the deflection basin. The parameters such as the load, plate pressure and plate radius when anlyzed with the deflection basin, enable us to estimate the stiffness profile of the pavement with respect to depth below the surface. Studies have shown that the outer deflection sensors respond primarily to the subgrade characteristics, while the inner sensors respond to the subgrade and upper pavement layers. The slope of the deflection basin at close proximity to the load is largely a function of the stiffness of the upper pavement layers.

The mid-panel FWD data is used to evaluate the deflection profile, and backcalculate the modulus of the concrete slab and the composite modulus of the soil using Bousdef. This information is helpful in comparing the performances of the sections and differentiate the effect on the performance due to the quality of the soil layers from the effect of the concrete properties.

The air and pavement temperatures during these tests varied by about 30°F and 20°F respectively. The temperature variations during these tests are shown in Figure A4-1. Three tests were conducted at each location. The actual loads used in the tests varied between 9730 to 9805 with a coefficient of variation of about 2.0. The three tests conducted at each point were then averaged to obtain a single deflection value for each test location. Then the actual deflections were linearly adjusted for the standard load of 9000 lb. The analysis is based on this converted FWD data and is included.

Some erratic results that may be attributed to the fragmentation of the slab due to extensive cracks at the test locations were discarded, then the deflection bowls were plotted for the mid-panel tests. All sections showed very similar deflection bowls with a difference within 1 mil. As the tests were conducted at considerable distances, individual deflection bowls were also plotted to observe the variations. The results are shown in Figure A4-2. The deflections of section MI2-1 were found to match well with the only acceptable test result available for MI2-2. The results are shown in Figure A4-3.

The following observations were made. The tests conducted at the edge of the slab for sections MI2-1 and MI2-2 showed considerably higher deflections compared to other sections. MI2-2 showed the highest deflection. For tests conducted near transverse joints, MI2-1 showed the highest deflection while MI2-2 showed a lower value.

Load Transfer (FWD)

Across transverse joints:

Section	Average Efficiency (%)	Measures per Section	Standard Deviation (%)	Coefficient of Variation (%)
MI1-1	65.8	9	22.6	34.3
MI1-2	79.2	12	5.1	6.4
MI1-3	57.2	13	27.2	47.6
MI1-4	83.4	10	14.9	17.9
MI2-1	58.5	11	22.4	38.3
MI2-2	52.4	9	13.9	26.6

Across joints between pavement and shoulder:

Section	Average Efficiency (%)	Measures per Section	Standard Deviation (%)	Coefficient of Variation (%)
MI1-1	43.5	10	24.0	55.1
MI1-2	32.1	11	8.2	25.6
MI1-3	48.2	10	9.0	18.6
MI1-4	34.5	3	5.1	14.7
MI2-1	34.7	3	43.5	125.4
MI2-2	39.5	4	28.6	72.3

Across cracks:

Section	Average Efficiency (%)	Measures per Section	Standard Deviation (%)	Coefficient of Variation (%)
MI1-1	54.2	7	42.8	79.0
MI1-2	36.6	10	36.0	98.4
MI1-3	55.2	9	36.8	66.6
MI1-4	61.7	3	39.7	64.4
MI2-1	92.3	1	—	—
MI2-2	30.8	13	21.7	70.4

Back Calculation of Elastic Modulus (FWD)

Ioannides[13] procedure:

A simplified outline of this method is given below.

1. Perform FWD tests using a plate of diameter = 300 mm (radius a = 5.9055 in)

2. Drop the weight and record the load, P in pounds and Deflections (mils) under the sensors at 0, 12, 24 and 36 inches away from the load.

3. Calculate *AREA* (inches) as

$$AREA = 6\{ 1+2 (D_{12}/D_o) +2 (D_{24}/D_o) + (D_{36}/D_o)\}$$

4. Calculate the radius of the relative stiffness, L (inches) as

$$L = 0.5 - 1.25(AREA) + 1.21(AREA)^2 - 0.1803(AREA)^3 + 0.011098(AREA)^4 - 0.0003075(AREA)^5 + 0.000003198(AREA)^6$$

5. Calculate Westergaard's interior deflection, d_o (dimensionless) as

$$d_o = [1 + (^1/_{2P}) \ln \{(^a/_{2L}) + 0.5772 - 1.25\} (^a/_L)^2] (^1/_8)$$

6. Backcalculate modulus of subgrade reaction k (psi / in) as

$$k = (^{d}{}_o/D_o) (^P/_L)^2)10^3$$

7. Backcalculate E (psi) knowing h (thickness) and m as

$$E = [\{12 (1 - m^2)/ h^3 \}(d_o/D_o) (PL)^2)]10^3$$

following assumptions were made in the calculations:

1. The dynamic liquid (DL) foundation concept was used in the analysis.
2. A Poisson's ratio of 0.15 was assumed for the concrete in the analysis
3. The slab thickness was assumed as 10"

For the *AREA* range of 25 to 33 inches, the radius of relative stiffness varies from 15 to 52 for the dense liquid concept. The same may vary from 20 to 40 for the elastic solid concept. Therefore, considerable variation can be expected in the estimation using the two concepts.

Back Calculation of k Value (FWD)

The elastic modulus of subgrade reaction (k) depends on the location of the test in the slab (edge or corner), size of the slab, embankment height, depth to the rigid layer, and other factors. A granular base of 4 to 6 inches will have no significant effect on k but a fill thicker than 12 inches may increase the k value. Bedrock or similar stiff layer at a shallow depth may increase k values as much as twice the level which would otherwise be assigned to the subgrade soil based on its classification, density, and other properties[14]. Therefore it is important to know the effect of these influencing factors before making any final conclusion based on the k value alone. The base layer has some influence on the back calculated concrete modulus too. Its primary effect on the backcalculation solution is an increase in the apparent modulus of the concrete slab; the effect of a base on the backcalculated k value is usually insignificant[14].

The results are summarized in Table A4-1 and shown in Figures A4-4 and A4-5. From Figure A4-4, it can be seen that individual values vary considerably, specially in section MI1-2. In figure A4-5 can be seen that section MI1-1 shows the highest modulus while MI1-2 the lowest. The second histogram shows the comparison of the elastic moduli of each test performed in the MI2-1 section with the only one test made in section MI2-2 which happens to be the one of the lowest values of back calculated elastic modules of the project.

Bousdef Program:

The elastic modulus obtained by the Ioannides method was compared to the solutions obtained by running the program Bousdef. This method, developed by Oregon State University is based on the Bousinesq theory[6]. The results compares favorably for the modulus range of 2 to 10 million psi. and are shown in Tables A4-6 and A4-7 and shown in Figures A4-4 and A4-5.

Results of FWD Testing

The FWD tests were conducted while the slabs were at different temperature gradients. The tests at the mid panels indicate that the recycled test sections show no material inferiority when compared to the control section. The recycled concrete on open-graded base on the West bound section at Galesburg (MI2-1) shows equally well or better performance than other sections. The number of tests available is not sufficient for an evaluation of the same in the East bound section (MI2-2), even though, the available result agrees. The erratic results at this section may be attributed to the fragmentation of the slab due to extensive cracks at the test locations.

FWD tests conducted near joints and slab edges can be effectively used to calculate the load transfer efficiencies. The load transfer efficiency of the section MI1-4 is found to be the highest. There is no considerable difference in the load transfer efficiencies of other sections. However, the load transfer efficiency of the west-bound section of the recycled concrete with open-graded base at Galesburg (MI2-1) is higher compared to its east-bound section (MI2-2). Worth mentioning is that individual tests at MI2-1 show lower values for the west-bound section compared to MI2-2. Therefore, an evaluation of the individual test results will be more appropriate than making a general comment on the superiority of one over the other.

The load transfer between slab and shoulder varies from test to test. Hence, it will be more appropriate to examine these results individually to assess their validity. In Sections MI2-1, the test locations at 87704 ft and 87214 ft should be investigated for the extremely low load transfer efficiency. The results of the load transfer efficiency analysis are tabulated in tables A4-2 to A4-5

UMKAK WK1
DATA BASE

NOTE THIS LOTUS FILE CREATED BY IMPORTING FWD NORMALIZED TEXT FILE TO LOTUS AND THEN AVERAGING THE THREE TEST DROPS TO PRODUCE ONE POINT

FWD DATA FILE C \SFWD\DATA\UMKAL.FWD
Project Number 39022-20736

Testing Location I-94 BETWEEN GALESBURG EXIT AND KALAMAZOO

Customer\Client WILL HANSEN, U OF M

Operator K.S. BANCROFT

Environment CLOUDY,COOL,WET - 12-06-94
CLOUDY,COLD,SNOWY - 12-08-94

Comment WBOL BETWEEN STA 880+00 - 870+00 FWD TEST 12-06-94
EBOL BETWEEN STA 870+00 - 880+00 FWD TEST 12-08-94

Date Created 12-06-1994 12-08-1994

Machine Type KUAB FWD Model 150
Software version 4 15

Load Mode 2 (3+3 large buffers, 7 stack weights)
Plate Radius 5 91 (in)

Drop Sequence 222
Record Drop? YYY

KEY: MID = SENSOR D0 IN MIDDLE OF SLAB OR LANE
OWP = SENSOR D0 IN OUTSIDE WHEEL PATH
MSE = SENSOR D0 ON PAVEMENT EDGE WITH SENSOR D2 ON SHOULDER
TJT = TRANSVERSE JOINT
TCK = TRANSVERSE CRACK
BJT = JOINT BETWEEN SENSOR D0 AND D1
AJT = JOINT BETWEEN SENSORS D0 AND D4 DISREGARD SENSOR D3
BCK = CRACK BETWEEN SENSOR D0 AND D1
ACK = CRACK BETWEEN SENSORS D0 AND D4 DISREGARD SENSOR D3

Channel	0	1	2	3	4	5	6	7	8
Distance	0.00	12.00	12.00	8 00	12.00	18.00	24 00	36.00	60 00 (in)
Position	CENTER	FRONT	LEFT	BEHIND	BEHIND	BEHIND	BEHIND	BEHIND	BEHIND

					temp. F		lbf	mils	mils	mils	mils	mils	mils	mils	mils	mils	
DIR	FEET	LANE	TEST	TYPE	AIR	PVMT	LOAD	D0	D1	D2	D3	D4	D5	D6	D7	D8	REMARKS
WBOL	87951	MID	CORE	NONE	41	40	9000	3.00	2.76	2.68	2.82	2.68	2.52	2.34	1.99	1.32	
WBOL	87970	OWP	TJT	BJT	41	41	9000	17.39	5.47	14.43	15.14	13.75	12.49	11.00	8.54	4.80	
WBOL	87970	OWP	TJT	AJT	41	41	9000	14.94	13.14	12.17	16.67	10.45	9.89	8.88	7.08	4.21	
WBOL	87938	OWP	TJT	BJT	41	40	9000	16.33	5.73	14.13	14.03	12.48	11.08	9.68	7.12	3.51	CORE
WBOL	87938	OWP	TJT	AJT	41	41	9000	19.31	16.42	16.88	22.05	6.57	6.24	5.62	4.49	2.50	CORE
WBOL	87804	OWP	TJT	BJT	41	40	9000	14.12	4.16	12.37	12.31	11.08	10.13	8.84	6.81	3.80	
WBOL	87804	OWP	TJT	AJT	40	40	9000	13.88	12.03	11.70	15.52	9.29	8.58	7.84	6.38	3.94	
WBOL	87747	MID	CORE	NONE	40	40	9000	3.36	3.31	3.26	3.27	3.09	2.94	2.75	2.39	1.68	
WBOL	87682	OWP	TJT	BJT	25	39	9000	17.19	10.46	15.04	15.32	14.14	13.18	11.80	9.51	5.92	
WBOL	87682	OWP	TJT	AJT	39	40	9000	13.61	11.76	12.02	15.01	11.84	10.11	9.29	7.81	5.07	
WBOL	87559	OWP	TJT	BJT	40	40	9000	13.75	9.61	12.09	11.86	10.80	9.85	8.73	6.78	3.75	
WBOL	87559	OWP	TJT	AJT	27	37	9000	10.58	8.99	9.39	11.80	11.37	10.26	9.21	7.49	4.39	
WBOL	87537	MID	CORE	NONE	23	39	9000	2.85	2.78	2.65	2.76	2.59	2.50	2.30	2.08	1.48	
WBOL	87490	OWP	TCK	BCK	31	39	9000	6.03	5.56	4.91	5.46	5.03	4.61	4.06	3.24	1.85	CORE
WBOL	87490	OWP	TCK	ACK	24	39	9000	6.97	6.03	5.60	5.72	5.14	4.78	4.23	3.31	1.88	CORE
WBOL	87478	OWP	TJT	BJT	29	39	9000	15.00	6.90	13.49	13.20	11.99	10.88	9.56	7.29	3.98	CORE
WBOL	87478	OWP	TJT	AJT	40	40	9000	11.63	9.87	10.41	13.14	10.35	9.78	8.82	7.01	4.04	CORE
WBOL	87437	OWP	TJT	BJT	40	40	9000	13.14	9.35	11.22	11.63	10.40	9.68	8.65	6.91	4.17	
WBOL	87437	OWP	TJT	AJT	27	39	9000	10.71	9.13	9.39	12.05	9.46	8.93	8.06	6.65	4.13	
WBOL	87335	MID	CORE	NONE	36	39	9000	3.35	3.26	3.16	3.23	3.09	2.95	2.75	2.45	1.73	
WBOL	87312	OWP	TJT	BJT	39	40	9000	13.20	12.41	11.76	11.93	10.86	10.20	9.16	7.49	4.75	

WBOL	87312	OWP	TJT	AJT	39	40	9000	11.27	9.99	10.13	12.45	12.43	11.52	10.54	8.70	5.75	
WBOL	87291	OWP	CORE	NONE	37	41	9000	7.77	6.75	6.73	6.99	6.45	5.94	5.39	4.38	2.76	CORE
WBOL	87190	OWP	TJT	BJT	29	38	9000	9.23	7.70	8.34	8.22	7.45	6.77	6.01	4.72	2.65	
WBOL	87190	OWP	TJT	AJT	23	38	9000	7.91	6.75	6.97	8.87	7.64	7.16	6.46	5.21	3.00	
WBOL	87149	OWP	TJT	BJT	26	39	9000	11.36	9.26	9.82	10.09	9.23	8.40	7.52	5.98	3.44	CORE
WBOL	87149	OWP	TJT	AJT	31	39	9000	10.06	8.59	8.67	9.79	8.99	8.32	7.54	6.08	3.59	CORE
WBOL	87067	OWP	TJT	BJT	31	39	9000	13.31	9.05	11.82	11.70	10.57	9.75	8.58	6.73	3.80	
WBOL	87067	OWP	TJT	AJT	32	39	9000	10.66	9.11	9.33	11.95	12.10	9.03	8.20	8.78	4.19	
WBOL	87049	MID	CORE	NONE	32	40	9000	3.05	2.92	2.87	2.96	2.81	2.70	2.48	2.12	1.48	
WBOL	87214	MSE	MS	NONE	39	40	9000	12.88	12.64	1.30	12.72	12.32	12.04	11.57	10.33	7.92	
WBOL	87416	MSE	MS	NONE	39	40	9000	9.66	9.35	8.21	9.56	9.23	9.02	8.66	7.75	5.98	
WBOL	87704	MSE	MS	NONE		40	9000	14.33	14.19	1.30	14.13	13.76	13.36	12.92	11.50	8.91	
EBOL	87026	OWP	TJT	BJT	24	21	9000	17.04	8.02	5.06	14.03	12.33	10.27	8.19	4.03	3.60	
EBOL	87026	OWP	TJT	AJT	24	22	9000	13.37	11.39	11.19	15.40	5.07	4.50	3.98	2.93	0.88	
EBOL	87042	OWP	TCK	BCK	25	23	9000	10.79	3.11	9.50	8.47	7.35	5.84	4.17	1.31	4.03	
EBOL	87042	OWP	TCK	ACK	24	23	9000	11.35	7.49	11.37	14.49	3.55	3.27	3.02	2.42	1.25	
EBOL	87080	OWP	TCK	BCK	24	22	9000	9.85	2.63	8.89	8.10	7.23	6.09	5.06	3.01	0.43	
EBOL	87080	OWP	TCK	ACK	24	22	9000	10.62	6.22	9.83	13.64	14.63	1.70	1.58	1.35	0.89	
EBOL	87128	OWP	TCK	BCK	24	22	9000	12.01	2.49	11.11	8.97	7.32	5.32	3.08	0.74	8.75	
EBOL	87128	OWP	TCK	ACK	25	22	9000	12.10	7.50	11.86	15.51	2.44	2.30	2.15	1.97	1.59	
EBOL	87147	OWP	TJT	BJT	25	23	9000	11.10	7.65	9.60	9.47	8.53	7.48	6.29	4.14	0.51	
EBOL	87147	OWP	TJT	AJT	24	23	9000	9.99	8.48	8.53	11.09	11.42	4.76	4.41	3.45	1.66	
EBOL	87163	OWP	TCK	BCK	24	22	9000	10.51	1.99	9.31	9.08	8.27	7.48	6.58	4.97	2.41	CORE
EBOL	87163	OWP	TCK	ACK	25	22	9000	12.89	10.30	11.83	1.68	1.52	1.51	1.44	1.26	0.94	CORE
EBOL	87270	OWP	TJT	BJT	25	23	9000	7.90	6.25	7.54	6.83	6.23	5.45	4.86	3.67	1.64	
EBOL	87270	OWP	TJT	AJT	24	23	9000	7.22	5.96	6.47	8.03	8.36	4.84	4.46	3.50	1.89	
EBOL	87275	MID	CORE	NONE	25	23	9000	3.39	3.56	3.29	3.18	3.02	2.81	2.66	2.30	1.48	
EBOL	87297	OWP	TCK	BCK	25	24	9000	11.71	2.16	10.41	9.68	8.48	7.15	5.79	3.13	1.34	
EBOL	87297	OWP	TCK	ACK	25	24	9000	10.79	7.25	10.13	13.40	14.42	1.83	1.72	1.52	1.11	
EBOL	87364	OWP	TCK	BCK	25	25	9000	13.11	3.75	12.35	11.06	10.08	8.94	7.95	5.90	2.88	
EBOL	87364	OWP	TCK	ACK	26	24	9000	16.57	14.04	15.55	1.52	1.33	1.27	1.22	1.10	0.86	
EBOL	87394	OWP	TJT	BJT	26	30	9000	10.16	6.54	9.14	8.96	8.17	7.41	6.56	5.17	2.91	
EBOL	87394	OWP	TJT	AJT	26	28	9000	8.86	7.83	7.84	9.71	9.91	6.35	5.79	4.76	2.88	
EBOL	87450	MID	CORE	NONE	26	26	9000	3.69	3.46	3.62	3.71	3.61	3.66	3.66	3.76	3.89	
EBOL	87486	OWP	TCK	BCK	27	23	9000	22.83	3.59	25.71	19.64	17.75	15.46	13.46	8.97	1.56	CORE
EBOL	87486	OWP	TCK	ACK	27	25	9000	18.27	12.42	22.15	3.03	2.80	2.60	2.41	2.03	1.28	CORE
EBOL	87516	OWP	TJT	BJT	27	28	9000	15.87	8.45	17.97	13.09	11.58	9.72	7.75	3.78	2.89	CORE
EBOL	87516	OWP	TJT	AJT	27	28	9000	12.65	9.51	12.08	6.47	5.90	5.23	4.62	3.32	1.13	CORE
EBOL	87570	MID	CORE	NONE	28	27	9000	7.48	6.64	6.07	7.98	8.10	8.34	8.69	9.36	1.75	
EBOL	87631	OWP	TJT	BJT	28	30	9000	10.28	4.52	9.40	8.77	7.85	6.71	5.59	3.49	0.82	CORE
EBOL	87631	OWP	TJT	AJT	28	29	9000	8.97	7.08	8.59	10.53	5.55	5.08	4.52	3.49	1.39	CORE
EBOL	87636	OWP	TCK	BCK	28	31	9000	7.89	4.03	7.57	6.55	5.92	5.03	4.26	2.78	0.64	CORE
EBOL	87636	OWP	TCK	ACK	28	30	9000	6.90	5.42	6.66	7.93	4.39	3.91	3.48	2.55	1.19	CORE
EBOL	87684	OWP	TCK	BCK	28	34	9000	10.03	3.41	9.59	7.84	6.62	5.02	3.65	1.22	1.25	
EBOL	87684	OWP	TCK	ACK	28	33	9000	15.33	10.07	13.99	4.04	3.72	3.43	3.13	2.59	1.64	
EBOL	87708	MID	CORE	NONE	28	34	9000	4.28	4.14	4.08	4.32	4.24	4.26	4.29	4.40	1.04	
EBOL	87754	OWP	TJT	BJT	28	33	9000	12.39	5.23	10.69	10.98	10.06	9.14	8.17	6.49	3.54	
EBOL	87754	OWP	TJT	AJT	29	33	9000	15.08	11.88	13.35	17.69	7.40	6.98	6.38	5.36	3.48	
EBOL	87780	OWP	TCK	BCK	29	33	9000	6.02	5.78	5.24	5.80	5.48	5.48	5.26	5.02	4.56	
EBOL	87780	OWP	TCK	ACK	28	31	9000	6.20	5.46	5.24	5.79	5.45	5.14	4.76	4.19	3.28	
EBOL	87827	OWP	TCK	BCK	29	29	9000	11.58	2.64	10.69	9.68	8.55	7.35	6.09	3.80	0.76	
EBOL	87827	OWP	TCK	ACK	29	29	9000	13.72	11.43	12.79	15.88	2.68	2.63	2.38	2.11	1.37	
EBOL	87866	OWP	TCK	BCK	28	29	9000	13.05	2.59	12.29	11.28	10.07	9.08	7.99	6.06	3.20	
EBOL	87866	OWP	TCK	ACK	29	28	9000	11.56	9.55	10.55	5.23	2.03	2.07	2.12	1.71	1.44	
EBOL	87878	OWP	TJT	BJT	29	29	9000	12.04	4.66	10.52	10.69	9.81	9.03	8.04	6.36	3.56	CORE
EBOL	87878	OWP	TJT	AJT	29	28	9000	10.51	8.94	9.23	11.73	12.03	4.68	4.48	3.89	2.74	CORE
EBOL	87938	MID	CORE	NONE	29	27	9000	5.54	5.12	5.33	5.86	5.87	6.14	6.37	6.91	1.65	
EBOL	87980	OWP	TCK	BCK	29	26	9000	11.69	2.22	10.67	10.02	8.93	7.90	6.96	5.19	2.47	
EBOL	87980	OWP	TCK	ACK	29	26	9000	11.87	9.44	11.98	13.91	1.96	1.91	1.80	1.65	1.29	
EBOL	88000	OWP	TJT	BJT	29	28	9000	9.48	4.34	9.20	7.98	7.14	6.20	5.37	3.87	1.68	
EBOL	88000	OWP	TJT	AJT	28	28	9000	12.78	9.48	11.16	15.31	16.09	4.68	4.17	3.33	1.84	
EBOL	87708	MSE	MS	NONE	34	36	9000	8.44	8.42	2.87	8.21	8.01	7.92	7.80	7.49	1.17	
EBOL	87570	MSE	MS	NONE	35	30	9000	22.13	8.35	4.82	17.57	14.94	11.60	7.87	1.77	1.07	
EBOL	87380	MSE	MS	NONE	33	28.	9000	17.25	18.82	3.60	15.87	14.77	13.73	12.60	10.15	6.04	
EBOL	87275	MSE	MS	NONE	31	28	9000	5.99	5.57	4.88	5.97	5.80	5.66	5.52	5.22	1.95	

UMLAW WK1
DATA BASE

NOTE THIS LOTUS FILE CREATED BY IMPORTING FWD NORMALIZED TEXT FILE TO LOTUS
AND THEN AVERAGING THE THREE DROPS TO PRODUCE ONE POINT

FWD DATA FILE C \SFWD\DATA\UMLAW FWD
Project Number 80023-20993

Testing Location : I-94 WBOL E. OF 64TH ST E'LY TO W OF M-51

Customer\Client : WILL HANSEN, U OF M

Operator KURT S BANCROFT

Environment CLOUDY,COOL

Comment VARIOUS LOCATIONS ON WESTBOUND OUTSIDE LANE(WBOL)
SECTION 4 - STA 415+00 - 410+00 FWD TEST 11-29-94
SECTION 1 - STA 652+00 - 648+00 FWD TEST 11-29-94
SECTION 2 - STA 645+00 - 640+00 FWD TEST 11-30-94
SECTION 3 - STA 515+00 - 510+00 FWD TEST 12-5-94

Date Created 11-29-1994

Machine Type KUAB FWD Model 150
Software Version 4 15

Load Mode 2 (3+3 large buffers 7 stack weights)
Plate Radius 5 91 (in)

Drop Sequence 222
Record Drop? YYY

KEY:
MID = SENSOR D0 IN MIDDLE OF SLAB OR LANE
OWP = SENSOR D0 IN OUTSIDE WHEEL PATH
MSE = SENSOR D0 ON PAVEMENT EDGE WITH SENSOR D2 ON SHOULDER
TJT = TRANSVERSE JOINT
TCK = TRANSVERSE CRACK
BJT = JOINT BETWEEN SENSORS D0 AND D1
AJT = JOINT BETWEEN SENSORS D0 AND D4 DISREGARD SENSOR D3
BCK = CRACK BETWEEN SENSORS D0 AND D1
ACK = CRACK BETWEEN SENSORS D0 AND D4 DISREGARD SENSOR D3

Channel	0	1	2	3	4	5	6	7	8
Distance	0 00	12 00	12 00	8 00	12.00	18 00	24 00	36.00	60 00 (in)
Position	CENTER	FRONT	LEFT	BEHIND	BEHIND	BEHIND	BEHIND	BEHIND	BEHIND

					temp. F.		lbf	mils	mils	mils	mils	mils	mils	mils	mils	mils	
SECT	FEET	LANE	TEST	TYPE	AIR	PVMT	LOAD	D0	D1	D2	D3	D4	D5	D6	D7	D8	REMARKS
4	41365	MID	CORE	NONE	30	33	9000	3.84	3.61	3.55	3.74	3.60	3.45	3.30	2.95	2.24	
4	41361	MID	CORE	NONE	30	34	9000	3.66	3.48	3.40	3.54	3.40	3.20	3.03	2.62	1.84	
4	41257	MID	CORE	NONE	26	33	9000	3.66	3.50	3.40	3.57	3.47	3.30	3.12	2.77	2.01	
4	41254	MID	CORE	NONE	26	33	9000	3.56	3.41	3.25	3.41	3.25	3.09	2.88	2.52	1.79	
4	41175	MID	CORE	NONE	35	34	9000	3.90	3.61	3.61	3.81	3.68	3.52	3.39	3.02	2.13	
4	41172	MID	CORE	NONE	35	34	9000	3.76	3.72	3.60	3.72	3.48	3.39	3.16	2.76	1.95	
4	41093	MID	CORE	NONE	8	32	9000	3.79	3.64	3.40	3.64	3.50	3.39	3.18	2.81	2.08	
4	41090	MID	CORE	NONE	17	33	9000	3.85	3.73	3.54	3.69	3.52	3.33	3.11	2.64	1.61	
4	41023	MID	CORE	NONE	35	34	9000	4.98	4.60	4.41	5.11	5.05	5.13	5.14	5.22	5.47	
4	41019	MID	CORE	NONE	35	34	9000	4.28	4.11	3.81	4.13	4.00	3.82	3.61	3.23	2.52	
4	41371	OWP	TJT	BJT	27	34	9000	7.59	5.65	6.88	6.51	6.07	5.42	4.92	3.66	2.16	
4	41361	OWP	TJT	AJT	25	34	9000	7.94	6.71	7.20	9.14	5.51	5.10	4.58	3.70	2.21	
4	41330	OWP	TJT	BJT	22	33	9000	7.52	6.12	6.87	6.53	5.95	5.31	4.69	3.64	2.09	
4	41330	OWP	TJT	AJT	22	33	9000	6.75	5.65	6.23	7.65	5.63	5.21	4.66	3.71	2.19	
4	41289	OWP	TJT	BJT	23	33	9000	7.49	6.93	6.88	6.63	6.09	5.53	4.87	3.84	2.24	
4	41289	OWP	TJT	AJT	22	32	9000	7.00	5.95	6.28	7.63	6.59	6.06	5.48	4.32	2.54	
4	41248	OWP	TJT	BJT	24	34	9000	8.56	8.24	7.79	7.48	6.83	6.16	5.38	4.19	2.35	
4	41248	OWP	TJT	AJT	24	33	9000	8.09	7.12	7.42	8.90	8.28	7.44	6.57	5.14	2.93	
4	41207	OWP	TJT	BJT	18	33	9000	7.45	6.28	6.70	6.50	5.99	5.40	4.73	3.69	2.01	
4	41207	OWP	TJT	AJT	30	33	9000	7.05	5.97	6.47	7.85	6.15	5.62	5.07	3.92	2.24	
4	41166	OWP	TJT	BJT	29	34	9000	7.77	3.51	7.07	6.69	6.11	5.41	4.79	3.69	2.12	
4	41166	OWP	TJT	AJT	27	34	9000	12.88	11.37	10.80	14.48	4.55	4.12	3.73	3.09	1.89	
4	41139	OWP	TCK	BCK	20	34	9000	7.33	1.55	6.70	6.31	5.80	5.12	4.56	3.51	2.00	
4	41139	OWP	TCK	ACK	20	35	9000	14.72	12.72	13.41	17.06	2.26	2.26	2.07	1.78	1.32	

4	41124	OWP	TJT	BJT	23	34	9000	8.10	7.78	7.25	7.11	6.50	5.90	5.16	4.06	2.28
4	41124	OWP	TJT	AJT	36	35	9000	7.71	6.68	6.88	8.42	7.52	6.82	6.07	4.83	2.85
4	41099	OWP	TCK	BCK	36	36	9000	8.76	5.56	7.45	7.68	6.96	6.36	5.60	4.43	2.54
4	41099	OWP	TCK	ACK	35	36	9000	12.73	10.87	10.76	14.72	4.27	4.07	3.72	3.13	2.08
4	41083	OWP	TJT	BJT	34	35	9000	7.85	6.66	7.20	6.83	6.27	5.64	5.02	3.86	2.14
4	41083	OWP	TJT	AJT	34	34	9000	7.05	5.97	6.48	7.86	6.26	5.77	5.17	4.09	2.39
4	41070	OWP	TCK	BCK	34	35	9000	5.16	5.19	4.43	4.85	4.60	4.21	3.90	3.30	1.99
4	41070	OWP	TCK	ACK	34	35	9000	5.16	4.66	4.71	5.35	5.12	4.79	4.37	3.62	2.30
4	41042	OWP	TJT	BJT	34	36	9000	7.63	6.74	7.01	6.62	6.06	5.49	4.85	3.70	1.94
4	41042	OWP	TJT	AJT	34	36	9000	6.71	5.75	6.18	7.43	6.43	5.87	5.22	4.12	2.28
4	41002	OWP	TJT	BJT	34	34	9000	8.83	7.84	8.05	7.86	7.16	6.41	5.64	4.39	2.43
4	41002	OWP	TJT	AJT	34	34	9000	7.37	6.25	6.78	8.26	7.36	6.79	6.02	4.82	2.74
4	41035	MSE	MS	NONE	34	34	9000	7.96	7.74	3.23	7.79	7.48	7.20	6.85	5.92	4.27
4	41186	MSE	MS	NONE	35	33	9000	10.95	10.58	3.57	10.91	10.47	10.11	9.73	8.80	7.03
4	41311	MSE	MS	NONE	35	34	9000	9.04	8.79	2.82	8.81	8.46	8.13	7.64	6.56	4.60
1	65154	MID	CORE	NONE	22	33	9000	4.73	4.26	4.13	4.88	4.89	4.94	5.03	5.20	5.56
1	65150	MID	CORE	NONE	24	33	9000	4.16	4.30	3.87	3.99	3.79	3.60	3.40	2.98	2.19
1	65058	MID	CORE	NONE	21	33	9000	2.80	2.68	2.57	2.73	2.64	2.51	2.41	2.14	1.62
1	65054	MID	CORE	NONE	23	33	9000	2.76	2.57	2.50	2.63	2.51	2.35	2.19	1.84	1.19
1	64975	MID	CORE	NONE	20	33	9000	2.89	2.72	2.68	2.83	2.71	2.57	2.44	2.18	1.42
1	64973	MID	CORE	NONE	19	33	9000	2.81	2.63	2.62	2.71	2.57	2.44	2.26	1.94	1.29
1	64935	MID	CORE	NONE	21	33	9000	3.03	2.77	2.79	2.98	2.91	2.80	2.74	2.49	1.60
1	64932	MID	CORE	NONE	18	33	9000	2.73	2.61	2.53	2.64	2.52	2.38	2.25	1.97	1.39
1	64853	MID	CORE	NONE	22	33	9000	3.16	2.85	2.84	3.08	2.99	2.90	2.79	2.57	1.55
1	64851	MID	CORE	NONE	27	34	9000	3.02	3.06	2.71	2.91	2.71	2.59	2.37	2.02	1.29
1	65201	OWP	TCK	BCK	16	33	9000	4.94	4.73	4.21	4.34	3.97	3.51	3.12	2.40	1.25
1	65201	OWP	TCK	ACK	19	33	9000	5.00	4.16	4.26	5.47	4.68	4.15	3.70	2.86	1.50
1	65187	OWP	TJT	BJT	20	33	9000	8.37	5.49	7.81	7.07	6.39	5.56	4.83	3.50	1.63
1	65187	OWP	TJT	AJT	23	33	9000	7.60	6.33	7.29	8.52	5.79	5.37	4.56	3.51	1.80
1	65146	OWP	TJT	BJT	17	33	9000	10.23	8.19	9.74	8.93	8.09	7.28	6.36	4.85	2.38
1	65146	OWP	TJT	AJT	20	32	9000	9.35	7.94	8.64	10.51	8.46	7.73	6.93	5.50	3.00
1	65132	OWP	TCK	BCK	19	33	9000	10.82	1.60	11.21	9.45	8.63	7.70	6.91	5.29	2.63
1	65132	OWP	TCK	ACK	32	34	9000	11.17	9.40	11.08	13.08	1.42	1.52	1.34	1.27	0.98
1	65104	OWP	TJT	BJT	33	36	9000	8.32	4.54	7.53	7.08	6.37	5.58	4.85	3.49	1.39
1	65104	OWP	TJT	AJT	33	36	9000	7.12	5.95	6.32	7.88	5.95	5.37	4.82	3.73	1.89
1	65077	OWP	TCK	BCK	33	36	9000	4.24	4.22	3.80	3.78	3.52	3.14	2.83	2.23	1.29
1	65077	OWP	TCK	ACK	31	35	9000	4.21	3.54	3.67	4.40	4.05	3.59	3.19	2.48	1.42
1	65063	OWP	TJT	BJT	26	34	9000	7.12	3.40	6.51	6.00	5.48	4.79	4.13	3.05	1.49
1	65063	OWP	TJT	AJT	24	33	9000	5.64	4.63	5.19	6.27	5.02	4.46	3.97	2.96	1.51
1	65050	OWP	TCK	BCK	29	35	9000	4.31	4.25	3.79	3.84	3.55	3.18	2.66	2.25	1.28
1	65050	OWP	TCK	ACK	29	35	9000	4.29	3.60	3.72	4.69	4.10	3.65	3.29	2.57	1.45
1	65022	OWP	TJT	BJT	29	36	9000	7.82	4.74	6.86	6.68	6.08	5.30	4.64	3.44	1.73
1	65022	OWP	TJT	AJT	28	35	9000	6.69	5.50	6.00	7.47	5.82	5.23	4.68	3.61	1.94
1	65009	OWP	TCK	BCK	28	34	9000	8.91	4.23	7.57	7.57	6.81	5.93	5.19	3.78	1.82
1	65009	OWP	TCK	ACK	24	34	9000	8.80	7.51	7.10	9.85	10.12	4.00	3.66	2.92	1.66
1	64981	OWP	TJT	BJT	25	35	9000	6.36	4.17	5.68	5.40	4.87	4.29	3.73	2.79	1.38
1	64981	OWP	TJT	AJT	25	35	9000	5.41	4.51	4.77	5.96	6.16	4.03	3.59	2.75	1.46
1	64939	OWP	TJT	BJT	27	34	9000	6.73	4.17	6.13	5.76	5.29	4.59	4.02	2.99	1.22
1	64939	OWP	TJT	AJT	27	33	9000	7.12	5.98	6.25	8.04	3.85	3.46	3.17	2.45	1.46
1	64912	OWP	TCK	BCK	27	36	9000	8.58	1.24	7.65	7.48	6.75	6.04	5.22	3.96	2.11
1	64912	OWP	TCK	ACK	34	36	9000	13.20	11.15	11.67	15.14	1.42	1.45	1.36	1.25	0.98
1	64899	OWP	TJT	BJT	34	34	9000	7.46	4.55	6.85	6.38	5.82	5.09	4.43	3.23	1.38
1	64899	OWP	TJT	AJT	34	34	9000	6.82	5.58	6.20	7.67	6.35	4.39	3.93	3.08	1.63
1	64887	OWP	TCK	BCK	34	35	9000	8.27	0.72	7.60	7.12	6.35	5.61	5.00	3.73	1.95
1	64887	OWP	TCK	ACK	34	35	9000	22.25	19.02	19.70	25.63	1.20	1.19	1.16	1.05	0.86
1	64858	OWP	TJT	BJT	34	36	9000	6.11	4.85	5.52	5.28	4.80	4.20	3.70	2.78	1.50
1	64858	OWP	TJT	AJT	34	36	9000	5.39	4.49	4.83	6.00	4.87	4.37	3.87	3.05	1.65
1	64817	OWP	TJT	BJT	35	34	9000	6.86	5.54	6.29	5.93	5.39	4.78	4.19	3.18	1.67
1	64817	OWP	TJT	AJT	34	34	9000	5.78	4.70	5.38	6.55	5.23	4.76	4.24	3.35	1.87
1	64853	MSE	MS	NONE	35	34	9000	8.31	7.82	1.62	8.28	8.17	7.98	7.83	7.34	1.68
1	64893	MSE	MS	NONE	34	34	9000	8.16	8.05	2.26	7.84	7.43	7.08	6.75	5.92	4.64
1	64921	MSE	MS	NONE	34	34	9000	7.78	7.22	5.42	7.84	7.62	7.63	7.08	6.86	6.35
1	64977	MSE	MS	NONE	35	34	9000	6.37	6.44	5.54	5.96	5.65	5.35	4.94	4.19	2.85
1	65029	MSE	MS	NONE	34	34	9000	7.50	6.65	3.28	7.52	7.35	7.20	7.02	6.46	5.41
1	65058	MSE	MS	NONE	18	35	9000	5.78	5.63	3.61	5.46	5.16	4.80	4.48	3.69	2.46
1	65086	MSE	MS	NONE	16	36	9000	10.48	10.92	2.38	9.62	9.09	8.36	7.70	6.16	3.39
1	65111	MSE	MS	NONE	21	35	9000	7.44	7.54	2.09	6.88	6.59	6.18	5.93	5.07	3.77
1	65154	MSE	MS	NONE	26	32	9000	14.40	15.83	5.27	13.40	12.61	11.81	9.29	7.80	4.43
1	65193	MSE	MS	NONE	32	33	9000	5.69	5.49	3.96	5.30	4.97	4.67	4.40	3.76	2.79
2	64483	MID	CORE	NONE	31	29	9000	3.88	3.36	3.62	4.02	3.98	4.07	4.16	4.26	4.16
2	64480	MID	CORE	NONE	31	29	9000	3.17	3.00	2.94	3.09	2.98	2.84	2.75	2.49	2.08
2	64395	MID	CORE	NONE	31	29	9000	4.05	4.57	3.81	3.60	3.31	2.96	2.61	1.97	0.98
2	64393	MID	CORE	NONE	31	30	9000	5.68	6.81	5.48	5.02	4.55	4.08	3.55	2.60	1.10
2	64278	MID	CORE	NONE	31	29	9000	3.44	3.14	3.22	3.50	3.42	3.45	3.41	3.36	2.37
2	64276	MID	CORE	NONE	31	30	9000	3.20	3.21	3.03	3.03	2.89	2.75	2.60	2.26	1.68
2	64151	MID	CORE	NONE	31	30	9000	3.22	3.17	3.03	3.08	2.95	2.80	2.65	2.32	1.73
2	64149	MID	CORE	NONE	31	29	9000	3.89	4.28	3.59	3.51	3.23	2.95	2.68	2.09	1.08
2	64032	MID	CORE	NONE	32	30	9000	4.89	4.34	4.58	5.14	5.10	5.33	5.41	4.28	2.56
2	64031	MID	CORE	NONE	32	30	9000	3.86	3.56	3.52	3.88	3.75	3.71	3.60	3.40	2.45

2	64488	OWP	TJT	BJT	31	30	9000	11.79	8.99	10.91	10.19	9.20	8.42	7.23	5.46	2.59	
2	64488	OWP	TJT	AJT	32	30	9000	10.16	8.49	9.52	11.44	9.26	8.65	7.77	6.21	3.39	
2	64446	OWP	TJT	BJT	32	30	9000	7.27	5.57	6.49	6.25	5.63	4.98	4.37	3.27	1.57	
2	64446	OWP	TJT	AJT	31	30	9000	6.33	5.26	5.62	7.01	5.52	5.05	4.42	3.44	1.80	
2	64433	OWP	TCK	BCK	32	30	9000	8.46	1.11	7.80	7.06	6.31	5.53	4.71	3.34	1.50	
2	64433	OWP	TCK	ACK	32	29	9000	8.94	7.11	8.22	10.41	1.01	1.05	0.94	0.89	0.70	
2	64427	OWP	CORE	NONE	32	30	9000	4.04	4.13	3.46	3.88	3.70	3.52	3.33	3.10	2.59	
2	64405	OWP	TJT	BJT	32	32	9000	8.89	6.37	8.03	7.63	6.94	6.16	5.39	3.99	1.99	
2	64405	OWP	TJT	AJT	32	31	9000	7.54	6.29	6.89	8.50	6.35	5.86	5.16	4.04	2.20	
2	64377	OWP	TCK	BCK	32	31	9000	12.09	1.65	10.92	10.30	9.27	8.22	7.07	5.24	2.13	
2	64377	OWP	TCK	ACK	32	31	9000	9.19	7.59	8.26	10.53	10.32	1.28	1.14	1.13	0.85	
2	64364	OWP	TJT	BJT	32	31	9000	8.73	7.02	7.88	7.73	7.15	6.51	5.79	4.57	2.48	
2	64364	OWP	TJT	AJT	32	31	9000	7.50	6.29	6.79	8.51	8.81	6.47	5.84	4.93	2.99	
2	64350	OWP	TCK	BCK	32	31	9000	7.66	7.72	6.91	6.87	6.32	5.80	5.14	4.07	2.27	
2	64350	OWP	TCK	ACK	32	31	9000	7.42	6.48	6.69	8.09	7.88	7.32	6.53	5.34	3.04	
2	64323	OWP	TJT	BJT	32	32	9000	11.14	9.41	10.49	9.77	8.86	8.04	7.00	5.33	2.33	
2	64323	OWP	TJT	AJT	32	31	9000	10.48	8.85	10.08	11.98	9.24	8.78	7.64	6.19	3.23	
2	64295	OWP	TCK	BCK	32	32	9000	9.56	1.68	8.79	8.16	7.40	6.56	5.70	4.17	1.77	
2	64295	OWP	TCK	ACK	32	32	9000	10.19	8.18	9.37	12.00	1.25	1.19	1.12	1.01	0.75	
2	64282	OWP	TJT	BJT	32	31	9000	6.95	6.04	6.28	5.93	5.36	4.69	4.03	2.84	0.87	CORE
2	64282	OWP	TJT	AJT	32	31	9000	6.71	5.59	6.06	7.56	5.46	4.92	4.32	3.25	1.38	CORE
2	64268	OWP	TCK	BCK	32	32	9000	14.89	1.52	14.52	12.96	11.59	10.47	9.16	6.99	3.43	CORE
2	64268	OWP	TCK	ACK	32	32	9000	11.59	9.84	10.60	13.43	1.15	1.24	1.08	1.02	0.84	CORE
2	64241	OWP	TJT	BJT	32	33	9000	9.41	6.79	8.59	8.21	7.47	6.69	5.88	4.48	2.18	
2	64241	OWP	TJT	AJT	32	33	9000	9.09	7.66	8.16	10.21	6.70	6.13	5.52	4.40	2.38	
2	64227	OWP	TCK	BCK	32	31	9000	15.75	1.87	13.91	13.76	12.42	11.31	9.99	7.75	4.01	
2	64227	OWP	TCK	ACK	32	31	9000	10.69	9.07	9.92	12.33	1.30	1.29	1.24	1.16	0.94	
2	64198	OWP	TJT	BJT	32	32	9000	8.73	7.12	7.73	7.73	7.11	6.50	5.74	4.62	2.51	
2	64198	OWP	TJT	AJT	32	32	9000	7.94	6.61	7.13	8.98	6.66	6.14	5.51	4.43	2.43	
2	64171	OWP	TCK	BCK	32	32	9000	13.41	2.10	12.32	11.49	10.47	9.21	8.06	5.99	2.09	
2	64171	OWP	TCK	ACK	32	32	9000	12.78	11.08	11.26	14.69	3.43	1.42	1.46	1.29	0.97	
2	64157	OWP	TJT	BJT	32	31	9000	7.87	5.84	7.14	6.84	6.23	5.60	4.91	3.71	1.78	
2	64157	OWP	TJT	AJT	32	31	9000	7.08	5.94	6.48	8.02	5.55	5.07	4.57	3.59	1.95	
2	64134	OWP	TCK	BCK	32	32	9000	10.63	2.16	10.26	8.95	8.00	6.89	5.80	3.68	0.37	
2	64134	OWP	TCK	ACK	31	31	9000	8.62	7.23	8.05	9.66	1.69	1.59	1.45	1.30	0.87	
2	64117	OWP	TJT	BJT	32	31	9000	8.19	6.62	7.65	7.18	6.53	6.01	5.32	4.17	2.29	
2	64117	OWP	TJT	AJT	32	31	9000	7.35	6.12	6.82	8.34	6.35	5.88	5.24	4.19	2.42	
2	64089	OWP	TCK	BCK	31	32	9000	7.05	5.25	6.42	5.91	5.34	4.67	4.02	2.88	1.23	
2	64099	OWP	TCK	ACK	31	32	9000	10.73	8.98	9.71	12.37	1.34	1.33	1.23	1.07	0.75	
2	64076	OWP	TJT	BJT	32	31	9000	7.63	6.41	6.82	6.67	6.13	5.52	4.96	3.87	2.08	
2	64076	OWP	TJT	AJT	32	31	9000	7.55	6.25	6.85	8.47	6.02	5.56	5.00	4.02	2.30	
2	64042	OWP	TCK	BCK	32	32	9000	5.76	5.07	4.73	5.22	4.92	4.57	4.24	3.67	2.76	CORE
2	64042	OWP	TCK	ACK	32	31	9000	5.09	4.65	4.30	5.20	5.06	4.62	4.25	3.58	2.40	CORE
2	64035	OWP	TJT	BJT	32	31	9000	8.09	6.76	7.21	7.10	6.51	5.84	5.23	4.08	2.21	
2	64035	OWP	TJT	AJT	32	31	9000	7.63	6.45	6.82	8.50	6.55	5.95	5.36	4.27	2.38	
2	64030	MSE	MS	NONE	31	31	9000	10.75	10.25	3.63	10.53	10.27	9.96	9.60	8.57	6.56	
2	64095	MSE	MS	NONE	31	32	9000	8.04	7.43	1.76	7.96	7.76	7.62	7.51	7.05	0.69	
2	64139	MSE	MS	NONE	31	32	9000	12.34	13.74	3.67	11.24	10.56	9.70	9.00	7.13	3.98	
2	64177	MSE	MS	NONE	31	32	9000	10.40	10.46	2.73	10.05	9.64	9.27	9.02	8.22	7.11	
2	64221	MSE	MS	NONE	32	32	9000	10.36	10.68	3.98	9.81	9.35	8.88	8.40	7.47	5.99	
2	64275	MSE	MS	NONE	32	32	9000	8.14	7.61	2.36	7.97	7.75	7.62	7.33	6.77	5.68	
2	64315	MSE	MS	NONE	32	32	9000	8.81	7.91	4.05	8.96	8.84	8.90	8.99	8.93	9.06	
2	64344	MSE	MS	NONE	32	33	9000	10.48	9.84	2.40	10.22	9.95	9.78	9.59	9.00	7.93	
2	64396	MSE	MS	NONE	32	32	9000	6.83	6.34	2.03	6.77	6.59	6.46	6.34	5.94	5.29	
2	64414	MSE	MS	NONE	32	32	9000	8.23	8.31	3.77	7.72	7.34	6.85	6.40	5.35	3.55	
2	64480	MSE	MS	NONE	32	32	9000	6.72	6.48	2.00	6.43	6.18	5.85	5.60	4.85	3.64	
3	51489	MID	CORE	NONE	53	51	9000	3.61	3.58	3.55	3.62	3.47	3.35	3.19	2.89	2.28	
3	51486	MID	CORE	NONE	53	50	9000	3.71	3.70	3.58	3.57	3.41	3.25	3.06	2.73	1.94	
3	51362	MID	CORE	NONE	53	51	9000	3.92	3.82	3.65	3.79	3.63	3.44	3.26	2.82	1.99	
3	51358	MID	CORE	NONE	53	50	9000	3.89	3.81	3.64	3.79	3.68	3.47	3.23	2.80	2.02	
3	51239	MID	CORE	NONE	53	51	9000	4.09	4.22	3.83	4.04	3.77	3.62	3.34	2.89	2.19	
3	51235	MID	CORE	NONE	53	50	9000	4.17	4.06	3.93	4.12	3.96	3.76	3.54	3.15	2.34	
3	51139	MID	CORE	NONE	53	50	9000	4.39	4.29	4.13	4.29	4.07	3.85	3.64	3.22	2.09	
3	51136	MID	CORE	NONE	52	50	9000	4.37	4.25	4.07	4.22	4.04	3.78	3.51	3.02	1.98	
3	51059	MID	CORE	NONE	53	51	9000	6.85	6.22	5.85	7.09	7.02	7.20	7.19	7.34	1.40	
3	51056	MID	CORE	NONE	53	50	9000	5.39	4.95	4.44	5.41	5.60	5.37	5.49	5.55	5.57	
3	51493	OWP	TJT	BJT	52	50	9000	6.53	6.29	5.88	6.07	5.67	5.28	4.86	4.25	3.27	CORE
3	51493	OWP	TJT	AJT	52	50	9000	6.29	5.46	5.75	6.84	5.97	5.43	4.92	3.90	2.41	CORE
3	51466	OWP	TCK	BCK	53	52	9000	10.55	3.39	9.94	9.20	8.36	7.51	6.67	5.35	3.20	
3	51466	OWP	TCK	ACK	53	51	9000	8.41	7.29	7.54	9.29	9.47	2.24	2.02	1.88	1.43	
3	51452	OWP	TJT	BJT	53	51	9000	6.41	6.32	5.79	5.77	5.30	4.74	4.28	3.50	2.14	CORE
3	51452	OWP	TJT	AJT	53	51	9000	6.53	5.58	5.96	7.17	6.06	5.42	4.88	3.90	2.40	CORE
3	51438	OWP	TCK	BCK	53	51	9000	5.52	5.52	5.06	5.18	4.77	4.51	4.16	3.58	2.56	
3	51438	OWP	TCK	ACK	53	51	9000	5.21	4.78	4.93	5.59	5.24	4.94	4.49	3.86	2.67	
3	51452	OWP	TCK	BJT	53	51	9000	10.13	2.64	9.32	8.95	8.11	7.40	6.58	5.31	3.26	
3	51452	OWP	TCK	ACK	53	51	9000	10.14	8.74	9.28	11.48	2.32	2.28	2.15	1.96	1.48	
3	51411	OWP	TJT	BJT	53	51	9000	7.01	6.26	6.51	6.32	5.76	5.20	4.67	3.78	2.48	
3	51411	OWP	TJT	AJT	39	51	9000	6.69	5.71	6.24	7.30	6.15	5.56	4.99	4.07	2.53	
3	51386	OWP	TCK	BCK	52	51	9000	5.29	5.34	4.89	4.86	4.58	4.24	3.87	3.27	2.20	

3	51386	OWP	TCK	ACK	52	51	9000	5.24	4.61	4.78	5.43	5.11	4.66	4.30	3.55	2.33	
3	51369	OWP	TJT	BJT	52	50	9000	6.32	5.41	5.80	5.58	5.16	4.60	4.17	3.29	2.08	
3	51369	OWP	TJT	AJT	52	51	9000	5.78	5.08	5.49	6.46	6.39	4.75	4.34	3.50	2.19	
3	51328	OWP	TJT	BJT	52	50	9000	8.26	6.27	7.50	7.26	6.63	6.01	5.31	4.21	2.57	
3	51328	OWP	TJT	AJT	52	50	9000	7.73	6.66	7.17	8.57	5.93	5.61	5.09	4.13	2.60	
3	51301	OWP	TCK	BCK	52	51	9000	6.79	5.60	6.20	6.00	5.53	4.95	4.50	3.55	2.17	
3	51301	OWP	TCK	ACK	52	51	9000	5.91	5.15	5.57	6.43	6.56	4.89	4.48	3.65	2.33	
3	51288	OWP	TJT	BJT	34	48	9000	7.23	4.55	6.69	6.39	5.88	5.20	4.72	3.75	2.34	
3	51288	OWP	TJT	AJT	40	49	9000	6.19	5.42	5.56	6.76	5.56	4.96	4.46	3.65	2.30	
3	51261	OWP	TCK	BCK	39	50	9000	9.01	2.66	8.40	7.88	7.22	6.48	5.82	4.60	2.75	
3	51261	OWP	TCK	ACK	40	50	9000	8.02	6.71	7.65	9.20	9.23	2.15	2.10	1.82	1.41	
3	51247	OWP	TJT	BJT	39	49	9000	7.53	5.94	6.84	6.71	6.12	5.60	5.03	4.12	2.56	CORE
3	51247	OWP	TJT	AJT	42	49	9000	7.31	6.37	6.64	8.15	5.71	5.25	4.75	3.90	2.59	CORE
3	51206	OWP	TJT	BJT	35	49	9000	10.63	4.77	9.30	9.31	8.31	7.52	6.63	5.27	3.24	
3	51206	OWP	TJT	AJT	52	50	9000	12.09	9.90	10.45	14.01	4.66	4.37	4.03	3.45	2.37	
3	51189	OWP	TCK	BCK	32	47	9000	15.10	3.18	13.86	12.62	11.00	9.33	7.71	4.45	1.09	
3	51189	OWP	TCK	ACK	40	48	9000	8.46	7.13	7.96	9.50	9.71	2.52	2.33	2.02	1.48	
3	51166	OWP	TJT	BJT	44	49	9000	9.17	3.43	8.47	8.24	7.37	6.55	6.05	4.69	2.83	
3	51166	OWP	TJT	AJT	43	49	9000	12.03	10.45	10.30	13.39	13.25	4.49	4.28	3.35	2.24	
3	51124	OWP	TJT	BJT	52	50	9000	11.45	3.47	10.32	9.91	8.88	7.97	6.97	5.38	2.80	CORE
3	51124	OWP	TJT	AJT	42	45	9000	12.04	10.43	10.86	13.90	6.34	5.82	5.25	4.32	2.81	CORE
3	51111	OWP	TCK	BCK	37	48	9000	13.80	2.10	13.73	12.43	11.09	9.90	8.72	6.44	3.24	
3	51111	OWP	TCK	ACK	41	47	9000	10.06	8.52	9.55	11.53	2.28	2.35	2.11	2.05	1.53	
3	51085	OWP	TJT	BJT	41	49	9000	8.56	2.90	7.76	7.23	6.52	5.70	4.95	3.71	1.93	
3	51085	OWP	TJT	AJT	39	47	9000	8.23	6.41	8.43	10.43	2.21	2.01	1.85	1.63	1.18	
3	51078	OWP	TCK	BCK	41	49	9000	10.11	2.64	10.73	9.43	8.29	6.84	5.43	2.93	1.79	CORE
3	51078	OWP	TCK	ACK	43	48	9000	10.65	8.07	10.85	13.92	3.12	2.93	2.60	2.22	1.54	CORE
3	51042	OWP	TJT	BJT	39	49	9000	8.78	3.04	7.97	7.48	6.71	5.85	5.06	3.76	1.98	
3	51042	OWP	TJT	AJT	50	50	9000	16.97	14.84	14.89	19.37	4.22	4.09	3.59	2.92	1.79	
3	51013	OWP	TCK	BCK	52	52	9000	6.81	6.08	6.09	5.90	5.37	4.72	4.10	3.04	1.32	CORE
3	51013	OWP	TCK	ACK	52	51	9000	8.90	7.28	7.30	10.09	5.46	4.82	4.19	3.08	1.41	CORE
3	51002	OWP	TJT	BJT	39	49	9000	8.95	2.48	8.28	7.65	6.92	6.13	5.30	3.99	2.14	
3	51002	OWP	TJT	AJT	52	50	9000	7.61	6.38	7.23	8.54	2.08	1.95	1.88	1.64	1.21	
3	51091	MSE	MS	NONE	37	48	9000	6.99	6.53	4.48	6.67	6.24	6.02	5.37	4.73	3.70	
3	51131	MSE	MS	NONE	52	50	9000	9.42	8.89	4.26	8.72	8.22	7.76	7.23	6.24	4.74	
3	51158	MSE	MS	NONE	52	51	9000	11.34	12.04	5.47	10.45	9.81	9.18	7.46	6.26	4.31	
3	51281	MSE	MS	NONE	52	49	9000	10.52	9.53	4.25	10.80	10.77	10.95	11.06	11.14	11.55	
3	51308	MSE	MS	NONE	52	51	9000	8.28	8.65	4.01	7.74	7.35	6.89	6.43	5.38	3.43	
3	51335	MSE	MS	NONE	52	50	9000	7.53	7.30	3.62	7.35	7.07	8.85	6.52	5.75	4.36	
3	51376	MSE	MS	NONE	52	49	9000	6.69	6.40	3.67	6.43	6.17	5.90	5.56	4.79	3.36	
3	51431	MSE	MS	NONE	52	49	9000	8.18	7.57	4.65	8.12	7.89	7.76	7.57	7.13	6.48	
3	51444	MSE	MS	NONE	52	49	9000	8.19	7.88	3.60	8.03	7.76	7.42	7.13	6.26	4.52	
3	51474	MSE	MS	NONE	52	52	9000	10.22	10.00	3.26	10.01	9.65	9.31	8.99	8.11	6.78	

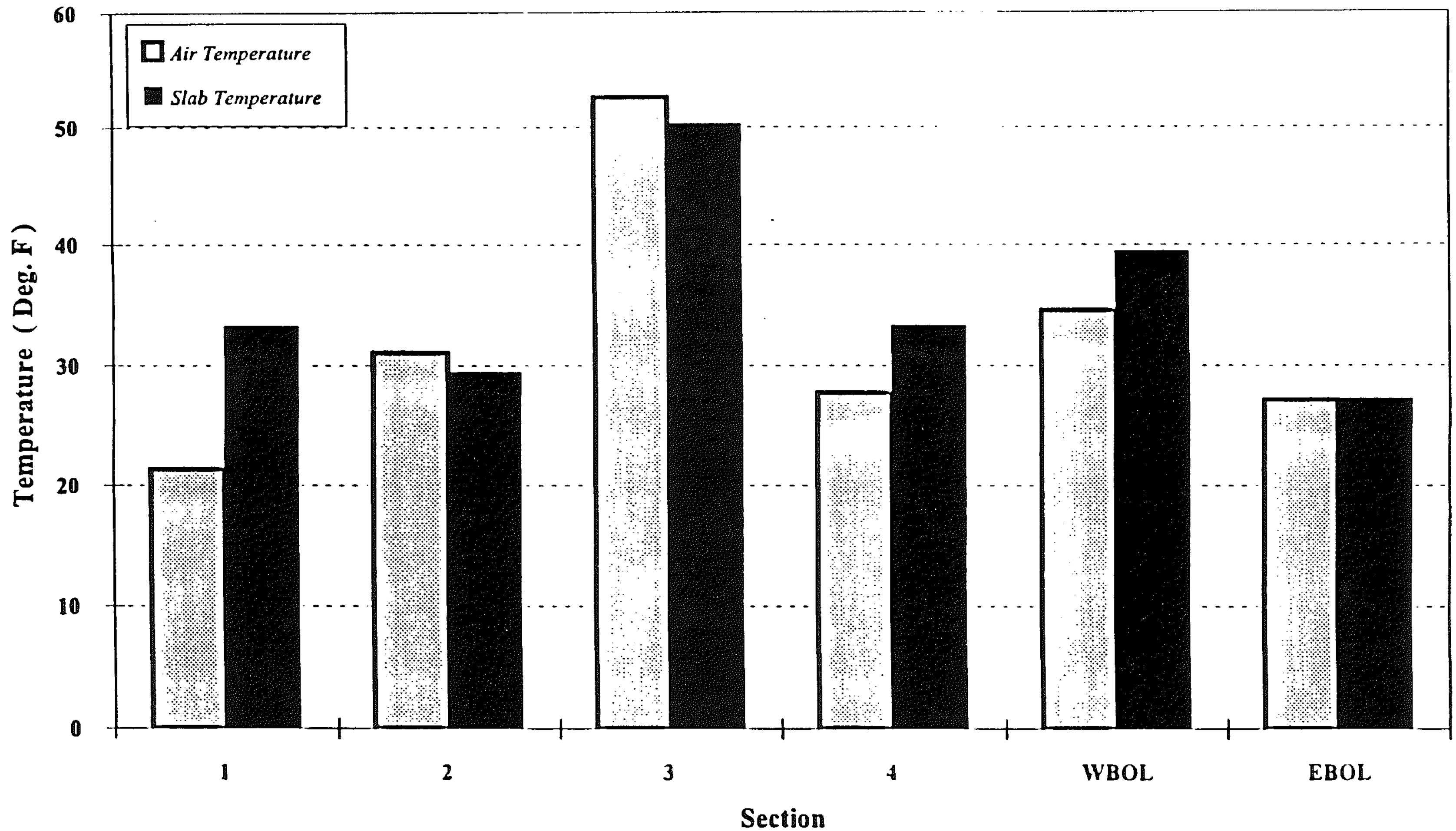
Air Temperature
Slab Temperature
60
50
40
30
20
10
0
Temperature (Deg. F)
1
2
3
4
WBOL
EBOL
Section

Figure A4-1

Deflections at Mid Slab

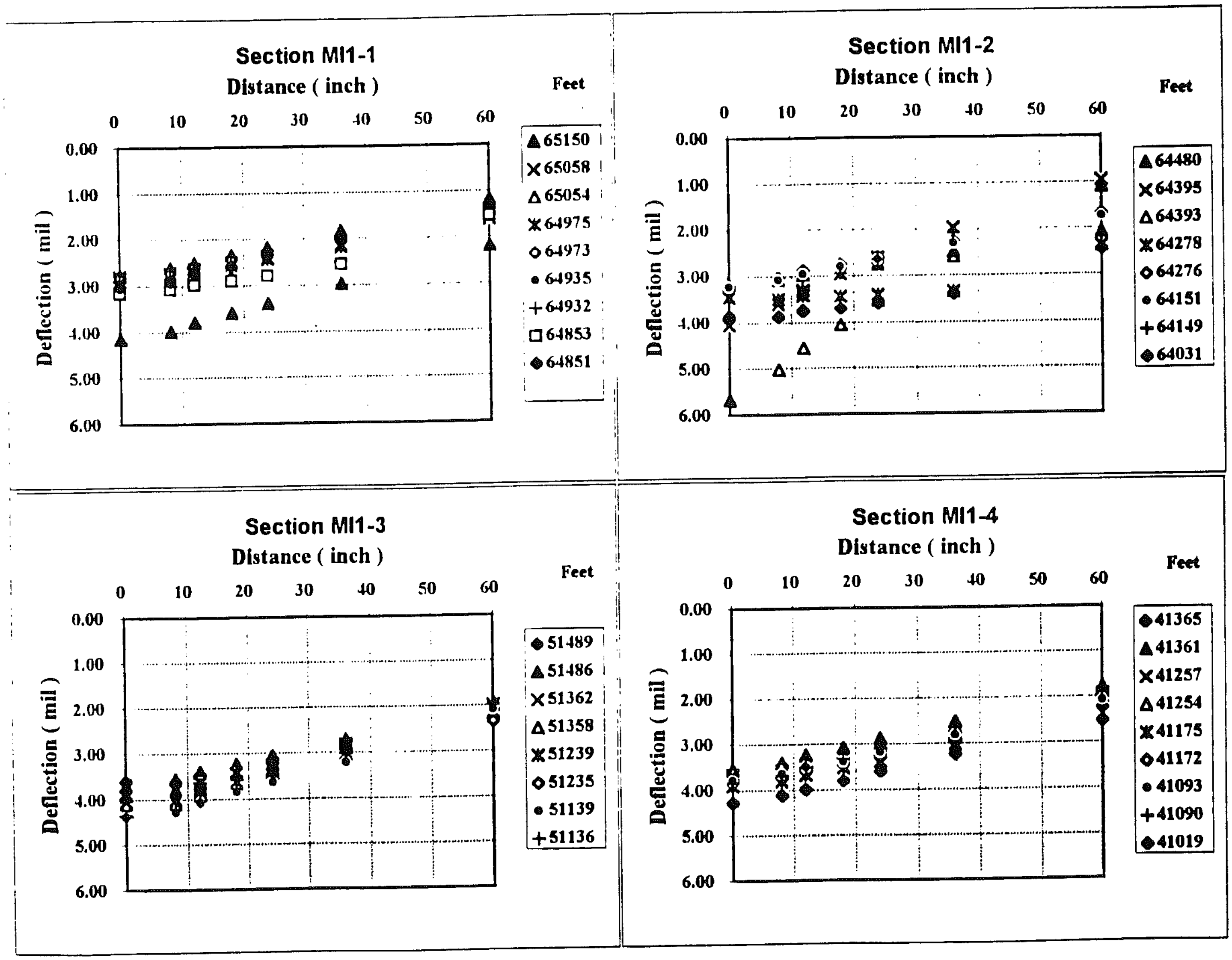

Figure A4-2

Deflections at Mid Slab

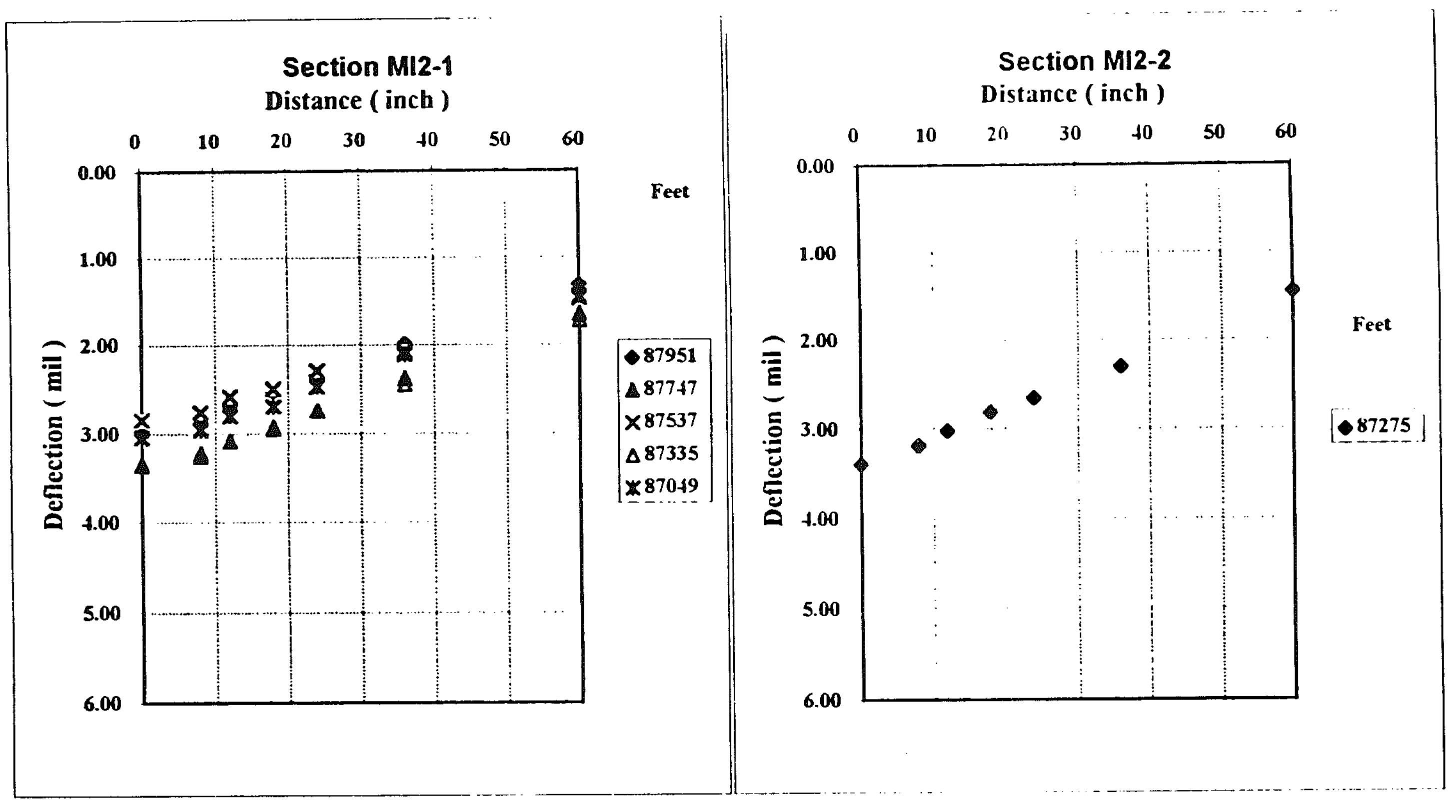

Note : Other FWD tests on MI2-2 have been neglected due to suspected error

Figure A4-3

Variation of Elastic Moduli (Ioannides Method) for various sections

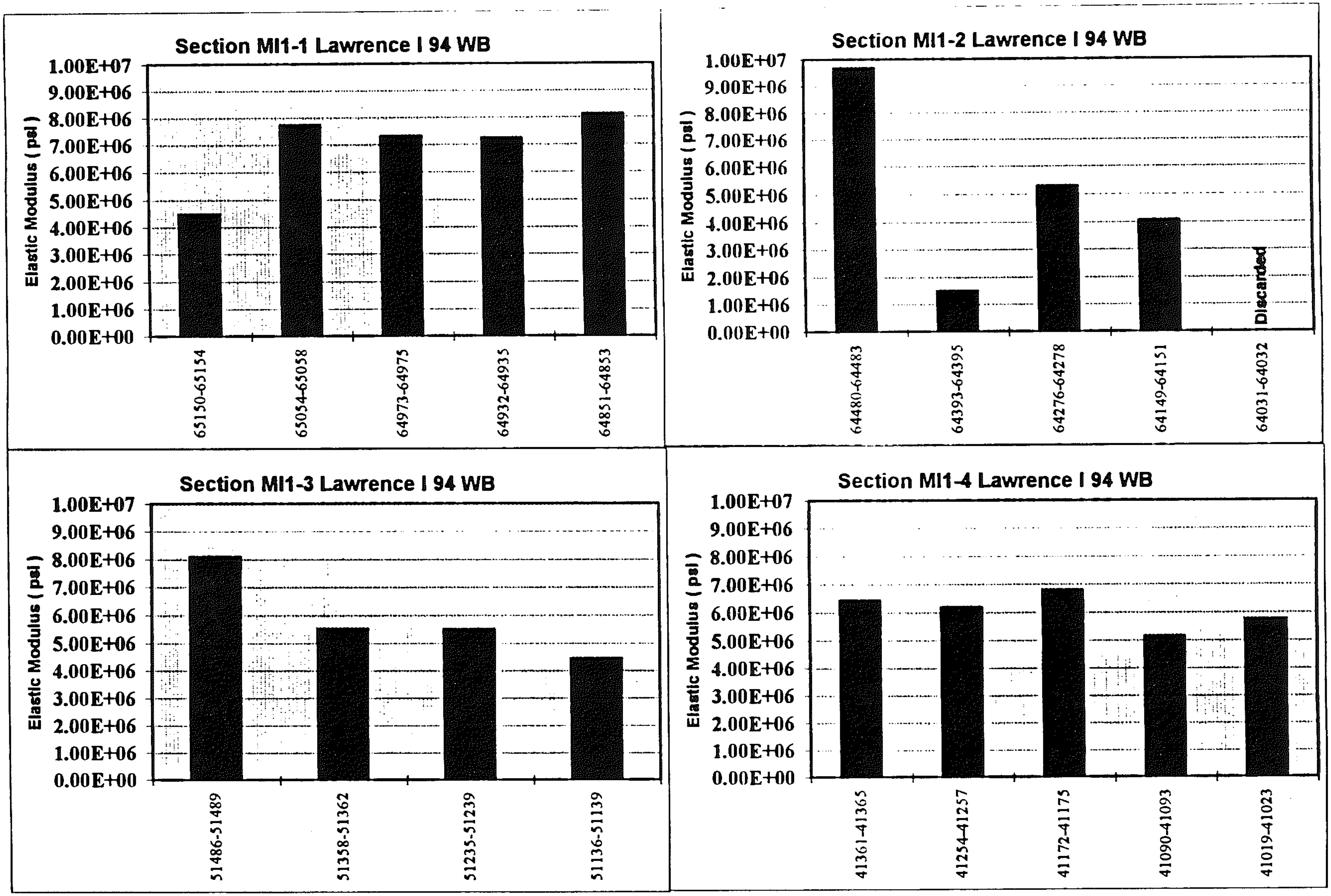

Figure A4-4

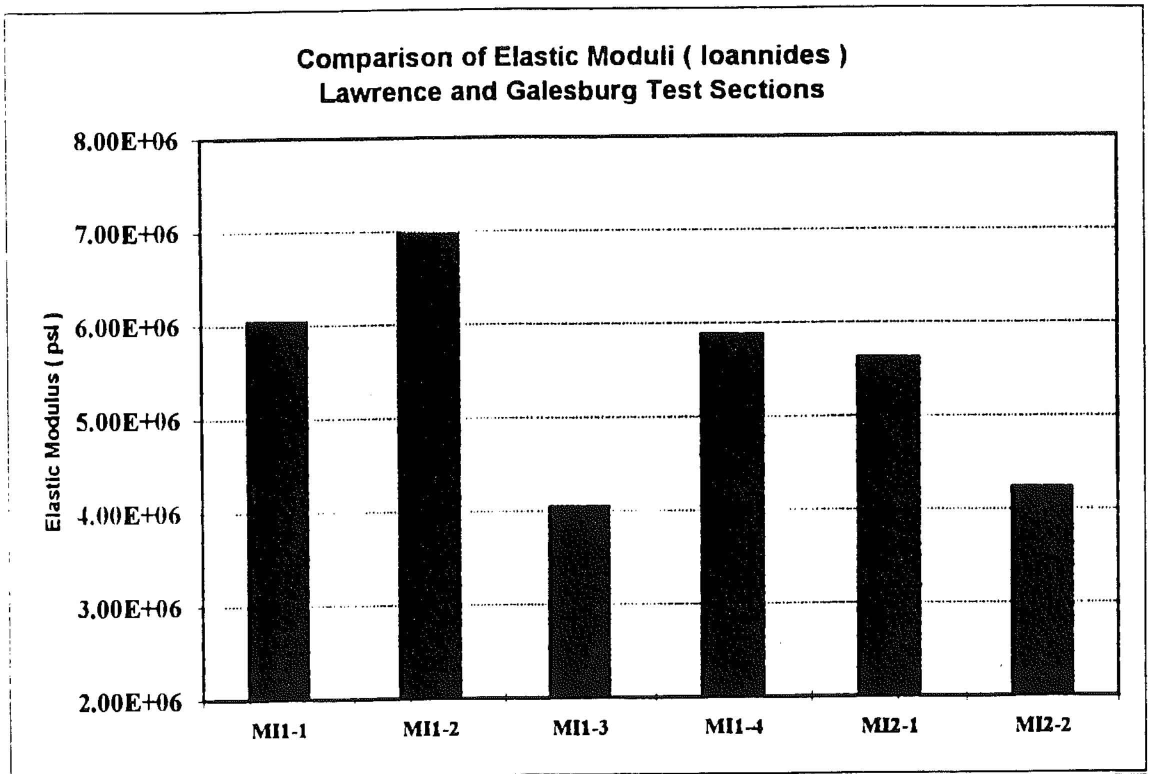
Comparison of Elastic Moduli (Ioannides)
Lawrence and Galesburg Test Sections
8.00E+06
7.00E+06
6.00E+06
5.00E+06
4.00E+06
3.00E+06
2.00E+06
Elastic Modulus (psi)
MI1-1
MI1-2
MI1-3
MI1-4
MI2-1
MI2-2

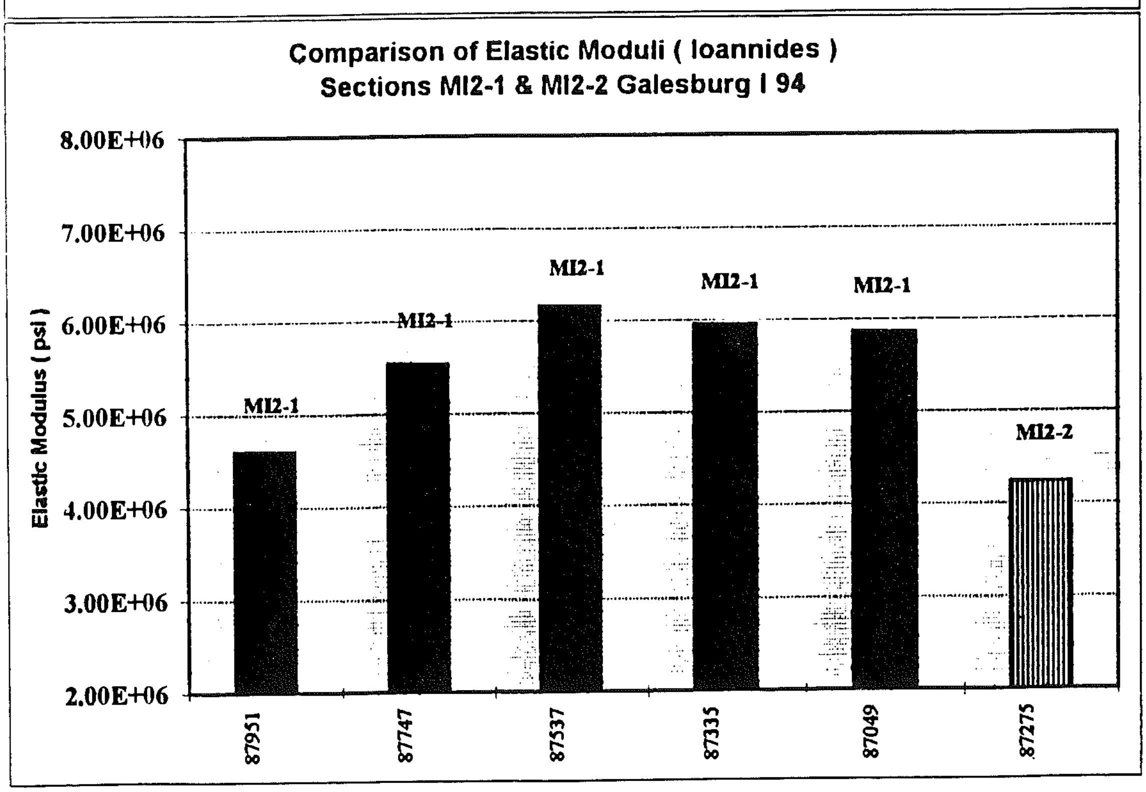
Comparison of Elastic Moduli (Ioannides)
Sections MI2-1 & MI2-2 Galesburg I 94
8.00E+06
7.00E+06
6.00E+06
5.00E+06
4.00E+06
3.00E+06
2.00E+06
Elastic Modulus (psi)
MI2-1
MI2-1
MI2-1
MI2-1
MI2-1
MI2-2
87951
87747
87537
87335
87049
87275

Figure A4-5

Summary of Findings:

Project		Lawrence Project CSN 80023-20993				Gailsberg Project CSN 39022-20736	
Section		MI1-1	MI1-2	MI1-3	MI1-4	MI2-1	MI2-2
Location		Lawrence I-94 WB	Lawrence I-94 WB	Lawrence I-94 WB	Lawrence I-94 WB	Galesburg I-94 WB	Galesburg I-94 EB
Station		648+17 - 652+25	603+07 - 648+17	496+56 - 515+33	407+50 - 436+20	823+62 - 922+73	825+11 - 888+00
Type of Pavement		Peastone	Recycled	Recycled	Recycled	Recycled	Recycled
Base Type		Open Graded	Open Graded	5 % Cement Stabilized Peastone Aggregate	Dense Graded	Open Graded	Open Graded
Mid Slab	Max. Deflections (mil)	3.21	3.93	4.44	3.93	3.12	4.87
E of concrete (million psi)	Predicted	7.25	3.26	5.88	6.08	5.62	4.23
K (psi/in)	Predicted	244	359	163	171	270	297*
E of concrete (million psi)	Actual	3.18	3.67	3.51	3.97	3.83	3.73
E of soil (psi)	Predicted	33201	25210	20754	22411	32217	18928
Edge of Slab	Max. Deflections (mil)	8.2	9.2	8.7	9.3	12.3	15.9
(No Joint & No Crack)	Comparative Influence Area	Medium	Medium	High	Medium	High	Low
	Load Transfer to Shoulder (%)	43.5	32.1	48.2	34.5	34.7	39.5
Outer Wheel Path	Max. Deflections (mil)	7.54	8.72	8.22	7.88	14	11.8
(Transverse Joint)	Comparative Influence Area	Medium	Medium	Medium	Medium	Medium	Low
	Load Transfer at Joint (%)	65.8	79.2	57.2	83.4	58.5	52.4

* based on single test

Note:

1 Peastone control section shows higher concrete modulus compared to the recycled sections
2 MI1-2 and MI2-2 show lowest predicted concrete modulus values resulting in higher deflections despite the higher modulus of subgrade reaction
3 The higher deflections at the outer wheel path combined with the low modulus of concrete and smaller influence area might have contributed to the deterioration of the sections at MI2-2
4 Even though, the section MI2-1 shows better concrete and base from the mid slab test, the higher deflections at outer wheel path may be due to the influence of the longitudinal edge drain below.
5 Even though, MI2-1 shows higher deflections, its a higher influence area might have contributed to its better performance.
6 Except for section MI1-4, the load transfer at joints are low due to high ESALs and contribute to the higher deflections compared to the mid slab tests.
7 Load transfer between slab and pavement is low for all sections resulting in higher deflections for the edge test.

Table A4-1

Load Transfer Between Adjacent Slabs (Based on Sensor Readings D0 and D1 with Transverse Joint Between D0 and D1)					
Section	**Station**	**Lane**	**Test**	**Type**	**Load Transfer %**
MI1-1	651+87	OWP	TJT	BJT	65.7
MI1-1	651+46	OWP	TJT	BJT	
MI1-1	651+04	OWP	TJT	BJT	54.6
MI1-1	650+63	OWP	TJT	BJT	47.7
MI1-1	650+22	OWP	TJT	BJT	60.6
MI1-1	649+81	OWP	TJT	BJT	65.6
MI1-1	649+39	OWP	TJT	BJT	62.0
MI1-1	648+99	OWP	TJT	BJT	61.0
MI1-1	648+58	OWP	TJT	BJT	79.3
MI1-1	648+17	OWP	TJT	BJT	80.7
				Average	**65.8**
				Standard Deviation	**22.6**
				Coef. of Variation	**34.3**
MI1-2	644+88	OWP	TJT	BJT	76.3
MI1-2	644+46	OWP	TJT	BJT	76.6
MI1-2	644+05	OWP	TJT	BJT	71.6
MI1-2	643+64	OWP	TJT	BJT	80.3
MI1-2	643+23	OWP	TJT	BJT	84.4
MI1-2	642+82	OWP	TJT	BJT	86.9
MI1-2	642+41	OWP	TJT	BJT	72.1
MI1-2	641+98	OWP	TJT	BJT	81.5
MI1-2	641+57	OWP	TJT	BJT	74.2
MI1-2	641+17	OWP	TJT	BJT	80.8
MI1-2	640+76	OWP	TJT	BJT	84.1
MI1-2	640+35	OWP	TJT	BJT	83.6
				Average	**79.2**
				Standard Deviation	**5.1**
				Coef. of Variation	**6.4**
MI1-3	514+93	OWP	TJT	BJT	96.3
MI1-3	514+52	OWP	TJT	BJT	98.6
MI1-3	514+11	OWP	TJT	BJT	89.3
MI1-3	513+69	OWP	TJT	BJT	85.5
MI1-3	513+28	OWP	TJT	BJT	75.9
MI1-3	512+88	OWP	TJT	BJT	63.0
MI1-3	512+47	OWP	TJT	BJT	78.9
MI1-3	512+06	OWP	TJT	BJT	44.9
MI1-3	511+66	OWP	TJT	BJT	37.4
MI1-3	511+24	OWP	TJT	BJT	30.3
MI1-3	510+85	OWP	TJT	BJT	33.9
MI1-3	510+42	OWP	TJT	BJT	34.7
MI1-3	510+02	OWP	TJT	BJT	27.2
				Average	**57.2**
				Standard Deviation	**27.2**
				Coef. of Variation	**47.6**

Table A4-2

Load Transfer Between Adjacent Slabs (Based on Sensor Readings D0 and D1 with Transverse Joint Between D0 and D1)					
Section	Station	Lane	Test	Type	Load Transfer %
MI1-4	413+71	OWP	TJT	BJT	74.4
MI1-4	413+30	OWP	TJT	BJT	81.3
MI1-4	412+89	OWP	TJT	BJT	92.5
MI1-4	412+48	OWP	TJT	BJT	96.3
MI1-4	412+07	OWP	TJT	BJT	84.3
MI1-4	411+66	OWP	TJT	BJT	45.2
MI1-4	411+24	OWP	TJT	BJT	96.0
MI1-4	410+83	OWP	TJT	BJT	84.9
MI1-4	410+42	OWP	TJT	BJT	88.3
MI1-4	410+02	OWP	TJT	BJT	88.7
				Average	**83.4**
				Standard Deviation	**14.9**
				Coef. of Variation	**17.9**
MI2-1	879+70	OWP	TJT	BJT	31.4
MI2-1	879+38	OWP	TJT	BJT	35.1
MI2-1	878+04	OWP	TJT	BJT	29.5
MI2-1	876+82	OWP	TJT	BJT	60.8
MI2-1	875+59	OWP	TJT	BJT	69.8
MI2-1	874+78	OWP	TJT	BJT	46.0
MI2-1	874+37	OWP	TJT	BJT	71.2
MI2-1	873+12	OWP	TJT	BJT	94.0
MI2-1	871+90	OWP	TJT	BJT	83.4
MI2-1	871+49	OWP	TJT	BJT	81.5
MI2-1	870+67	OWP	TJT	BJT	68.0
				Average	**58.5**
				Standard Deviation	**22.4**
				Coef. of Variation	**38.3**
MI2-2	870+26	OWP	TJT	BJT	47.1
MI2-2	871+47	OWP	TJT	BJT	69.0
MI2-2	872+70	OWP	TJT	BJT	79.1
MI2-2	873+94	OWP	TJT	BJT	64.3
MI2-2	875+16	OWP	TJT	BJT	53.2
MI2-2	876+31	OWP	TJT	BJT	44.0
MI2-2	877+54	OWP	TJT	BJT	42.2
MI2-2	878+78	OWP	TJT	BJT	38.7
MI2-2	880+00	OWP	TJT	BJT	45.8
				Average	**52.4**
				Standard Deviation	**13.9**
				Coef. of Variation	**26.6**

Table A4-3

Load Transfer Between Slabs and Shoulder
(Based on Sensor Readings D0 and D2 with Shoulder Joint Between D0 and D2)

Section	Station	Lane	Test	Type	Load Transfer %
MI1-1	648+53	MSE	MS	NONE	19.5
MI1-1	648+93	MSE	MS	NONE	27.7
MI1-1	649+21	MSE	MS	NONE	69.7
MI1-1	649+77	MSE	MS	NONE	86.9
MI1-1	650+29	MSE	MS	NONE	43.7
MI1-1	650+58	MSE	MS	NONE	65.9
MI1-1	650+86	MSE	MS	NONE	22.7
MI1-1	651+11	MSE	MS	NONE	28.1
MI1-1	651+54	MSE	MS	NONE	36.6
MI1-1	651+93	MSE	MS	NONE	69.7
				Average	**43.5**
				Standard Deviation	**24**
				Coef. of Variation	**55.1**
MI1-2	640+30	MSE	MS	NONE	33.8
MI1-2	640+95	MSE	MS	NONE	21.9
MI1-2	641+39	MSE	MS	NONE	29.8
MI1-2	641+77	MSE	MS	NONE	26.2
MI1-2	642+21	MSE	MS	NONE	38.4
MI1-2	642+75	MSE	MS	NONE	29.0
MI1-2	643+15	MSE	MS	NONE	46.0
MI1-2	643+44	MSE	MS	NONE	22.9
MI1-2	643+96	MSE	MS	NONE	29.7
MI1-2	644+14	MSE	MS	NONE	45.8
MI1-2	644+80	MSE	MS	NONE	29.7
				Average	**32.1**
				Standard Deviation	**8.2**
				Coef. of Variation	**25.6**
MI1-3	510+91	MSE	MS	NONE	64.1
MI1-3	511+31	MSE	MS	NONE	45.2
MI1-3	511+58	MSE	MS	NONE	48.3
MI1-3	512+81	MSE	MS	NONE	40.4
MI1-3	513+08	MSE	MS	NONE	48.4
MI1-3	513+35	MSE	MS	NONE	48.1
MI1-3	513+76	MSE	MS	NONE	54.9
MI1-3	514+31	MSE	MS	NONE	56.8
MI1-3	514+44	MSE	MS	NONE	43.9
MI1-3	514+74	MSE	MS	NONE	31.9
				Average	**48.2**
				Standard Deviation	**9.0**
				Coef. of Variation	**18.6**
MI1-4	410+35	MSE	MS	NONE	40.6
MI1-4	411+86	MSE	MS	NONE	32.6
MI1-4	413+11	MSE	MS	NONE	31.2
				Average	**34.5**
				Standard Deviation	**5.1**
				Coef. of Variation	**14.7**
MI2-1	872+14	MSE	MS	NONE	10.1
MI2-1	874+16	MSE	MS	NONE	85.0
MI2-1	877+04	MSE	MS	NONE	9.1
				Average	**34.7**
				Standard Deviation	**43.5**
				Coef. of Variation	**125.4**
MI2-2	877+08	MSE	MS	NONE	34.0
MI2-2	875+70	MSE	MS	NONE	21.8
MI2-2	873+80	MSE	MS	NONE	20.9
MI2-2	872+75	MSE	MS	NONE	81.4
				Average	**39.5**
				Standard Deviation	**28.6**
				Coef. of Variation	**72.3**

Table A4-4

Load Transfer Between Transverse Cracks (Based on Sensor Readings D0 and D1 with Transverse Joint Between D0 and D1)					
Section	**Station**	**Lane**	**Test**	**Type**	**Load Transfer %**
MI1-1	652+01	OWP	TCK	BCK	95.8
MI1-1	651+32	OWP	TCK	BCK	14.8
MI1-1	650+77	OWP	TCK	BCK	99.5
MI1-1	650+50	OWP	TCK	BCK	98.6
MI1-1	650+09	OWP	TCK	BCK	47.5
MI1-1	649+12	OWP	TCK	BCK	14.5
MI1-1	648+87	OWP	TCK	BCK	8.7
				Average	**54.2**
				Standard Deviation	**42.8**
				Coef. of Variation	**79.0**
MI1-2	644+33	OWP	TCK	BCK	13.1
MI1-2	643+77	OWP	TCK	BCK	13.6
MI1-2	643+50	OWP	TCK	BCK	100.8
MI1-2	642+95	OWP	TCK	BCK	17.6
MI1-2	642+68	OWP	TCK	BCK	10.2
MI1-2	642+27	OWP	TCK	BCK	11.9
MI1-2	641+71	OWP	TCK	BCK	15.7
MI1-2	641+34	OWP	TCK	BCK	20.3
MI1-2	640+89	OWP	TCK	BCK	74.4
MI1-2	640+42	OWP	TCK	BCK	88.0
				Average	**36.6**
				Standard Deviation	**36.0**
				Coef. of Variation	**98.4**
MI1-3	514+66	OWP	TCK	BCK	32.2
MI1-3	514+38	OWP	TCK	BCK	100.1
MI1-3	513+86	OWP	TCK	BCK	100.9
MI1-3	513+01	OWP	TCK	BCK	82.6
MI1-3	512+61	OWP	TCK	BCK	29.6
MI1-3	511+89	OWP	TCK	BCK	21.0
MI1-3	511+11	OWP	TCK	BCK	15.2
MI1-3	510+78	OWP	TCK	BCK	26.1
MI1-3	510+13	OWP	TCK	BCK	89.2
				Average	**55.2**
				Standard Deviation	**36.8**
				Coef. of Variation	**66.6**
MI1-4	411+39	OWP	TCK	BCK	21.1
MI1-4	410+99	OWP	TCK	BCK	63.3
MI1-4	410+70	OWP	TCK	BCK	100.6
				Average	**61.7**
				Standard Deviation	**39.7**
				Coef. of Variation	**64.4**
MI2-1	874+90	OWP	TCK	BCK	92.3
MI2-2	870+42	OWP	TCK	BCK	28.9
MI2-2	870+80	OWP	TCK	BCK	26.7
MI2-2	871+28	OWP	TCK	BCK	20.8
MI2-2	871+63	OWP	TCK	BCK	18.9
MI2-2	872+97	OWP	TCK	BCK	18.4
MI2-2	873+64	OWP	TCK	BCK	28.6
MI2-2	874+86	OWP	TCK	BCK	15.7
MI2-2	876+36	OWP	TCK	BCK	51.1
MI2-2	876+84	OWP	TCK	BCK	34.0
MI2-2	877+80	OWP	TCK	BCK	96.1
MI2-2	878+27	OWP	TCK	BCK	22.8
MI2-2	878+66	OWP	TCK	BCK	19.9
MI2-2	879+80	OWP	TCK	BCK	19.0
				Average	**30.8**
				Standard Deviation	**21.7**
				Coef. of Variation	**70.4**

Table A4-5

Back Calculation of Elastic Modulus (Ioannides 1989 Method & Bousdef)

Sheet 1/2

SECT	FEET	P lb	D0 0	D4 12	D5 24	D6 36	Ioannides AREA (in)	Ioannides L (in)	Ioannides d0	Ioannides k psi/in	Ioannides E psi	Bousdef E psi	Remarks
MI1-1	65154	9000	4.73	4.89	5.03	5.20	37.773	198.605	0.1249	6.03	1.10E+08	9.00E+06	Disc
MI1-1	65150	9000	4.16	3.79	3.40	2.98	31.083	37.744	0.1234	187.60	4.47E+06	4.70E+06	
MI1-1	65058	9000	2.80	2.64	2.41	2.14	32.190	46.101	0.1239	187.13	9.92E+06	8.66E+06	
MI1-1	65054	9000	2.76	2.51	2.19	1.84	30.442	34.303	0.1232	341.30	5.54E+06	4.70E+06	
MI1-1	64975	9000	2.89	2.71	2.44	2.18	31.894	43.511	0.1238	203.36	8.55E+06	7.03E+06	
MI1-1	64973	9000	2.81	2.57	2.26	1.94	30.805	36.150	0.1233	302.58	6.06E+06	5.17E+06	
MI1-1	64935	9000	3.03	2.91	2.74	2.49	33.314	58.968	0.1243	106.15	1.51E+07	6.93E+06	Disc
MI1-1	64932	9000	2.73	2.52	2.25	1.97	31.267	38.905	0.1235	269.02	7.23E+06	6.63E+06	
MI1-1	64853	9000	3.16	2.99	2.79	2.57	32.823	52.693	0.1241	127.31	1.15E+07	6.85E+06	
MI1-1	64851	9000	3.02	2.71	2.37	2.02	30.192	33.171	0.1231	332.91	4.73E+06	4.22E+06	
MI1-1						Average				243.90	7.25E+06	6.00E+06	
						Standard Deviation				78.48	2.55E+06	1.53E+06	
						Coefficient of Variation				32.2	35.1	25.6	
MI1-2	64483	9000	3.88	3.98	4.16	4.26	37.756	197.666	0.1249	7.41	1.33E+08	9.00E+06	Disc
MI1-2	64480	9000	3.17	2.98	2.75	2.49	32.425	48.372	0.1240	150.58	9.67E+06	9.00E+06	Disc
MI1-2	64395	9000	4.05	3.31	2.61	1.97	26.464	23.685	0.1216	481.68	1.78E+06	3.00E+06	
MI1-2	64393	9000	5.68	4.55	3.55	2.60	25.859	22.687	0.1213	373.57	1.16E+06	3.00E+06	
MI1-2	64278	9000	3.44	3.42	3.41	3.36	35.669	109.310	0.1248	27.29	4.57E+07	9.00E+06	Disc
MI1-2	64276	9000	3.20	2.89	2.60	2.26	30.793	36.083	0.1233	266.09	5.29E+06	6.13E+06	
MI1-2	64151	9000	3.22	2.95	2.65	2.32	31.180	38.346	0.1235	234.70	5.95E+06	6.36E+06	
MI1-2	64149	9000	3.89	3.23	2.66	2.09	27.427	25.393	0.1220	438.00	2.14E+06	3.00E+06	
MI1-2	64032	9000	4.89	5.10	5.41	4.28	37.047	161.521	0.1249	8.81	7.03E+07	4.36E+06	Disc
MI1-2	64031	9000	3.86	3.75	3.60	3.40	34.164	72.792	0.1245	54.83	1.81E+07	8.39E+06	Disc
MI1-2						Average				358.80	3.26E+06	4.30E+06	
						Standard Deviation				106.75	2.19E+06	1.78E+06	
						Standard Deviation				106.75	2.19E+06	1.78E+06	
						Coefficient of Variation				29.8	67.2	41.4	
MI1-3	51489	9000	3.61	3.47	3.19	2.89	32.961	54.351	0.1242	104.88	1.07E+07	7.32E+06	
MI1-3	51486	9000	3.71	3.41	3.06	2.73	31.341	39.391	0.1235	192.97	5.45E+06	5.30E+06	
MI1-3	51362	9000	3.92	3.63	3.26	2.82	31.387	39.698	0.1236	179.86	5.24E+06	4.57E+06	
MI1-3	51358	9000	3.89	3.68	3.23	2.80	31.628	41.423	0.1237	166.60	5.75E+06	4.64E+06	
MI1-3	51239	9000	4.09	3.77	3.34	2.89	31.126	38.007	0.1234	188.21	4.61E+06	5.42E+06	
MI1-3	51235	9000	4.17	3.96	3.54	3.15	32.080	45.102	0.1238	131.29	6.37E+06	5.11E+06	
MI1-3	51139	9000	4.39	4.07	3.64	3.22	31.505	40.520	0.1236	154.46	4.88E+06	3.67E+06	
MI1-3	51136	9000	4.37	4.04	3.51	3.02	30.893	36.637	0.1234	189.41	4.00E+06	3.22E+06	
MI1-3	51059	9000	6.85	7.02	7.19	7.34	37.341	175.628	0.1249	5.32	5.94E+07	1.16E+06	Disc
MI1-3	51056	9000	5.39	5.60	5.49	5.55	36.849	152.664	0.1249	8.94	5.70E+07	9.00E+06	Disc
MI1-3						Average				163.46	5.88E+06	4.91E+06	
						Standard Deviation				31.58	2.09E+06	1.24E+06	
						Coefficient of Variation				19.3	35.5	25.4	

Table A4-6

Back Calculation of Elastic Modulus (Ioannides 1989 Method & Bousdef)

Sheet 2/2

							Ioannides					Bousdef	
SECT	FEET	P lb	D0 0	D4 12	D5 24	D6 36	AREA (in)	L (in)	d0	k psi/in	E psi	E psi	Remarks
MI1-4	41365	9000	3.84	3.60	3.30	2.95	32.177	45.980	0.1239	137.33	7.20E+06	7.65E+06	
MI1-4	41361	9000	3.66	3.40	3.03	2.62	31.383	39.670	0.1236	193.07	5.61E+06	4.76E+06	
MI1-4	41257	9000	3.66	3.47	3.12	2.77	32.124	45.494	0.1239	147.02	7.39E+06	5.79E+06	
MI1-4	41254	9000	3.56	3.25	2.88	2.52	30.933	36.866	0.1234	229.69	4.98E+06	4.95E+06	
MI1-4	41175	9000	3.90	3.68	3.39	3.02	32.377	47.893	0.1240	124.60	7.69E+06	6.54E+06	
MI1-4	41172	9000	3.76	3.48	3.16	2.76	31.578	41.053	0.1236	175.44	5.85E+06	4.91E+06	
MI1-4	41093	9000	3.79	3.50	3.18	2.81	31.620	41.361	0.1237	171.65	5.89E+06	5.75E+06	
MI1-4	41090	9000	3.85	3.52	3.11	2.64	30.764	35.925	0.1233	223.32	4.36E+06	3.88E+06	
MI1-4	41023	9000	4.98	5.05	5.14	5.22	36.835	152.038	0.1249	9.76	6.11E+07	9.00E+06	Disc
MI1-4	41019	9000	4.28	4.00	3.61	3.23	31.875	43.357	0.1238	138.55	5.74E+06	5.96E+06	
MI1-4						Average				171.19	6.08E+06	5.58E+06	
						Standard Deviation				38.09	1.13E+06	1.11E+06	
						Coefficient of Variation				22.2	18.5	19.9	
MI2-1	87951	9000	3.00	2.68	2.34	1.99	30.053	32.588	0.1230	347.43	4.60E+06	5.34E+06	
MI2-1	87747	9000	3.36	3.09	2.75	2.39	31.094	37.814	0.1234	230.99	5.54E+06	4.99E+06	
MI2-1	87537	9000	2.85	2.59	2.30	2.08	30.911	36.739	0.1234	288.27	6.16E+06	6.72E+06	
MI2-1	87335	9000	3.35	3.09	2.75	2.45	31.300	39.119	0.1235	216.64	5.95E+06	5.63E+06	
MI2-1	87049	9000	3.05	2.81	2.48	2.12	30.964	37.041	0.1234	265.35	5.86E+06	5.94E+06	
MI2-1						Average				269.74	5.62E+06	5.72E+06	
						Standard Deviation				51.77	6.15E+05	6.58E+05	
						Coefficient of Variation				19.2	10.9	11.5	
MI2-2	87275	9000	3.39	3.02	2.66	2.30	30.201	33.210	0.1231	296.51	4.23E+06	4.02E+06	
MI2-2	87450	9000	3.69	3.61	3.66	3.76	35.788	113.031	0.1248	23.84	4.56E+07	9.00E+06	Disc
MI2-2	87570	9000	7.48	8.10	8.69	9.36	40.451	416.867	0.1250	0.87	3.07E+08	1.21E+06	Disc
MI2-2	87708	9000	4.28	4.24	4.29	4.40	36.103	123.498	0.1248	17.22	4.70E+07	1.95E+06	Disc
MI2-2	87938	9000	5.54	5.87	6.37	6.91	40.013	370.515	0.1250	1.48	3.27E+08	1.85E+06	Disc
MI2-2						Average (single value)				296.51	4.23E+06	4.02E+06	

Table A4-7

Appendix 5: Gradation Analysis

Samples of base, subbase and subgrade materials collected from all midpanel core locations were tested for their grain size distribution. The loss of fines on washing (particles passing #200 sieve as per MTM 108-94 and ASTM C117-90[15,16]) was determined for all subbase and subgrade samples before performing the full sieving (MTM 109-88 and ASTM C136-92[17-18]). In the case of the base materials, loss on washing was determined only for two samples, which visually showed higher content of fines. These were dense graded base course samples from MI1-4

The filter criteria was verified for the subgrade-subbase and subbase-base interfaces based on section average values of grain size parameters for each test section. The permeability of each layer was determined using Hazen's empirical correlation[19].

The first page of this appendix shows the data and calculations to determine the percentage of fines contained in each sample. The low percentage of fines in the subgrade materials shows that the foundation is generally granular (less than 12% fines).

The second page shows the laboratory data of retained weights in each sieve from the mechanical sieving that leads to the percentage of passing material for each size shown in the third page. Note that the finer sieves (from #50 to #200) were not used for analyzing base materials with the exception of the MI1-4 samples because of their coarse gradations. MI1-4 is dense graded with higher content of fines. The subbase and subgrade materials also contain a higher percentage of fines, meriting the use of the smaller sieves.

Grain size distribution curves for base, subbase and subgrade materials of the Lawrence project are shown, followed by similar information for the Galesburg project. The shape of the curves for the MI1-4 section base samples show that this section is a well graded material as opposed to the poorly graded materials of the other test sections.

The last page of this appendix shows the verification of the filter qualities of each layer related to the adjacent layers. A fail indication in this chart implies that migration of fines is possible in the interface of the analyzed layers, assuming all soils meet the filter criteria requirements at the time of placement.

The values of permeability estimated by the Hazen's empirical correlation should be considered only roughly in their order of magnitude because of the large variations that result from the different densities and particle structure that are possible in the field. As can be seen in the heading of the chart, the permeability is calculated based only in one parameter of the grain size distribution (D_{10}) and a constant (C) that depends on the kind of material[19].

Also in this analysis the dense graded base material, section MI1-4 shows its difference from the other sections. In this case a very low permeability (coefficient of water conductivity) is seen compared with the other base materials of the project.

Loss on Wash Calculations

	Before Washing			After Washing			Weight Loss	Loss %	Average Loss %
	Pan	Pan+sand	sand	Pan	Pan+sand	sand			
BASE									
MI1-4-Mix #1	356.57	1052.99	696.42	354.61	999.53	644.92	51.50	7.39	8.80
MI1-4-Mix #2	356.61	1128.70	772.09	370.28	1063.57	693.29	78.80	10.21	
SUBBASE									
MI1-1-M2	356.53	1032.92	676.39	364.61	945.08	580.47	95.92	14.18	10.59
MI1-1-M3	73.04	656.57	583.53	73.15	590.41	517.26	66.27	11.36	
MI1-1-M4	356.66	1019.08	662.42	307.22	928.45	621.23	41.19	6.22	
MI1-2-M2	365.03	1089.50	724.47			690.35	34.12	4.71	8.30
MI1-2-M3	73.17	636.83	563.66	342.16	865.90	523.74	39.92	7.08	
MI1-2-M4	396.21	1100.09	703.88	356.62	968.18	611.56	92.32	13.12	
MI1-3-M2	356.65	1073.83	717.18	364.61	1037.47	672.86	44.32	6.18	6.30
MI1-3-M3	73.18	617.72	544.54	73.15	578.53	505.38	39.16	7.19	
MI1-3-M5	73.24	976.09	902.85	73.15	925.95	852.80	50.05	5.54	
MI1-4-M1	73.13	865.34	792.21	73.15	826.65	753.50	38.71	4.89	6.54
MI1-4-M5	73.15	890.32	817.17	73.15	823.41	750.26	66.91	8.19	
MI2-1-M2	73.15	957.85	884.70	73.15	876.74	803.59	81.11	9.17	8.21
MI2-1-M3	73.15	912.15	839.00	297.25	1067.58	770.33	68.67	8.18	
MI2-1-M4	73.15	471.38	398.23	73.15	442.43	369.28	28.95	7.27	
MI2-2-M2	73.15	1041.39	968.24	73.15	985.10	911.95	56.29	5.81	5.98
MI2-2-M3	73.14	760.69	687.55	73.15	718.54	645.39	42.16	6.13	
MI2-2-M4	73.15	790.84	717.69	73.15	747.82	674.67	43.02	5.99	
SUBGRADE									
MI1-1-M2	73.07	666.90	593.83	297.29	797.45	500.16	93.67	15.77	17.34
MI1-1-M4	73.27	733.53	660.26	290.05	825.48	535.43	124.83	18.91	
MI1-2-M2	73.15	657.72	584.57	354.66	904.30	549.64	34.93	5.98	10.68
MI1-2-M3	73.18	602.15	528.97	90.67	573.26	482.59	46.38	8.77	
MI1-2-M4	73.25	607.80	534.55	73.15	515.32	442.17	92.38	17.28	
MI1-3-M2	73.11	704.78	631.67	364.54	986.00	621.46	10.21	1.62	6.64
MI1-3-M3	73.16	618.78	545.62	425.48	937.18	511.70	33.92	6.22	
MI1-3-M4	73.07	657.74	584.67	294.78	808.82	514.04	70.63	12.08	
MI1-4-M2	73.07	933.10	860.03	73.15	748.41	675.26	184.77	21.48	11.18
MI1-4-M3	73.18	781.30	708.12	458.69	1130.88	672.19	35.93	5.07	
MI1-4-M4	73.15	771.75	698.60	396.10	1045.99	649.89	48.71	6.97	
MI2-1-M1	73.16	943.83	870.67	354.54	1167.94	813.40	57.27	6.58	6.58
MI2-2-M4	73.15	894.49	821.34	73.15	864.99	791.84	29.50	3.59	3.59

Sieve Analysis Calculations

	Weight Retained (g)												
	1	3/4	1/2	3/8	#4	#8	#16	#30	#50	#100	#200	Pan	% error *
BASE													
MI1-1-Trial 1	0	100	420	130	130	30	50	10				60	-7.5
MI1-1-Trial 2	0	210	340	110	130	50	10	10				70	-7.5
MI1-1- Trial 3	50	160	340	130	140	20	10	10				40	-11.1
MI1-2-Trial 1	20	170	430	170	90	20	10	10				60	-2.0
MI1-2-Trial 2	0	180	400	140	140	50	20	20				70	2.0
MI1-2-Trial 3	0	270	390	140	100	50	20	10				50	2.9
MI1-3-Trial 1	0	0	0	20	890	80	0	0				0	-1.0
MI1-3-Trial 2	0	0	0	30	860	110	0	0				0	0.0
MI1-3-Trial 3	0	0	0	30	880	80	0	0				0	-1.0
MI1-4-Mix #1		0.00	125.00	58.01	85.91	49.20	29.07	27.79	88.74	125.08	41.98	12.25	-0.3
MI1-4-Mix #2		25.49	44.98	41.04	79.89	52.88	35.11	40.51	132.63	175.48	57.14	7.91	0.0
MI2-1-Trial 1	150	210	330	130	80	20	20	10				50	0.0
MI2-1-Trial 2	100	230	340	120	90	10	10	10				50	-4.2
MI2-1-Trial 3	70	300	330	120	80	30	20	10				60	2.0
MI2-2-Trial 1	30	120	170	120	240	100	50	40				110	-2.0
MI2-2-Trial 2	20	150	200	150	230	90	40	30				80	-1.0
MI2-2-Trial 3	40	70	180	110	280	130	60	40				90	0.0
SUBBASE													
MI1-1-M2		50.16	14.01	20.58	53.05	38.22	35.63	49.73	161.57	125.43	29.19	1.90	-0.2
MI1-1-M3		0.00	62.34	32.67	40.77	33.48	30.36	44.58	115.26	114.20	32.31	10.18	-0.2
MI1-1-M4		0.00	11.87	10.61	27.87	23.77	21.97	40.66	167.35	224.05	79.64	12.13	-0.2
MI1-2-M2		0.00	3.57	6.34	6.45	5.26	4.06	13.05	230.63	333.14	80.22	6.62	-0.1
MI1-2-M3		0.00	5.40	2.35	16.95	13.26	17.42	40.97	181.51	192.92	43.17	8.70	-0.2
MI1-2-M4		9.16	23.85	10.68	27.51	17.49	14.20	23.83	185.18	225.19	65.28	8.68	-0.1
MI1-3-M2		0.00	14.53	19.18	41.01	16.74	7.57	8.40	50.85	318.33	176.00	20.11	0.0
MI1-3-M3		0.00	4.28	1.66	16.59	6.99	4.50	6.60	57.88	273.49	117.17	15.46	-0.2
MI1-3-M5		44.71	11.57	6.80	27.23	11.46	7.66	11.44	102.96	451.84	160.45	14.48	-0.3
MI1-4-M1		16.91	16.13	6.87	10.85	8.53	10.56	26.90	247.37	296.66	91.88	20.98	0.0
MI1-4-M3		115.85	3.65	20.58	33.73	24.52	19.87	25.44	127.71	230.69	174.36	7.93	-0.1
MI1-4-M5		0.00	23.41	15.48	18.59	15.68	16.52	32.02	229.27	307.00	80.76	8.85	-0.4
MI2-1-M2		0.00	16.70	11.96	45.87	39.61	40.34	87.07	421.22	103.74	29.42	5.05	-0.3
MI2-1-M3		37.68	60.78	24.81	61.43	56.81	59.64	90.62	263.52	86.56	23.80	4.52	0.0
MI2-1-M4		19.24	43.10	47.12	54.26	37.83	31.55	32.94	63.25	27.97	9.01	2.98	0.0
MI2-2-M2		79.15	87.68	82.63	141.16	88.58	78.60	90.74	164.89	75.83	17.93	3.00	-0.2
MI2-2-M3		56.83	37.84	34.40	90.86	61.13	53.56	61.21	159.15	70.75	13.16	3.89	-0.4
MI2-2-M4		34.49	64.83	35.60	58.71	87.19	27.19	68.45	141.03	135.25	17.93	3.56	-0.1
SUBGRADE													
MI1-1-M2		96.30	0.00	4.39	25.41	28.43	27.93	41.37	100.89	114.86	44.60	14.92	-0.2
MI1-1-M4		44.54	4.90	8.37	27.44	21.56	22.37	43.95	131.00	141.98	60.85	27.62	-0.2
MI1-2-M2		0.00	28.42	13.26	20.14	18.60	25.75	57.00	176.84	157.60	42.92	7.65	-0.3
MI1-2-M3		52.20	52.07	40.66	32.80	13.66	15.28	32.54	83.84	98.11	37.51	22.70	-0.3
MI1-2-M4		0.00	6.77	10.69	10.55	8.00	15.10	32.90	115.92	153.76	59.20	26.28	-0.7
MI1-3-M2		0.00	0.00	0.00	7.25	1.23	1.05	6.65	366.14	191.91	42.92	5.46	0.2
MI1-3-M3		0.00	5.45	0.00	4.70	2.97	3.66	9.87	105.46	276.10	87.73	9.50	-1.2
MI1-3-M4		0.00	3.20	3.40	4.29	3.34	2.12	2.50	11.54	39.52	316.36	126.15	-0.3
MI1-4-M2		0.00	15.67	6.45	9.79	9.33	12.05	26.45	207.94	278.21	89.23	18.28	-0.3
MI1-4-M3		0.00	0.00	1.78	14.99	9.91	13.16	28.67	225.86	306.84	62.23	8.18	-0.1
MI1-4-M4		0.00	4.55	9.88	10.37	7.64	14.42	30.16	233.23	265.42	63.09	11.60	0.1
MI2-1-M1		76.88	26.78	28.01	54.68	64.92	69.43	109.59	275.00	79.11	23.50	4.66	-0.1
MI2-2-M4		23.28	12.70	13.87	25.91	2.19	41.16	56.69	324.79	250.48	36.67	2.85	-0.2

* % error is the error associated with the difference in the weight of the entire sample before and after sieving
Weight retained was measured to the nearest ten grams for most base course samples; therefore, higher error is noted

Sieve Analysis Calculations (2)

	% passing										
# mm.	25.400	19.100	12.700	9.500	4.750	2.360	1.148	0.600	0.300	0.178	0.075
	1"	3/4"	1/2"	3/8"	#4	#8	#16	#30	#50	#100	#200
BASE											
MI1-1-Trial 1	100.00	89.25	44.09	30.11	16.13	12.90	7.53	6.45			
MI1-1-Trial 2	100.00	77.42	40.86	29.03	15.05	9.68	8.60	7.53			
MI1-1- Trial 3	94.44	76.67	38.89	24.44	8.89	6.67	5.56	4.44			
MI1-2-Trial 1	97.96	80.61	36.73	19.39	10.20	8.16	7.14	6.12			
MI1-2-Trial 2	100.00	82.35	43.14	29.41	15.69	10.78	8.82	6.86			
MI1-2-Trial 3	100.00	73.79	35.92	22.33	12.62	7.77	5.83	4.85			
MI1-3-Trial 1	100.00	100.00	100.00	97.98	8.08	0.00	0.00	0.00			
MI1-3-Trial 2	100.00	100.00	100.00	97.00	11.00	0.00	0.00	0.00			
MI1-3-Trial 3	100.00	100.00	100.00	96.97	8.08	0.00	0.00	0.00			
MI1-4-MIx #1		100.00	82.00	73.65	61.28	54.20	50.01	46.01	33.23	15.22	9.18
MI1-4-Mix #2		96.70	90.87	85.55	75.20	68.35	63.80	58.55	41.37	18.64	11.23
MI2-1-Trial 1	85.00	64.00	31.00	18.00	10.00	8.00	6.00	5.00			
MI2-1-Trial 2	89.58	65.63	30.21	17.71	8.33	7.29	6.25	5.21			
MI2-1-Trial 3	93.14	63.73	31.37	19.61	11.76	8.82	6.86	5.88			
MI2-2-Trial 1	96.94	84.69	67.35	55.10	30.61	20.41	15.31	11.22			
MI2-2-Trial 2	97.98	82.83	62.63	47.47	24.24	15.15	11.11	8.08			
MI2-2-Trial 3	96.00	89.00	71.00	60.00	32.00	19.00	13.00	9.00			
SUBBASE											
MI1-1-M2		92.57	90.50	87.45	79.60	73.94	68.66	61.30	37.38	18.81	14.48
MI1-1-M3		100.00	89.30	83.69	76.69	70.94	65.73	58.07	38.28	18.67	13.13
MI1-1-M4		100.00	98.20	96.60	92.38	88.79	85.47	79.32	54.00	20.11	8.07
MI1-2-M2		100.00	99.51	98.63	97.74	97.01	96.45	94.65	62.77	16.72	5.63
MI1-2-M3		100.00	99.04	98.62	95.61	93.25	90.16	82.87	50.61	16.32	8.64
MI1-2-M4		98.70	95.31	93.79	89.88	87.39	85.37	81.98	55.66	23.64	14.36
MI1-3-M2		100.00	97.97	95.30	89.58	87.24	86.19	85.02	77.93	33.53	8.99
MI1-3-M3		100.00	99.21	98.91	95.86	94.57	93.74	92.53	81.89	31.59	10.04
MI1-3-M5		95.04	93.75	93.00	89.97	88.70	87.85	86.58	75.15	24.98	7.16
MI1-4-M1		97.87	95.83	94.96	93.59	92.52	91.18	87.79	56.57	19.13	7.53
MI1-4-M3		84.26	83.76	80.97	76.38	73.05	70.35	66.89	49.54	18.20	
MI1-4-M5		100.00	97.13	95.23	92.94	91.02	88.99	85.06	56.91	19.22	9.30
MI2-1-M2		100.00	98.11	96.75	91.55	87.06	82.49	72.62	24.86	13.10	9.77
MI2-1-M3		95.51	88.26	85.30	77.98	71.21	64.10	53.30	21.88	11.56	8.73
MI2-1-M4		95.17	84.34	72.51	58.88	49.38	41.46	33.19	17.31	10.28	8.02
MI2-2-M2		91.81	82.74	74.19	59.58	50.42	42.29	32.90	15.84	7.99	6.13
MI2-2-M3		91.70	86.18	81.16	67.89	58.97	51.15	42.21	18.97	8.64	6.72
MI2-2-M4		95.19	86.15	81.19	73.00	60.85	57.06	47.51	27.85	8.99	6.49
SUBGRADE											
MI1-1-M2		83.75	83.75	83.01	78.73	73.93	69.22	62.24	45.22	25.84	18.32
MI1-1-M4		93.25	92.50	91.23	87.07	83.80	80.41	73.74	53.88	32.35	23.12
MI1-2-M2		100.00	95.13	92.85	89.40	86.21	81.79	72.02	41.69	14.66	7.30
MI1-2-M3		90.11	80.24	72.54	66.32	63.73	60.84	54.67	38.79	20.20	13.09
MI1-2-M4		100.00	98.73	96.72	94.73	93.23	90.38	84.20	62.39	33.46	22.32
MI1-3-M2		100.00	100.00	100.00	98.85	98.66	98.49	97.44	39.58	9.26	2.48
MI1-3-M3		100.00	98.99	98.99	98.12	97.57	96.89	95.06	75.51	24.32	8.05
MI1-3-M4		100.00	99.45	98.87	98.13	97.56	97.20	96.77	94.79	88.01	33.75
MI1-4-M2		100.00	98.17	97.42	96.28	95.19	93.79	90.71	66.48	34.06	23.66
MI1-4-M3		100.00	100.00	99.75	97.63	96.23	94.37	90.32	58.40	15.03	6.23
MI1-4-M4		100.00	99.35	97.94	96.45	95.36	93.30	88.98	55.62	17.65	8.63
MI2-1-M1		91.16	88.08	84.86	78.58	71.11	63.13	50.53	18.92	9.82	7.12
MI2-2-M4		97.16	95.61	93.92	90.76	90.49	85.48	78.56	38.96	8.42	3.94

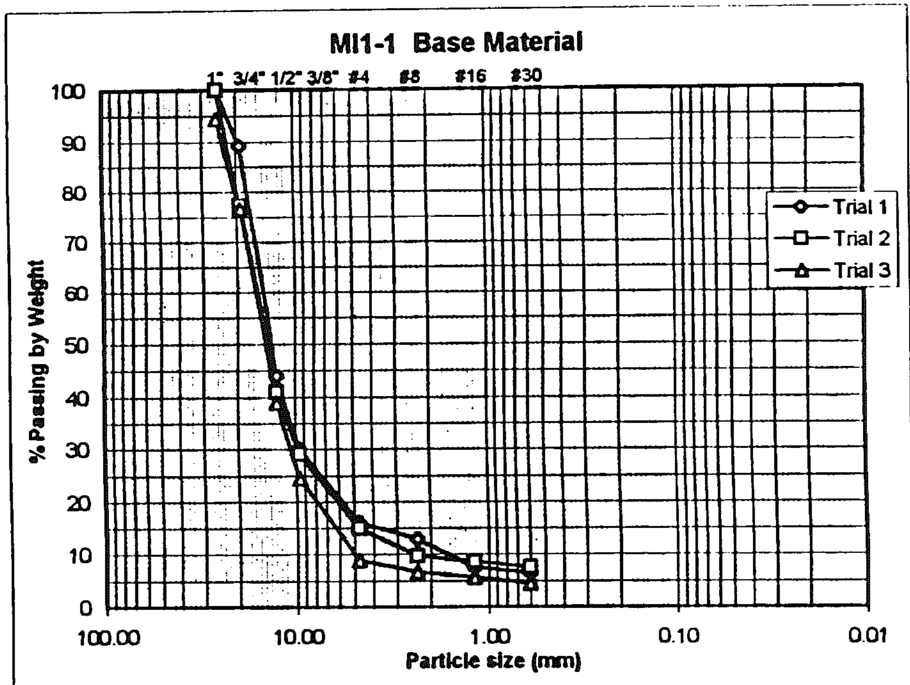
MI1-1 Base Material
1" 3/4" 1/2" 3/8" #4 #8 #16 #30
% Passing by Weight
Particle size (mm)
Trial 1
Trial 2
Trial 3

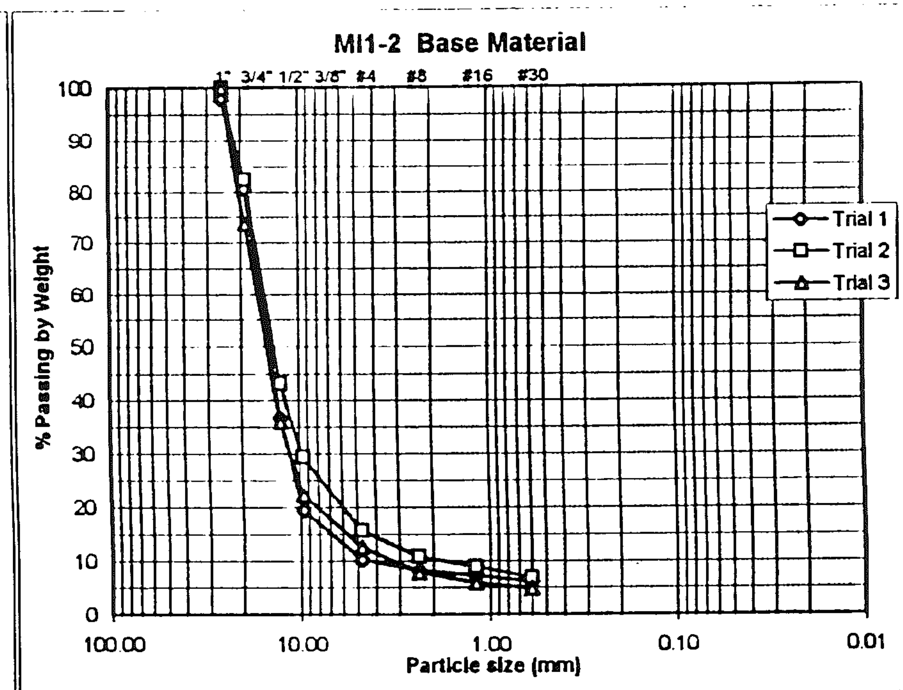
MI1-2 Base Material
1" 3/4" 1/2" 3/8" #4 #8 #16 #30
% Passing by Weight
Particle size (mm)
Trial 1
Trial 2
Trial 3

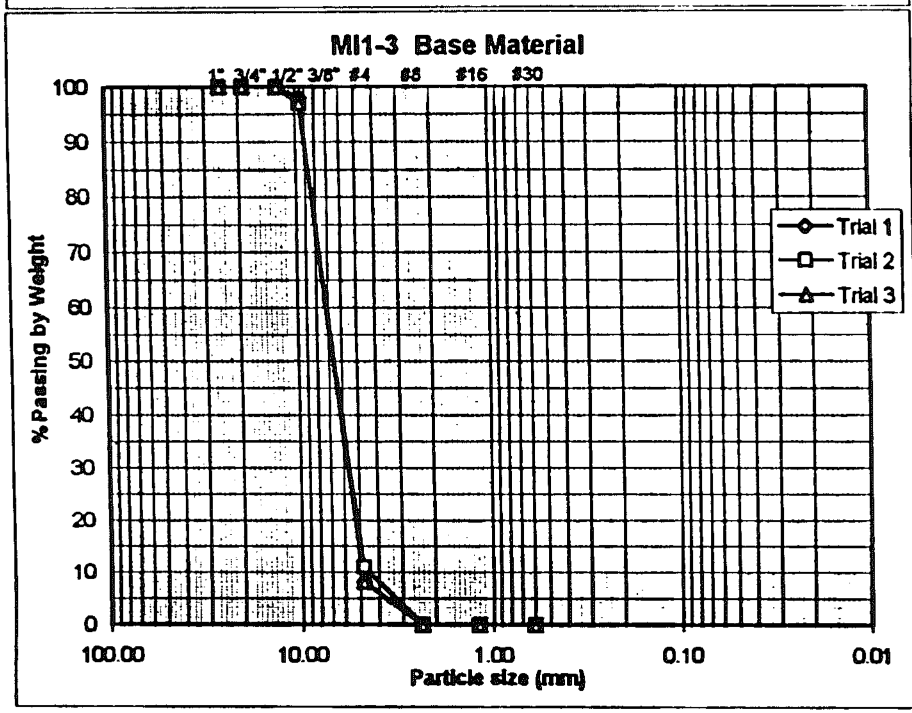
MI1-3 Base Material
1" 3/4" 1/2" 3/8" #4 #8 #16 #30
% Passing by Weight
Particle size (mm)
Trial 1
Trial 2
Trial 3

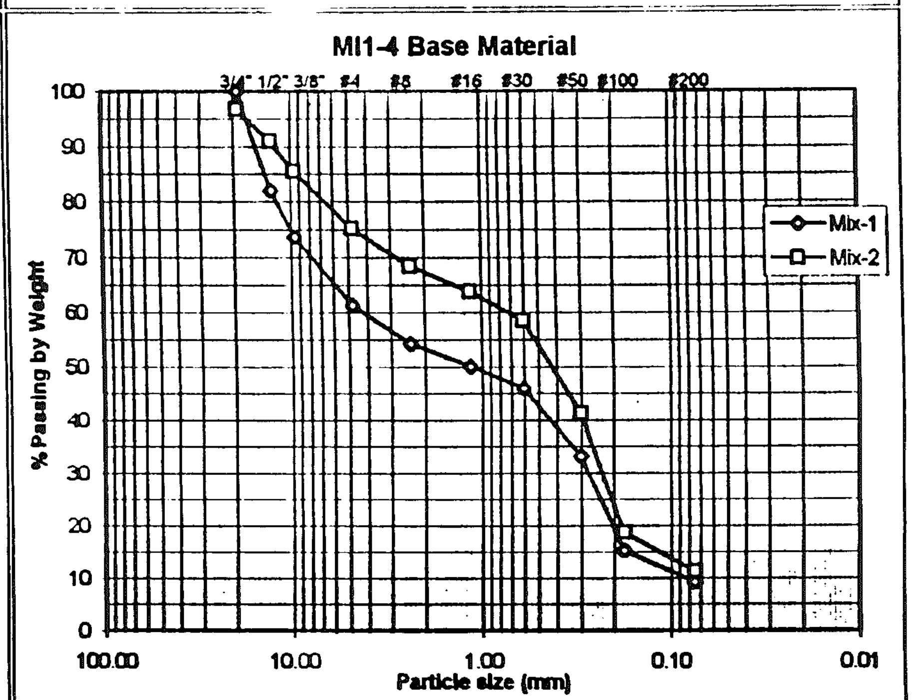
MI1-4 Base Material
3/4" 1/2" 3/8" #4 #8 #16 #30 #50 #100 #200
% Passing by Weight
Particle size (mm)
Mix-1
Mix-2

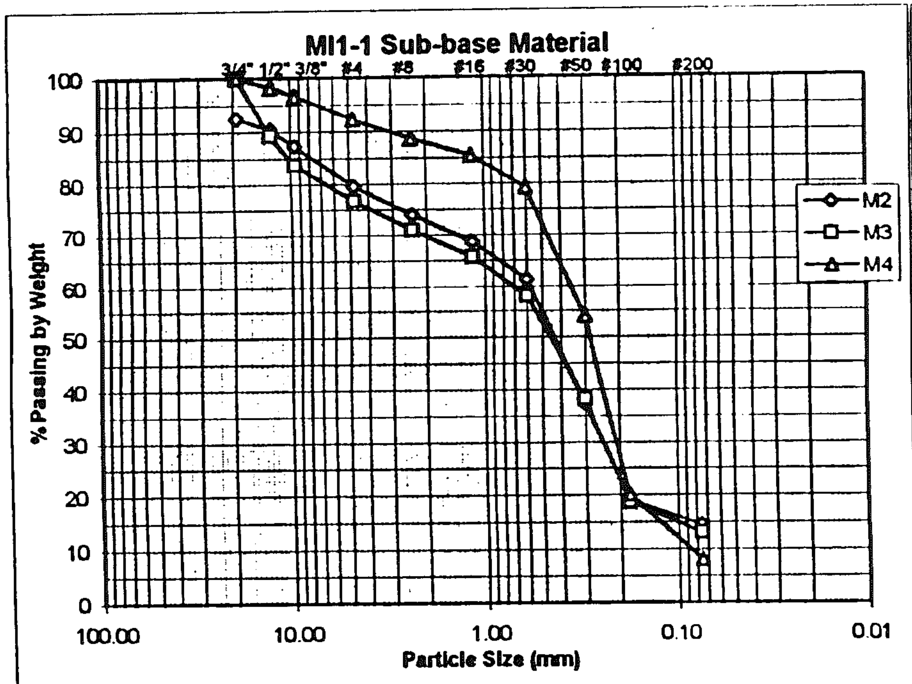
MI1-1 Sub-base Material
3/4" 1/2" 3/8" #4 #8 #16 #30 #50 #100 #200
% Passing by Weight
100
90
80
70
60
50
40
30
20
10
0
100.00
10.00
1.00
0.10
0.01
Particle Size (mm)
M2
M3
M4

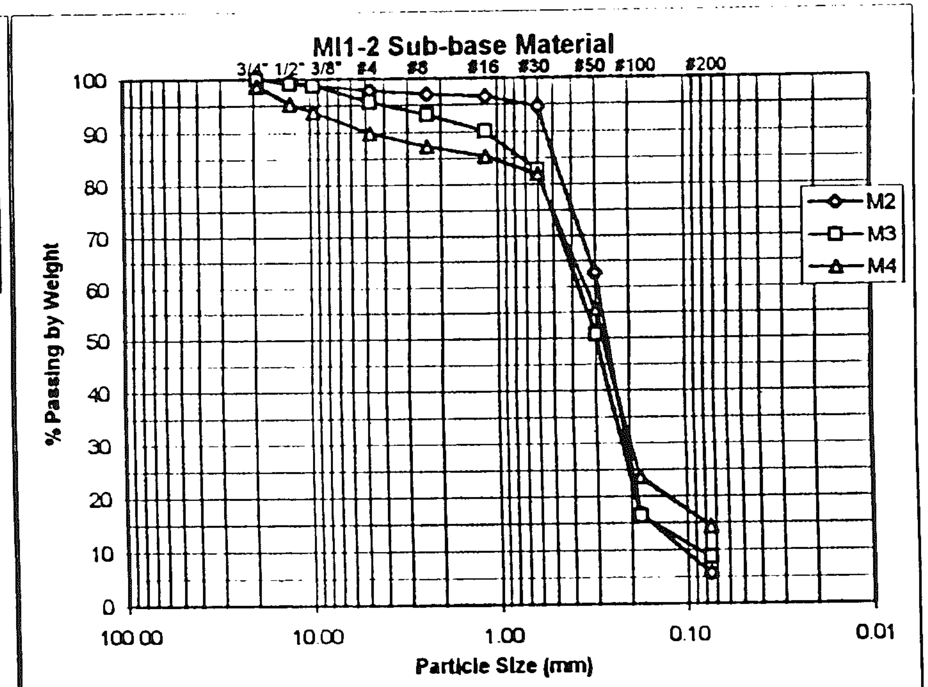
MI1-2 Sub-base Material
3/4" 1/2" 3/8" #4 #8 #16 #30 #50 #100 #200
% Passing by Weight
100
90
80
70
60
50
40
30
20
10
0
100.00
10.00
1.00
0.10
0.01
Particle Size (mm)
M2
M3
M4

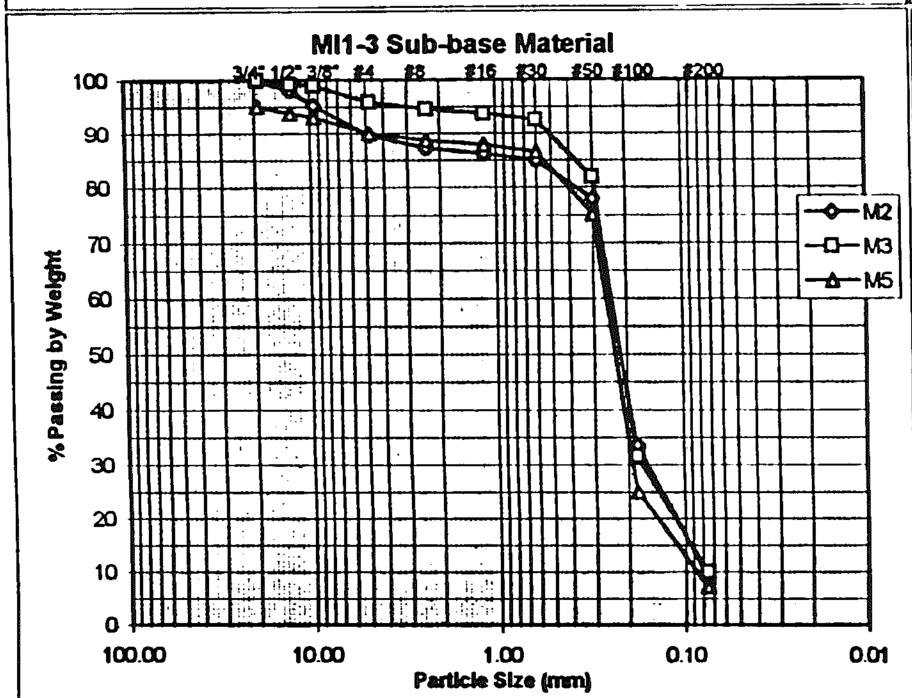
MI1-3 Sub-base Material
3/4" 1/2" 3/8" #4 #8 #16 #30 #50 #100 #200
% Passing by Weight
100
90
80
70
60
50
40
30
20
10
0
100.00
10.00
1.00
0.10
0.01
Particle Size (mm)
M2
M3
M5

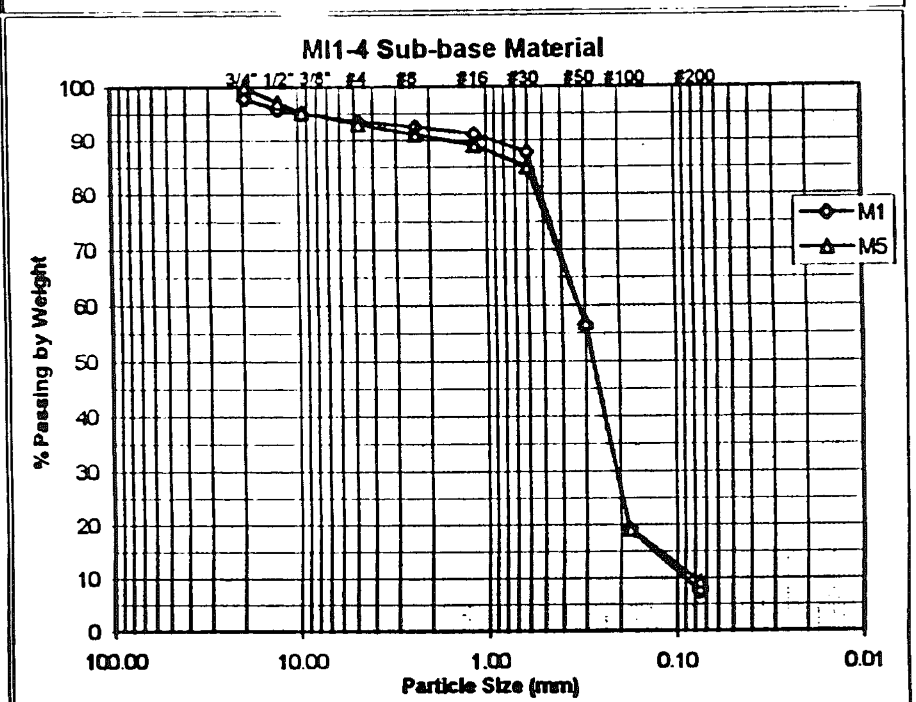
MI1-4 Sub-base Material
3/4" 1/2" 3/8" #4 #8 #16 #30 #50 #100 #200
% Passing by Weight
100
90
80
70
60
50
40
30
20
10
0
100.00
10.00
1.00
0.10
0.01
Particle Size (mm)
M1
M5

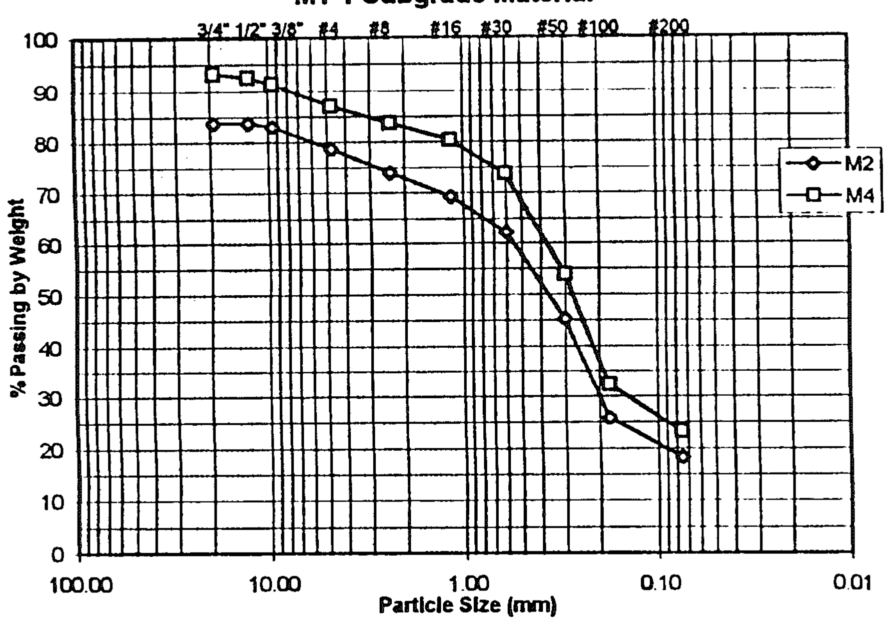

M1-1 Subgrade Material

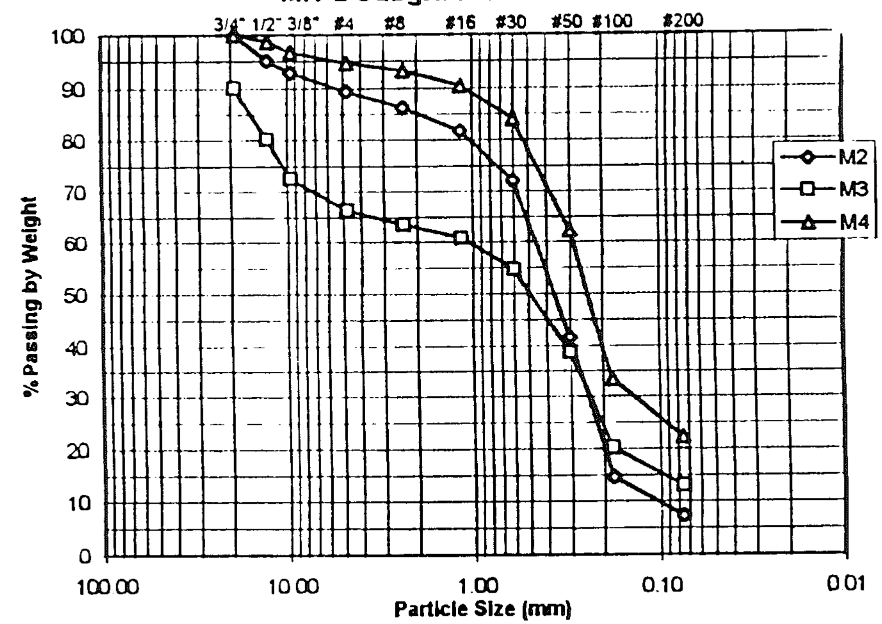

MI1-2 Subgrade Material

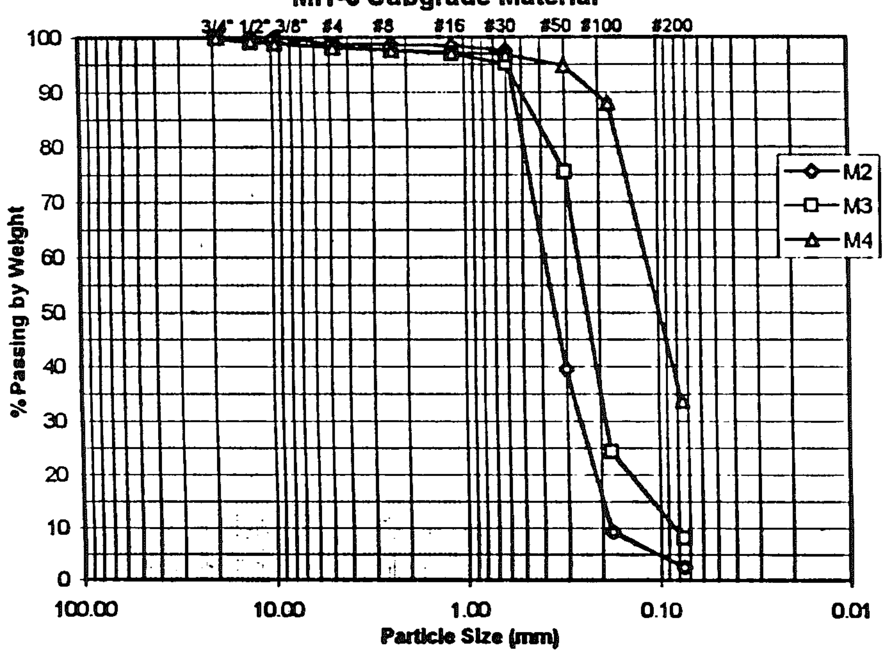

MI1-3 Subgrade Material

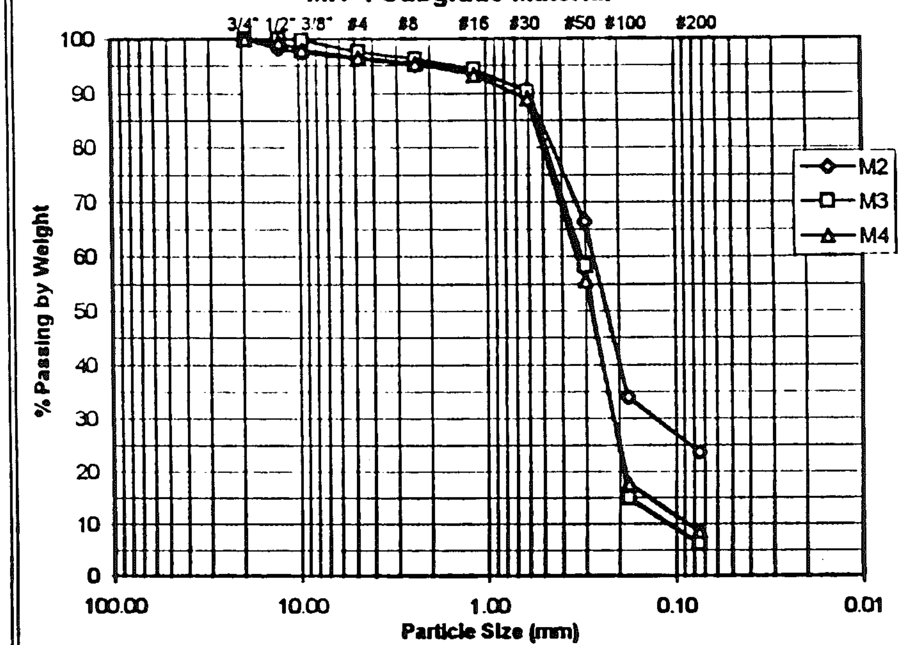

MI1-4 Subgrade Material

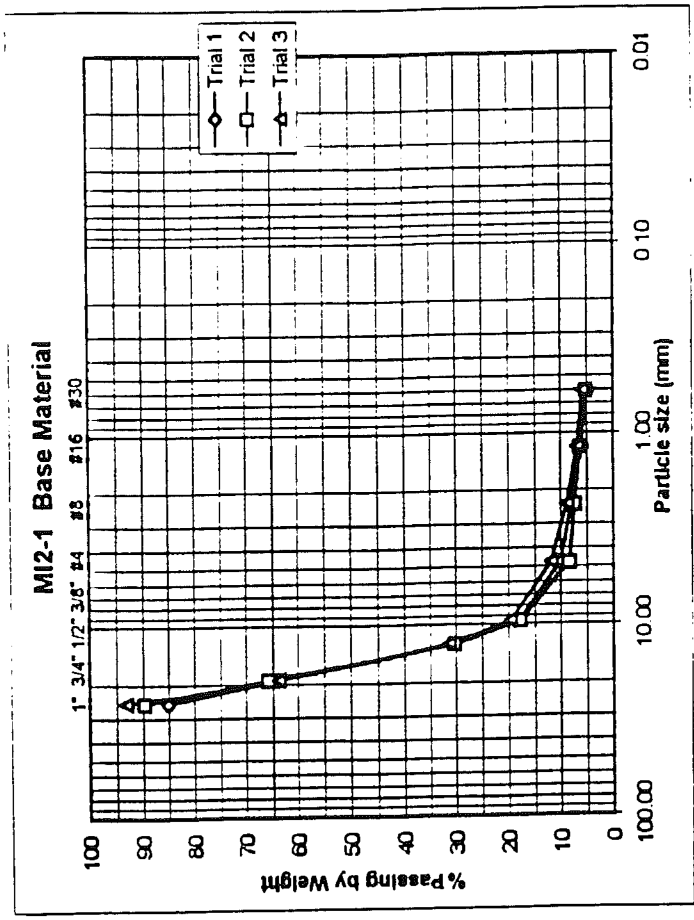
MI2-1 Base Material
Trial 1
Trial 2
Trial 3
% Passing by Weight
Particle size (mm)
100.00
10.00
1.00
0.10
0.01
1" 3/4" 1/2" 3/8" #4 #8 #16 #30
100
90
80
70
60
50
40
30
20
10
0

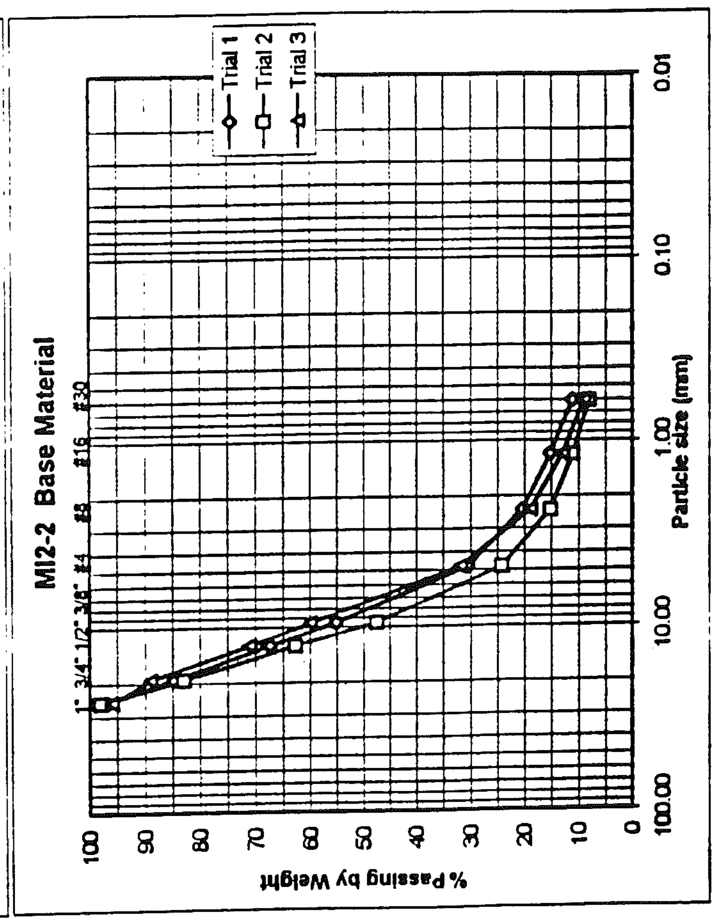
MI2-2 Base Material
Trial 1
Trial 2
Trial 3
% Passing by Weight
Particle size (mm)
100.00
10.00
1.00
0.10
0.01
1" 3/4" 1/2" 3/8" #4 #8 #16 #30
100
90
80
70
60
50
40
30
20
10
0

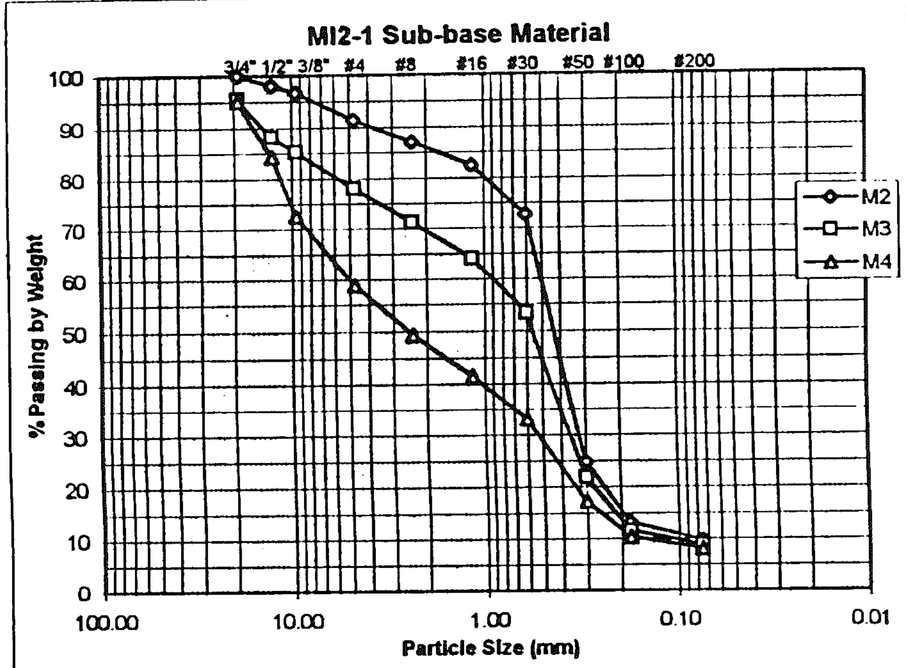
MI2-1 Sub-base Material
3/4" 1/2" 3/8" #4 #8 #16 #30 #50 #100 #200
% Passing by Weight
Particle Size (mm)
M2
M3
M4

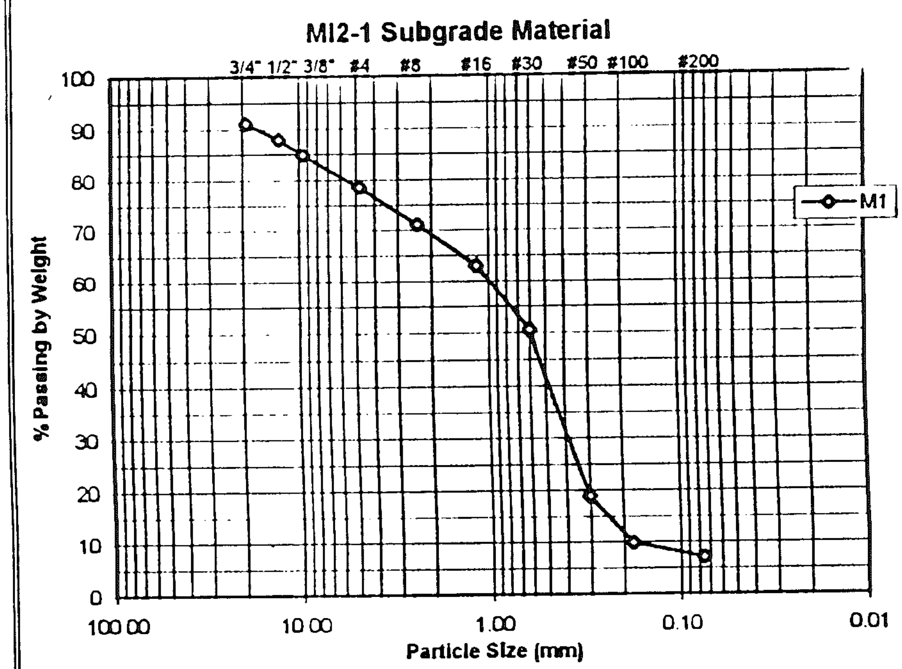
MI2-1 Subgrade Material
3/4" 1/2" 3/8" #4 #8 #16 #30 #50 #100 #200
% Passing by Weight
Particle Size (mm)
M1

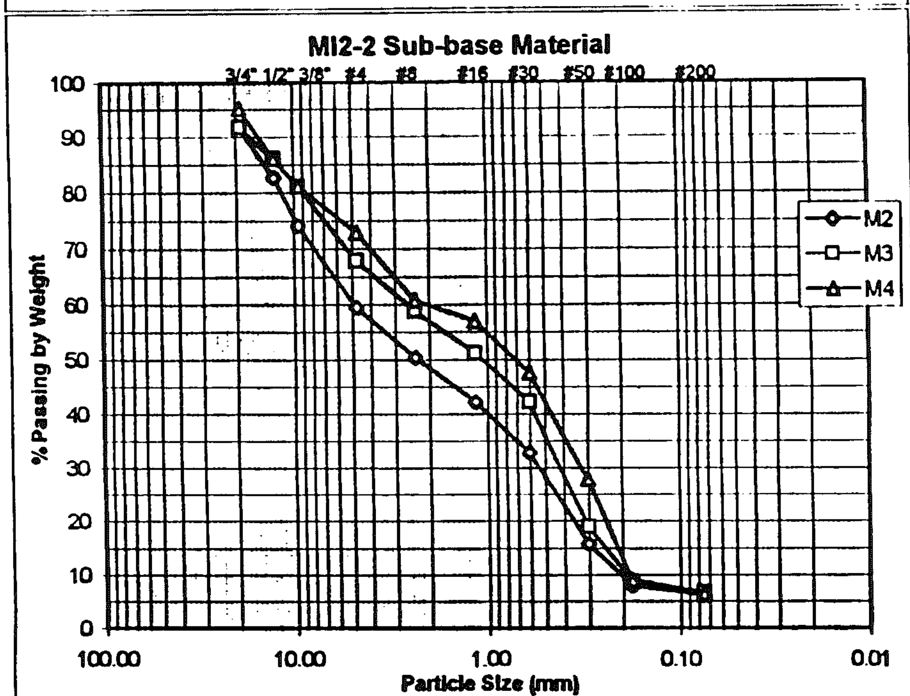
MI2-2 Sub-base Material
3/4" 1/2" 3/8" #4 #8 #16 #30 #50 #100 #200
% Passing by Weight
Particle Size (mm)
M2
M3
M4

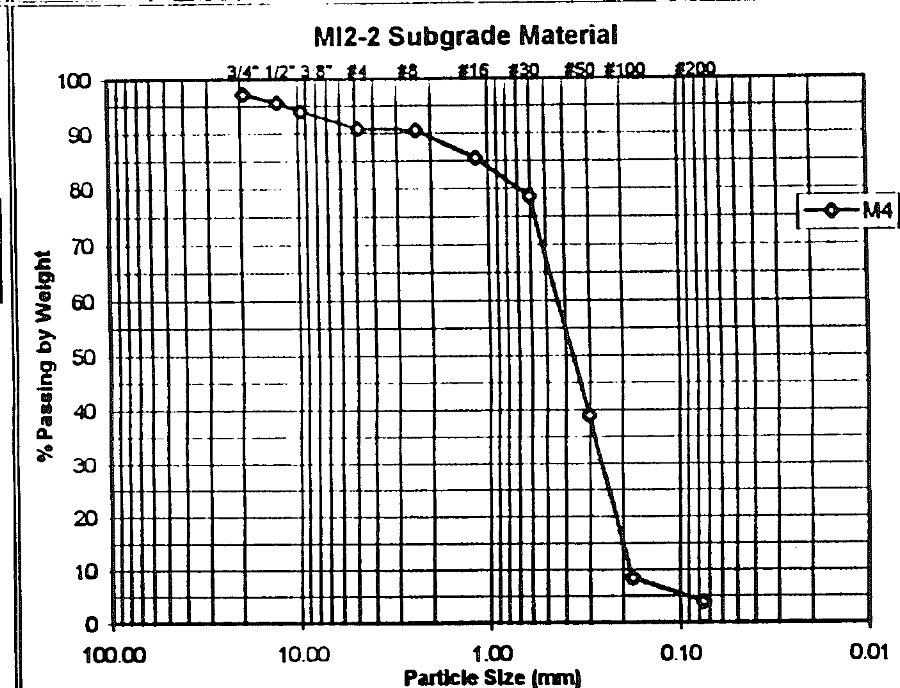
MI2-2 Subgrade Material
3/4" 1/2" 3/8" #4 #8 #16 #30 #50 #100 #200
% Passing by Weight
Particle Size (mm)
M4

FILTER CRITERIA AND PERMEABILITY VALUES OF FOUNDATION LAYERS

	D85	D60	D50	D15	D10	D5	Filter Criteria: D5 >=0.074	D15f/D85s <=5		D15f/D15s >=5		D50f/D50s <=25		D60f/D10f <=25		Permeability: k=C(D10)^2 (cm/sec) Hazen's C	k (cm/s)	k (ft/day)	
Base																			
MI1-1 (avg)	20.33	15.67	14.67	4.57	3.000	0.800	ok	0.73	ok	44.19	ok	46.81	Fail	5.22	ok	1.20	10.800	30614	*
MI1-2 (avg)	21.00	16.00	14.67	5.50	3.267	0.600	ok	7.17	Fail	37.50	ok	51.76	Fail	4.90	ok	1.20	12.805	36299	*
MI1-3 (avg)	8.50	7.00	6.50	5.00	4.700	3.833	ok	10.00	Fail	50.00	ok	30.47	Fail	1.49	ok	1.20	26.508	75141	*
MI1-4 (avg)		2.35	0.81	0.16	0.075	0.074	ok	0.26	ok	1.03	Fail	3.00	ok	31.33	Fail	0.80	0.005	13	
MI2-1 (avg)	23.67	18.00	16.00	7.17	4.433	0.667	ok	1.00	ok	32.09	ok	14.24	ok	4.06	ok	1.20	23.585	66856	*
MI2-2 (avg)	19.33	11.17	8.57	1.63	0.825	<0.6	ok ?	0.13	ok	6.45	ok	6.27	ok	13.54	ok	0.90	0.615	1744	
Sub-base																			
MI1-1 (avg)	6.23	0.53	0.31	0.10	0.080	<0.074	Fail	0.01	ok	>1.40	Fail ?	0.98	ok	6.67	ok	0.80	0.005	15	
MI1-2 (avg)	0.77	0.34	0.28	0.15	0.095	<0.074	Fail	0.03	ok	1.07	Fail	0.77	ok	3.61	ok	0.80	0.007	21	
MI1-3 (avg)	0.50	0.24	0.21	0.10	0.080	<0.074	Fail	0.28	ok	0.65	Fail	0.97	ok	3.06	ok	0.80	0.005	14	
MI1-4 (avg)	0.60	0.31	0.27	0.15	0.085	<0.074	Fail	0.27	ok	0.83	Fail	1.03	ok	3.65	ok	0.80	0.006	16	
MI2-1 (avg)	7.20	2.13	1.12	0.22	0.117	<0.074	Fail	0.02	ok	0.89	Fail	1.87	ok	18.29	ok	0.81	0.011	31	
MI2-2 (avg)	13.00	3.13	1.37	0.25	0.197	<0.074	Fail	0.21	ok	1.27	Fail	3.80	ok	15.93	ok	0.82	0.032	90	
Subgrade																			
MI1-1 (avg)	11.50	0.46	0.32	<0.074	<0.074	<0.074										0.54	<0.003	<8	
MI1-2 (avg)	5.87	0.58	0.37	0.14	0.100	<0.074										0.55	0.005	16	
MI1-3 (avg)	0.36	0.26	0.22	0.16	0.135	0.100										0.57	0.010	29	
MI1-4 (avg)	0.55	0.29	0.26	0.18	0.100	<0.074										0.55	0.005	16	
MI2-1 (avg)	10.00	1.00	0.60	0.25	0.180	<0.074										0.59	0.019	54	
MI2-2 (avg)	1.20	0.42	0.36	0.20	0.180	0.090										0.59	0.019	54	

* Values of permeability appear unusually high

Appendix 6: Petrographic Analysis

Two mid panel core samples from each test section have been petrographically analyzed by the PC LABORATORIET A/S in Denmark using the Method ASTM C-856: "Practice for Petrographic Examination of Hardened Concrete"[20]. This appendix contains the information of the analysis presented in 3 summary sheets of the petrographic macroanalysis and 3 summary sheets of the petrographic microanalysis of all samples. A table of the quantitative determination of microcracks and some representative microphotos are also presented. The summary sheets show the information organized in columns to be easily compared. Note that in the macroanalysis tables, many of the descriptors are used for the whole recycled concrete and for the recycled aggregate (which is itself a concrete).

Section MI1-1 is a virgin aggregate concrete that doesn't contain recycled concrete but has a relatively inhomogeneous distribution of cement paste. All the other sections (MI1-2 to MI2-2) contain high volume of homogeneusly distributed recycled concrete which is distinguished only by its gray value and small differences in structure. Variations in the homogeneity of distribution of the cement paste and the water cement ratio are detected in the analysis. The number of adhesion microcracks and cement paste microcracks is variable. Fine early cracks are distinguished by their smooth run through the concrete as opposed to the later stage cracks that penetrate aggregates and have run sharply through the concrete. Some of the recycled concrete fragments have a large amount of later stage cracks, possibly formed in the recycling procedure.

Alkali-silica reactivity (ASR) is detected in 4 samples from the various test sections. ASR is not associated with cracking, though, and is only found in minor amounts.

The microanalysis chart reveals that all samples have the same type of minerals in the aggregates. The recycled concrete fragments do not contain fly ash, although it is present in the new cement paste.

The final chart shows the amount of microcracking observed in the cement paste and adhesion zones of the thin section samples. In general, the number of microcracks is higher in the cement paste than in the adhesion zones with the exception of section MI1-1 (the peastone concrete). Microcracks are also more frequent in the new cement paste than in the recycled aggregate in the recycled concretes examined.

Finally, microphotos are shown that were taken from cores in each section. They are intended to show general trends in the concrete, though they may not be statistically representative of all of the concrete. Because the areas studied in these microphotos are very small, they may not give a completely accurate account of the composition of the concretes as a whole.

Summary Sheet of Petrographic Analysis - MACROANALYSIS. LAWRENCE

Sample	Cut Area (mm)	Type of Concr	Aggregate					Trapped Air			Temp Steel	Comments
			Shape	Max. Size (mm)	Orientation	Quantity	Type	Amount	Max Size (mm)	Distri-bution		
MI1-1-M2	252 x 140	new	rounded to elongated	8	slightly preferred orientation parallel to surface	50%	chert calcareous rock fine sandstone granite other rock fragm.	moderate	5 x 5			
MI1-1-M4	264 x 140	new	rounded to elongated	8	slightly preferred orientation parallel to surface	52%	chert calcareous rock fine sandstone granite other rock fragm.	moderate	5 x 5		*10 and 5 mm steel 115 mm from top. *good cement paste adhesion to reinf.	
MI1-2-M2	270 x 140	new	rounded to elongated	15	no preferred orientation	low	chert calcareous rock sandstone granite other rock fragm.	low	10 x 10		*10 mm steel 115 mm from top. *good cement paste adhesion to reinf.	*difficult to distinguish between new and recycled concrete.
		recy-cled	sub-rounded	4 to 30		high	similar to new	higher than new		middle and bottom of core.		*good adhesion with new conc. *high amount of recycled concr.
MI1-2-M4	270 x 140	new	rounded to elongated	15	no preferred orientation	low	chert calcareous rock sandstone granite other rock fragm.	low	10 x 15			*difficult to distinguish between new and recycled concrete.
		recy-cled	sub-rounded	4 to 30		high	similar to new	higher than new				*good adhesion with new concrete. *high amount of recycled concrete.

Summary Sheet of Petrographic Analysis - MACROANALYSIS. LAWRENCE

Sample	Cut Area (mm)	Type of Concr	Aggregate					Trapped Air			Temp. Steel	Comments
			Shape	Max. Size (mm)	Orientation	Quantity	Type	Amount	Max Size (mm)	Distri-bution		
MI1-3-M2	265 x 140	new	rounded to elongated	20	no preferred orientation	low	chert calcareous rock sandstone some granite and other rock fragm.	moderate	10 x 20	largest air voids in the lower part	*10 mm steel 105 mm from top. *good cement paste adhesion to reinf.	*good adhesion with reinforcement *difficult to distinguish between new and recycled concrete.
		recy-cled	sub-rounded	4 to 30		high	similar to new	higher than new				*good adhesion with new conc. *high amount of recycled concrete.
MI1-3-M4	245 x 140	new	rounded to elongated	15	no preferred orientation	low	chert calcareous rock sandstone some granite and other rock fragm.	low	10 x 15			*difficult to distinguish between new and recycled concrete.
		recy-cled	sub-rounded	4 to 30		high	similar to new	higher than new				*good adhesion with new conc. *high amount of recycled concrete.
MI1-4-M2	250 x 140	new	rounded to elongated	15	no preferred orientation	low	chert calcareous rock sandstone some granite and other rock fragm.	moderate	10 x 20		*10 mm steel 70 mm from top. *partial cement paste adhesion to reinf.	*difficult to distin-guish between new and recycled
		recy-cled	sub-rounded	4 to 30		high	similar to new	higher than new				*good adhesion with new conc. *high amount of recycled concrete.
MI1-4-M4	245 x 140	new	rounded to elongated	15	no preferred orientation	low	chert calcareous rock sandstone some granite and other rock fragm.	low	10 x 15			*difficult to distinguish between new and recycled concrete.
		recy-cled	sub-rounded	4 to 30		high	similar to new	higher than new				*good adhesion with new conc. *high amount of recycled concrete.

Summary Sheet of Petrographic Analysis - MACROANALYSIS. LAWRENCE

Sample	Cut Area (mm)	Type of Concr	Aggregate					Trapped Air			Temp. Steel	Comments
			Shape	Max. Size (mm)	Orientation	Quantity	Type	Amount	Max Size (mm)	Distri-bution		
MI2-1-M2	270 x 140	new	rounded to elongated	15	no preferred orientation	low	chert calcareous rock sandstone some granite and other rock fragm.	moderate	10 x 20		*10 mm steel 120 mm from top. *partial cement paste adhesion to reinf.	*partial adhesion with reinforcement *difficult to distin-guish between new and recycled
		recy-cled	sub-rounded	4 to 30		high	similar to new	higher than new				*good adhesion with new conc. *high amount of recycled concrete.
MI2-1-M4	280 x 140	new	rounded to elongated	15	no preferred orientation	low	chert calcareous rock sandstone granite other rock fragm.	moderate	5 x 10			*difficult to distinguish between new and recycled concrete.
		recy-cled	sub-rounded	4 to 30		high	similar to new	higher than new				*good adhesion with new conc. *high amount of recycled concrete.
MI2-2-M2	250 x 140	new	rounded to elongated	15	no preferred orientation	low	chert calcareous rock sandstone some granite and other rock fragm.	moderate	10 x 20		*10 mm steel 130 mm from top. *partial cement paste adhesion to reinf.	*partial adhesion with reinforcement *difficult to distin-guish between new and recycled
		recy-cled	sub-rounded	4 to 30		high	similar to new	higher than new				*good adhesion with new conc. *high amount of recycled concrete.
MI2-2-M4	245 x 140	new	rounded to elongated	15	no preferred orientation	low	chert calcareous rock sandstone some granite and other rock fragm.	low	10 x 15			*difficult to distinguish between new and recycled concrete.
		recy-cled	sub-rounded	4 to 30		high	similar to new	high				*good adhesion with new conc. *high amount of recycled concrete.

Summary Sheet of Petrographic Analysis - MICROANALYSIS.

Section	Aggregate Minerals		alkali-silica gels	Carbonation Depth		Flyash	Water-cement ratio	Cement paste distribution	Cracks			Comments
	0-2 mm	2-4 mm		In Concr (mm)	Along Cracks (mm)				Adhesion Crks New-Recycled	Through C. Paste	Through Aggregate	
MI1-1-M2	rounded quarts	dolomite chert sandstone schist granite rocks	•in schist and porous opal chert •present in air voids	3.5	20	no	0.35 to 0.55	inhomo-geneous	In bottom part up to 0 1mm x 2mm	minor amount in top and middle part		•no cracks in connection to the alkalisilica gel.
MI1-1-M4	rounded quarts	dolomite chert sandstone schist granite rocks calcareous rock	not present	6		no	0.35 to 0.55	inhomo-geneous	yes (table2)			•similar microstructure as MI1-1-M2 •relatively high amount of entrained air.
MI1-2-M2	rounded quarts	dolomite chert sandstone schist granite rocks		5	9	yes only in new concr.	0.35 to 0.6 higher in recycled concrete	inhomo-geneous in the upper part	•in upper and middle part •minor amount at bottom	at surface fine cracks 0 5mm x 30mm	some micro-cracks penetrate	•high water cement ratio in the adhesion zone with recycled concrete. •ettringite like minerals precipitated in air voids. •some recycled fragments are carbonated.
MI1-2-M4	rounded quarts	dolomite chert sandstone schist granite rocks		2		yes			yes, due to air voids along the grain border.	many		•similar microstructure as MI1-1-M2 •similar structure to MI1-2-M2 •some cracks are very soft.

Summary Sheet of Petrographic Analysis - MICROANALYSIS.

Section	Aggregate Minerals		alkali-silica gels	Carbonation Depth		Flyash	Water-cement ratio	Cement paste distribution	Cracks			Comments
	0-2 mm	2-4 mm		In Concr. (mm)	Along Cracks (mm)				Adhesion Crks. New-Recycled	Through C. Paste	Through Aggregate	
MI1-3-M2	rounded quarts	dolomite chert sandstone schist granite rocks	some	2	6	yes only in new concr.	0.35 to 0.6 higher in recycled concrete	inhomogeneous in the upper part	in the upper part of the core	high amount in some areas.	some micro-cracks penetrates	•only minor areas of entrapped air •ettringite like minerals precipitated in air voids. •some recycled fragments are carbonated.
MI1-3-M4	rounded quarts	dolomite chert sandstone schist granite rocks		2	12	yes only in new concr.	0.4 to 0.6	inhomogeneous	moderate	•at surface fine cracks 25mm length •high amount in some areas	some micro-cracks penetrates	•ettringite like minerals precipitated in air voids. •some recycled fragments are carbonated.
MI1-4-M2	rounded quarts	dolomite chert sandstone schist granite rocks		2	7	yes only in new concr.	0.35 to 0.4 not homogeneous distribution but slightly higher in middle sect. and in recycled concrete.		good adhesion in top section	•thin at surface >50mm length •high amount in some areas.	sharp cracks penetrates	•higher amount of adhesion cracks and micro-separation in middle sect. •ettringite like minerals precipitated in air voids. •high air void content in some recycled fragments
MI1-4-M4	rounded quarts	dolomite chert sandstone schist granite rocks	•in air voids some in connection with fine cracks •schist with cracks and ASG near air voids.	2	6	yes only in new concr.	0.35 to 0.55	inhomogeneous	yes, in minor amount	•thin at surface 25mm length		•ettringite like minerals precipitated in air voids. •variations in water cement ratios of recycled concrete •high amount of air voids in cement paste of recycled concrete.

Summary Sheet of Petrographic Analysis - MICROANALYSIS.

Section	Aggregate Minerals		alkali-silica gels	Carbonation Depth		Flyash	Water-cement ratio	Cement paste distribution	Cracks			Comments
	0-2 mm	2-4 mm		In Concr. (mm)	Along Cracks (mm)				Adhesion Crks. New-Recycled	Through C. Paste	Through Aggregate	
MI2-1-M2	rounded quarts	dolomite chert sandstone schist granite rocks		1	4	yes only in new concr.	0.45 Lower in recycled conr.	homo-geneous	few	•in the upper 20mm •high amount in some areas.	no	•ettringite like minerals precipitated in air voids. •variations in water cement ratios of recycled concrete •some recycled concr. high air void content
MI2-1-M4	rounded quarts	dolomite chert sandstone schist granite rocks		1		yes only in new concr.	0.35 to 0.4 higher in adhe-sion zone with recycled conr.	inhomo-geneous	minor amount	•high amount in some areas.		•ettringite like minerals precipitated in air voids. •variations in water cement ratios of recycled concrete
MI2-2-M2	rounded quarts	dolomite chert sandstone schist granite rocks	present in one area with partly dissolved material.	2	4	yes only in new concr.	0.4 to to •higher in adhe-sion zone with recycled conr. •lower in recycled concr.	homo-geneous	few good adhesion in middle and lower part	at surface •high amount in some areas.	no	•ettringite like minerals precipitated in air voids. •variations in water cement ratios of recycled concrete •some recycled concr. high air void content
MI2-2-M4	rounded quarts	dolomite chert sandstone schist granite rocks		2	6	yes only in new concr.	0.35 to 0.6 •same in recy-cled concrete	inhomo-geneous	minor amount	•high amount in some areas.		•ettringite like minerals precipitated in some air voids. •variations in water cement ratios of recycled concrete •cement paste partly car-bonated in some recycled concrete fragments

Quantitative Determination of Microcracks.

Core	Thin Section	Alkali-silica Reaction	Microcracks/mm²			
			New Concrete		Old Concrete (recycled)	
			Cement Paste	Adhesion	Cement Paste	Adhesion
MI1-1-M2	Surface Mid. Bottom	X	0.14	0.57*	--	--
MI1-1-M4	Surface		0.09	0.12	--	--
MI1-2-M2	Surface Mid Bottom		0.52*	0.34	0.38	0.21
MI1-2-M4	Surface		0.95*	0.22	0.14	0.07
MI1-3-M2	Surface Mid Bottom	X	0.60*	0.26	0.46	0.21
MI1-3-M4	Surface		0.71*	0.31	0.33	0.14
MI1-4-M2	Surface Mid Bottom		0.53*	0.22	0.16	0.02
MI1-4-M4	Surface	X	0.41	0.21	0.31	0.14
MI2-1-M2	Surface Mid Bottom		0.23	0.10	0.14	0.05
MI2-1-M4	Surface		0.22	0.14	0.17	0.16
MI2-2-M2	Surface Mid Bottom	X	0.41	0.14	0.84*	0.18
MI2-2-M4	Surface		0.78*	0.36	0.33	0.12

Cracks less than 0.01mm are considered in this quantitative determination in 10 fields of sight (5.8mm^2) on each thin section.
(*) High amount of microcracks.

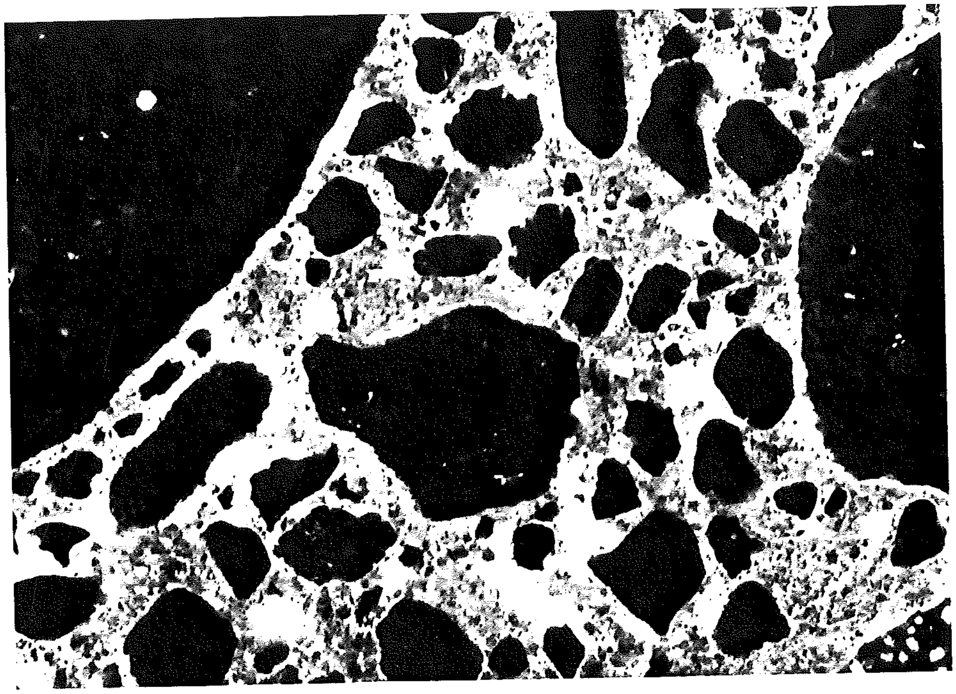

Microphoto of a sample from section MI1-1, taken in fluorescent light. Scale: 1cm = .26mm. The cement paste is in good condition, while cracking is seen in the adhesion zones.

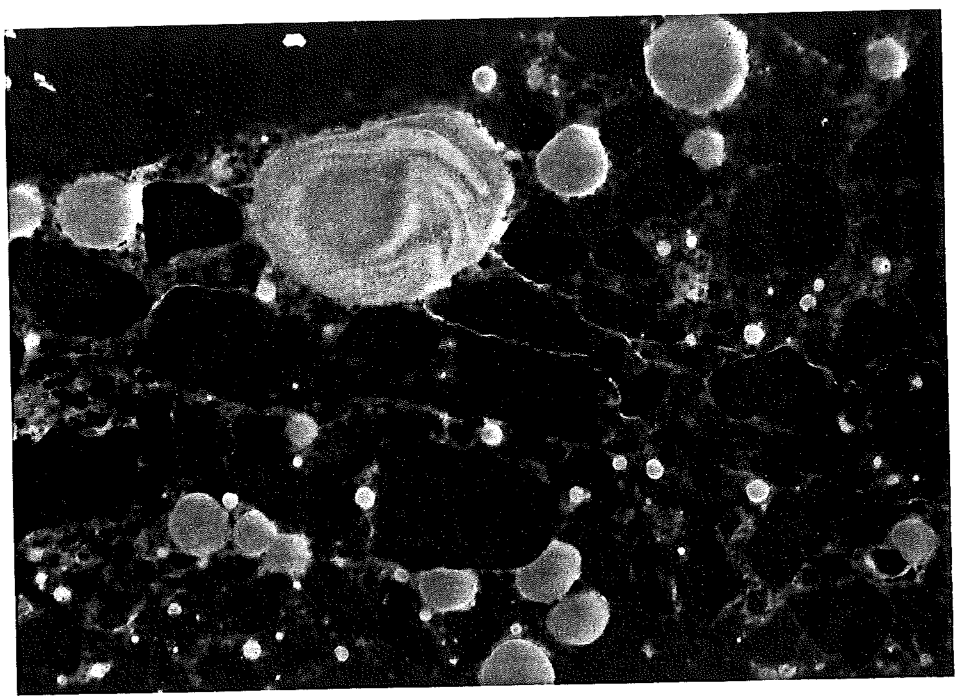

Microphoto of a sample from section MI1-2, taken in fluorescent light. Scale: 1cm = 0.26mm. Cracking has occurred through the cement paste, around aggregate, and through aggregate.

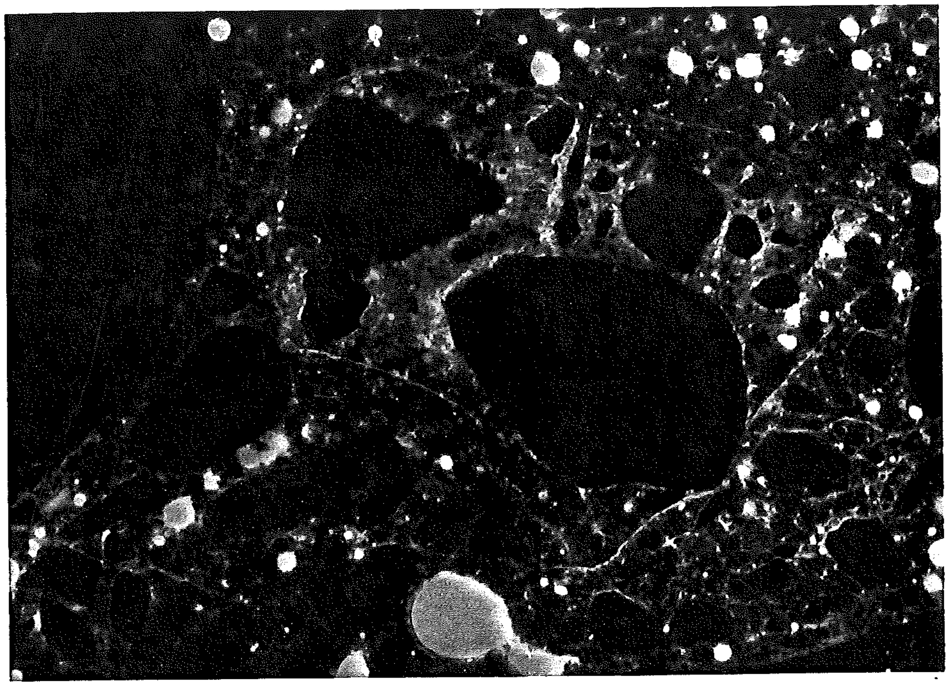

Microphoto of a sample from section MI1-3, taken in fluorescent light. Scale 1cm = 0.26mm. High amounts of cracking are found in the cement paste.

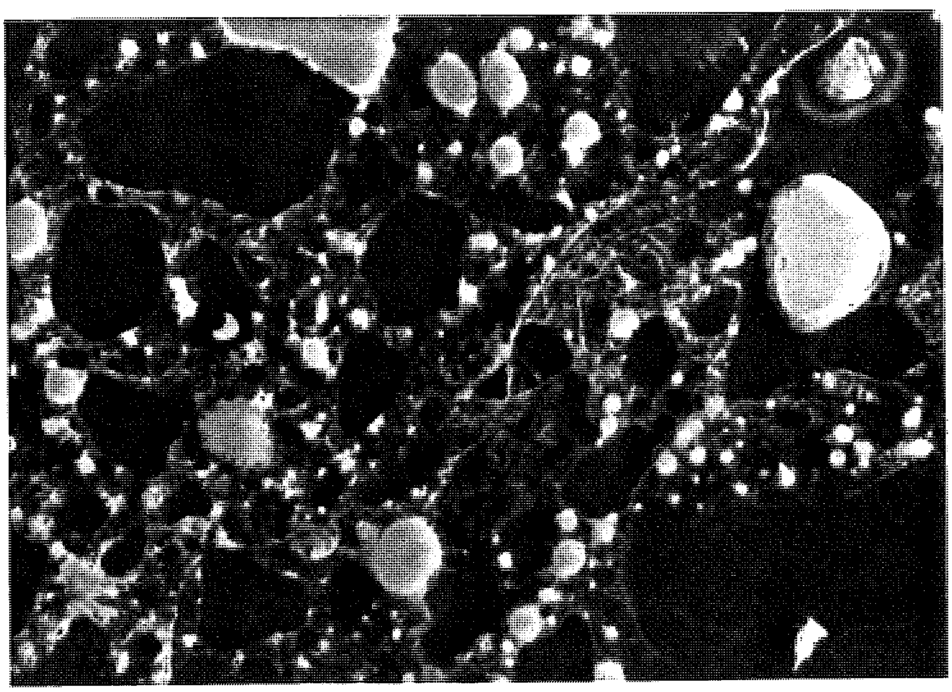

Microphoto of a sample from section MI1-4, taken in fluorescent light. Scale: 1cm = 0.26mm. Cracking is seen through the cement paste and through aggregates.

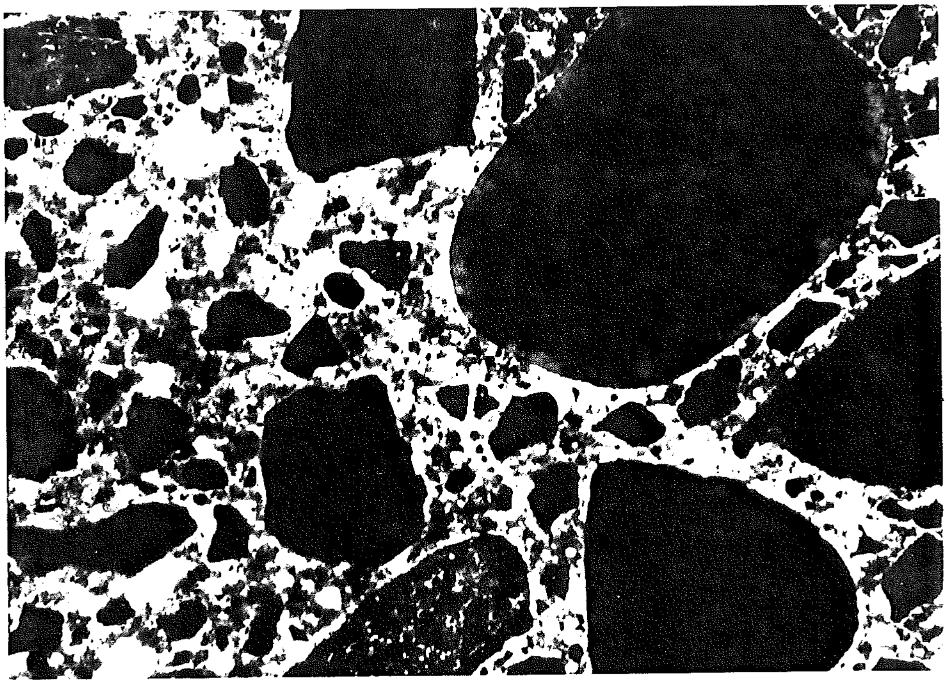

Microphoto of a sample from section MI2-1, taken in fluorescent light. Scale 1cm = 0.26 mm. Few microcracks are found in this concrete. In this photo, virtually no microcracking is detected.

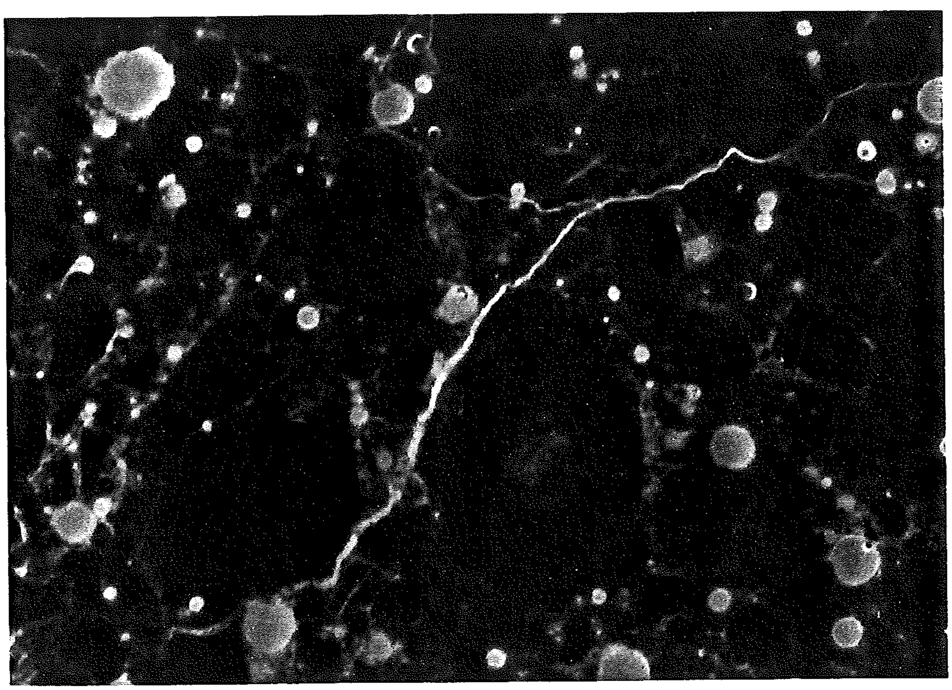

Microphoto of a sample from section MI2-2, taken in fluorescent light. Scale: 1cm = 0.26mm. Cracking is seen running mainly through the cement paste and around aggregates.

Appendix 7: Construction Data and Mix Design

This appendix gives an indication of field conditions at the time of concrete placement for the 6 test sections. In addition, comments from the contractor and from inspectors' reports have been added, providing clues to the early performances of each pavement section. Finally, this appendix includes mix design information for the various pavement sections.

The mix design information has been compiled from databases provided by MDOT and the construction contractor. Temperature information is based on data collected at weather stations near the work sites on their respective placement dates. From mix design information provided, some assumptions had to be made, such as unit weights of the materials. Estimations for recycled aggregate properties were made based on testing of the Brighton aggregate. Other unit weights were assumed based on values typical for these materials. The row labeled "sum" should add up to 1 cu.yd. (27 cf) and gives an indication of the accuracy of these estimates.

AIR TEMPERATURE ON THE DAY OF CONCRETE PLACEMENT
(Data collected from weather stations located close to the project section)

Section	Date	Temperature (Deg. F)		Location
		Low	High	
MI1-1	8/15/84	58	85	Kalamazoo
		51	86	Benton Harbor
MI1-2	8/14/84	60	86	Kalamazoo
		51	78	Benton Harbor
MI1-3	8/9/84	68	90	Kalamazoo
		63	92	Benton Harbor
MI1-4	9/4/84	49	68	Kalamazoo
		43	71	Benton Harbor
MI2-1	5/29/86	58	81	Kalamazoo
	5/29/86	54	83	Battle Creek
	5/30/86	58	83	Kalamazoo
	5/30/86	56	82	Battle Creek
MI2-2	7/13/85	66	88	Kalamazoo
	7/13/85	65	87	Battle Creek
	7/15/85	70	86	Kalamazoo
	7/15/85	68	83	Battle Creek

Temperature data is compiled from "Climatological Data: Michigan" U.S. Department of Commerce.

COMMENTS:

Section	Comments
MI1-1	Weak looking mix with bleeding during normal vibration had to be discarded. Overrun due to deep wet cores.
MI1-2	Weather warm-sunny, many problems, mix setting up very fast
MI1-3	Weather warm-sunny
MI1-4	Weather cloudy and rainy
MI2-1	Higher quality materials, better quality mix. Original concrete pavement was stronger, difficult to remove and break up.
MI2-2	The original roadway was formed of two layers of different concrete. When recycled these layers were mixed together.

CONCRETE COMPONENTS

		LAWRENCE								GALESBURG			
	Unit Weight γ	MI1-1		MI1-2		MI1-3		MI1-4		MI2-1		MI2-2	
		W lb.	Vol. Cu.ft	W lb.	Vol. Cu.ft	W lb.	Vol. Cu.ft	W lb.	Vol. Cu.ft	W lb.	Vol. Cu.ft	W lb.	Vol. Cu.ft
Fine Aggregate Natural	165	1490	9.0	691	4.2	691	4.2	1004	6.1	1493	9.0	1458	8.8
Recycled	147	0	0.0	690	4.7	690	4.7	430	2.9	0	0.0	0	0.0
Coarse Aggregate Natural	165	1730	10.5	0	0.0	0	0.0	0	0.0	0	0.0	0	0.0
Recycled	147	0	0.0	1497	10.2	1497	10.2	1497	10.2	1536	10.5	1536	10.5
Recycled % Fine		0		50		50		30		0		0	
Coarse		0		100		100		100		100		100	
Cement Type		1		1		1		1		1A		1A	
Cement Quantity	197	470	2.4	480	2.4	480	2.4	480	2.4	526	2.7	480	2.4
Fly Ash	156	72	0.5	72	0.5	72	0.5	72	0.5	0	0.0	72	0.5
Water	62.4	230	3.7	314	5.0	314	5.0	299	4.8	291	4.7	291	4.7
Added Water		106		235		237		202		201		202.7	
Water Reducing (oz/cwt)		5		5		5		5		0		5	
Air Entraining	62.4	0.78	0.0	1.203	0.0	1.147	0.0	1.137	0.0	N/A*	0.0	0.658	0.0
Water/cement Ratio		0.49		0.65		0.65		0.62		0.55		0.61	
Water/Cementitius Ratio		0.42		0.57		0.57		0.54		0.55		0.53	
Sum.			26.1		27.0		27.0		26.9		26.8		26.9

* N/A indicates information is not available

Appendix 8: Dynamic Cone Penetrometer Testing

The Dynamic Cone Penetration (DCP) Test is widely used in pavement evaluation for determination of the California Bearing Ratio (CBR) and compaction rates in base and subbase foundation layers. Even though several correlations were found in the literature, it seems to be true that each correlation is accurate only for the kind of soil for which it was established[21]. Many factors influence the interpretation of the test, producing some level of uncertainty when these relationships are used in other soil types and field conditions.

One of the most widely accepted forms of interpretation of DCP data is to correlate the number of blows of the DCP to the "N" value of the Standard Penetration Test (SPT) based on energy equations. Empirical correlations of DCP and SPT field test results also exist, but these relationships are only valid for specific soils and field conditions in which they were tested[22].

In this particular study, the DCP blow count was used directly as a qualitative representation of the mechanical properties of the base and subbase layers of the pavement. Because the high penetration resistance encountered in the field frequently exceeded the valid ranges of the available correlations, numerical calculations to determine the CBR or the field density could not be made.

When large gravel particles are centered in the line of penetration, the number of blows increases, typically producing incomplete penetration that leads to unreasonably high values for the number of DCP blows. For this reason, the larger values of DCP blows are capped to 160 which is a number approximately 95% of the maximum number of blows for 3 inches of completed penetration.

The thickness of the base is four inches; therefore, penetrations from 3 to 6 inches correspond partially to base layers and partially to subbase layers. The number of blows correspondent to penetration from 0 to 3 inches was selected as a representative value for the base layer. Penetrations from 9 to 12 inches were more frequently interrupted by large particles; therefore, penetration from 6 to 9 inches was selected for representative values of DCP number of blows for subbase.

Graphs of representative DCP resistance of base and subbase layers at each core location are presented in this appendix followed by graphs of section averages. The last graph shows the overall base and subbase DCP resistance together with the predicted modulus from the Falling Weight Deflectometer (FWD) test.

The predicted modulus of the FWD tests corresponds mainly to the subgrade material and was used in conjunction with the DCP resistance of the base and subbase to give the complete qualitative information regarding the foundation layers of each section of the project. The empirical correlation suggested by Tom Bemham[23] was used to calculate the effective modulus of the base-subbase layer. The result of this analysis is also included in this appendix.

Dynamic Cone Penetration field data.

Section	Depth	DCP blow/3in Field	Capped
MI1-1-M1	0-3	21	
MI1-1-M1	3-6	51	
MI1-1-M1	6-9	90	
MI1-1-M1	9-12	133	
MI1-1-M2	0-3	36	
MI1-1-M2	3-6	72	
MI1-1-M2	6-9	90	
MI1-1-M2	9-12	96	
MI1-1-M3	0-3	30	
MI1-1-M3	3-6	42	
MI1-1-M3	6-9	67	
MI1-1-M3	9-12	57	
MI1-1-M4	0-3	24	
MI1-1-M4	3-6	55	
MI1-1-M4	6-9	83	
MI1-1-M4	9-12	60	
MI1-1-M5	0-3	36	
MI1-1-M5	3-6	42	
MI1-1-M5	6-9	99	
MI1-1-M5	9-12	111	
MI1-2-M1	0-3	14	
MI1-2-M1	3-6	42	
MI1-2-M1	6-9	91	
MI1-2-M1	9-12	70	
MI1-2-M2	0-3	32	
MI1-2-M2	3-6	30	
MI1-2-M2	6-9	74	
MI1-2-M2	9-12	76	
MI1-2-M3	0-3	34	
MI1-2-M3	3-6	56	
MI1-2-M3	6-9	129	
MI1-2-M3*	9-12	50	150
MI1-2-M4	0-3	24	
MI1-2-M4	3-6	25	
MI1-2-M4**	6-9	45	
MI1-2-M4	9-12	20	
MI1-2-M5	0-3	23	
MI1-2-M5	3-6	23	
MI1-2-M5	6-9	52	
MI1-2-M5	9-12	40	
MI1-3-M1	0-3	53	
MI1-3-M1	3-6	89	
MI1-3-M1	6-9	135	
MI1-3-M1	9-12	133	
MI1-3-M2	0-3	35	
MI1-3-M2	3-6	47	
MI1-3-M2	6-9	116	
MI1-3-M2	9-12	141	

Section	Depth	DCP blow/3in Field	Capped
MI1-3-M3	0-3	24	
MI1-3-M3	3-6	74	
MI1-3-M3	6-9	120	
MI1-3-M3	9-12	160	
MI1-3-M4	0-3	17	
MI1-3-M4	3-6	32	
MI1-3-M4	6-9	43	
MI1-3-M4	9-12	58	
MI1-3-M5	0-3	33	
MI1-3-M5	3-6	78	
MI1-3-M5	6-9	92	
MI1-3-M5	9-12	112	
MI1-4-M1	0-3	30	
MI1-4-M1	3-6	42	
MI1-4-M1	6-9	58	
MI1-4-M1	9-12	63	
MI1-4-M2	0-3	29	
MI1-4-M2	3-6	45	
MI1-4-M2	6-9	56	
MI1-4-M2	9-12	83	
MI1-4-M3	0-3	38	
MI1-4-M3**	3-6	85	
MI1-4-M3	6-9	57	
MI1-4-M3	9-12	49	
MI1-4-M4	0-3	24	
MI1-4-M4	3-6	30	
MI1-4-M4	6-9	46	
MI1-4-M4	9-12	60	
MI1-4-M5	0-3	21	
MI1-4-M5	3-6	48	
MI1-4-M5	6-9	53	
MI1-4-M5	9-12	86	
MI2-1-M1	0-3	18	
MI2-1-M1	3-6	27	
MI2-1-M1	6-9	48	
MI2-1-M1	9-12	168	
MI2-1-M2	0-3	44	
MI2-1-M2	3-6	83	
MI2-1-M2	6-9	131	
MI2-1-M2 +	9-12	100	160
MI2-1-M3	0-3	30	
MI2-1-M3	3-6	111	
MI2-1-M3 ++	6-9	100	160
MI2-1-M3	9-12		
MI2-1-M4	0-3	45	
MI2-1-M4+++	3-6	150	160
MI2-1-M4	6-9		160
MI2-1-M4	9-12		

Section	Depth	DCP blow/3in Field	Capped
MI2-1-M5	0-3	34	
MI2-1-M5	3-6	97	
MI2-1-M5 +	6-9	100	160
MI2-1-M5	9-12		
MI2-2-M1	0-3	25	
MI2-2-M1	3-6	48	
MI2-2-M1	6-9	136	
MI2-2-M1 !	9-12	100	160
MI2-2-M2	0-3	19	
MI2-2-M2	3-6	31	
MI2-2-M2	6-9	60	
MI2-2-M2	9-12	59	
MI2-2-M3	0-3	22	
MI2-2-M3	3-6	93	
MI2-2-M3 !	6-9	100	160
MI2-2-M3	9-12		
MI2-2-M4	0-3	25	
MI2-2-M4	3-6	65	
MI2-2-M4	6-9	150	
MI2-2-M4 +	9-12	100	160
MI2-2-M5	0-3	29	
MI2-2-M5	3-6	67	
MI2-2-M5 +	6-9	100	160
MI2-2-M5	9-12		

* 50/1"
** rock
\+ 100/1"
++100/.25"
+++ 150/2"
! 100/2"

Note: All values of number of blows that seem to be extremely high due to the presence of large solid particles were capped to a 160 number of blows value (95% of the maximum 3 inches penetration value in this project)

DCP Representative values and averages

Section	Base				Sub-base			
	Representative	Average	St. Dev.*	C. Var.*	Representative	Average	St. Dev.*	C. Var.*
MI1-1-M1	21				90			
MI1-1-M2	36				90			
MI1-1-M3	30				67			
MI1-1-M4	24				83			
MI1-1-M5	36	29.4	6.8	23.3	99	85.8	11.9	13.9
MI1-2-M1	14				91			
MI1-2-M2	32				74			
MI1-2-M3	34				129			
MI1-2-M4	24				45			
MI1-2-M5	23	25.4	8.0	31.4	52	78.2	33.7	43.1
MI1-3-M1	53				120			
MI1-3-M2	35				135			
MI1-3-M3	24				116			
MI1-3-M4	17				43			
MI1-3-M5	33	32.4	13.6	42.0	92	101.2	36.0	35.6
MI1-4-M1	30				58			
MI1-4-M2	29				56			
MI1-4-M3	38				57			
MI1-4-M4	24				46			
MI1-4-M5	21	28.4	6.5	22.9	53	54.0	4.8	9.0
MI2-1-M1	18				48			
MI2-1-M2	44				131			
MI2-1-M3	30				111			
MI2-1-M4	45				160			
MI2-1-M5	34	34.2	11.1	32.5	160	122.0	46.3	37.9
MI2-2-M1	25				136			
MI2-2-M2	19				60			
MI2-2-M3	22				93			
MI2-2-M4	25				150			
MI2-2-M5	29	24.0	3.7	15.6	67	101.2	40.4	39.9

* St. Dev. and C. Var. refer to Standard Deviation and Coefficient of Variation Respectively.

Note: The representative value of DCP blow count for the base material is directly taken from the first 3 inches of penetration. For subbase, the penetration from 6 to 9 inches has been selected. This value is chosen because blow counts from 3 to 6 inches of depth are influenced by the base material and blow counts from 9 to 12 inches are found to be frequently influenced by large particles in the line of penetration.

Summary of DCP averages

Section	Base	Sub-base	Base + Sub-base
MI1-1	29.4	85.8	115.2
MI1-2	25.4	78.2	103.6
MI1-3	32.4	101.2	133.6
MI1-4	28.4	54.0	82.4
MI2-1	34.2	122.0	156.2
MI2-2	24.0	101.2	125.2

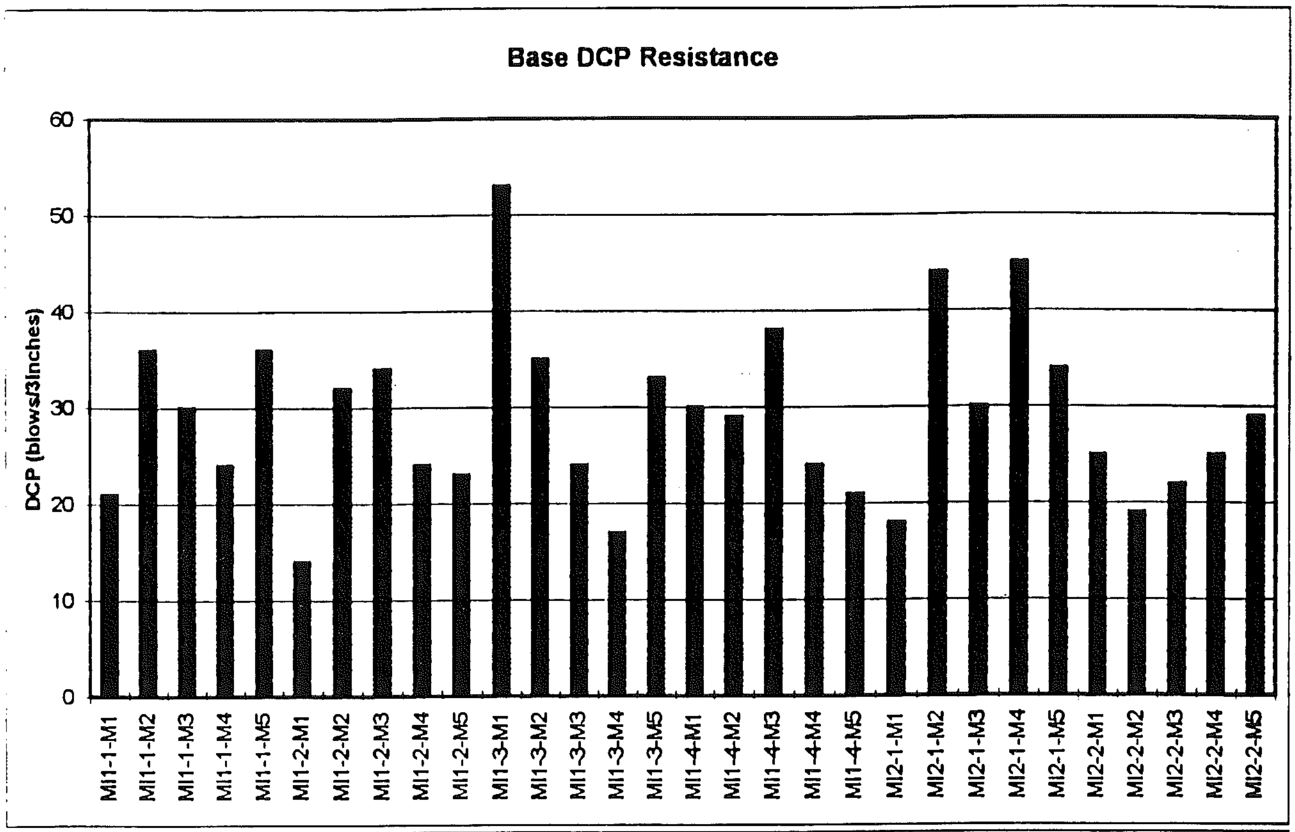
Base DCP Resistance
DCP (blows/3inches)
60
50
40
30
20
10
0
MI1-1-M1
MI1-1-M2
MI1-1-M3
MI1-1-M4
MI1-1-M5
MI1-2-M1
MI1-2-M2
MI1-2-M3
MI1-2-M4
MI1-2-M5
MI1-3-M1
MI1-3-M2
MI1-3-M3
MI1-3-M4
MI1-3-M5
MI1-4-M1
MI1-4-M2
MI1-4-M3
MI1-4-M4
MI1-4-M5
MI2-1-M1
MI2-1-M2
MI2-1-M3
MI2-1-M4
MI2-1-M5
MI2-2-M1
MI2-2-M2
MI2-2-M3
MI2-2-M4
MI2-2-M5

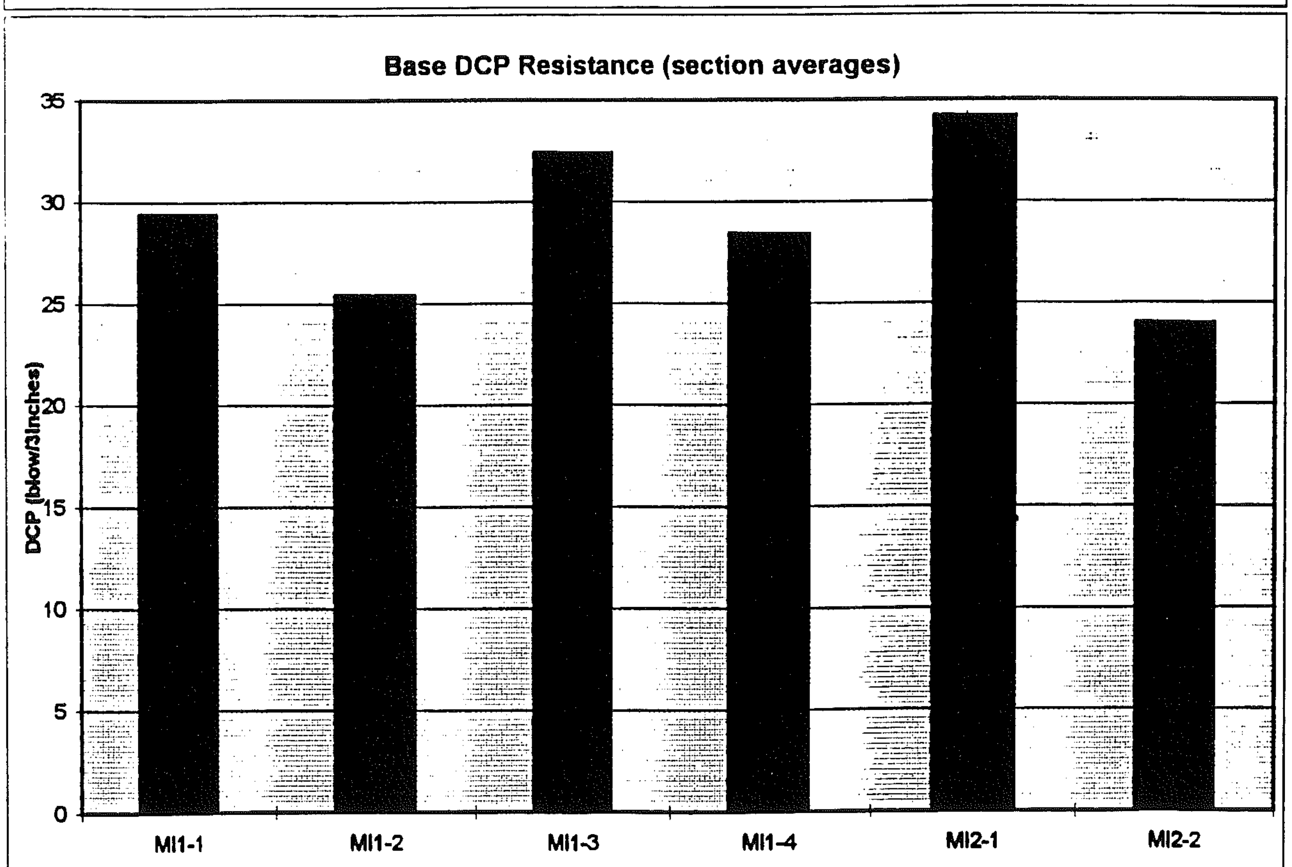
Base DCP Resistance (section averages)
DCP (blow/3inches)
35
30
25
20
15
10
5
0
MI1-1
MI1-2
MI1-3
MI1-4
MI2-1
MI2-2

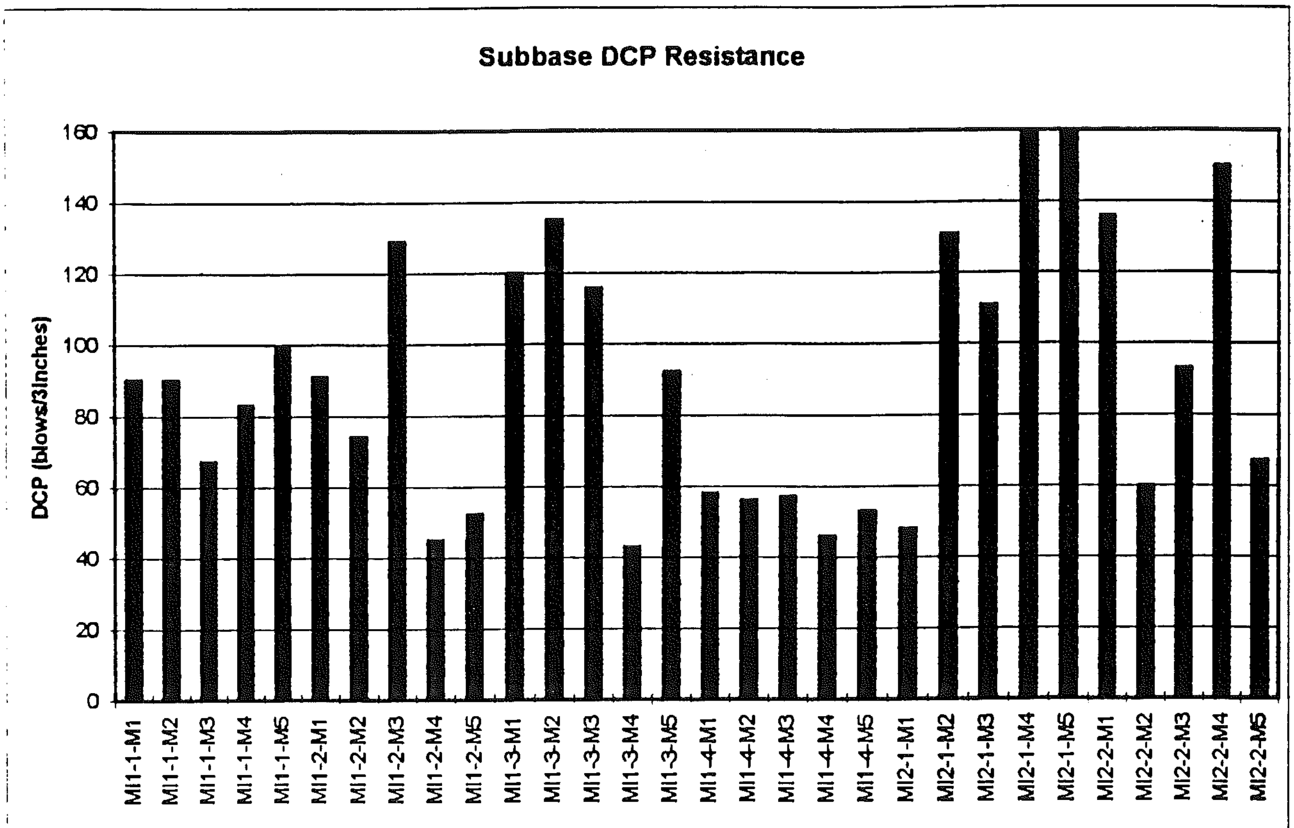

Subbase DCP Resistance
DCP (blows/3inches)
0
20
40
60
80
100
120
140
160
MI1-1-M1
MI1-1-M2
MI1-1-M3
MI1-1-M4
MI1-1-M5
MI1-2-M1
MI1-2-M2
MI1-2-M3
MI1-2-M4
MI1-2-M5
MI1-3-M1
MI1-3-M2
MI1-3-M3
MI1-3-M4
MI1-3-M5
MI1-4-M1
MI1-4-M2
MI1-4-M3
MI1-4-M4
MI1-4-M5
MI2-1-M1
MI2-1-M2
MI2-1-M3
MI2-1-M4
MI2-1-M5
MI2-2-M1
MI2-2-M2
MI2-2-M3
MI2-2-M4
MI2-2-M5

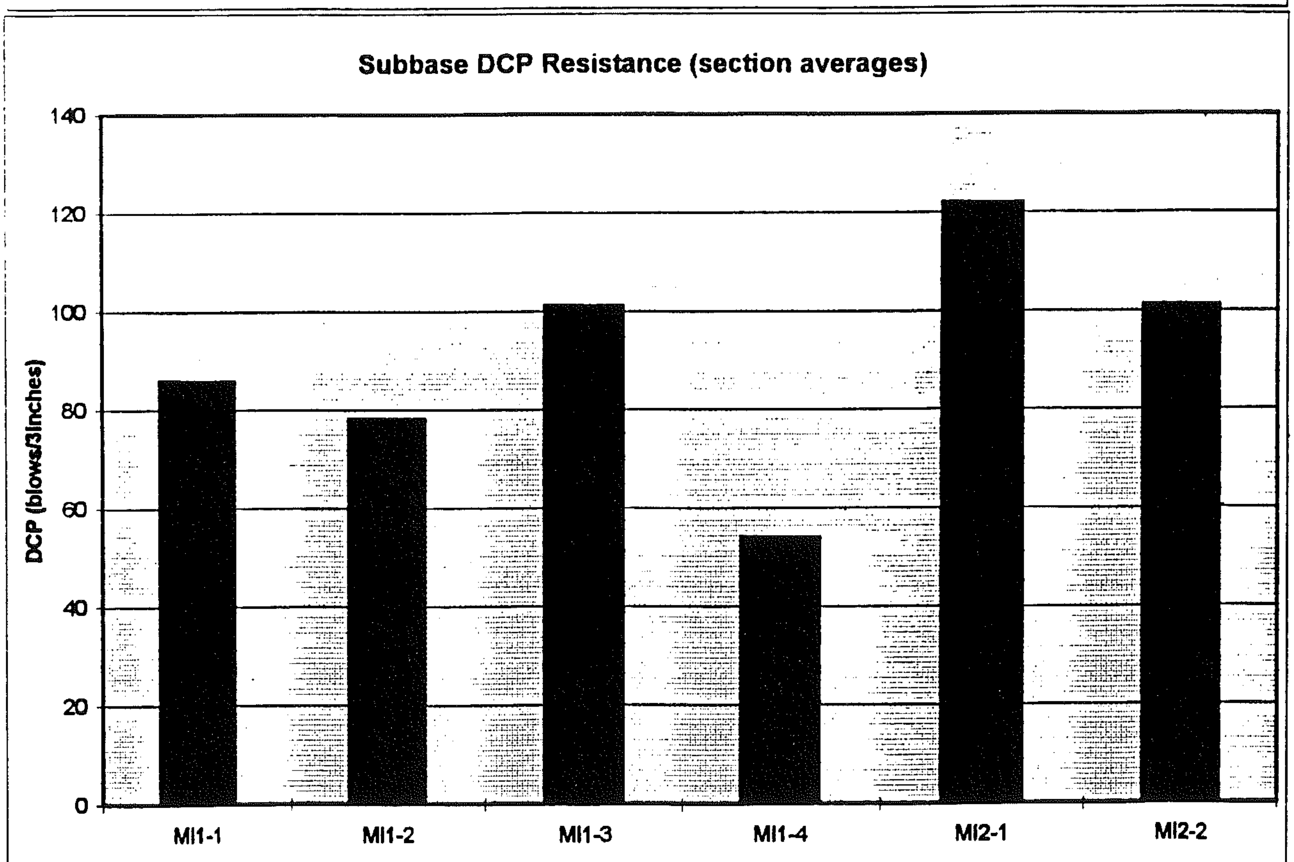

Subbase DCP Resistance (section averages)
DCP (blows/3inches)
0
20
40
60
80
100
120
140
MI1-1
MI1-2
MI1-3
MI1-4
MI2-1
MI2-2

Dynamic Cone Penetrometer Test
(Calculation of Soil Modulus)

Section Number	Depth (in)	DCP Blows (for 3")	log(mm/blow)	Eff. Mod #	Average
MI1-1-M1	0-3	21	0.55	41242	
MI1-1-M1	3-6	51	0.17	107289	
MI1-1-M1	6-9	90	-0.08	197855	
MI1-1-M1	9-12	133	-0.25	301370	
MI1-1-M2	0-3	36	0.32	73717	
MI1-1-M2	3-6	72	0.02	155570	
MI1-1-M2	6-9	90	-0.08	197855	
MI1-1-M2	9-12	96	-0.11	212103	
MI1-1-M3	0-3	30	0.40	60569	
MI1-1-M3	3-6	42	0.25	87036	
MI1-1-M3	6-9	67	0.05	143961	
MI1-1-M3	9-12	57	0.12	120950	
MI1-1-M4	0-3	24	0.49	47624	
MI1-1-M4	3-6	55	0.13	116383	
MI1-1-M4	6-9	83	-0.04	181325	
MI1-1-M4	9-12	60	0.10	127823	
MI1-1-M5	0-3	36	0.32	73717	
MI1-1-M5	3-6	42	0.25	87036	
MI1-1-M5	6-9	99	-0.12	219254	
MI1-1-M5	9-12	111	-0.17	248019	**140,035**
MI1-2-M1	0-3	14	0.73	26644	
MI1-2-M1	3-6	42	0.25	87036	
MI1-2-M1	6-9	91	-0.08	200225	
MI1-2-M1	9-12	70	0.03	150919	
MI1-2-M2	0-3	32	0.37	64931	
MI1-2-M2	3-6	30	0.40	60569	
MI1-2-M2	6-9	74	0.01	160231	
MI1-2-M2	9-12	76	-0.01	164902	
MI1-2-M3	0-3	34	0.34	69314	
MI1-2-M3	3-6	56	0.13	118665	
MI1-2-M3	6-9	129	-0.24	291616	
MI1-2-M3*	9-12	50	0.18	105024	
MI1-2-M4	0-3	24	0.49	47624	
MI1-2-M4	3-6	25	0.48	49766	
MI1-2-M4**	6-9	45	0.22	93753	
MI1-2-M4	9-12	20	0.57	39130	
MI1-2-M5	0-3	23	0.51	45490	
MI1-2-M5	3-6	23	0.51	45490	
MI1-2-M5	6-9	52	0.16	109558	
MI1-2-M5	9-12	40	0.27	82579	**100,673**
MI1-3-M1	0-3	53	0.15	111830	
MI1-3-M1	3-6	89	-0.07	195487	
MI1-3-M1	6-9	135	-0.26	306256	
MI1-3-M1	9-12	133	-0.25	301370	
MI1-3-M2	0-3	35	0.33	71513	
MI1-3-M2	3-6	47	0.20	98251	
MI1-3-M2	6-9	116	-0.19	260078	
MI1-3-M2	9-12	141	-0.27	320947	
MI1-3-M3	0-3	24	0.49	47624	
MI1-3-M3	3-6	74	0.01	160231	
MI1-3-M3	6-9	120	-0.20	269754	
MI1-3-M3	9-12	160	-0.33	367781	
MI1-3-M4	0-3	17	0.64	32844	
MI1-3-M4	3-6	32	0.37	64931	
MI1-3-M4	6-9	43	0.24	89271	
MI1-3-M4	9-12	58	0.11	123238	
MI1-3-M5	0-3	33	0.36	67120	
MI1-3-M5	3-6	78	-0.02	169583	
MI1-3-M5	6-9	92	-0.09	202596	
MI1-3-M5	9-12	112	-0.17	250428	**175,557**

Section Number	Depth (in)	DCP Blows (for 3")	log(mm/blow)	Eff. Mod #	Average
MI1-4-M1	0-3	30	0.40	60569	
MI1-4-M1	3-6	42	0.25	87036	
MI1-4-M1	6-9	58	0.11	123238	
MI1-4-M1	9-12	63	0.08	134722	
MI1-4-M2	0-3	29	0.41	58396	
MI1-4-M2	3-6	45	0.22	93753	
MI1-4-M2	6-9	56	0.13	118665	
MI1-4-M2	9-12	83	-0.04	181325	
MI1-4-M3	0-3	38	0.30	78139	
MI1-4-M3**	3-6	85	-0.05	186037	
MI1-4-M3	6-9	57	0.12	120950	
MI1-4-M3	9-12	49	0.18	102763	
MI1-4-M4	0-3	24	0.49	47624	
MI1-4-M4	3-6	30	0.40	60569	
MI1-4-M4	6-9	46	0.21	96000	
MI1-4-M4	9-12	60	0.10	127823	
MI1-4-M5	0-3	21	0.55	41242	
MI1-4-M5	3-6	48	0.19	100505	
MI1-4-M5	6-9	53	0.15	111830	
MI1-4-M5	9-12	86	-0.06	188396	**106,979**
MI2-1-M1	0-3	18	0.62	34931	
MI2-1-M1	3-6	27	0.44	54069	
MI2-1-M1	6-9	48	0.19	100505	
MI2-1-M1	9-12	168	-0.35	387633	
MI2-1-M2	0-3	44	0.23	91510	
MI2-1-M2	3-6	83	-0.04	181325	
MI2-1-M2	6-9	131	-0.24	296490	
MI2-1-M2 +	9-12	100	-0.12	221641	
MI2-1-M3	0-3	30	0.40	60569	
MI2-1-M3	3-6	111	-0.17	248019	
MI2-1-M3 ++	6-9	100	-0.12	221641	
MI2-1-M4	0-3	45	0.22	93753	
MI2-1-M4 +++	3-6	150	-0.30	343075	
MI2-1-M5	0-3	34	0.34	69314	
MI2-1-M5	3-6	97	-0.11	214485	
MI2-1-M5 +	6-9	100	-0.12	221641	**177,538**
MI2-2-M1	0-3	25	0.48	49766	
MI2-2-M1	3-6	48	0.19	100505	
MI2-2-M1	6-9	136	-0.26	308701	
MI2-2-M1 I	9-12	100	-0.12	221641	
MI2-2-M2	0-3	19	0.60	37026	
MI2-2-M2	3-6	31	0.38	62747	
MI2-2-M2	6-9	60	0.10	127823	
MI2-2-M2	9-12	59	0.10	125529	
MI2-2-M3	0-3	22	0.53	43362	
MI2-2-M3	3-6	93	-0.09	204970	
MI2-2-M3 I	6-9	100	-0.12	221641	
MI2-2-M4	0-3	25	0.48	49766	
MI2-2-M4	3-6	65	0.06	139336	
MI2-2-M4	6-9	150	-0.30	343075	
MI2-2-M4 +	9-12	100	-0.12	221641	
MI2-2-M5	0-3	29	0.41	58396	
MI2-2-M5	3-6	67	0.05	143961	
MI2-2-M5 +	6-9	100	-0.12	221641	**148,894**

* 50/1" ** rock + 100/1" ++100/.25" +++ 150/2"
I 100/2"

Using equation, log(Modulus)= -1.0775 log(mm/blow)+3.0495
Derived from Burham, 1993 data

Appendix 9: Crack Analysis

Crack and joint analysis has been performed in two separate studies. One study was a visual examination of two cracks and two joints from each section performed at the University of Michigan. Evidence of the infiltration of fines, presence and severity of wear and abrasions, and condition of the temperature steel were examined. A table showing the results of this study is found on pate A9-2

The second study examined surface texture of one joint core and of one crack core for each test section. Each core was given a visual rating from "poor" to "very good" in three categories: volumetric surface texture, macro-texture, and gross-texture. This study was conducted at the University of Minnesota.

Joint Core Information

Identification	Fines/Deposits	Dowel Condition	Abrasions	Movement	Other Comments
MI1-1-J1	yellowish deposits throughout		None	Tight; Likely non-moving	
MI1-1-J3	yellowish deposits throughout		Few	Tight; Likely non-moving	
MI1-2-J1		Tight/secure		Tight; Likely non-moving	No faulting. Edges at top of joint (mainly on approach side) show wear
MI1-2-J3	many white deposits		None	Tight; Possible movement	No faulting.
MI1-3-J1	Yellow deposits in top 1/2 of core		None	Tight/fixed; Likely non-moving	
MI1-3-J3	Many gray deposits	very loose; no epoxy on bottom; bar corroded	Some	Possible movement	Dowel allows vertical movement of 2-3mm
MI1-4-J1	Many gray deposits		Few	Some fixed points	Large vertical crack, 1/2" gap. Horizontal crack close to the bottom
MI1-4-J3	Some beige deposits		None	Well fixed; Likely non-moving	Horizontal crack at 2" from bottom
MI2-1-J1	Fairly clean except for dirt/rust below dowel	Rusted and loose. Green epoxy is corroded and missing for lower area	None		Bottom of hole for dowel shows wear
MI2-1-J3			None	Likely non-moving	Smooth holes along crack fit aggregate

Crack Core Information

Identification	Type of Cracking	Fines/Deposits	Rebar Condition	Abrasions	Movement	Other Comments
MI1-1-C1		Dark gray deposits in top half	Corroded	Some	Loose, Likely moving	Horizontal crack at rebar level in approach side. 1" height wedge missing at top on leave side.
MI1-1-C3	Cracked on an angle. Open about 1/4" along side of core.	Dark gray deposits throughout crack	Broken and severely corroded			3/4" height wedge missing at top
MI1-2-C1	Tight	Appears to have clay in edges	From exterior, rebar appears in good condition		Tight	No faulting
MI1-2-C3		Dark gray deposits at top and down side	Broken and severely corroded	Many	Likely a moving crack	Two small pieces broken at top, split aggregates and wear.
MI1-3-C1		Many gray deposits	Broken and severely corroded	Many (deep)	No fixed points. Slides easily.	Horizontal crack above rebar (clean and shows no signs of wear)
MI1-3-C3		Some gray deposits	Broken and severely corroded	Some	Well fixed; Likely non-moving	
MI1-4-C1		Many brown deposits (clay)	Broken and corroded	Some	Likely small movement	Some fixed points.
MI1-4-C3		White deposits in top			Tight	Crack more open at top (1/4") than bottom. At bottom crack is tight
MI2-2-C1		Some deposits (silt)		Few		Abrasions on coarse aggregate indicate relative displacement downward on traffic leaving side of core.
MI2-2-C3		Fairly clean		Vertical lines of abrasion		aggregates along crack seem to have worn the bottom of corresponding holes on approach side smooth. Leave side

* Core could not be opened along joint or crack

University of Minnesota Crack Texture Study

Test Procedures

Volumetric Surface Texture (VST) Testing

The VST test was developed at the University of Minnesota to provide an estimate of the load transfer potential available across a fractured concrete surface through aggregate or grain interlock. It may also provide an indication of the degree of surface abrasion that has taken place since fracture. The test apparatus consists of a spring-loaded probe with digital readout that is mounted on a frame over a computer-controlled microscope stage of the type typically used for performing linear traverse or other measurements of concrete air void systems. The digital readout measures the distance from an arbitrarily established datum to the fractured surface at any chosen point. These distances are recorded electronically for each point in a predetermined grid pattern across the fractured surface (a 0.125-in grid was used for this work) to define the 3-dimensional profile of the fractured surface. The average measurement area was about 25 square inches.

When the test is complete, the surface texture is quantified by a volumetric surface texture ratio (VSTR). The VSTR is the ratio of the volume of texture per unit surface area (given in units of cm^3/cm^2). A VSTR below 0.22 cm^3/cm^2 typically indicates poor surface texture, while values above 0.27 cm^3/cm^2 are typically associated with good surface texture.

Visual Examination

Each core was also examined visually to assess the surface texture and provide documentation of any unusual conditions that might explain or contribute to the VST measurements obtained. A visual rating is given to both "gross texture" and "macrotexture." The gross texture was defined as the texture provided by the path along which the crack propagated, while macrotexture refers to actual surface texture of the fractured plane (a function of the type of coarse aggregate used and the path of fracture). The following rating scale was used to rate both aspects of the crack texture:: VG-very good; G-good; F-fair; P-poor; and VP-very poor.

Test Results and Observations

Each core was examined visually and subjected to the VST test (as described previously). The results of these tests are summarized in Table 1. The core identification code consists of several parts: first the project identification (i.e., MI1 for the Lawrence location, MI2 for the Galesburg location), then a one-digit section identifier within the project. followed by a J (indicating a core through a joint) or a C (a core through a crack).

A brief summary and interpretation of the test results follows.

Table 1. Surface texture data summary.

Surface Texture				
Core Identification		VSTR (cm^3/cm^2)	Visual Rating macro	Visual Rating gross
MI1	1J	0.2265	P	P
	1C	0.3033	P	F
	2J	0.2435	G	F
	2C	0.2758	P	G-F
	3J	0.3537	F	F
	3C	0.2005	P-F	P
	4J	0.2626	VG	F
	4C	0.0995	P	P
MI2	1J	0.2742	G	G
	1C	0.5059	P	G
	2J	0.1804	F-P	F
	2C	0.5609	P	G

Project MI1: I-94 near Lawrence

Section MI1-1: Virgin Peastone Gravel, Open-Graded Base

Table 1 indicates that the texture of the crack face (MI1-1-C2) was greater than that of the joint face (MI1-1-J2). This is probably due at least in part to the fact that the transverse crack was still being held tight by the wire mesh reinforcing, which was still intact and had to be cut to perform the VST measurement. It was noted that the face of the crack did not exhibit any signs of abrasion. It was also noted that the crack meandered roughly along the transverse wire at this location.

The crack beneath the sawed joint (MI1-1-J2) appeared to have propagated along a fairly straight plane which provided little gross texture for load transfer. The small aggregate top size (reported as 8 mm) also contributed to the low VSTR measured for this core. It was also noted that the bottom portion of the dowel found in this core was beginning to exhibit signs of corrosion.

Section MI1-2: 100% Recycled CA, 50% Recycled FA, Open-Graded Base.

The crack for core MI1-2-C2 (taken through a transverse crack) propagated along an inclined plane and through the aggregate, producing relatively poor macrotexture (because of going through the aggregate, rather than around) but fair-to-good gross texture (because of the inclined crack plane. The longitudinal steel was ruptured and severely corroded; as a result, some areas of the crack face showed signs of abrasion and the crack was severely spalled.

The crack for the core MI1-2-J2 (taken through a transverse joint) exhibited good macrotexture and fair gross texture. This crack appeared to propagate around many aggregate particles, which increased the macrotexture. Some spalling was observed at the bottom of the core.

The overall difference between the VST measurements for the joint and crack cores was not great because one exhibited better macrotexture while the other showed improved gross texture. Joint texture was improved over that found in section MI1-1, presumably due mainly to the greater macrotexture in MI1-2 associated with the use of the larger sized recycled aggregate particles (15 mm observed) in MI1-2 (compared with the 8-mm peastone used in section MI1-1). The crack texture in MI1-2 was good, but still lower than that of MI1-1, which was still tight and had not been subject to abrasion.

Section MI1-3: 100% Recycled CA, 50% Recycled FA, 5% Cement-Stabilized Peastone Base.

The crack associated with core MI1-3-C2 (transverse crack) appears to have propagated through the aggregate and along a relatively straight plane, thereby providing poor-to-fair macrotexture, poor gross texture, and overall poor texture (VST = 0.2005). In addition, the longitudinal steel had ruptured and was severely corroded, and the center portion of the crack face appeared to have been worn down to the point where good contact between the slab faces would be improbable. Severe spalling was also observed at the crack.

The crack at the joint (core MI1-3-J2) appeared to go around most of the natural aggregate particles, and the surface texture appeared to be unabraded, indicating that the dowel load transfer system was still carrying most of the load across the joint and that differential vertical movements were not great. The surface texture measurement of this specimen was the greatest of any in section MI1. The dowel was not corroded, but some signs of wear were observed along the bottom of the dowel.

Section MI1-4: 100% Recycled CA, 30% Recycled FA, Dense-Graded Base

The crack for core MI1-4-C2 (transverse crack) propagated along a relatively straight plane and through most of the recycled and natural aggregate particles. The natural (original) coarse aggregate particles appeared to be have a small top size. These factors contributed to the extremely low VSTR (0.0995) obtained for this core. Severe spalling was noted at both the top and bottom of the core, which decreased the effective thickness of the slab from 24 cm to 16 cm at this location. The longitudinal wire had ruptured and was severely corroded.

The crack associated with core MI1-4-J2 (transverse joint) appears to have propagated around the aggregate particles but on a relatively straight plane, thereby providing very good macrotexture and fair gross texture. Although some concrete bearing failures were present around the dowel and some corrosion was observed on the bottom of the dowel, it appears to be preventing significant abrasion of the crack surface at this time. The overall effect of these factors was a relatively good VSTR of 0.2626.

<u>Project MI2: I-94 near Galesburg</u>

Section MI2-1: 100% Recycled CA, Open-Graded Base, Westbound Lanes

The crack associated with core MI2-1-C2 (transverse crack) was very tight and the mesh reinforcement had to be cut to expose the crack faces. The crack had propagated through the aggregate particles and along a curved plane. An extremely high VSTR (0.5059) was measured in spite of the lack of macrotexture because of the global interlock provided by the curved plane of cracking. Two layers of longitudinal steel were found: the upper layer was 8 cm from the top of the core and the lower layer was 12 cm below the top layer. Presumably, this is why the crack was held so tightly. Neither steel wire showed any sign of corrosion.

Both the gross and macro texture for core MI2-1-J2 (transverse joint) are good, which is reflected in the good VSTR (0.2742). This VSTR is lower than that of the crack core from the same project (M2-1-C2) because the global or gross crack texture of the crack was much greater for the transverse crack. In this case, it appears that the gross texture has a disproportionately large influence on the VSTR because the meander of the vertical crack face creates a large volume of interlock potential per unit of surface area. However, both VSTR numbers are high enough to expect good aggregate or grain interlock load transfer capacity.

It was noted that the natural portion of the recycled concrete aggregate in M2-1-C2 appeared to be gap-graded, with both large and small particles sizes but no intermediate sizes. In addition, the dowel was corroded on both the top and bottom, but not on either side.

Section MI2-2: 100% Recycled CA, Open-Graded Base, Eastbound Lanes

The crack associated with core MI2-2-C2 (transverse crack) propagated through the majority of the aggregate particles and along approximately a 17 degree incline, thereby providing poor macrotexture but good gross texture. A large fragment at the bottom of the approach side of the core was broken off, reducing the effective thickness from 26 cm to 20 cm. The longitudinal steel was severely corroded.

Core MI2-2-J2 (transverse joint) also propagated through the majority of the aggregate particles but did so on a relatively straight vertical plane. This resulted in a much lower VSTR (0.1804) compared to that of MI2-2-C2 (VSTR = 0.5609). There did not appear to be many natural aggregate particles at the crack face. Some spalling was also observed on the bottom of the leave side of the core.

Appendix 10: Freeze-Thaw Durability Testing

Freeze-thaw durability testing was performed on concrete beams made with recycled coarse aggregate in order to examine the durability of recycled aggregate in pavement concrete. Testing was performed following the Michigan Test Methods 113-115 and corresponding ASTM specifications. The aggregate was tested to determine its bulk specific gravity, percent absorption capacity, and unit weight. The mix design followed the requirements of cement content, consistency, air content, and coarse aggregate contents specified in the MTM standards.

The coarse aggregate was 24 hour vacuum saturated prior to mixing. The unit weight, slump, air content, and temperature were tested on the freshly mixed concrete and the strength of the concrete was tested at ages of 7 and 28 days. The freeze-thaw machine used in this project automatically freezes and thaws the beams about eight times every 24 hours using cold air to freeze and water to thaw. The temperature limits are zero and forty degrees Fahrenheit.

A total of nine beams (three for each batch) were tested. The length of each specimen was measured in a length comparator to 0.0001" approximately every 30 cycles except for initial readings which were taken more frequently. The percent expansion was recorded and plotted after each reading until the specimen reached 0.1% expansion or 300 cycles.

In the appendix is found a summary of the testing results, followed by aggregate properties and data specific to the three batches and freeze-thaw testing.

Of the three batches made, only one meets the current MTM vacuum saturation procedure specifications. While all batches were brought to the required vacuum pressure, batches 1 and 3 lost vacuum during backfilling of the chamber with water to give the pressure indicated in the summary sheet. M-DOT has since indicated that such pressure loss is not acceptable. The batches with slightly lower vacuum pressure are presented because they indicate a significantly improved performance of recycled aggregates under a lower degree of vacuum saturation.

UNIVERSITY OF MICHIGAN
MATERIALS DEPARTMENT

Freeze-Thaw No.	Recycled I-96
Job No.	MCPA Recycled Concrete Project
Laboratory No.	UM Concrete
Date	7/18/95

REPORT OF TEST
FREEZE-THAW DURABILITY IN CONCRETE

Report on sample of	Recycled I 96 at Brighton
Date sampled	9/15/94
Source of material	Crushing plant-Milford
Sampled from	Stockpile
Submitted by	Phil Mohr
Intended use	MCPA study

PROPERTIES OF COARSE AGGREGATE

Bulk Specific Gravity (dry basis)	2.35
Absorption (%) by Vacuum Saturation	5.26
Unit Weight of Agg. (dry, loose, pcf)	84.39

		BATCH NUMBER			
CONCRETE MIX DATA		1	2	3	Average
Date Made		11/10/94	11/15/94	11/22/94	
Slump (inches)		2	2.5	2.75	2.42
Unit weight of Concrete (pcf)		141.82	141.02	140.60	141.15
Actual Cement Content (pcy)		530	524	524	526
Water-cement ratio by weight		0.43	0.46	0.44	0.45
Air Content (%)		6.2	6.6	8.2	7.0
Compressive Strength (psi)	7 days	4220	3435	3175	3610
	28 days	4644	4416	4726	4595

Vacuum Pressure (in-hg)*		28.0	28.6	27.4	
Freeze-Thaw Durability (% Expansion per 100 cycles)	Beam 1	0.025	0.107	0.032	
	Beam 2	0.023	0.063	0.038	
	Beam 3	0.021	0.083	0.039	
	Average	0.023	0.084	0.036	0.048

REMARKS:
*MTM specifies 28.5$\pm$0.2 in-hg of vacuum pressure.

UNIVERSITY OF MICHIGAN
MATERIALS DEPARTMENT

Freeze-Thaw No.	Recycled I-96
Job No.	MCPA Recycled Concrete Project
Laboratory No.	UM Concrete
Date	6/27/95

AGGREGATE PROPERTIES TEST

Report on sample of Recycled I 96 at Brighton

CONDITION OF SAMPLE	INDICATION	1 HOUR VACUUM SATURATION + 23 HOUR COLD WATER IMMERSION	
SATURATED SURFACE DRY	B	11.41	11.41
SATURATED SAMPLE IN WATER	C	6.80	6.81
OVEN DRY IN AIR	A	10.84	10.84
MOISTURE CONTENT OF SAMPLE	B - A	0.57	0.57
VOLUME OF SAMPLE (cc)	B - C	4.61	4.60
BULK SPECIFIC GRAVITY (OVEN DRY BASIS)	A / B - C	2.35	2.36
	AVERAGE	2.35	
BULK SPECIFIC GRAVITY (SSD BASIS)	B / B - C	2.48	2.48
	AVERAGE	2.48	
ABSORPTION PERCENT	B - A / A	5.26	5.26
	AVERAGE	5.26	

OVEN DRY LOOSE UNIT WEIGHT CALCULATIONS

		SAMPLE 1	SAMPLE 2
EMPTY BUCKET WEIGHT	D	14.28	14.28
FILLED BUCKET WEIGHT	E	56.23	56.72
VOLUME OF BUCKET	F	0.50	0.50
SAMPLE WEIGHT	E - D	41.95	42.44
UNIT WEIGHT (pcf)	E - D / F	83.90	84.88
	AVERAGE	84.39	

UNIVERSITY OF MICHIGAN
MATERIALS DEPARTMENT

Freeze-Thaw No.	Recycled I-96
Job No.	MCPA Recycled Concrete Project
Laboratory No.	UM Concrete
Date	7/18/95

MIX DESIGN

Report on sample of Recycled I 96 at Brighton

		LAB NO.	SP. GR.	ABS%
CEMENT	Lafarge Type I		3.15	
COARSE AGGREGATE	Recycled I-96		2.35	5.26
FINE AGGREGATE	BIN		2.64	1.32

MATERIAL	WEIGHT (pcy)	BATCH PROPORTIONS (pounds) BATCH = 1.971 (cf)			
CEMENT	517	37.74	TOTAL CEMENT		
COARSE AGGREGATE	1700		PASS	RET	%
		31.03	1"	3/4"	25
		31.03	3/4"	1/2"	25
		31.03	1/2"	3/8"	25
		31.03	3/8"	#4	25
		124.10	TOTAL COARSE AGGREGATE		
FINE AGGREGATE	1194	87.16	TOTAL FINE AGGREGATE		
ABSORBED WATER	FREE WATER				
C. AGG 89.39					
F. AGG 15.76	330	24.09	TOTAL WATER		
TOTAL 105.15					

TOTAL AGGREGATE CONTAINS 41 % FINE AGGREGATE

UNIVERSITY OF MICHIGAN
MATERIALS DEPARTMENT

Freeze-Thaw No.	94-recycled I 96 -1
Job No.	MCPA recycled concrete project
Laboratory No.	UM Concrete
Date	6/6/95

BATCH SHEET

Report on sample of Recycled I 96 at Brighton

COARSE AGGREGATE	
CANS	2 & 3
WEIGHT	24.47
1" - 3/4"	31.03
	55.50
3/4" - 1/2"	31.03
	86.52
1/2" - 3/8"	31.03
	117.55
3/8" - #4	31.03
TOTAL	148.57
FINE AGGREGATE	
M.C.	0.0265
PAILS	1 & 2
WEIGHT	4.56
DRY SAND	87.16
MOISTURE	2.31
TOTAL	94.03
CEMENT	
PAIL	3
WEIGHT	2.02
CEMENT	37.74
TOTAL	39.76

BATCH NO.	1
COARSE AGGREGATE	Recycled I 96
VACUUM SATURATION	28
DATE BATCH MADE	11/10/94

WATER MEASUREMENT

COARSE AGG. + CANS	148.57	
+ TOTAL WATER	24.09	24.09
- RESERVE WATER	4	4
TOTAL	168.66	20.09

RESERVE WATER

	before	after	
full weight	4	3.01	
beaker	0.4	0.4	
	4.4	2.61	1.39

WATER USED IN BATCH 21.48

WATER	21.48
+ MOISTURE	2.31
TOTAL WATER USED IN BATCH	23.79

SUMMARY OF PROPORTIONS	
Coarse aggregate as designed	124.10
Fine aggregate as designed	87.16
Cement as designed	37.74
Total water of batch	23.79
Total weight of batch	272.79

WEIGHT OF CONC. AND CONTAINER	85.23
WEIGHT OF EMPTY CONTAINER	14.32
WEIGHT OF CONCRETE	70.91
TEMPERATURE	72
AIR ENTRAINING ADMIXTURE	34cc
SLUMP	2.0
AIR CONTENT	6.2

UNIVERSITY OF MICHIGAN
MATERIALS DEPARTMENT

Freeze-Thaw No.	94-recycled I 96 -1
Job No.	MCPA recycled concrete project
Laboratory No.	UM Concrete
Date	6/6/95

BATCH SHEET

Report on sample of Recycled I 96 at Brighton

COARSE AGGREGATE

CANS	2 & 3
WEIGHT	24.42
1" - 3/4"	31.03
	55.45
3/4" - 1/2"	31.03
	86.47
1/2" - 3/8"	31.03
	117.50
3/8" - #4	31.03
TOTAL	148.52

FINE AGGREGATE

M.C.	0.0279
PAILS	1 & 2
WEIGHT	4.11
DRY SAND	87.16
MOISTURE	2.43
TOTAL	93.70

CEMENT

PAIL	3
WEIGHT	2.19
CEMENT	37.74
TOTAL	39.93

SUMMARY OF PROPORTIONS

Coarse aggregate as designed	124.10
Fine aggregate as designed	87.16
Cement as designed	37.74
Total water of batch	25.08
Total weight of batch	274.08

BATCH NO.	2
COARSE AGGREGATE	Recycled I 96
VACUUM SATURATION	28.6
DATE BATCH MADE	11/15/94

WATER MEASUREMENT

COARSE AGG. + CANS	148.52	
+ TOTAL WATER	24.09	24.09
- RESERVE WATER	4	4
TOTAL	168.61	20.09

RESERVE WATER

	before	after	
full weight	4	1.9	
beaker	0.46	0.46	
	4.46	1.44	2.56

WATER USED IN BATCH 22.65

WATER	22.65
+ MOISTURE	2.43
TOTAL WATER USED IN BATCH	25.08

WEIGHT OF CONC. AND CONTAINER	84.86
WEIGHT OF EMPTY CONTAINER	14.35
WEIGHT OF CONCRETE	70.51
TEMPERATURE	76
AIR ENTRAINING ADMIXTURE	35cc
SLUMP	2.5
AIR CONTENT	6.6

UNIVERSITY OF MICHIGAN
MATERIALS DEPARTMENT

Freeze-Thaw No.	94-recycled I 96 -1
Job No.	MCPA recycled concrete project
Laboratory No.	UM Concrete
Date	6/6/95

BATCH SHEET

Report on sample of Recycled I 96 at Brighton

COARSE AGGREGATE

CANS	1 & 3
WEIGHT	24.47
1" - 3/4"	31.03
	55.50
3/4" - 1/2"	31.03
	86.52
1/2" - 3/8"	31.03
	117.55
3/8" - #4	31.03
TOTAL	148.57

FINE AGGREGATE

M.C.	0.035
PAILS	1 & 2
WEIGHT	3.95
DRY SAND	87.16
MOISTURE	3.05
TOTAL	94.16

CEMENT

PAIL	3
WEIGHT	2.14
CEMENT	37.74
TOTAL	39.88

SUMMARY OF PROPORTIONS

Coarse aggregate as designed	124.10
Fine aggregate as designed	87.16
Cement as designed	37.74
Total water of batch	24.16
Total weight of batch	273.16

BATCH NO.	3
COARSE AGGREGATE	Recycled I 96
VACUUM SATURATION	27.4
DATE BATCH MADE	11/22/94

WATER MEASUREMENT

COARSE AGG. + CANS	148.57	
+ TOTAL WATER	24.09	24.09
- RESERVE WATER	4	4
TOTAL	168.66	20.09

RESERVE WATER

	before	after	
full weight	4	3.41	
beaker	0.43	0.43	
	4.43	2.98	1.02

WATER USED IN BATCH 21.11

WATER	21.11
+ MOISTURE	3.05
TOTAL WATER USED IN BATCH	24.16

WEIGHT OF CONC. AND CONTAINER	83.66
WEIGHT OF EMPTY CONTAINER	13.36
WEIGHT OF CONCRETE	70.30
TEMPERATURE	
AIR ENTRAINING ADMIXTURE	36cc
SLUMP	2.8
AIR CONTENT	8.2

UNIVERSITY OF MICHIGAN
MATERIALS DEPARTMENT

Freeze-Thaw No.	94-recycled I 96 -1
Job No.	MCPA recycled concrete project
Laboratory No.	UM Concrete
Date	6/6/95

YIELD DATA

Report on sample of Recycled I 96 at Brighton

	BATCH NUMBER 1	2	3	
UNIT WEIGHT OF CONCRETE	141.82	141.02	140.60	(pcf)
VOLUME OF ONE BATCH OF CONCRETE	1.9235	1.9436	1.9428	(cf / batch)
CEMENT USED FOR ONE CY OF CONCRETE	530	524	524	(pcy)
NET FREE WATER USED FOR ONE CY OF CONCRETE	228.78	243.28	230.61	(pcy)
WATER CEMENT RATIO	0.43	0.46	0.44	W/C

UNIVERSITY OF MICHIGAN
MATERIALS DEPARTMENT

Freeze-Thaw No.	94-recycled I 96 -1
Job No.	MCPA recycled concrete project
Laboratory No.	UM Concrete
Date	6/6/95

COMPRESSIVE STRENGTH TESTS

Report on sample of Recycled I 96 at Brighton	BATCH NUMBER 1	2	3
Date of mix	11/10/94	11/15/94	11/22/94
7 day breaks A & B	11/17/94	11/22/94	11/30/94
28 day breaks C & D	12/8/94	12/13/94	12/21/94

BATCH NO.	SPECIMEN NO.	DIAMETER (inches)	AREA (square inches)	LOAD (pounds)	STRENGTH (psi)	AVERAGE (psi)
1	A	4.00	12.57	53560	4262	
	B	4.00	12.57	52490	4177	4220
	C	4.00	12.57	56970	4534	
	D	4.00	12.57	59750	4755	4644
2	A	4.00	12.57	42040	3345	
	B	4.00	12.57	44300	3525	3435
	C	4.00	12.57	56140	4467	
	D	4.00	12.57	54850	4365	4416
3	A	4.00	12.57	39350	3131	
	B	4.00	12.57	40440	3218	3175
	C	4.00	12.57	59790	4758	
	D	4.00	12.57	58980	4693	4726

REMARKS:

Batch 3: 8 day & 29 day breaks

FREEZE-THAW DURABILITY EXPANSION WORKSHEET

U - MICH

IDENTIFICATION: RECYCLED 1-1
BATCH MADE: 11/10/94
INITIAL READING: 0.1049

BEAM NUMBER: 55
STARTING DATE: 11/24/94
GAGE LENGTH: 13.5

NUMBER OF CYCLES	COMPARATOR READING	EXPANSION CONTRACTION	PERCENT EXPANSION
0	0.1049		
7	0.1049	0.0000	0.0000
34	0.1052	0.0003	0.0022
67	0.1057	0.0008	0.0059
91	0.1061	0.0012	0.0089
106	0.1070	0.0021	0.0156
140	0.1080	0.0031	0.0230
180	0.1093	0.0044	0.0326
196	0.1102	0.0053	0.0393
213	0.1109	0.0060	0.0444
230	0.1122	0.0073	0.0541
253	0.1129	0.0080	0.0593
286	0.1142	0.0093	0.0689
311	0.1160	0.0111	0.0822

INTERPOLATION

300	**0.1152**	**0.0103**	**0.0764**

% EXPANSION / 100 CYCLES **0.0255**

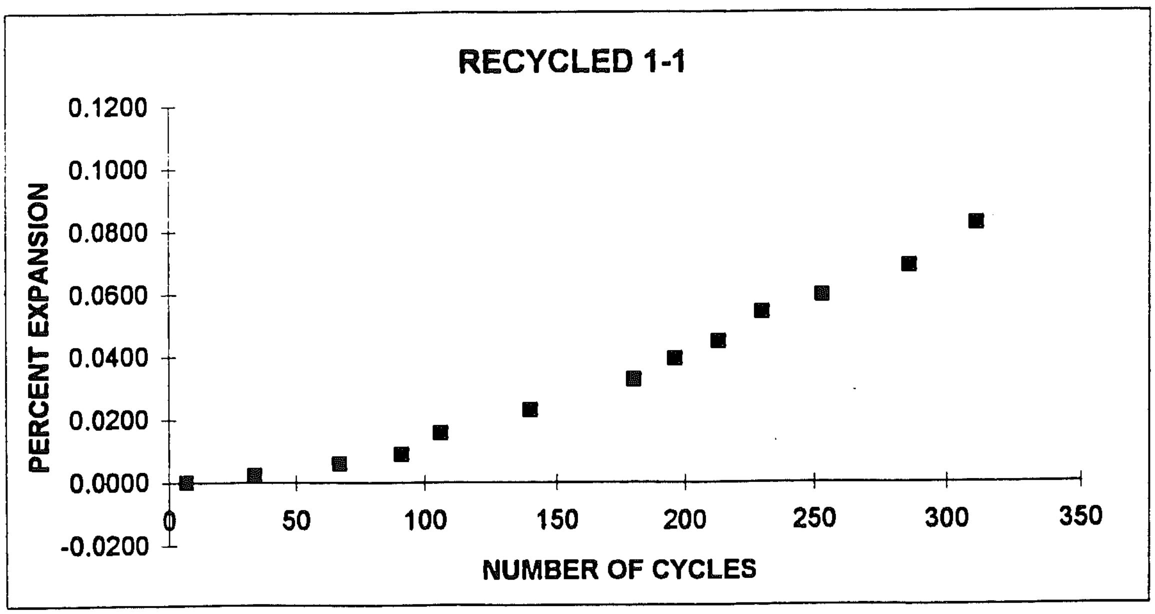

FREEZE-THAW DURABILITY EXPANSION WORKSHEET

U - MICH

IDENTIFICATION: RECYCLED 1-2
BATCH MADE: 11/10/94
INITIAL READING: 0.1900

BEAM NUMBER: 56
STARTING DATE: 11/24/94
GAGE LENGTH: 13.5

NUMBER OF CYCLES	COMPARATOR READING	EXPANSION CONTRACTION	PERCENT EXPANSION
0	0.1900		
7	0.1900	0.0000	0.0000
34	0.1905	0.0005	0.0037
67	0.1909	0.0009	0.0067
91	0.1913	0.0013	0.0096
106	0.1921	0.0021	0.0156
140	0.1926	0.0026	0.0193
180	0.1935	0.0035	0.0259
196	0.1944	0.0044	0.0326
213	0.1949	0.0049	0.0363
230	0.1957	0.0057	0.0422
253	0.1967	0.0067	0.0496
286	0.1982	0.0082	0.0607
311	0.1999	0.0099	0.0733

INTERPOLATION

300	**0.1992**	**0.0092**	**0.0678**

% EXPANSION / 100 CYCLES **0.0226**

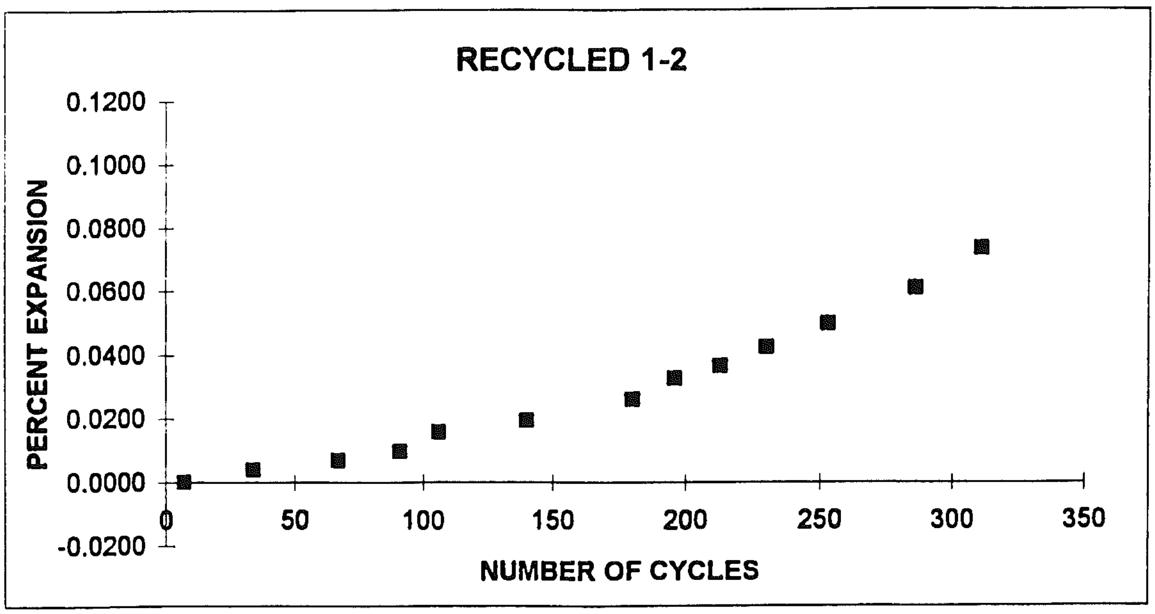

FREEZE-THAW DURABILITY EXPANSION WORKSHEET

U - MICH

IDENTIFICATION: RECYCLED 1-3
BATCH MADE: 11/10/94
INITIAL READING: 0.1224

BEAM NUMBER: 57
STARTING DATE: 11/24/94
GAGE LENGTH: 13.5

NUMBER OF CYCLES	COMPARATOR READING	EXPANSION CONTRACTION	PERCENT EXPANSION
0	0.1224		
7	0.1222	-0.0002	-0.0015
34	0.1225	0.0001	0.0007
67	0.1228	0.0004	0.0030
91	0.1232	0.0008	0.0059
106	0.1240	0.0016	0.0119
140	0.1248	0.0024	0.0178
180	0.1260	0.0036	0.0267
196	0.1268	0.0044	0.0326
213	0.1272	0.0048	0.0356
230	0.1280	0.0056	0.0415
253	0.1289	0.0065	0.0481
286	0.1302	0.0078	0.0578
311	0.1316	0.0092	0.0681

INTERPOLATION

300	**0.1310**	**0.0086**	**0.0636**

% EXPANSION / 100 CYCLES **0.0212**

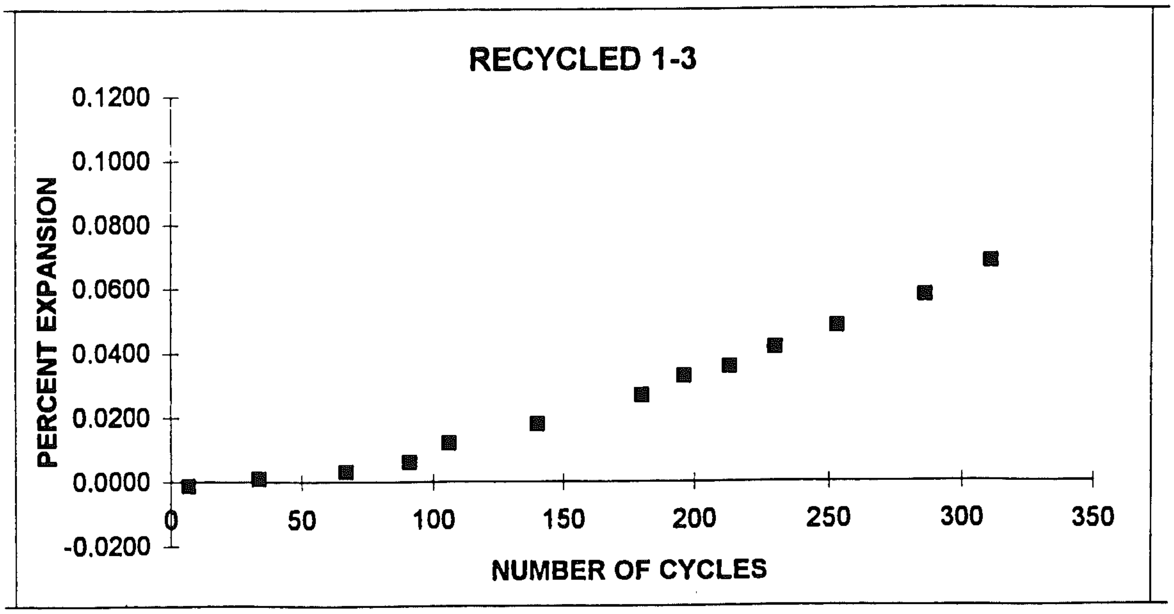

FREEZE-THAW DURABILITY EXPANSION WORKSHEET

U - MICH

IDENTIFICATION: RECYCLED 2-1
BATCH MADE: 11/15/94
INITIAL READING: 0.1407

BEAM NUMBER: 58
STARTING DATE: 11/29/94
GAGE LENGTH: 13.5

NUMBER OF CYCLES	COMPARATOR READING	EXPANSION CONTRACTION	PERCENT EXPANSION
0	0.1407		
7	0.1418	0.0011	0.0081
25	0.1424	0.0017	0.0126
49	0.1446	0.0039	0.0289
64	0.1473	0.0066	0.0489
98	0.1552	0.0145	0.1074

INTERPOLATION

94	**0.1542**	**0.0135**	**0.1000**

% EXPANSION / 100 CYCLES **0.1067**

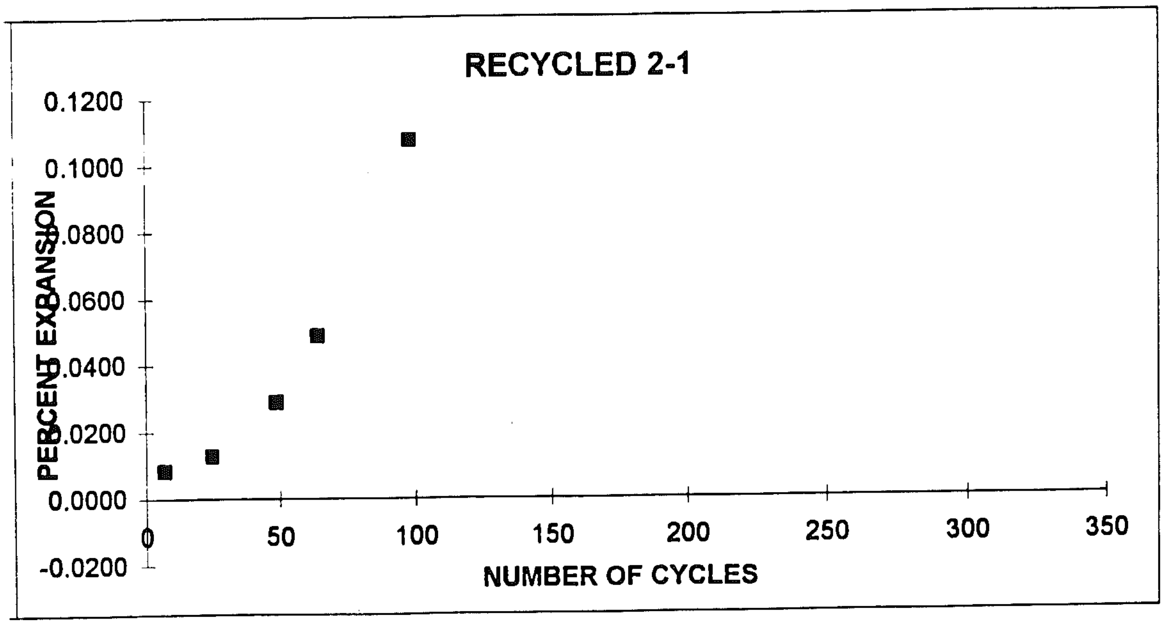

FREEZE-THAW DURABILITY EXPANSION WORKSHEET

U - MICH

IDENTIFICATION: RECYCLED 2-2
BATCH MADE: 11/15/94
INITIAL READING: 0.1766

BEAM NUMBER: 59
STARTING DATE: 11/29/94
GAGE LENGTH: 13.5

NUMBER OF CYCLES	COMPARATOR READING	EXPANSION CONTRACTION	PERCENT EXPANSION
0	0.1766		
7	0.1770	0.0004	0.0030
25	0.1774	0.0008	0.0059
49	0.1777	0.0011	0.0081
64	0.1791	0.0025	0.0185
98	0.1818	0.0052	0.0385
138	0.1871	0.0105	0.0778
154	0.1893	0.0127	0.0941
171	0.1920	0.0154	0.1141

INTERPOLATION

159	**0.1901**	**0.0135**	**0.1000**

% EXPANSION / 100 CYCLES **0.0629**

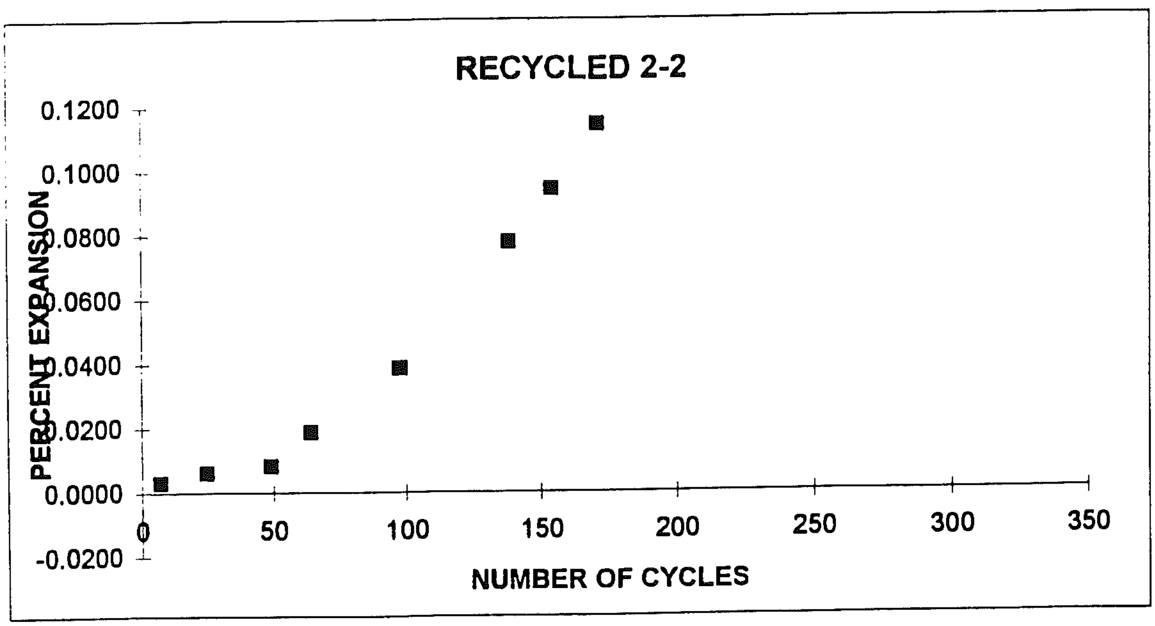

FREEZE-THAW DURABILITY EXPANSION WORKSHEET

U - MICH

IDENTIFICATION: RECYCLED 2-3
BATCH MADE: 11/15/94
INITIAL READING: 0.1569

BEAM NUMBER: 60
STARTING DATE: 11/29/94
GAGE LENGTH: 13.5

NUMBER OF CYCLES	COMPARATOR READING	EXPANSION CONTRACTION	PERCENT EXPANSION
0	0.1569		
7	0.1581	0.0012	0.0089
25	0.1587	0.0018	0.0133
49	0.1594	0.0025	0.0185
64	0.1615	0.0046	0.0341
98	0.1667	0.0098	0.0726
138	0.1733	0.0164	0.1215

INTERPOLATION

120	**0.1704**	**0.0135**	**0.1000**

% EXPANSION / 100 CYCLES **0.0830**

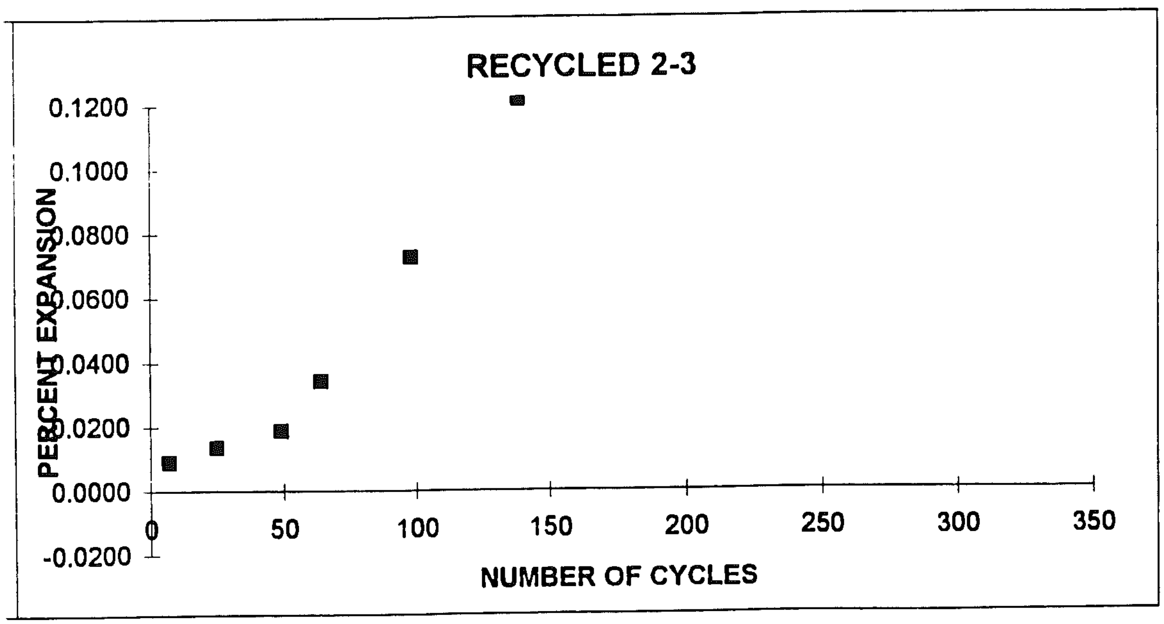

FREEZE-THAW DURABILITY EXPANSION WORKSHEET

U - MICH

IDENTIFICATION: RECYCLED 3-1
BATCH MADE: 11/22/94
INITIAL READING: 0.1308

BEAM NUMBER: 61
STARTING DATE: 12/7/94
GAGE LENGTH: 13.5

NUMBER OF CYCLES	COMPARATOR READING	EXPANSION CONTRACTION	PERCENT EXPANSION
0	0.1308		
8	0.1308	0.0000	0.0000
42	0.1321	0.0013	0.0096
82	0.1328	0.0020	0.0148
98	0.1334	0.0026	0.0193
115	0.1338	0.0030	0.0222
132	0.1343	0.0035	0.0259
155	0.1356	0.0048	0.0356
188	0.1365	0.0057	0.0422
213	0.1378	0.0070	0.0519
228	0.1393	0.0085	0.0630
245	0.1400	0.0092	0.0681
268	0.1418	0.0110	0.0815
303	0.1438	0.0130	0.0963

INTERPOLATION

300	**0.1436**	**0.0128**	**0.0950**

% EXPANSION / 100 CYCLES **0.0317**

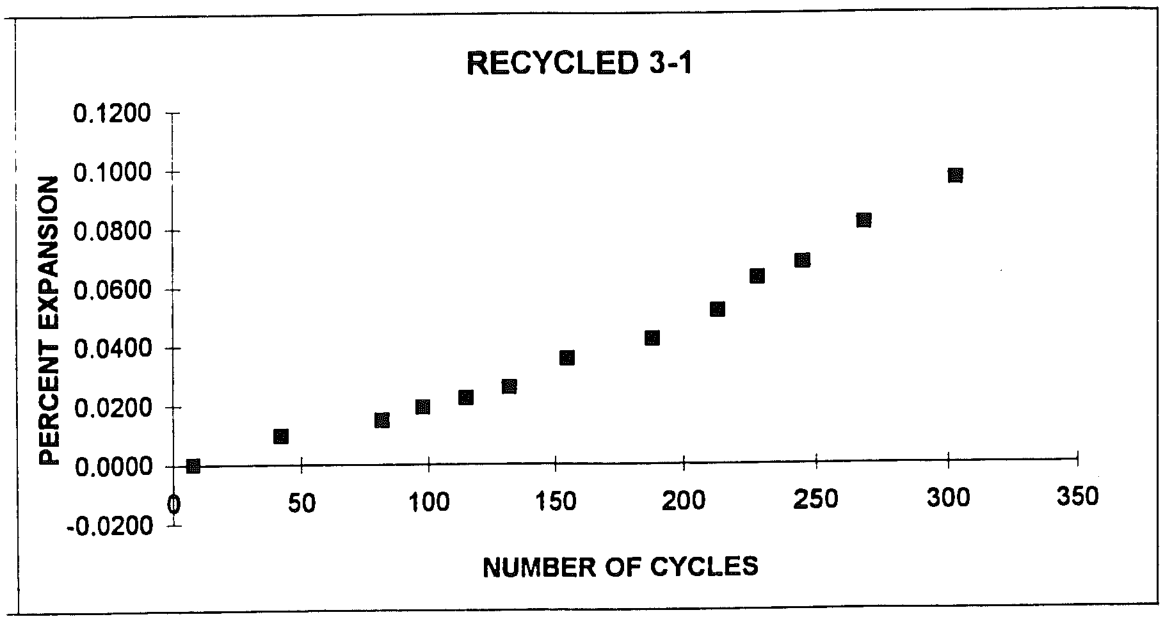

FREEZE-THAW DURABILITY EXPANSION WORKSHEET

U - MICH

IDENTIFICATION: RECYCLED 3-2
BATCH MADE: 11/22/94
INITIAL READING: 0.1551

BEAM NUMBER: 62
STARTING DATE: 12/7/94
GAGE LENGTH: 13.5

NUMBER OF CYCLES	COMPARATOR READING	EXPANSION CONTRACTION	PERCENT EXPANSION
0	0.1551		
8	0.1550	-0.0001	-0.0007
42	0.1560	0.0009	0.0067
82	0.1571	0.0020	0.0148
98	0.1579	0.0028	0.0207
115	0.1583	0.0032	0.0237
132	0.1594	0.0043	0.0319
155	0.1606	0.0055	0.0407
188	0.1627	0.0076	0.0563
213	0.1645	0.0094	0.0696
228	0.1661	0.0110	0.0815
245	0.1674	0.0123	0.0911
268	0.1692	0.0141	0.1044

INTERPOLATION

260	**0.1686**	**0.0135**	**0.1000**

% EXPANSION / 100 CYCLES **0.0384**

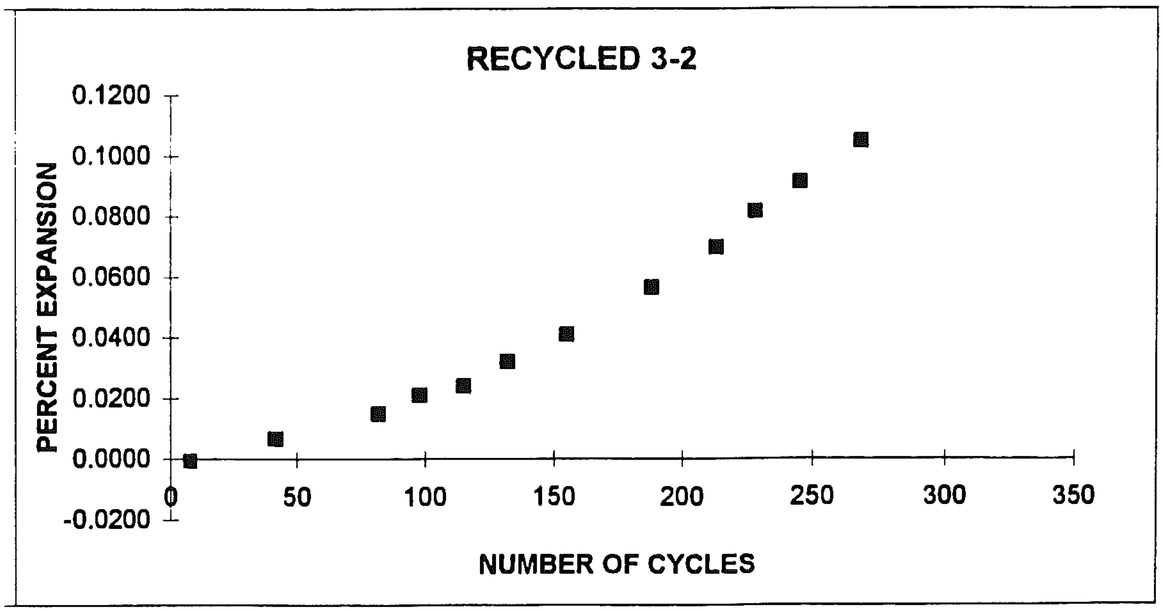

FREEZE-THAW DURABILITY EXPANSION WORKSHEET

U - MICH

IDENTIFICATION: RECYCLED 3-3
BATCH MADE: 11/22/94
INITIAL READING: 0.1602

BEAM NUMBER: 63
STARTING DATE: 12/7/94
GAGE LENGTH: 13.5

NUMBER OF CYCLES	COMPARATOR READING	EXPANSION CONTRACTION	PERCENT EXPANSION
0	0.1602		
8	0.1599	-0.0003	-0.0022
42	0.1615	0.0013	0.0096
82	0.1626	0.0024	0.0178
98	0.1635	0.0033	0.0244
115	0.1639	0.0037	0.0274
132	0.1652	0.0050	0.0370
155	0.1668	0.0066	0.0489
188	0.1683	0.0081	0.0600
213	0.1700	0.0098	0.0726
228	0.1718	0.0116	0.0859
245	0.1728	0.0126	0.0933
268	0.1751	0.0149	0.1104

INTERPOLATION

254	**0.1737**	**0.0135**	**0.1000**

% EXPANSION / 100 CYCLES **0.0394**

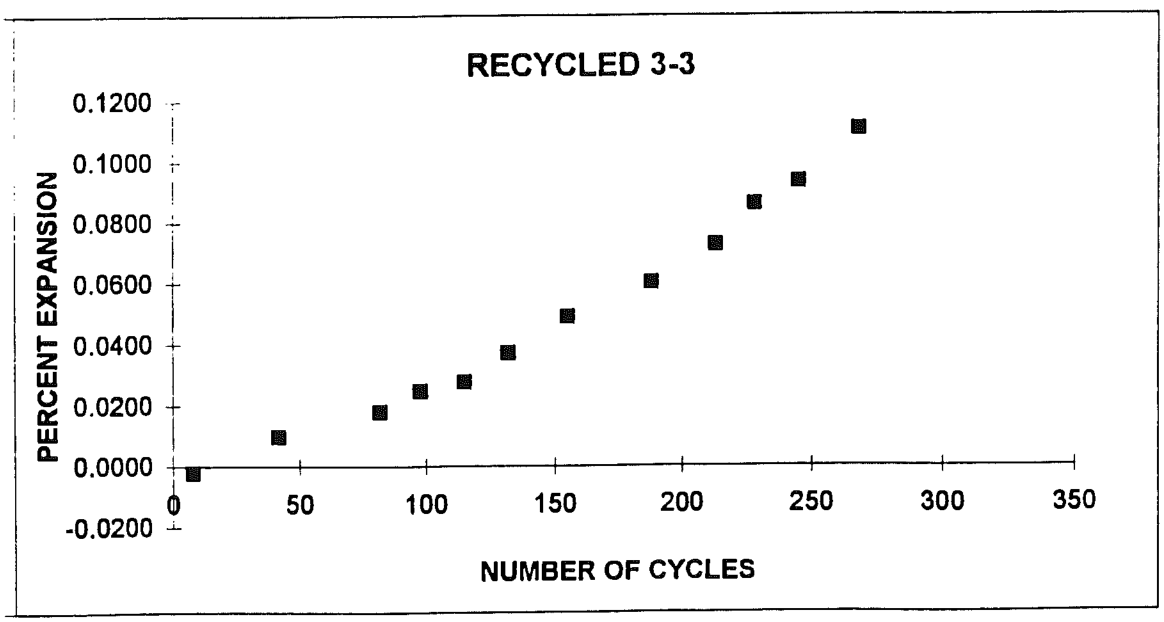

Appendix 11: Traffic Analysis

The magnitude, configuration and the number of repetitions of heavy axle loads actually applied on a pavement influence its performance to a great extent. In the AASHTO procedure for the design of pavements, the axle loads are represented by the number of 18-kip equivalent single axle loads or ESAL's which will produce the same damage as that of the axle in question. The Federal Highway Administration's W-4 truck weight tables give the number of axles observed in a pavement within a series of load groups. These numbers are then converted into ESAL's by multiplying with a corresponding truck equivalency factor for each group. In the AASHTO design procedure, a rigid pavement is designed for the given material characteristics, to a certain thickness sufficient to keep the pavement in a serviceable condition for the level of traffic expected throughout its design period. The serviceability soon after construction and the lowest acceptable limit are respectively termed as the present and terminal serviceability indices.

The four pavement sections at Lawrence and two sections at Galesburg are analyzed in terms of the AASHTO serviceability concept. An initial serviceability index of 4.5 and terminal serviceability index of 2.5 are used in the analysis. As per AASHTO, the terminal serviceability index of 2.5 yields an unacceptable ride quality level for about 55% of the public. The traffic level in each of these sections is calculated based on an MDOT estimate of the traffic. The initial traffic is backcalculated using the growth rate reported for the period from 1993 to 1995, i.e. 2.1%.

The material characteristics used in the analysis are based on field testing, laboratory analysis and backcalculation results. A reliability of 90%, standard deviation of 0.35 and subbase thickness of 10 inches are assumed for all sections. Assuming fair drainage quality (water removed within a week), a drainage coefficient of 1.0 (about 5 % of the time the pavement structure is exposed to moisture levels approaching saturation) is assumed in the analysis. The thickness of the slab used in the analysis is the average of all full depth cores taken from a section. The 28 day flexural strength and modulus of elasticity value are estimated from the present laboratory test results. The 28 day compressive strength is assumed as 80% of the 9 to 11 year compressive strength. The flexural strength is assumed as 9 times (8 to 10 is used in the literature) the square root of the compressive strength. Similarly the 28 day modulus of elasticity is calculated from the relationship that it is proportional to the square root of the compressive strength at the same age[24]. The subgrade modulus is estimated from the FWD backcalculation using the Bousdef computer program and the subbase modulus from a correlation of the CPT results[23].

As per the FWD tests, the load transfer across slabs varies from section to section. Therefore, a load transfer coefficient of 2.8 is assumed for sections with low load transfer efficiency and 2.5 for those with better transfer efficiency (MI1-2 and MI1-4). For tied PCC plain jointed pavements AASHTO recommends a range of 2.5 to 3.1 as load transfer coefficient (AASHTO, 1993). The loss of support is another important factor used in the AASHTO design procedure to account for the potential loss of support arising from factors such as subbase erosion. For unbound granular materials AASHTO recommends a range of 1.0 to 3.0 (AASHTO, 1993) for the loss of support. Keeping the comparative subbase and subgrade qualities in view, a loss of support of 1.5 is used for all sections except MI1-4 where a value of 1.0 is used. In section MI1-4, the foundation layers are found to be more uniform than in the other sections. A loss of support of 1.0 would have been more appropriate for MI2-1, however, it is kept at 1.5 for purpose of comparison with MI2-2. The allowable ESAL's for each section, based on the available and assumed design inputs, are calculated. The pavement is supposed to have reached its threshold serviceability level, if this allowable ESAL's exceeds the estimated actual ESAL's. It is to be noted that this analysis is based entirely on the serviceability of the pavement which is indirectly a measure of the ride quality and does not directly represent the fatigue failure of the section. The various design inputs used in each section are attached.

AASHTO SERVICEABILITY CHECK

(BASED ON AASHTO DESIGN GUIDE FOR DESIGN OF PAVEMENT STRUCTURES, 1993)

Data Item	MI1-1	MI1-2	MI1-3	MI1-4
Age, years (as of 1995)	11	11	11	11
Reliability (%)	90	90	90	90
Design Terminal Serviceability, Pt	2.5	2.5	2.5	2.5
Initial Serviceabilty Index, Pi	4.5	4.5	4.5	4.5
Traffic Growth Rate (%)	2.1	2.1	2.1	2.1
Current Yearly ESAL	1,640,310	1,640,310	1,640,310	1,640,310
Estimated Initial ESAL	1,305,097	1,305,097	1,305,097	1,305,097
Total ESAL	15,962,528	15,962,528	15,962,528	15,962,528
Lane Distribution Factor	0.85	0.85	0.85	0.85
Total ESAL (Design Lane)	**13,568,149**	**13,568,149**	**13,568,149**	**13,568,149**
Overall Standard Deviation	0.35	0.35	0.35	0.35
Subbase Thickness (in)	**10**	**10**	**10**	**10**
Measured PCC Thickness (in)	**10.2**	**10.3**	**9.7**	**9.4**
Current Concrete Compressive Strength, CS (psi)	5244	6166	6785	6553
Estimated 28 Day Concrete Compressive Strength (psi)	4195.2	4932.8	5428	5242.4
Current Flexural Strength, FS = 9*sqrt[CS] (psi)	651.74	706.71	741.34	728.56
Estimated 28 Day Flexural Strength = .8*FS (psi)	**521.39**	**565.37**	**593.07**	**582.84**
Current PCC Elastic Modulus, Ec (psi)	3,180,000	3,670,000	3,510,000	3,970,000
Estimated 28 Day PCC Elastic Modulus (psi)	**2,844,278**	**3,282,548**	**3,139,439**	**3,550,876**
Load Transfer Coefficient	**2.8**	**2.5**	**2.8**	**2.5**
Drainage Coefficient	**1.0**	**1.0**	**1.0**	**1.0**
Loss of Support Factor	**1.5**	**1.5**	**1.5**	**1.0**
Composite K value (FWD-Back Calculated)	244	359	163	171
Composite K (DNPS86 output)	211	263	208	199
Composite Elastic Modulus of Soil (FWD-Back Calculated)	33201	25210	20754	22411
Assumed Subbase Modulus (DCP Correlation)	**140,035**	**100,673**	**175,557**	**105,979**
Roadbed Modulus (Based on FWD)	**33201**	**25210**	**20754**	**22411**

AASHTO SERVICEABILITY CHECK

(BASED ON AASHTO DESIGN GUIDE FOR DESIGN OF PAVEMENT STRUCTURES, 1993)

Data item	East Bound	West Bound
Age, years (as of 1995)	10	9
Reliability (%)	90	90
Design Terminal Serviceability, Pt	2.5	2.5
Initial Serviceabilty Index, Pi	4.5	4.5
Traffic Growth Rate (%)	2.1	2.1
Current Yearly ESAL	2,153,500	2,007,500
Estimated Initial ESAL	1,749,393	1,665,037
Total ESAL	19,243,174	16,307,765
Lane Distribution Factor	0.85	0.85
Total ESAL (Design Lane)	**16,356,698**	**13,861,600**
Overall Standard Deviation	0.35	0.35
Subbase Thickness (in)	**10**	**10**
Measured PCC Thickness (in)	**10.1**	**10.4**
Current Concrete Compressive Strength, CS (psi)	5901	6775
Estimated 28 Day Concrete Compressive Strength (psi)	4720.8	5420
Current Flexural Strength, FS = 9*sqrt[CS] (psi)	691.36	740.79
Estimated 28 Day Flexural Strength	**553.09**	**592.63**
Current PCC Elastic Modulus, Ec (psi)	3,730,000	3,830,000
Estimated 28 Day PCC Elastic Modulus (psi)	**3,336,213**	**3,425,656**
Load Transfer Coefficient	**2.8**	**2.8**
Drainage Coefficient	**1.0**	**1.0**
Loss of Support Factor	**1.5**	**1.5**
Composite K value (FWD-Back Calculated)	297*	270
Composite K (DNPS86 output)	192	270
Composite Elastic Modulus of Soil (FWD-Back Calculated)	18928	32217
Assumed Subbase Modulus (DCP Correlation)	**148,894**	**177,538**
Roadbed Modulus (Based on FWD)	**18928**	**32217**

* Based on only one test

AASHTO Serviceability Check

Section	Age in years (Until 1995)	Load repetitions (ESAL's)		Remarks
		Total allowable	Estimated Actual* to date	
MI1-1	11	11,176,010	13,658,149	Fail
MI1-2	11	20,168,810	13,658,149	Pass
MI1-3	11	11,279,980	13,658,149	Fail
MI1-4	11	15,698,400	13,658,149	Pass
MI2-1	9	18,481,760	13,861,600	Pass
MI2-2	10	10,845,930	16,356,698	Fail

* Based on data obtained from MDOT

7. References

7.1 Cited References

1. "AASHTO Guide for Design of Pavement Structures", American Association of State Highway and Transportation Officials, Washington, D.C. 1993.
2. "Standard Test Method for Obtaining and Testing Drilled Cores and Sawed Beams of Concrete," (C42-90). *1991 Annual Book of ASTM Standards*, Volume 04.02. Philadelphia: ASTM, 1991.
3. "Standard Test Method for Static Modulus of Elasticity and Poisson's Ratio of Concrete in Compression," (C469-87a). *1991 Annual Book of ASTM Standards*, Volume 04.02. Philadelphia: ASTM, 1991.
4. RILEM Committee DRC 37. *Rilem Report 6: Recycling of Demolished Concrete and Masonry*. London: E & FN SPON, 1992.
5. *Climatological Data, Michigan*. United States Department of Commerce. August 1984, Vol 99, No. 8; September 1984, Vol 99, No. 9; July 1985, Vol 100, No. 7; May 1985, Vol 101, No. 5.
6. Huang, Yang H. *Pavement Analysis and Design*. Englewood Cliffs: Prentice Hall, 1993.
7. "Subgrades and Subbases for Concrete Pavements," *Concrete Paving Technology*. Portland Cement Association, 1991.
8. "Method of Selection and Preparation of Coarse Aggregate Samples for Freeze-Thaw Testing," Michigan Test Method 113-91. Michigan Department of Transportation.
9. "Method for Making Concrete Specimens for Freeze-Thaw Testing of Concrete Course Aggregate," Michigan Test Method 114-89. Michigan Department of Transportation.
10. "Method of Testing Concrete for Durability by Rapid Freezing in Air and Thawing in Water," Michigan Test Method 115-90. Michigan Department of Transportation.
11. Fergus, James S. "Laboratory Investigation and Mix Proportions for Utilizing Recycled Portland Cement Concrete Aggregate," Michigan Department of Transportation. pp. 144-160.
12. Forster, Stephen W. "Recycled Concrete as Aggregate," *Concrete International*. October 1986, pp. 34-40.
13. Ioannides, A. Barenberg E. "Interpretation of Falling Weight Deflectometer Results Using Principles of Dimensional Analysis," 1989.
14. Darter, M., Hall, K., Kuo, C. "Support Under Concrete Pavements" Appendices NCHRP, TRB, National Research Council, Dec. 1994.
15. "Materials Finer Than No. 200 (75μm) Sieve in Mineral Aggregates by Washing", Michigan Test Method 108-94. Michigan Department of Transportation.
16. "Standard Test Method for Materials Finer than 75μm (No. 200) Sieve in Mineral Aggregates by Washing." (C117-90). *1991 Annual Book of ASTM Standards*, Volume 04. Philadelphia: ASTM, 1991.

17. "Sieve Analysis of Fine, Dense Graded, Open Graded, and Coarse Aggregates in the Field." Michigan Test Method 109-88. Michigan Department of Transportation.
18. "Standard Test Method for Sieve analysis of Fine and Coarse Aggregates." (C136-92). *1992 Annual Book of ASTM Standards*, Volume 04. Philadelphia: ASTM, 1992.
19. "Drainable Pavement Systems: Participant Notebook", Demonstration Project 87, Federal Highway Administration, Washington DC., March 1992.
20. "Practice for Petrographic Examination of Hardened Concrete." (C-856) *1991 Annual Book of ASTM Standards*, Volume 04. Philadelphia: ASTM, 1991.
21. "Penetration Testing in the UK.", Telford. London, United Kingdom, 1989.
22. "Proceedings of the European Symposium on Penetration Testing ESOPT: Volume 2:1 General Reports, Discussions, and other Activities." Swedish Geotechnical Society, 1975.
23. Burnham, T. and Johnson, D. "In Situ Foundation Characterization Using the Dynamic Cone Penetrometer", Minnesota Department of Transportation, Minnesota, 1993.
24. ERES Consultants, Inc. "Pavement Design Principles and Practices", National Highway Institute, Federal Highway Administration. Washington, D.C. 1987.

7.2 Other References

1. "A Study of the Use of Recycled Paving Material - Report to Congress," Report No. FHWA-RD-93-147; EPA/600/R-93/095, Federal Highway Administration, Environmental Protection Agency, June 1993.
2. Arnold, Chuck. "Concrete Recycling," *Materials and Technology Engineering and Science*. Michigan Department of Transportation Materials and Technology Division, May 1988.
3. Darter, Michael I. "Initial Evaluation of Michigan JRCP Crack Deterioration." Report Prepared for Michigan Concrete Paving Association, 1989.
4. Das, Braja M. *Principles of Geotechnical Engineering*, Second Edition. Boston: PWS-KENT Publishing Company, 1990.
5. Malott, Don. "Notes on Concrete Recycling and Associated Specification Changes," *Materials and Technology Engineering and Science*. Michigan Department of Transportation Materials and Technology Division, May 1988.
6. "Pavement Deflection Analysis Course - Participant Workbook, Volumes I - II. Federal Highway Administration National Highway Institute. Prepared by Dynatest Consulting, Inc. in collaboration with Soils and Materials Engineering, Inc.
7. *Penetration Testing in the UK*. Institution of Civil Engineers. London: Thomas Telford, 1989.
8. "Practice for Dealing with Outlying Observations," (E178). *1991 Annual Book of ASTM Standards*, Philadelphia: ASTM, 1991.
9. "Recycling Concrete Pavement," *Concrete Paving Technology*. American Concrete Pavement Association, 1993.
10. Schmid, Werner E. "Evaluation of Vibratory Compaction Field Tests," *In Situ Measurement of Soil Properties*. New York: American Society of Civil Engineers, 1975.
11. Smiley, David L. and Demetrius Parker. "Ten-Year Performance Review of Michigan's Concrete Recycled Pavements." Report Prepared for Michigan State University Concrete Technology Seminar VIII.
12. "Specification for Apparatus for Use in Measurement of Length Change of Hardened Cement Paste, Mortar, and Concrete," (C490). *1991 Annual Book of ASTM Standards*, Volume 04.02. Philadelphia: ASTM, 1991.
13. "Standard Practice for Capping Cylindrical Concrete Specimens," (C617-87). *1991 Annual Book of ASTM Standards*, Volume 04.02. Philadelphia: ASTM, 1991.
14. "Standard Practice for Making and Curing Concrete Test Specimens in the Laboratory," (C192-90a). *1991 Annual Book of ASTM Standards*, Volume 04.02. Philadelphia: ASTM, 1991.
15. "Standard Test Method for Compressive Strength of Cylindrical Concrete Specimens," (C39-86). *1991 Annual Book of ASTM Standards*, Volume 04.02. Philadelphia: ASTM, 1991.

16. "Standard Test Method for Total Moisture Content of Aggregate by Drying," (C566-89). *1991 Annual Book of ASTM Standards*, Volume 04.02. Philadelphia: ASTM, 1991.
17. Tammirinne, M. "Factors Effecting the Dynamic Penetration Resistance," *Proceedings of the European Symposium on Penetration Testing*. Stockholm: National Swedish Building Research, 1975.
18. Tavakoli, Mostafa and Parviz Soroushian. "Aggregates from Recycled Concrete." Michigan State University, Department of Civil and Environmental Engineering.
19. "Test Method for Air Content of Freshly Mixed Concrete by the Volumetric Method," (C173). *1991 Annual Book of ASTM Standards*, Volume 04.02. Philadelphia: ASTM, 1991.
20. "Test Method for Resistance of Concrete to Rapid Freezing and Thawing," (C666). *1991 Annual Book of ASTM Standards*, Volume 04.02. Philadelphia: ASTM, 1991.
21. "Test Method for Resistance to Degradation of Small-Size Coarse Aggregate by Abrasion and Impact in the Los Angeles Machine," (C131). *1991 Annual Book of ASTM Standards*, Volume 04.02. Philadelphia: ASTM, 1991.
22. "Test Method for Slump of Portland Cement Concrete," (C143). *1991 Annual Book of ASTM Standards*, Volume 04.02. Philadelphia: ASTM, 1991.
23. "Test Method for Specific Gravity and Absorption of Coarse Aggregate," (C127). *1991 Annual Book of ASTM Standards*, Volume 04.02. Philadelphia: ASTM, 1991.
24. "Test Method for Temperature of Freshly-Mixed Portland Cement Concrete," (C1064). *1991 Annual Book of ASTM Standards*, Volume 04.02. Philadelphia: ASTM, 1991.
25. "Test Method for Unit Weight and Voids in Aggregate," (C29). *1991 Annual Book of ASTM Standards*, Volume 04.02. Philadelphia: ASTM, 1991.
26. "Test Method for Unit Weight, Yield, and Air Content (Gravimetric) of Concrete," (C138). *1991 Annual Book of ASTM Standards*, Volume 04.02. Philadelphia: ASTM, 1991.
27. Yrjanson, William A. "Recycling of Portland Cement Concrete Pavements," National Cooperative Highway Research Program Synthesis of Highway Practice. Transportation Research Board, National Research Council, Washington, D.C., December 1989.